

Production of wax esters in *Camelina sativa*

Dissertation

for the award of the degree

“Doctor rerum naturalium”

of the Georg-August-Universität Göttingen

within the doctoral program “BIONUTZ”

of the Georg-August University School of Science (GAUSS)

submitted by

Dan Yu

from Fuxin, China

Göttingen, 2016

Members of the Thesis Committee

Prof. Dr. Ivo Feußner

Department of Plant Biochemistry, Albrecht-von-Haller-Institute for Plant Sciences, Georg-August University of Göttingen

Prof. Dr. Christiane Gatz

Department of Plant Molecular Biology, Albrecht-von-Haller-Institute for Plant Sciences, Georg-August University of Göttingen

Prof. Dr. Andrea Polle

Forest Botany and Tree Physiology, Faculty of Forest Science and Ecology, Georg-August University of Göttingen

Members of the Examination Board

Reviewer

Prof. Dr. Ivo Feußner

Department of Plant Biochemistry, Albrecht-von-Haller-Institute for Plant Sciences, Georg-August University of Göttingen

Reviewer

Prof. Dr. Christiane Gatz

Department of Plant Molecular Biology, Albrecht-von-Haller-Institute for Plant Sciences, Georg-August University of Göttingen

Prof. Dr. Andrea Polle

Forest Botany and Tree Physiology, Faculty of Forest Science and Ecology, Georg-August University of Göttingen

Prof. Dr. Volker Lipka

Department of Plant Cell Biology, Schwann-Schleiden Centre, Georg-August University of Göttingen

PD Dr. Thomas Teichmann

Department of Plant Cell Biology, Albrecht-von-Haller-Institute for Plant Sciences, University of Göttingen

Dr. Marcel Wiermer

Department of Plant Cell Biology, Schwann-Schleiden Centre, Georg-August University of Göttingen

Date of the oral examination: 14th December, 2016

Affidavit

I declare that I wrote the doctoral thesis on my own and did not use other sources or aids than quoted.

Dan Yu

Göttingen, November 2016

INDEX

1 INTRODUCTION	1
1.1 Natural resources of wax esters	2
1.2 Role of wax esters in nature	3
1.3 Chemical and physical properties of wax esters	3
1.4 Industrial applications of wax esters	4
1.5 Enzymatic basis of wax ester biosynthesis	6
1.5.1 Fatty acyl reductases	8
1.5.2 Wax synthases	12
1.6 Heterologous synthesis of wax esters	16
1.7 Biosynthesis of neutral lipids in plants	17
1.7.1 Fatty acid synthesis, elongation and desaturation	17
1.7.2 Biosynthesis of triacylglycerols	19
1.7.3 Biosynthesis of wax esters through acyl reduction pathway	21
1.8 <i>C. sativa</i> as an oilseed platform for metabolic engineering	21
1.8.1 Oil content and composition of <i>C. sativa</i>	22
1.8.2 Agronomic traits of <i>C. sativa</i>	23
1.8.3 Biotechnological tools of manipulating lipid metabolism in <i>C. sativa</i>	25
1.8.4 Biosynthesis of unusual lipids in <i>C. sativa</i>	26
1.8.5 Biosynthesis of wax esters in <i>C. sativa</i>	27
2 OBJECTIVES	28
3 MATERIALS	29
3.1 Chemicals	29
3.2 Machines and equipments	29
3.3 Softwares and web-based services	31
3.4 Kits and consumables	32
3.5 Standards and markers	33
3.6 Mediums, buffers and antibiotics	33
3.7 Columns for chromatography	35
3.8 Enzymes	35
3.9 Strains and organisms	36
3.10 Oligonucleotides	37
3.11 DNA constructs	40
3.12 Transgenic plants	43
4 METHODS	45
4.1 Molecular biology methods	45

INDEX

4.1.1 Standard PCR	45
4.1.2 Overlap extension PCR	45
4.1.3 Colony PCR.....	45
4.1.4 Restriction of DNA	46
4.1.5 Separation of DNA by agarose gel-electrophoresis.....	46
4.1.6 Ligation of DNA.....	47
4.1.7 Cloning of artificial microRNAs	48
4.1.8 Gateway technology.....	50
4.1.9 Preparation of competent <i>E. coli</i> cells.....	50
4.1.10 Transformation of <i>E. coli</i>	51
4.1.11 Plasmid preparation	51
4.1.12 Preparation of competent <i>S. cerevisiae</i> cells.....	51
4.1.13 Transformation of <i>S. cerevisiae</i>	52
4.1.14 Cultivation of <i>S. cerevisiae</i>	52
4.1.15 Preparation of competent <i>A. tumefaciens</i> cells	53
4.1.16 Transformation of <i>A. tumefaciens</i>	53
4.1.17 Transformation of <i>A. thaliana</i>	53
4.1.18 Transformation of <i>C. sativa</i> via vacuum floral dipping.....	53
4.1.19 Sterilization of seeds of <i>C. sativa</i> for germination experiment	54
4.1.20 Cultivation of <i>E. coli</i> expression culture for protein purification.....	54
4.2 Biochemical methods	55
4.2.1 Preparation of cell pellets for protein purification.....	55
4.2.2 Protein purification.....	56
4.2.3 Size exclusion chromatography (SEC).....	56
4.2.4 Desalting chromatography	57
4.2.5 SDS polyacrylamide gel electrophoresis (SDS-PAGE)	58
4.2.6 Measurement of protein concentration.....	59
4.2.7 DTNB-based <i>in vitro</i> test of acyltransferase activity.....	60
4.3 Imaging methods	61
4.3.1 Gold particle preparation for bombardment	61
4.3.2 Particle bombardment	61
4.3.3 Microscopy	62
4.4 Analytical methods	62
4.4.1 Wax ester extraction from <i>S. cerevisiae</i>	62
4.4.2 Wax ester extraction from seeds of <i>C. sativa</i> and <i>A. thaliana</i>	62
4.4.3 Thin layer chromatography analysis.....	62

4.4.4 Transesterification of <i>C. sativa</i> cotyledons	63
4.4.5 GC-FID analysis of fatty acid profile of <i>C. sativa</i> seed oil	63
4.4.6 Wax ester analysis via GC-MS	63
4.4.7 GC-FID analysis of wax esters and TAGs	64
4.4.8 Nano-ESI-MS/MS analysis of wax ester molecular species.....	65
4.5 Statistical methods.....	65
5 RESULTS	66
5.1 Fusion of <i>MaFAR</i> with <i>ScWS</i> to locate <i>MaFAR</i> to the ER.....	66
5.1.1 Expression of <i>ScWS-MaFAR</i> in <i>S. cerevisiae</i>	67
5.1.2 Expression of <i>ScWS-MaFAR</i> in seeds of <i>A. thaliana</i>	68
5.2 Bifunctional enzyme <i>AbWSD1</i> from <i>A. baylyi</i> ADP1	73
5.2.1 Co-expression of <i>MaFAR</i> with <i>AbWSD1</i> in seeds of <i>A. thaliana</i>	74
5.2.2 Optimization of <i>AbWSD1</i>	75
5.2.3 Co-expression of <i>MaFAR</i> with optimized <i>AbWSD1</i> in seeds of <i>A. thaliana</i>	78
5.3 Wax synthases from <i>M. aquaeolei</i> VT8.....	83
5.3.1 Identification of a fifth putative wax synthase in <i>M. aquaeolei</i> VT8	83
5.3.2 Expression of five putative <i>MaWSs</i> in <i>S. cerevisiae</i>	84
5.3.3 Co-expression of <i>MaFAR</i> with <i>MaWS2</i> in seeds of <i>A. thaliana</i>	85
5.3.4 Purification of heterologously expressed <i>MaWS5</i>	88
5.4 Down-regulation of TAG biosynthesis in seeds of <i>C. sativa</i>	92
5.5 Optimization of wax ester composition in the seeds of <i>C. sativa</i>	98
5.5.1 Modification of fatty acid profile of <i>C. sativa</i> seeds	98
5.5.2 Crossing wax ester producing lines with a high oleic line.....	102
6 DISCUSSION	107
6.1 Fusion of <i>MaFAR</i> with <i>ScWS</i> to locate <i>MaFAR</i> to the ER.....	107
6.1.1 Enzymatic activities of the <i>ScWS-MaFAR</i> fusion protein	107
6.1.2 Substrate specificities of the <i>ScWS-MaFAR</i> fusion protein.....	108
6.2 Bifunctional enzyme <i>AbWSD1</i> from <i>A. baylyi</i> ADP1	109
6.2.1 <i>AbWSD1</i>	109
6.2.2 <i>TMMmAWAT2-AbWSD1</i>	110
6.3 Wax synthases from <i>M. aquaeolei</i> VT8.....	111
6.3.1 <i>MaWS1</i>	111
6.3.2 <i>MaWS2</i>	111
6.3.3 <i>MaWS3</i>	112
6.3.4 <i>MaWS4</i>	113
6.3.5 <i>MaWS5</i>	113

INDEX

6.4 Down-regulation of CsDGAT1 by amiRNAs.....	114
6.5 Optimization of wax ester composition in the seeds of <i>C. sativa</i>	116
6.5.1 Modification of fatty acid profile by amiRNAs	116
6.5.2 <i>MaFAR/ScWS</i> &HO crosses	117
6.6 The threshold of wax ester yield and the white cotyledon phenotype.....	118
7 OUTLOOK	120
8 ABSTRACT.....	122
9 REFERENCES	123
SUPPLEMENTARY MATERIALS	137
LIST OF ABBREVIATIONS	153
LIST OF FIGURES.....	156
LIST OF TABLES.....	160
ACKNOWLEDGEMENTS.....	163
CURRICULUM VITAE.....	165

1 INTRODUCTION

In the modern world, the growth of the global economy heavily relies on mineral fuels, such as coal, petroleum and natural gas. They are mainly used for energy production and as raw materials. The blooming economy of developing countries will dramatically increase the demand for more materials and products, resulting in a greater requirement for energy. Even though there may be no immediate shortage of fossil fuels, the increasing difficulties to exploit fossil carbon resources, the current instable supply of petroleum, and the continuous fluctuation of their prices have attracted a widespread attention on alternative energy resources. Furthermore, more serious concerns regarding to the utilization of fossil carbon resources arise in these years, as they have created undesirable damages to the environment. Burning fossil carbon resources for more than one century has already caused the emission of a huge amount of CO₂ that has resulted in the global warming and meteorological disasters. In addition, the production of industrial chemicals from fossil carbon resources has led to water and soil pollutions, as well as the emission of toxic gas and dust. As consequence, the public consciousness for clean and renewable energy resources is growing rapidly considering that the global economy need to develop sustainably. Overall, it is imminent to find renewable energy resources in consideration of the environmental, economic and geopolitical reasons.

In recent years, the biotechnology has become increasingly important for a sustainable economy. Biotechnological solutions utilize the knowledge of life science to create novel and commercially products, at the same time reduce the consumption of raw materials and negative impacts on the eco-system (En Route to the Knowledge-Based Bio-Economy, 2007). Plant oil represents one of the major resources to provide environmental friendly, sustainable and renewable industrial feedstocks. It will probably take the place of fossil carbon resources in a lot of industrial applications (Vanhercke *et al.*, 2013). Plant oil and plant-derived resources have mostly been used for the production of biofuels that are mainly used in transportation purposes (Du *et al.*, 2008). In order to produce ethanol and biodiesel, crop plants, such as sugar cane, corn and maize, have been cultivated in large scale in some countries, like U.S.A and Brazil. However, there is always an argument that food crops should not be burnt for transportation, taking the consideration that a part of the population on earth is still suffering from starving and lack of nutrients (International Centre for Trade and Sustainable Development, 2011; Committee on world food security, 2013). On the other hand, it is unrealistic that the plant oil can fulfill the worldwide requirement of the oil for energy and transportation purposes. In 2009, the United State consumed a total of 94.6 quads of energy, whilst the bio-based oil could only contribute 3.88 quads (Altman and Hasegawa, 2012). If 40% of the fossil oil is replaced with the renewable plant oil, meanwhile the global increasing demand for the food oil is still satisfied, the production of the plant oil would have to grow from the current 139 million tons per year up to over 400 million tons per year (Carlsson *et al.*, 2011). This would be an extremely huge challenge to the agricultural industry.

In the long-term view, selling a small amount of the plant oil for energy production at a low price is meaningless for both economical profits and social implications. In contrast, utilizing plant oils as chemical feedstocks could be a commercially attractive alternative (Biermann *et al.*, 2000). For instance, erucic acid, a very long-chain fatty acid is used for the production of erucamide, which is an important slipping agent for producing extruded polyethylene films (Friedt and Luhs, 1998; Dyer, 2008). China wool oil accumulated in the nut of *Vernicia fordii*, has excellent drying properties; therefore it is widely used for furniture protection (Vanhercke *et al.*, 2013). Currently, fatty acids and triacylglycerols (TAGs) are plant oils mostly used in industrial applications. Wax esters are also a species of the plant oil with a relatively high commercial value, so that they are commonly used in the cosmetic, food coating and lubrication industries.

1.1 Natural resources of wax esters

Wax esters are a group of highly hydrophobic neutral lipids existing in a wide range of organisms (Iven *et al.*, 2013; DeWitt *et al.*, 1982; Kahn and Kolattukudy, 1973). The content of wax esters varies within and among different species. They are commonly found as a part of the cuticle of plant leave surfaces, fruits and seed coats. Wax esters account for only 0.1% - 0.2% of the surface lipids in *A. thaliana* leaves, and account for 0.7% - 2.9% of the surface lipids in the stem (Jenks *et al.*, 1995). Only a few plant species accumulate big amounts of wax esters. The thick coating of waxes on the leaf surface of carnauba palm (*Copernicia cerifera*) contains up to 85% of wax esters, which are composed of C₃₀ - C₃₄ alcohols linked to C₁₆ - C₂₀ fatty acids (Taube, 1952). Jojoba (*S. Chinensis*) was discovered to accumulate wax esters in the seed embryos (Pollard *et al.*, 1979; Ohlrogge *et al.*, 1978). The liquid waxes extracted from jojoba seeds account for nearly half of the seed weight, and consist mainly of 20:1 (22%), 22:1 (21%) and 24:1 (4%) fatty alcohols linked to 18:1 (6%), 20:1 (35%) and 22:1 (7%) fatty acids (Miwa, 1971; Lassner *et al.*, 1999). Wax esters are also found in the cuticle surfaces of arthropods and insects (Chung and Carroll, 2015). Bee wax, secreted by the glands under the abdomen of bees, contains 35% - 80% of wax esters that consist of C₄₀ - C₄₆ molecular species (Tulloch, 1970). In animals, sebaceous glands secrete mostly nonpolar lipids composed of wax esters that are components of the sebum on the skin surface. Wool wax (lanolin) is rich in wax esters, containing up to 50% of total waxes (Truter, 1956). Wax esters are also accumulated in a variety of tissues of marine animals (Benson and Lee, 1972; Carlsson *et al.*, 2011). Spermaceti oil contains up to 76% of wax esters, which is composed of a range of saturated, monounsaturated and polyunsaturated fatty acids that are esterified with saturated and monounsaturated fatty alcohols. Oleyl - oleate (18:1/18:1) is the major component of spermaceti oil (Benson and Lee, 1972). Wax esters are also commonly synthesized in a diversity of microorganisms. *M. hydrocarbonoclasticus* synthesizes isoprenoid wax esters as a storage compound under nitrogen or phosphorous limiting conditions (Holtzapple and Schmidt-Dannert, 2007). *A. baylyi*

ADP1 accumulates neutral lipids as 10% - 20% of cellular dry weight, which are mainly composed of wax esters (Perez *et al.*, 2010).

1.2 Role of wax esters in nature

Wax esters fulfill a myriad of specialized functions in organisms. For instance, wax esters is a significant part of the cuticular layer of plant epidermal cells, helping plants against the diffusion of water and solutes (Fixter *et al.*, 1986; Miwa, 1971), as well as against UV radiation or attacks from pathogens and insects (Jetter and Kunst, 2008). Although, most of the eukaryotes and prokaryotes accumulate TAGs as storage lipids, wax esters are found to be the main energy storage compounds in some species of Gram-negative genus *Acinetobacter* (Kalscheuer *et al.*, 2007; Fixter *et al.*, 1986), in some marine hydrocarbonoclastic bacteria (Holtzapple and Schmidt-Dannert, 2007; Bryn *et al.*, 1977), as well as the seeds of jojoba (Ohlrogge *et al.*, 1978). Furthermore, wax esters are the constructional materials of the bee wax to build honeycombs, and serve to restrict movement of water across the cuticle of insects (Aichholz and Lorbeer, 2000). In birds and mammals, wax esters give a waterproof layer on feathers and fur, to prevent the skin from desiccation (Biester *et al.*, 2012), and help to regulate buoyancy in the spermaceti organ in the heads of sperm whales (Rowland and Domergue, 2012; Pond and Tarling, 2011).

1.3 Chemical and physical properties of wax esters

At the molecular level, straight-chain wax esters are composed of primary long-chain fatty alcohols and long-chain fatty acids in various combinations, including different chain lengths and a variety of desaturation degrees. Wax esters can cover a wide range of chemical and physical properties, due to the characters of the each esterified moiety. The melting temperature (T_m) of wax esters may range from below 0 °C to higher than 75 °C (Patel *et al.*, 2001). The main factor affecting T_m is the total chain length of wax esters. Short-chain wax esters are normally more stable and have lower melting temperatures. Taking the fully saturated wax esters as an example, the T_m of these wax esters is increased by 1 - 2 °C with every additional carbon atom (Patel *et al.*, 2001). Besides, the T_m of wax esters with the same number of carbon atoms can also be divers, if the ester bond is located at a different position. In detail, the T_m of "symmetric" wax esters is 1 - 5 °C higher than those with acid and alcohol moieties of different chain lengths (Patel *et al.*, 2001).

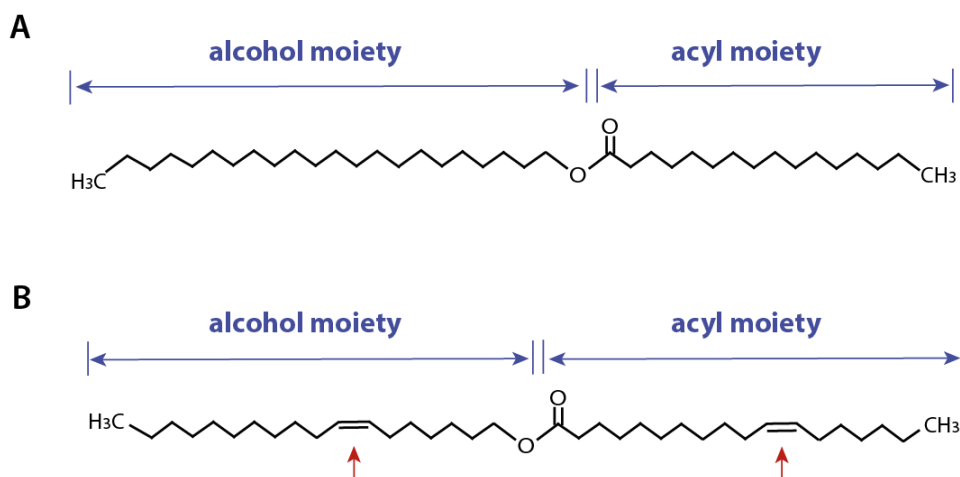


Figure 1.1 Chemical structures of wax esters. Wax esters can vary in chain length of acyl moiety and alcohol moiety (blue arrows), the grade of desaturation and the positions of double bonds of each moiety (red arrows). The name of a wax ester molecule is describe as fatty alcohol moiety/fatty acyl moiety. **(A)** Docosanyl - hexadecanoate (22:0/16:0). **(B)** Oleyl - oleate (18:1/18:1).

Furthermore, the desaturation types of wax esters also affect their chemical and physical properties. The wax esters containing saturated alcohol and acyl moieties melt at 38 - 73 °C. Saturated wax esters have a higher T_m and are more likely to be solid at room temperature, whilst unsaturated wax esters have a lower T_m and are more probably to be liquid oil at room temperature (<https://wikipedia.org>). Introduction of a double bond into either the alcohol or the acyl moiety of a wax ester molecule will decrease the T_m by ~ 30 °C (Patel *et al.*, 2001). The position of the double bond within a wax ester molecule is also important. For example, the T_m of octadecenyl - octadecanoate (18:1/18:0) is 27 °C, and thus 10 °C lower than that of octadecanoyl - octadecenoate (18:0/18:1), although they have the same chain length and unsaturation degree. Additionally, the degree of unsaturation also affect the oxidation stability of a wax ester molecule. In general, the oxidation rate increases with the number of double bond (Hagemann and Rothfus, 1979).

In summary, there are many different combinations of alcohol moiety and acyl moiety, and each combination will give a special set of characters to a wax ester molecule. The molecular species of wax esters have effects on their physical property, quality, and suitability for various industrial applications.

1.4 Industrial applications of wax esters

Wax esters display diverse commercial applications, due to their various chemical and physical properties. They are widely utilized in lubrication, production of candles, cosmetics, polishes, surface coatings and inks. For each application purpose, wax esters with specialized properties are applied. For example, the wax esters used as a desired lubricant should have a low T_m and high oxidation

stability. Hence, it is desirable to use the wax ester species that are composed of monounsaturated alcohols and acids with medium or long carbon chains. 18:1/18:1 is a popular lubricant due to its longevity and excellent performance (Heilmann *et al.*, 2012; Iven *et al.*, 2015).

The application of wax esters in daily life and industry started from the end of the 19th century, when the waxes derived from spermaceti oil were diffusely used as lubricants and lamp oils (Tower, 1907). The market of spermaceti waxes shrank at the beginning of the 20th century with the increasing popularity of mineral waxes. However, spermaceti waxes were later reused as an addition agent in high pressure industrial lubricants, resulting in the prosperity of the whaling industry in the 1960s. At that time, around 30 thousand of whales were hunted for commercial usage per year, leading to the extinction of sperm whales (Whitehead, 2009). Whale hunting has been banned by the Endangered Species Act (USA) from the 1980s to save the sperm whales from extinction (<https://iwc.int/commercial>).

Although wax esters are very common in nature, the abundance of wax esters for industrial applications is very limited, because only a few organisms can accumulate large amounts of wax esters. Since the forbidden of the whale hunting, a suitable replacement of spermaceti oil had not been available for a long time, until the natural wax esters from jojoba oil were found. Currently, the only natural resource of wax esters for commercial application is the slow-growing desert shrub jojoba. The jojoba plant is special for accumulating wax esters instead of TAGs as an energy storage compound in seeds. The oil content of jojoba seed accounts for 50% of seed dry weight, which consist of almost entirely wax esters (97%; Rowland and Domergue, 2012). These odorless waxes (C₃₈ - C₄₄) consist of a narrow mixture of straight-chain esters of primary long-chain fatty alcohols and long-chain fatty acids with only one double bond in each moiety (Bart, 2013; Miwa, 1971). Jojoba oil is relatively resistant to oxidation. Its melting temperature is relatively low (around 7 °C; Bassam, 1997). Jojoba oil is also recognized for its high thermal stability, high flash and fire points, and high viscosity index (Wisniak, 1987). So, jojoba oil stands out as a lubricant among various kinds of plant oils. However, the lubricant processed from jojoba oil is less favorable to be applied in cold condition (Lassner *et al.*, 1999). Jojoba oil is unique unsaturated oil and difficult to be synthesized chemically. Moreover, jojoba plant grows mainly in moderate temperate zones. The production of jojoba seeds is still limited, and not sufficient for the global requirement (Miwa, 1971). Therefore, jojoba oil is an expensive material. Currently, jojoba oil is mainly used for the production of high value products, and as an additive in cosmetics and medicines (Bart, 2013).

According to a recent report, the global lubricant market accounted for \$144.45 billion in 2015, and is estimated to reach \$162.3 billion by 2019 at an annual rate of 2.5% of growth (<http://www.marketsandmarkets.com/PressReleases/lubricant-additives.asp>). Nowadays, the lubricants derived from mineral oil are still the major type in lubricant market, due to the low cost and easy availability. However, natural wax esters perform comparably well to the wax esters from mineral

oil, because of their hydrolytic stability, oxidation stability as well as shear stability (Carlsson *et al.*, 2006). It is supposed that most of the common industrial lubricants could be replaced by bio-based lubricants with equivalent quality (Mang, 1998). Therefore, the production of plant-derived wax esters for lubrication probably has a huge economical potential. Furthermore, the utilization of bio-based wax esters would reduce the atmospheric and the water contaminations caused by the processing of fossil fuels. The utilization of bio-based lubricants to decrease environmental contaminations is a present tendency in the lubricant market (Nagendramma and Kaul, 2012). So, the utilization of natural wax esters in the field of lubrication is economically beneficial, sustainably developed and thus extremely prospective.

1.5 Enzymatic basis of wax ester biosynthesis

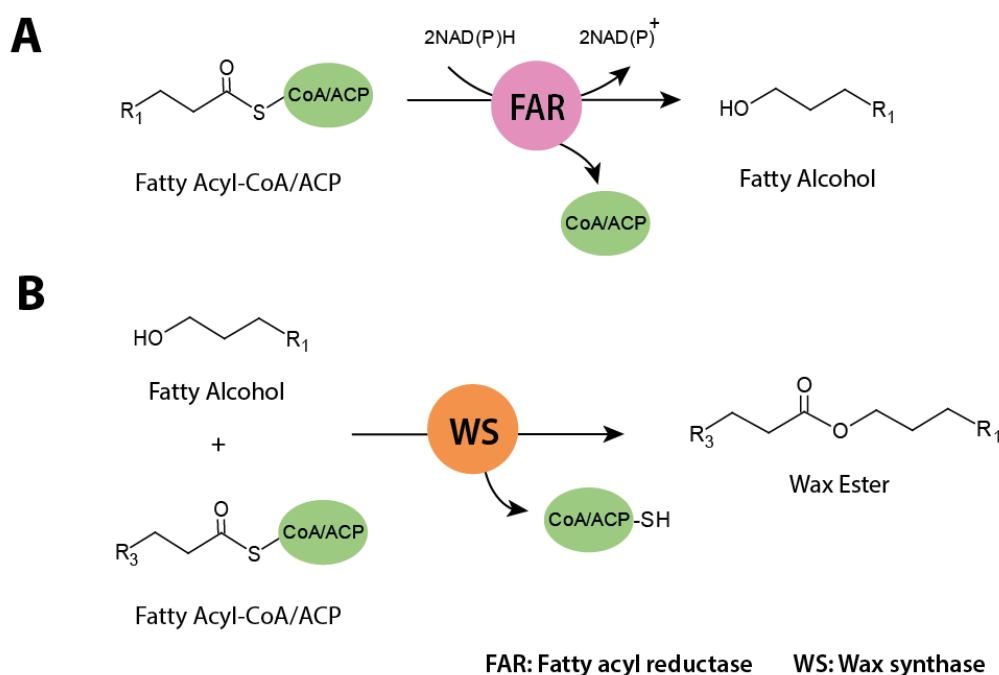


Figure 1.2 Two-step enzymatic reactions of wax ester synthesis. (A) Fatty acyl reductase catalyzes the NAD(P)H-dependent reduction of either fatty acyl-CoA or fatty acyl-ACP to the corresponding fatty alcohol and release free CoA or ACP. (B) Wax synthase catalyzes the esterification of a fatty alcohol molecule with a fatty acyl-ACP or a fatty acyl-CoA molecule to the corresponding wax ester, and releases free CoA-SH at the same moment. Abbreviations: ACP, acyl carrier protein; CoA, coenzyme A; FAR, fatty acyl reductase; WS, wax synthase. Figure is modified from Hofvander *et al.* (2011), Willis *et al.* (2011).

In general, the biosynthesis of wax esters is a two-step process involving two enzymes (Figure 1.2). The first reaction is catalyzed by a fatty acyl reductase (FAR), which reduce a fatty acyl-CoA or a fatty acyl-ACP molecule to the corresponding primary fatty alcohol molecule using NAD(P)H molecules as the reductant. The second enzymatic reaction is the esterification of a fatty acyl-CoA or a fatty acyl-

ACP molecule with a fatty alcohol molecule, and this reaction is catalyzed by a second enzyme called wax synthase (WS). The biosynthesis pathway of wax esters widely exist among various species of cells in both prokaryotes and eukaryotes. While, the subcellular localization of wax ester biosynthesis is distinct in different types of organisms. The identified FARs and WSs from various species of organisms also showed distinctive enzymatic characteristics.

The fatty acyl-ACP or fatty acyl-CoA is one of the two precursors for wax ester biosynthesis. They are the products of fatty acids esterified to acyl-ACPs in the case of plant plastids and prokaryotes, or esterified to acyl-CoAs in the case of eukaryotes. Fatty acids are produced by the process of long-chain fatty acid synthesis, which is highly conserved in both prokaryotes and eukaryotes with only few exceptions (Rottem, 1980). The fatty acids with C₁₆ - C₁₈ chain length are synthesized by a repeated cycle of condensation, reduction and dehydration reactions adding two carbon units to the elongating fatty acid chain (Haslam *et al.*, 2016; Bansal *et al.*, 2016; Li-Beisson *et al.*, 2013). These enzymatic reactions are catalyzed by the FASII in plants, prokaryotes as well as mitochondria (White *et al.*, 2005; Figure 1.3 A and B), and by the FASI in mammals and insects (White *et al.*, 2005; Figure 1.3 C and D).

In plants, the formation of fatty alcohols occurs in plastids or at the endoplasmic reticulum (ER), with regard to the localization of FARs. The final step of wax biosynthesis are localized at the ER or within the ER membrane (Figure 1.3 A). There are two main pathways for the wax biosynthesis in plant cells. An acyl reduction pathway produces primary alcohols and wax esters. An alkane forming pathway, results in the formation of secondary alcohols, aldehydes, alkanes as well as ketones. In plant epidermal cells, the generating waxes are then transported across the plasma membrane and cell walls, and finally arrive at the cuticle of leaves and stems (Li-Beisson *et al.*, 2013). In the embryo cells of jojoba seeds, the resulting wax esters are stored as energy compounds in lipid droplets (Ohlrogge *et al.*, 1978; Pollard *et al.*, 1979).

In most prokaryotes, such as *Acinetobacter*, the reduction reaction of a fatty acyl-CoA or a fatty acyl-ACP to a fatty alcohol molecule is thought to be catalyzed by two separate enzymes (Reiser and Somerville, 1997; Schirmer *et al.*, 2010; Figure 1.3B). Firstly, a fatty acyl-CoA or a fatty acyl-ACP molecule is reduced to a corresponding long-chain aldehyde by a NADPH dependent FAR, then, the resulting fatty aldehyde is further reduced to a fatty alcohol by an undiscovered enzyme called aldehyde reductase (FALDR; Alvarez, 2016). Differently, two FARs from *M. aqualeolei* VT8, *MaFAR1* (Maqu_2220) and *MaFAR2* (Maqu_2507), were found to directly catalyze a single step reduction of a fatty acyl-ACP or a fatty acyl-ACP molecule to a fatty alcohol molecule (Hofvander *et al.*, 2011; Willis *et al.*, 2011; Liu *et al.*, 2013). The fatty alcohols generated in bacteria are finally esterified with fatty acyl-CoAs or fatty acyl-ACPs in the cytosol by WSs or the bifunctional wax ester synthase/acyl-CoA: diacylglycerol acyltransferase (WS/DGAT) enzymes (Rude and Schirmer, 2009; Kalscheuer and Steinbüchel, 2003).

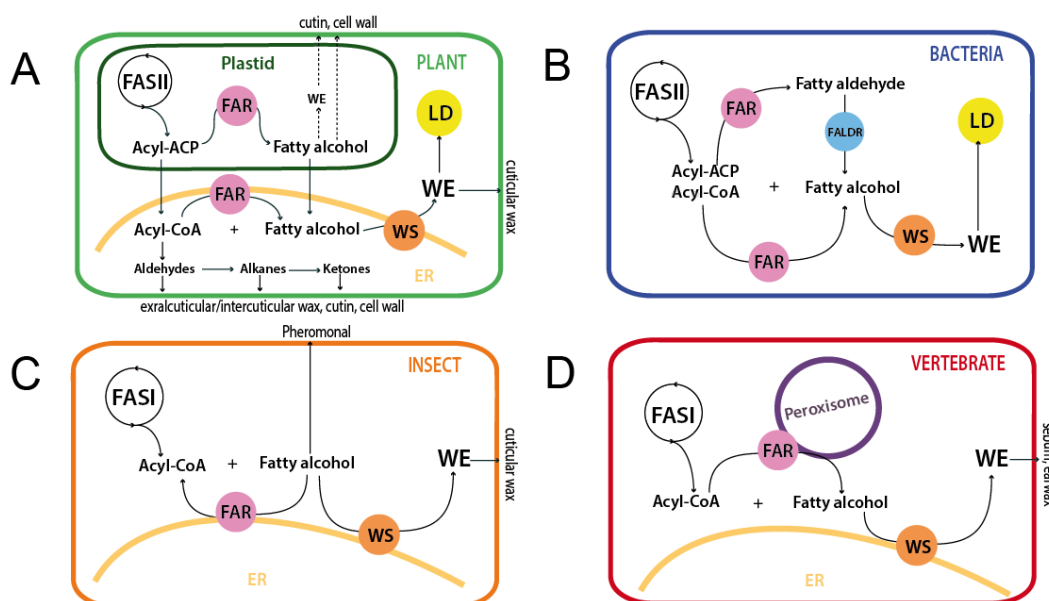


Figure 1.3 Hypothetical wax biosynthesis pathway in (A) plant, (B) bacteria, (C) insect and (D) vertebrate. Dashed lines show the hypothetical routes for plastid fatty alcohols, which might be also involved in the structure of cutin and cell wall. Abbreviations: ACP, acyl carrier protein; CoA, coenzyme A; ER, endoplasmic reticulum; FALDR, fatty aldehyde reductase; FAR, fatty acyl reductase; FASI, type I fatty acid synthesis complex; FASII, type II fatty acid synthesis complex; LD, lipid droplet; WE, wax ester; WS, wax synthase. Figure is modified from White *et al.* (2005), Li-Beisson *et al.* (2013), Kawelke (2014), Burdett *et al.* (1991), Jaspers *et al.* (2014), Liu *et al.* (2013) and Willis *et al.* (2011).

In insects, the biosynthesis pathway of wax esters is possibly localized at the ER membrane of specific types of cells (Figure 1.3C), such as pheromone gland cells. Because the identified FARs and WSs from insects were found to be localized to the ER (Jaspers *et al.*, 2014). In vertebrates, the reduction of fatty acyl-CoAs to primary fatty alcohols probably occurs in the peroxisomes, as the identified FARs from vertebrates such as the FARs from *Mus musculus* were reported to be localized to the peroxisome, while the esterification reaction to produce wax esters occurs at the ER (Burdett *et al.*, 1991; Cheng and Russell, 2004; Figure 1.3 D).

1.5.1 Fatty acyl reductases

The FARs reduce either a fatty acyl-CoA or a fatty acyl-ACP molecule to a corresponding fatty alcohol by using two molecules of NADPH or NADH as the co-substrate (Riendeau and Meighen, 1985). Evolutionarily related series of FARs are broadly distributed in all kingdoms. According to the phylogenetic analyses, FARs are divided into four main groups: plant-type, bacterial-type, insect-type and vertebrate-type (Figure 1.4).

The plant-type FARs are further divided into two sub-groups depending on their subcellular localizations and substrate specificities. Most of the plant-type FARs are the ER-localized enzymes, predicted to contain two C-terminal transmembrane domains, and use fatty acyl-CoAs as substrates (Metz *et al.*, 2000; Schwacke *et al.*, 2003). Several FARs from *A. thaliana* (AtFAR1, 4, 5, 7, 8) and the FAR from jojoba seeds (ScFAR) belong to this subgroup. The cuticle-associated enzyme from *A. thaliana* (AtFAR3) also belong to the ER-localized sub-group, while its sequence was predicted to contain an N-terminal transmembrane domain (Rowland *et al.*, 2006). Interestingly, a FAR from *M. aqualeolei* (MaFAR1, Maqu_2220) also belongs to the plant type group, catalyzing the four electron reduction of a fatty acyl-CoA or a fatty acyl-ACP directly to a fatty alcohol molecule (Hofvander *et al.*, 2011), although it is a cytosolic enzyme originated from bacteria. A few plant-type FARs, including AtFAR2 and AtFAR6, have been identified to be plastid-localized enzymes that utilize fatty acyl-ACPs as substrates (Chen *et al.*, 2000; Doan *et al.*, 2011; Shi *et al.*, 2011). These plastidial isoforms of FARs were predicted not to contain any transmembrane domain and to represent putatively soluble enzymes.

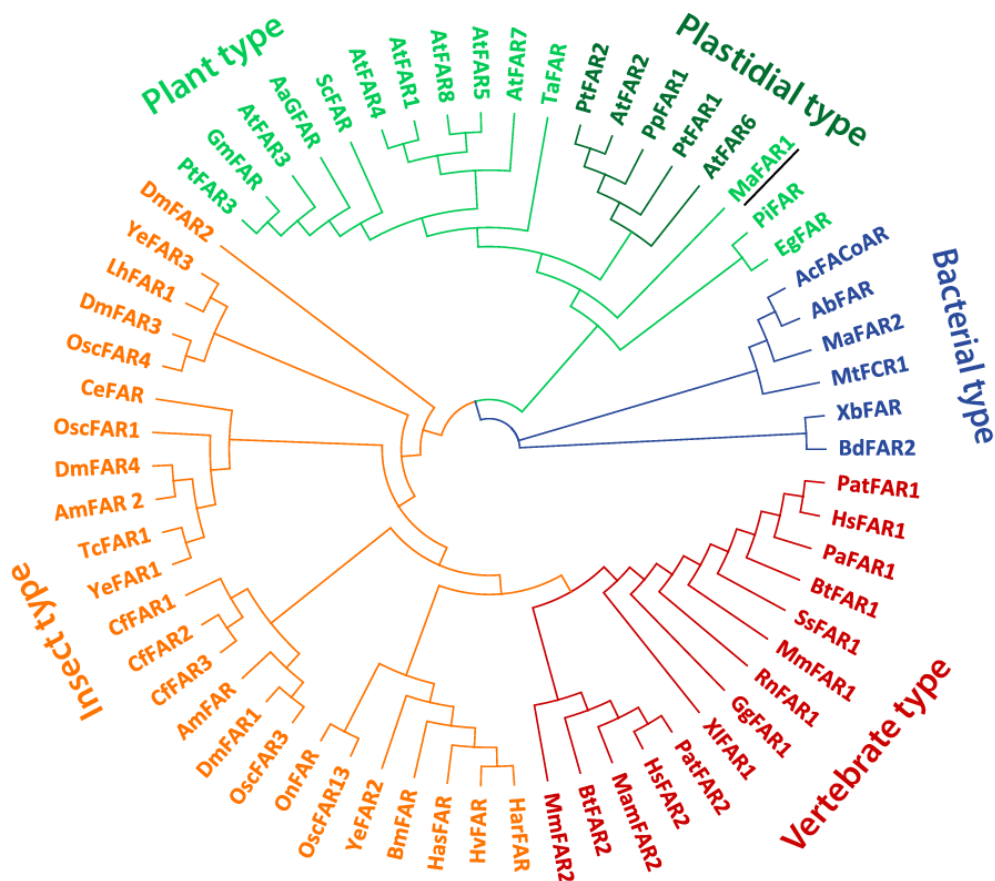


Figure 1.4 Phylogenetic tree showing relationships among different types of fatty acyl reductases. UniProt IDs or GenenBank IDs are listed behind respective enzyme abbreviations. FAR, fatty acyl reductase; Ab, *Acinetobacter baylyi*; Ac, *Acinetobacter calcoaceticus*; Am, *Apis mellifera*; At, *A. thaliana*; Bm, *Bombyx mori*; Bt, *Bos Taurus*; Ce, *Caenorhabditis elegans*; Cf, *Calanus finmarchicus*; Dm, *Drosophila melanogaster*; Gg, *Gallus gallus*; Har, *Helicoverpa armigera*; Has, *Helicoverpa assulta*; Hs, *Homo sapiens*; Hv, *Heliothis virescens*; Lh, *Lygus hesprus*; Ma,

M. aqueolei; Mam, *Macaca mulatta*; Mm, *Mus musculus*; Mt, *Mycobacteria tuberculosis*; On, *Ostrinia nubilalis*; Osc, *Ostrinia scapularis*; Pa, *Pongo abelii*; Pat, *Pan troglodytes*; Pi, *Phytophthora infestans*; Pt, *Populus trichocarpa*; Rn, *Rattus norvegicus*; Sc, *Simmondsia chinensis*; Suc, *Sus ccrofa*; Ta, *Triticum aestivum*; Tc, *Tribolium castaneum*; Xl, *Xenopus laevis*; Ye, *Yponomeuta evonymella*; Xb, *Xenorhabdus bovienin*. AaGFAR : E9KL86, AbFAR : Q6F7B8, AcFACoAR : D0S4I2, AmFAR : D9MX52, AtFAR1 : Q39152, AtFAR2 : Q08891, AtFAR3 : Q93ZB9, AtFAR4 : Q9LXN3, AtFAR5 : Q0WRB0, AtFAR6 : B9TSP7, AtFAR7 : Q9FMQ9, AtFAR8 : Q1PEI6, BdFAR2 : I1H9P9, BmFAR : Q7YTA9, BtFAR2 : Q0P5J1, CeFAR : Q9TZL9, CfFAR1 : G3KIJ8, CfFAR2 : G3KIJ9, CfFAR3 : G3KIK0, DmFAR4 : Q8MS59, DmFAR2 : Q960W6, DmFAR3 : A1ZAI3, DmFAR4 : A1ZAI5, EgFAR : D7PN08, GgFAR1 : Q5ZM72, GmFAR : I1M4E4, HarFAR : I3PN86, HasFAR : I3PN85, HsFAR1 : Q8WVX9, HsFAR2 : Q96K12, HvFAR : D2SNU9, LhFAR1: A0A0A9XVU3, MaFAR1 : A1U2T0, MaFAR12 : A1U3L3, MamFAR: F7AH86, MmFAR1 : Q922J9, MmFAR2 : Q7TNT2, MtFCR1 : O50417, OscFAR13 : B6SDC3, OnFAR: D3U9W3, OsFAR1 : Q0IZI9, OsFAR3 : Q7XRZ6, OsFAR4 : Q6ZJ06, PaFAR1 : Q5R834, PatFAR1: H2R2T3, PatFAR2: H2Q5N6, Pi: D0NE51, PpFAR1 : A9RVF6, PtFAR1 : B9IHM0, PtFAR2 : B9IID5, PtFAR3 : B9H1Z2, PtFAR3-1 : B9H1F3, RnFAR1 : Q66H50, ScFAR1 : Q9XGY7, SucFAR1 : G8ENM4, TaFAR9 : Q8L4C3, TcFAR1 : D2A5A7, XIFAR1 : Q7ZXF5, YeFAR1 : D7P5E2, YeFAR2 : D7P5E3, YeFAR3 : D7P5E4, XbFAR : D3UWE4. Sequence multiple alignment and the construction of phylogenetic tree was performed by Geneious 7.0 with the MUSCLE Alignment method in the default settings. Underlined FARs were studied in this work.

Many genes encoding putative FARs were found in diverse species of insects. The FAR from *Drosophila melanogaster* (*DmFAR1*) was reported to be important for the gas filling of the tracheal tubes during *Drosophila* embryogenesis, and it is localized to the ER when expressed in *Drosophila* S2 cells (Jaspers *et al.*, 2014). The vertebrate-type and insect-type FARs were poorly studied compared with the plant-type FARs. Only two vertebrate-type FARs from *Mus musculus* (*MmFAR1* and *MmFAR2*) were relatively well studied. *MmFAR1* utilizes saturated and unsaturated substrates of C₁₆ - C₁₈ chain length, while *MmFAR2* prefers saturated substrates with the same chain length. Both enzymes were shown to be localized to the peroxisomal membrane with two predicted transmembrane domains at the C-terminus (Burdett *et al.*, 1991; Heilmann *et al.*, 2012). Several bacterial-type FARs were already identified, including the ones from *A. calcoaceticus* and *M. aqualeolei* VT8. The sequence of bacterial-type FARs were reported not to contain any predicted transmembrane domain, and thus were most likely to be soluble enzymes. However, when some of these enzymes were expressed in *E. coli* for protein purification, they were not as soluble as expected (Willis *et al.*, 2011; Hofvander *et al.*, 2011).

All FARs are members of the extended short chain dehydrogenase/reductase (SDR) family, sharing a NAD(P)H-binding Rossmann-fold domain (Kallberg *et al.*, 2010; Rowland *et al.*, 2012). A conserved GXXGXX(G/A) motif exists in the Rossmann-fold domain and is possibly a NAD(P)H-binding site. There is also a conserved YXXXK motif in the Rossmann-fold domain, which is believed to be the catalytic motif of the SDR family enzymes.

The plant-type, insect-type and vertebrate-type FARs are around 450-500 amino acids in length, and contain a fatty acyl reductase (FAR_C) domain except for the Rossmann-fold domain. The FAR_C domain was originally named as 'male sterile', because the first cloned FAR gene was found to encode

MALE STERILITY2 from *A. thaliana* (Aarts *et al.*, 1993). The plastidial isoforms enzymes of the plant-type FARs also contain an N-terminal extension as long as 50 - 120 amino acids (Figure 1.5 A).

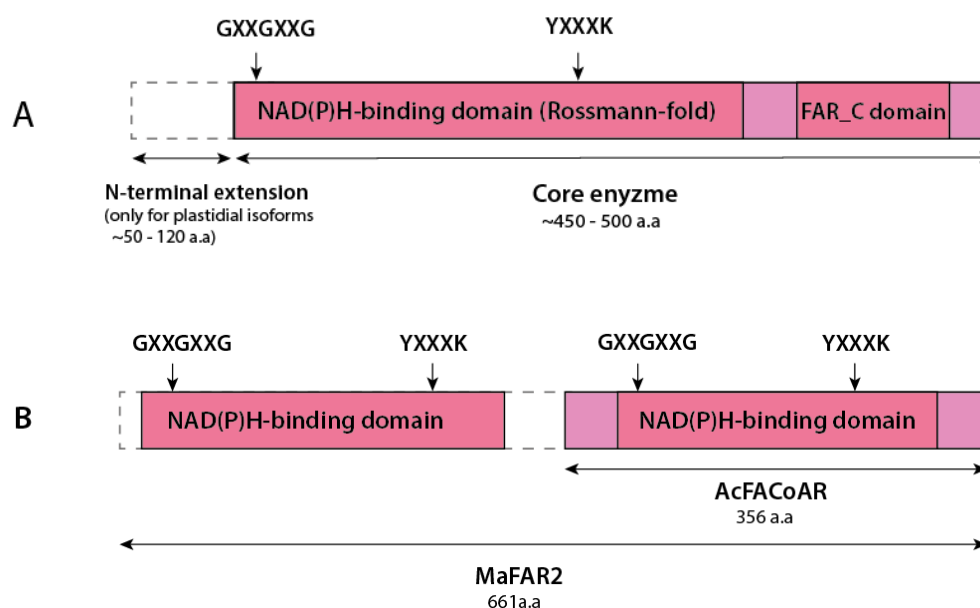


Figure 1.5 Domain structure of fatty acyl reductase. (A) Plant-type, insect-type and vertebrate-type FARs. Dash lines indicate an N-terminal extension that is only found in the plastidial isoforms of plant-type FARs. The approximate positions of the GXXGXX(G/A) as NAD(P)H binding motif and the catalytic YXXXX motif are indicated with black arrow. The FAR_C domain in C-terminal of the enzyme was ever called male sterility domain, because some of FARs cause male sterility upon gene disruption. **(B)** Bacterial-type FARs. The structural domain of a fatty acyl-CoA reductase from *A. calcoaceticus* (AcFACoAR) is shown as a model of most of bacterial-type FARs, reducing fatty acyl-CoAs/ACPs to fatty aldehydes. MaFAR2 from *M. aquaeolei* VT8 is a special bacterial-type FAR catalyzing the four electron reduction of a fatty acyl-CoA/ACP to a fatty alcohol by a two-step reaction. MaFAR2 contains two NAD(P)H binding domains and two catalytic YXXXX motifs. Figure is modified from Aarts *et al.* (1993), Willis *et al.* (2011), Rowland and Domergue (2012) and Kawelke (2014).

The bacterial-type FARs are normally shorter than the other three types of FARs, containing around 350 amino acids. Most of the bacterial-type FARs can only catalyze the reduction of a fatty acyl-CoA or a fatty acyl-ACP to a fatty aldehyde molecule, and do not contain the FAR_C domain found in the other three groups of FARs (Figure 1.5B). However, a FAR from *M. aquaeolei* VT8 (MaFAR2, Maqu_2507) is special, as it catalyzes the four electron reduction of a fatty acyl-CoA or a fatty acyl-ACP to a fatty alcohol by a two-step reaction (Willis *et al.*, 2011; Guo *et al.*, 2015). Its C-terminal domain shares similarity to the majority of fatty acyl-CoA reductase from *A. calcoaceticus* (AcFACoAR), and reduces fatty acyl-CoAs to the fatty aldehydes. Its N-terminal domain is distinctive from AcFACoAR, and catalyzes the reduction of the fatty aldehydes further to the fatty alcohols (Willis *et al.*, 2011; Figure 1.5 B).

Different types of FARs have diverse substrate specificities, in regard to the chain length and the unsaturation degree of acyl chain. The *AtFAR5* and *AtFAR8* from *A. thaliana* showed a relatively narrow substrate specificity, mainly using 18:0-CoA and 16:0-CoA upon heterologous expression in yeast (Chacon *et al.*, 2013). In contrast, the FARs from bacteria were reported to utilize a wide range of fatty acyl-CoAs/ACPs as substrates (Hofvander *et al.*, 2011; Willis *et al.*, 2011). Moreover, the same FAR might show different substrate specificities with the high dependency on the fatty acyl substrate pools in different hosts. For example, the FAR from jojoba seed (*ScFAR*) shows the highest activities to 16:0-CoA and 18:0-CoA in an *in vitro* assay (Miklaszewska and Banas, 2016). While, high levels of C_{20:1} and C_{22:1} fatty alcohols were detected in the native wax esters of jojoba seeds (Lardizabal *et al.*, 2000). The domain structures or amino acid residues that affect the substrate specificities of FARs have not been well studied. Only two amino acid residues were identified as the key residues determining the substrate chain length specificities in *AtFAR5* and *AtFAR8* (Chacon *et al.*, 2013).

1.5.2 Wax synthases

WSs belong to the family of acyltransferases that catalyze the esterification of an activated acyl moiety with an acyl acceptor. WSs catalyze the esterification of fatty acyl-CoAs/ACPs with fatty alcohols yielding wax esters; however, acyl-CoA: diacylglycerol acyltransferases (DGATs), another member of acyltransferases, catalyzes the condensation of fatty acyl-CoAs with diacylglycerols (DAGs) yielding TAGs. With the increasing numbers of WSs were discovered and analyzed, it was found that a part of WSs also exhibit DGAT activity, thus acting as bifunctional enzymes, such as the *WSD1* from *A. thaliana* and many WSs from bacteria (Li *et al.*, 2008; Villa *et al.*, 2013). At the same time, it has been reported that a number of DGATs are also able to catalyze the biosynthesis of wax esters (Du *et al.*, 2014). According to the phylogenetic analyses of WS sequences, WSs are divided into three groups found in many organisms, including higher plants, vertebrate and bacteria. These three groups of WSs are no homologous to each other (Figure 1.6).

The first group of WSs are widely found in higher plants, fungi and yeast. These WSs have no obvious sequence similarity, but share an origin with DGAT1 enzymes. Therefore, they are called as DGAT1/plant-type WSs. A respective DGAT1/ plant-type WS consists of about 350 residues, and contains multiple (normally 6 - 8) predicted transmembrane domains, so that are localized to the ER membrane. A histidine residue in one of the transmembrane domains of the WS is the potential catalytic site of the enzyme (Figure 1.7 A).

To date, the knowledge about DGAT1/plant-type WSs is still very limited. The first identified WS belonging to this group is from the embryo of jojoba seed (Wu *et al.*, 1981). The wax synthase from jojoba embryos (*ScWS*) is predicted to have seven transmembrane domains, with three transmembrane domains at the direct N-terminus, two located in the middle, and the last two

encoded at the C-terminus of its sequence (Figure 1.7 A). In the *in vitro* assays, ScWS showed significant activity with a wide range of saturated and monounsaturated acyl-CoAs with a chain length from C₁₄ to C₂₄, with C_{20:1} acyl-CoA as the most favorite substrate; and it showed the highest activity towards C_{18:1} and C_{18:2} fatty alcohols (Lardizabal *et al.*, 2000). The second characterized enzyme of the DGAT1/plant-type family is the WS from *Euglena gracilis* (EgWS). EgWS is predicted to have seven transmembrane domains. However, unlike ScWS using very long-chain substrates, EgWS was reported to utilize shorter chain substrates (C₁₂ - C₁₆), with myristic acid being the most favored acyl substrate and palmitic alcohol as the most favored alcohol substrates (Teerawanichpan and Qiu, 2010).

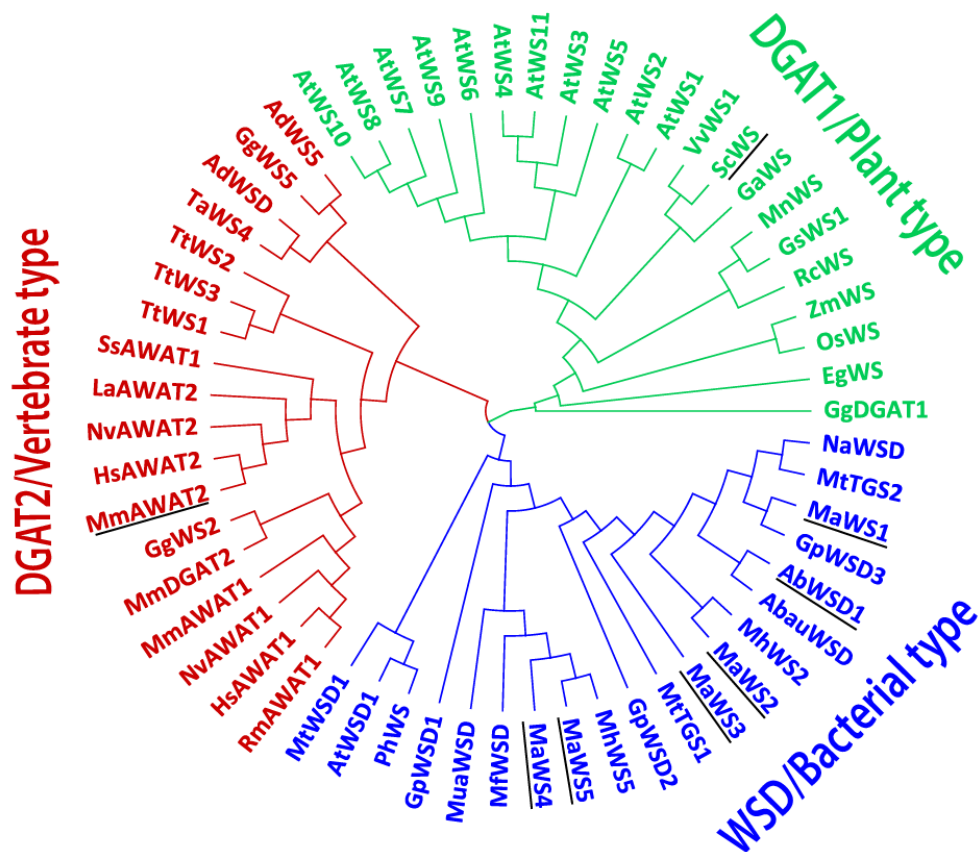


Figure 1.6 Phylogenetic tree showing relationships among different types of wax synthases. UniProt IDs or GeneBank IDs are listed behind the respective enzyme abbreviations. AWAT : acyl-CoA wax alcohol acyltransferase, WS : wax synthase, WSD : bifunctional wax synthase/diacylglycerol O-acyltransferase, Ab, *Acinetobacter baylyi*; Abau, *Acinetobacter baumannii*; Ac, *Acinetobacter calcoaceticus*; Ad, *Anser anser domesticus*; Ar, *Acinetobacter radioresistens*; At, *A. thaliana thaliana*; Eg, *Euglena gracilis*; Ga, *Genlisea aurea*; Gg, *Gallus gallus*; Gs, *Glycine Soja*; Gp, *Gordonia polyisoprenivorans*; Hs, *Homo sapiens*; La, *Loxodonta African*; Ma, *M. VT8*; Mf, *Myxococcus fulvus*; Mh, *M. hydrocarbonoclasticus*; Mm, *Mus musculus*; Mm, *Morus notabilis*; Mt, *Medicago truncatula*; MtTGS1, *Mycobacteria tuberculosis*; MtWSD1, *Medicago truncatula*; Mua, *Mucor ambiguous*; Na, *Nocardia asteroides*; Nv, *Neovison vison*; Os, *Oryza sativa*; Ph, *Petunia hybrid*; Rm, *Macaca mulatta*; Sc, *Simmondsia chinensis*; Ss, *Sus scrofa*; Ta, *Tyoto alba*; Tt, *Tetrahymena thermophile*; Vv, *Vitis vinifera*; Zm, *Zea mays*. AbauWSD : D0CDL4, AbWSD1 : Q8GGG1, AdWSD : H6W8E5, AcWSD : N8N9S3, AdWS5 : H6W8E9, ArWSD : K6VXX4, AtWS1 : Q9FJ72, AtWS2 : Q9FJ73, AtWS3 : Q9FJ74, AtWS4 : Q9FJ75, AtWS5 : Q9FJ76, AtWS6 : 9FJ77,

AtWS7 : Q9FJ78, AtWS8 : Q9LNL1, AtWS9 : Q4PT07, AtWS10 : Q3ED15, AtWS11 : , AtWSD1 : Q93ZR6, EgWS : D7PN09, GaWS:S8CGW7, GgDGAT1: E1BTG6, GgWS2 : H6W8E6, GgWS5 : Q5ZJD8, GsWS: A0A0B2RKV5, GpWSD1 : 6MTQ1, GpWSD2 : H6MS36, GpWSD3 : H6MYJ4, HsAWAT1 : Q58HT5, HsAWAT2 : Q6E213, LaAWAT2 : 3T8K5, MaWS1: ABM17275, MaWS2:ABM20141, MaWS3: ABM17947, MaWS4:ABM20442, MaWS5: ABM20482, MfWSD: A0A0F7DYG7, MhWS2 : A3RE51, MmAWAT1 : A2ADU9, MmAWAT2 : Q6E1M8, MmDGAT2 : Q9DCV3, MnWS:W9QUP2, MtTGS1 : P9WKC9, MtTGS2: P9WKC7, MtWSD1 : G7JTU6, MuaWSD: A0A0C9N7W4, NaWSD : 5E762, NvAWAT1 : U6DU75, NvAWAT2 : U6CZ66, OsWS : Q6K7A7, PhWS : A3QME3, RmAWAT1 : F6SLT8, ScWS : 9XGY6, SsAWAT2 : K7GQC2, TaWS4 : H6W8E7, TaWS5 : H6W8E8, TtWS1 : I7MN05, TtWS2 : Q24DK3, TtWS3 : Q22SB3, VvWS : Q84XY9, ZmWS : K7TU84. Sequence multiple alignment and construction of phylogenetic tree was performed by Geneious 7.0 with MUSCLE Alignment method in the default settings. Underlined WSs were studied in this work.

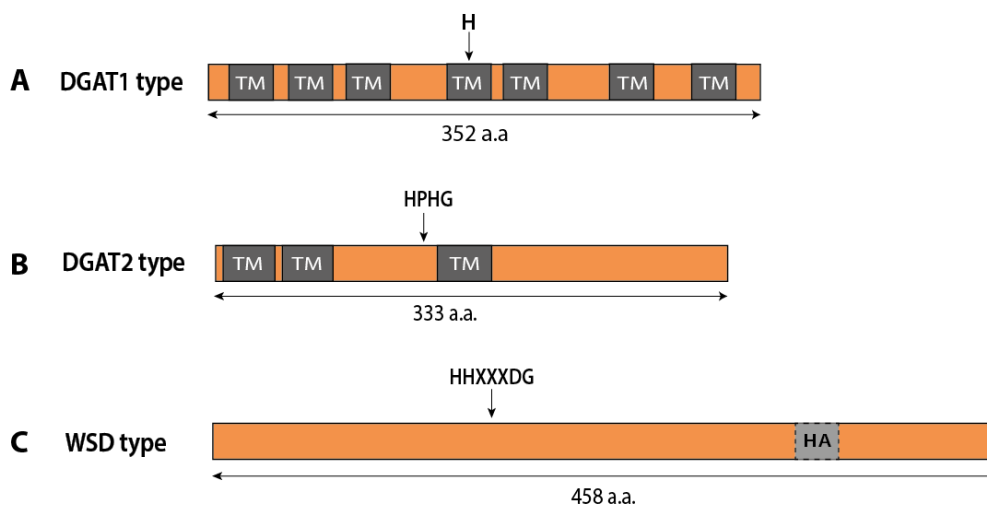


Figure 1.7 Domain structure of three types of wax synthases. (A) DGAT1/plant-type WSs are mostly found in higher plants and localized to the ER. A respective enzyme normally contains 6-8 predicted transmembrane domains. A histidine residue in one of the transmembrane domain of the enzyme is indicated with a black arrow as possible active site. The structure domain of a WS from jojoba seed (*ScWS*) was shown as a model of DGAT1/plant-type WSs. **(B)** DGAT2/vertebrate-type WSs contain 2-3 predicted transmembrane domains and localized to the ER. A highly conserved HPHG motif between the second and the third transmembrane domain is the anticipated active site of the enzyme. The structure domain of a WS from *Mus musculus* (*MmAWAT2*) was shown as a model of DGAT2/vertebrate-type WSs. **(C)** Bifunctional wax synthase/diacylglycerol O-acyltransferase (WSD) type enzymes show both WS and DGAT activity. They are mostly from bacteria and predicted to be soluble, while some of them contain hydrophobic areas in the sequence and might associate with membranes. The highly conserved HHXXXDG motif could be a potential active site of the enzyme. The structure domain of a WS from *A. baylyi* ADP1 (*AbWSD1*) was shown as a model of WSD/bacterial-type WSs. Figure is modified from Kawelke (2014).

The DGAT2/vertebrate-type WSs are commonly found in mammals, and cluster with the sequence of DGAT2 family. The enzymes belonging to DGAT2/vertebrate-type are smaller than those of DGAT1/plant-type, with approximately 320 residues on average. The DGAT2/vertebrate-type WSs as well as DGAT2s are predicted to contain one to three transmembrane domains. For example, the

mouse WS (*MmAWAT2*) has three predicted transmembrane domains, two of them are located at the N-terminus and are separated by a short stretch of 4 - 5 amino acids, and the third one is located in the middle of its sequence. A highly conserved HPHG motif between the second and the third transmembrane domain is possibly the active motif of this enzyme (Figure 1.7 B). *MmAWAT2* was reported to have high activities to the fatty acyl-CoAs with C₁₂ - C₁₆ carbons, and prefer to utilize unsaturated long-chain alcohols (C₁₈ - C₂₂) than the saturated ones (Miklaszewska *et al.*, 2013).

The third family of WSs are mostly found in bacteria, and completely unrelated to the other two groups. A lot of WSD/bacterial-type WSs were found to have a bifunctional WS/DGAT activity, producing both wax esters and TAGs (Holtzapple and Schmidt-Dannert, 2007; Kalscheuer and Steinbüchel, 2003; Röttig and Steinbüchel, 2013). A typical WSD/bacterial-type WS consists of 450 - 500 amino acids on average, containing a highly conserved HHXXXDG motif that is assumed to be the catalytic motif of the enzyme (Figure 1.7 C). The WSD/bacterial-type WSs are normally predicted to contain no transmembrane domains in their sequences. While, some WSD/bacterial-type WSs seem to contain hydrophobic stretches, which allow the enzymes to be partly located in cytosol whilst partly associated with membranes or lipid inclusions. There is also a speculation that the activities and substrate specificities of WSD/bacterial-type WSs could be affected by whether they are exposed to a hydrophobic (membrane associated) or a hydrophilic (cytosolic) environment (Wältermann *et al.*, 2005; Stöveken *et al.*, 2005).

Only a few WSD/bacterial-type WSs were studied. The first identified WSD/bacterial-type WS is the *AbWSD1* from *A. baylyi* ADP1, which is regarded as a bacterial model enzyme for wax ester and TAG biosynthesis (Kalscheuer and Steinbüchel, 2003). In an *in vitro* assay, *AbWSD1* equally accepted a broad range of fatty acyl-CoAs and fatty alcohols for wax ester synthesis, whilst showed preference to C_{16:1} and C_{18:1} alcohols (Stöveken *et al.*, 2005; Kalscheuer and Steinbüchel, 2003). A number of WS/DGAT enzymes in prokaryotes were found since the characterization of *AbWSD1*. Two enzymes from *M. aquaeolei* VT8 (*MaWS1* and *MaWS2*) were identified belong to the WSD/bacterial-type (Holtzapple and Schmidt-Dannert, 2007; Figure 1.6). One WS from *A. thaliana* (*AtWSD1*) and one WS from the *Petunia* hybrid (*PhWS1*) were identified to be WS/DGAT enzymes (Li *et al.*, 2008; King *et al.*, 2007). Additionally, WS/DGAT-like enzymes seem to be widely distributed in other eukaryotes organisms, including wheat, soybean and several animals (Röttig and Steinbüchel, 2013; Li *et al.*, 2008).

The general catalytic mechanism of WSs starts with the histidine residues in the conserved catalytic motif (Figure 1.8; Röttig and Steinbüchel, 2013). The importance of histidine residues in the conserved HHXXXDG motif of the WSD/bacterial-type WSs has been indicated by measuring the enzymatic activities of single amino acid mutants. The activity of *AbWSD1* decreased significantly, if the second histidine residue (His 133) of its HHXXXDG motif was replaced by leucine (Stöveken *et al.*, 2009). Similarly, for the *MaWS2* from *M. aquaeolei* VT8, the alanine mutant of the second histidine (His 141) was poorly active *in vitro* (Villa *et al.*, 2014). Comparatively, the catalytic mechanisms of DGAT1/plant-

type and DGAT2/vertebrate-type WSs are even less studied, since these enzymes are ER membrane-associated, and are therefore difficult to be purified.

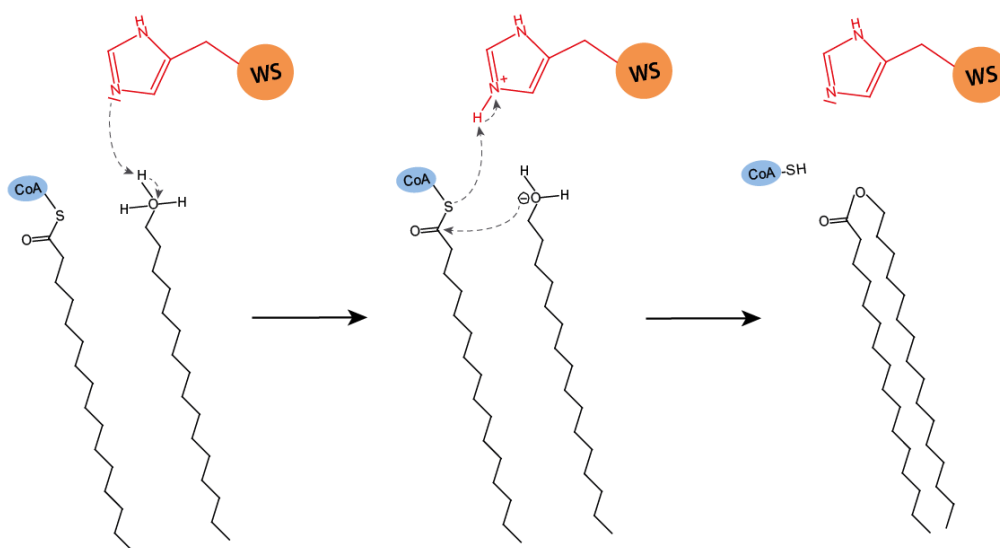


Figure 1.8 Proposed catalytic mechanism of wax synthases. A catalytic histidine residue of the active motif (H for DGAT1/plant-type WS, HPHG for DGAT2/vertebrate-type, HHXXXDG for WSD/bacterial-type) acts as a base, and abstracts a proton from the hydroxyl group of a fatty alcohol molecule. The resulting oxyanion acts as a nucleophile and attacks the thioester bond of a fatty acyl-CoA molecule, resulting in a cleavage of the thioester bond, and the formation of a new oxoester bond between the acyl chain and the fatty alcohol anion. The cleaved CoA-S molecule is protonated by the catalytic histidine residue of the protein, thereby restoring the initial situation of the enzyme. Figure is modified from Röttig and Steinbüchel (2013).

The WSs can naturally accept a broad range of substrates, such as straight-chain acyl groups with chain length from C₈ to C₂₂ and primary alcohols with chain length from C₁₂ to C₂₄ (Barney *et al.*, 2012; Shi *et al.*, 2012; Miklaszewska and Banas, 2016). Even though there is an increasing interest in utilizing WSs to produce a range of industrial compounds, only a few studies focused on identifying the potential structure domains or amino residues responsible for the substrates specificities of WSs. It was reported that the first two transmembrane domains of *MmAWAT2* are important for the specificity of this enzyme to the acyl chain length (Kawelke and Feussner, 2015). The replacement of alanine 360 residue of *MaWS1* or glycine 355 residue of *AbWSD1* to a bigger amino residue (isoleucine) improved the binding of small fatty alcohol substrates (C₈ and C₁₀) to the active site, while the accessibility of larger fatty alcohols (C₁₂ - C₁₈) was not blocked (Barney *et al.*, 2013).

1.6 Heterologous synthesis of wax esters

The diversity of identified FARs and WSs offers valuable biotechnological tools to produce tailored wax esters upon heterologous expression systems. The jojoba wax synthase (*ScWS*) was ever co-expressed

with jojoba FAR (ScFAR) in the seeds of *A. thaliana*. The resulting wax esters accounted for 49% of total seed oil in the transgenic plants (Kathryn *et al.*, 2000). Later, the most commonly used platform for producing wax esters changed to microorganisms. Jojoba oil-like wax esters were synthesized in *E. coli* by heterologous co-expression of jojoba FAR with the bifunctional *AbWSD1* from *A. baylyi* ADP1. The resulting yield of wax esters was up to 1% of the cellular dry weight, predominantly consisting of palmitoyl – oleate (16:0/18:1) and 18:1/18:1 (Kalsheuer *et al.*, 2006). Expression of *AbWSD1* in a quadruple mutant strain *S. cerevisiae* H1246 and feeding yeast cells with long-chain fatty alcohols also resulted in the accumulation of wax esters (Kalsheuer *et al.*, 2004). In recent years, plants have been suggested as a platform for production of valuable oil. Transient expression of a chloroplasts-directed FAR from *M. aquaeolei* VT8 together with the *AtPES2* in leaf tissue of *N. benthamina* led to the accumulation of wax esters up to 1.6 nmol mg⁻¹ FW (Aslan *et al.*, 2014). When different combinations of FARs with WSs were stably expressed in *A. thaliana* under a seed-specific promoter, 5 - 100 mg g⁻¹ wax esters were produced in seeds of the transgenic lines (Iven *et al.*, 2015; Heilmann *et al.*, 2012). Although the formation of wax esters was successfully established in heterologous hosts by expression of wax forming enzymes, the amounts of accumulated wax esters were still not sufficient for industrial applications.

1.7 Biosynthesis of neutral lipids in plants

Lipids play many important functions in living organisms. The lipids can broadly be divided into two groups: polar lipids, including phospholipids and glycolipids; neutral lipids (non-polar lipids), such as acylglycerols, steryl esters and wax esters. In plants, polar lipids make up the major constituent of cell membrane and organelles, and operate as the signal molecules in anti-biotic and anti-abiotic pathways. Neutral lipids, particularly TAGs, serve as intracellular storage molecules for free fatty acids and DAGs. TAGs are involved in the catabolism for energy production required by cells. Wax esters are uncommon storage compounds, but more often provide a hydrophobic coating of tissue, protecting against water loss and pathogen attacks. The abilities for biosynthesis pathways of neutral lipids are abroad distributed in different species of plants. The biosynthesis of neutral lipids starts from the synthesis of fatty acids happen in plastids, and is closely related to the fatty acyl editing pathway.

1.7.1 Fatty acid synthesis, elongation and desaturation

Briefly, plant *de novo* fatty acid biosynthesis occurs in the plastid instead of in the cytosol as in other eukaryotes. In plant plastids, the fatty acyl-CoAs up to C₁₈ chain length are made, and these fatty acyl-CoA are later transported to the ER for further editing or for TAG formation (Figure 1.9 and Figure 1.10). The fatty acid biosynthesis starts from the formation of malonyl-CoA from acetyl-CoA catalyzed

by the acetyl-CoA carboxylase (ACC; Konishi *et al.*, 1996). Then, the production of C₁₈ fatty acyl-ACP are catalyzed by monofunctional enzymes forming the type II fatty acid synthase complex (FASII; Brown *et al.*, 2006). Two-carbon units are added to the elongating fatty acid chain in four consecutive steps: (1) the condensation of C₂ moiety from acetyl-CoA to form malonyl-CoA; (2) the reduction of beta-ketoacyl-ACP; (3) the dehydration of beta-hydroxyacyl-ACP; (4) the reduction of enoyl-ACP. Ketoacyl-ACP synthase III (KASIII) catalyze the initial condensation reaction of malonyl-ACP and acetyl-CoA, yielding C₄ product (3-ketobutyryl-ACP). The subsequent condensations of 3-ketobutyryl-ACP to palmitoyl-ACP (16:0-ACP) need the second enzyme named as KASI (Li-Bession *et al.*, 2013). The final elongation of palmitoyl-ACP to stearoyl-ACP (18:0-ACP) is catalyzed by a ketoacyl-ACP synthase II (KASII; Pidkowich *et al.*, 2007; Kunst *et al.*, 2008). Afterwards, stearoyl-ACP (18:0-ACP) is efficiently desaturated to oleatoyl-ACP (18:1-ACP) by a stromal stearoyl-ACP desaturase (SAD; Yao *et al.*, 2003). Long-chain acyl groups (16:0-ACP and 18:1-ACP) then either enter the eukaryotes glycerolipid pathway or are further hydrolyzed by the acyl-ACP thioesterase (Fata/B) to release free fatty acids (Salas and Ohlrogge, 2002). These free fatty acids (FFA) are subsequently connected to CoA esters catalyzed by a long chain acyl-CoA synthase (LACS), and then are exported to the ER (Bates *et al.*, 2007; Li-Beisson *et al.*, 2013).

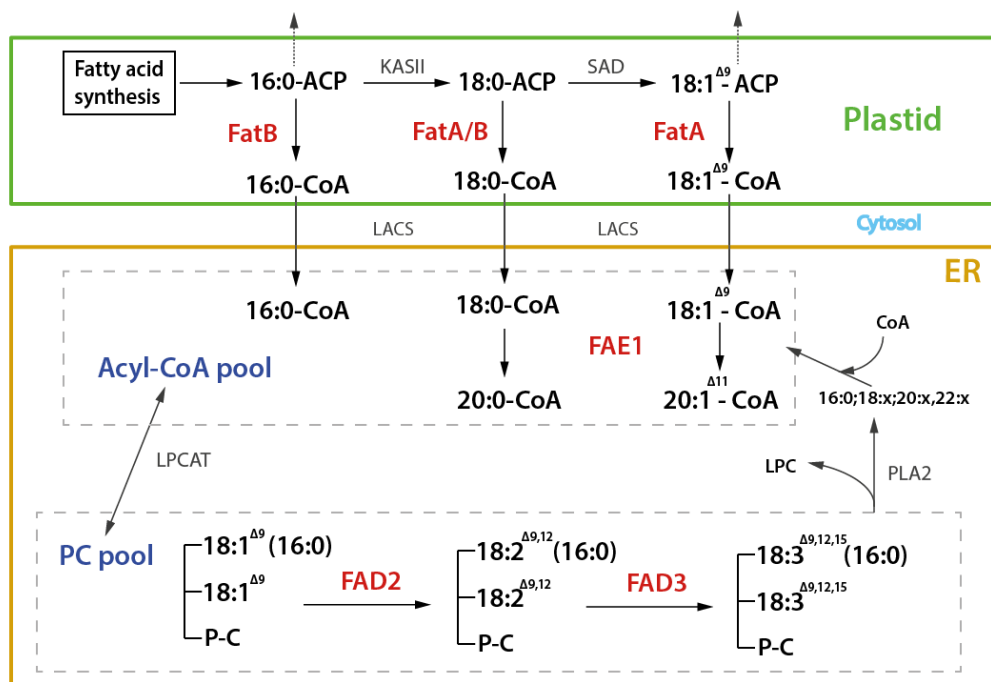


Figure 1.9 Overview of fatty acid biosynthesis, elongation and desaturation pathways in a plant cell. Dash borders indicate the acyl-CoA and PC pools within the ER. The names of enzymes studied in this study are indicated with red color. Abbreviations, ACP, acyl carrier protein; CoA, coenzyme A; ER, endoplasmic reticulum; FAE1, fatty acyl-CoA elongase1; FAD2, oleate desaturase; FAD3, linoleate desaturase; Fata/B, fatty acyl thioesterase; KAS, keto acyl-ACP synthase; LACS, long-chain acyl-CoA synthase; LPCAT, 2-lysophosphatidylcholine

acyltransferase; LPC, 2-lysophosphatidylcholine; PC, phosphatidylcholine; PLA2, phospholipase A2; SAD, stearoyl desaturase. Figure is modified from Li-Beisson (2013), Bansal and Durrett (2015).

Newly synthesized fatty acyl-CoAs (16:0-CoA, 18:1-CoA) are transported to the ER and enter a pool of acyl-CoA, where C₁₈ acyl-CoAs are elongated further to C₂₀ acyl-CoAs, a reaction that is catalyzed by fatty acid elongase 1 (FAE1). The acyl groups of fatty acyl-CoAs can be also esterified to phosphatidylcholine (PC). As parts of the PC molecules, they can be further desaturated by fatty acid desaturases (FADs). The oleate desaturase (FAD2) and linoleate desaturase (FAD3) convert a PC-bound oleate to a linoleate, and then further to a linolenate. A PC acyl editing pathway cycles fatty acyl groups between the acyl-CoA pool and the PC pool without the net synthesis of PC (Bansal *et al.*, 2016). The acyl editing cycle probably also need a 2-lysophosphatidylcholine acyltransferase (LPCAT), which catalyzes the reverse reactions of the CoA: PC exchange, producing lyso-PC and acyl-CoA, and later re-esterifying lyso-PC (Stymne and Stobart, 1984; Bansal *et al.*, 2016; Wang *et al.*, 2012; Bates and Browse, 2011). The acyl editing cycle is also proceed by the rapid cleavage of fatty acyl from the first and second carbon of glycerol molecule (*sn*-1 and *sn*-2 position) of PC, which is catalyzed by a phospholipase (PLA2). This reaction generates lyso-PC molecules and releases FAAs that are later re-esterified to the CoA by a long chain acyl-CoA synthase (LACS; Kunst *et al.*, 2008; Chen *et al.*, 2011). The rate of the acyl editing cycle seems to be much faster than the fatty acid synthesis, and the newly synthesized acyl-CoAs are more rapidly esterified into PC molecules than be incorporated into DAGs or TAGs. Thus, the TAG synthesis and phospholipid synthesis utilize a mixture of saturated and polyunsaturated acyl-CoA substrates (Li-Beisson *et al.*, 2013; Bansal *et al.*, 2016).

1.7.2 Biosynthesis of triacylglycerols

TAG is a very efficient way for plant cells to accumulate fatty acids for energy and carbon resources. TAGs are the major components of seed oil for most of crops. Furthermore, they are also accumulated in other plant tissues, including pollen tubes, senescing leaves and flower petals (Zhang *et al.*, 2009; Kaup *et al.*, 2002). The biosynthesis of TAGs occurs in the ER, and the forming TAGs are finally stored in the lipid droplets.

The pathway of TAG biosynthesis is normally referred as the glycerol phosphate pathway or the Kennedy Pathway (Figure 1.10; Bates *et al.*, 2013). This pathway starts with the acylation of a glycerol-3-phosphate (G3P) by a glycerol-3-phosphate acyltransferase (GPAT) forming a lysophosphatidic acid (LPA; Bansal *et al.*, 2016). Then, a lyso-phosphatidic acid acyltransferase (LPAAT) is responsible for the second acylation by the addition of a second acyl-CoA, producing phosphatidic acid (PA; Cagliari, 2010). In the next step, PA is dephosphorylated to create *de novo* DAGs, which is catalyzed by a phosphatidic acid phosphatase (PAP). Except for the DAG pool formed through the Kennedy Pathway, there are other reactions also important for TAG biosynthesis in plant cells. In *A. thaliana*, the phosphocholine

head group of PC molecules can be transferred to DAG by a phosphatidylcholine: diacylglycerol choline phosphotransferase (PDCT), which is critical for more desaturated fatty acyl groups flowing into the DAG pool and subsequently into TAGs (Lu *et al.*, 2009; Bansal *et al.*, 2016). In addition, there are other mechanisms responsible for converting fatty acyl groups from the PC pool to the DAG pool, such as the reverse reaction of a CDP-choline: diacylglycerol choline phosphotransferase (CPT) and the action of a phospholipase (Slack *et al.*, 1983; Bansal *et al.*, 2016).

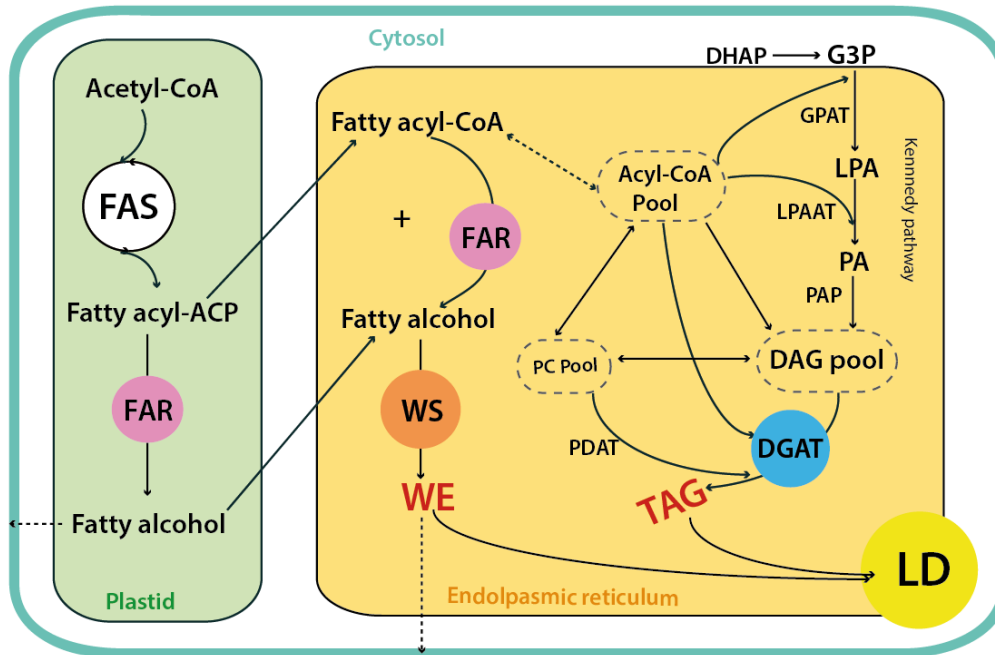


Figure 1.10 Hypothesis pathways of wax ester and TAG biosynthesis in plant seeds. Dash borders indicate the acyl-CoA, DAG and PC pools within the ER; black arrows indicate the orientations of catalytic reaction or transportation. Abbreviations, FAS, fatty acid synthase complex; ACP, acyl carrier protein; CoA, coenzyme A; DAG, diacylglycerol; DGAT, acyl-CoA: diacylglycerol acyltransferase; DHAP, dihydroxyacetone phosphate; FAR, fatty acyl-CoA/ACP reductase; G3P, glycerol-3-phosphate; GPAT, glycerol-3-phosphate acyltransferase; LD, lipid droplet; LPA, lysophosphatidic acid; LPAAT, lyso-phosphatidic acid acyltransferase; PA, phosphatidic acid; PAP, phosphatidic acid phosphatase; PC, phosphatidylcholine; PDAT, phospholipid: diacylglycerol acyltransferase; triacylglycerol, TAG; WE, wax ester; WS, wax synthase. Figure is modified from Bates *et al.* (2013), Haslam *et al.* (2016), Heilmann *et al.* (2013), Kunst *et al.* (2008).

TAGs can be synthesized in two different acyltransferase pathways using DAGs as a substrate. One pathway is that the acyl group of acyl-CoA can be transferred to the *sn*-3 position of DAGs by DGAT to form TAGs. Two different classes of DGAT enzymes (DGAT1 and DGAT2) have been identified to be important for TAG biosynthesis by previous studies (Hobbs *et al.*, 1999; Shockly *et al.*, 2006), while DGAT3 is a soluble protein and not closely involved in the neutral lipid production (Saikat *et al.*, 2006). In most of plant species, such as *A. thaliana*, the enzyme DGAT1 is responsible for the biosynthesis of major TAGs from DAGs (Routaboul *et al.*, 1999; Nykiforuk *et al.*, 2002). As an alternative pathway,

DAGs can be acylated with phospholipids as the acyl donors, the *sn*-2 acyl group of PC molecules is transferred to DAGs to form TAGs by a phospholipid: diacylglycerol acyltransferase (PDAT; Mhaske *et al.*, 2005; Zhang *et al.*, 2009). Once TAG molecules are synthesized, they will form a structure called lipid droplet (LD) or oil body (Li-Bession *et al.*, 2013; Figure 1.10). This organelle is made of a hydrophobic TAG core surrounded by a phospholipid monolayer with a variety of different proteins, including oleosin, caleosin and lipases (Li-Bession *et al.*, 2013). Oleosin is the most abundant protein around LDs, and is important for the size of LDs and the stabilization of TAG core (Jolivet *et al.*, 2004; Shimada *et al.*, 2008; Siloto *et al.*, 2006). Other proteins, such as caleosin and lipase seem to play key roles in the TAG mobilization during seed germination (Poxleitner *et al.*, 2006).

1.7.3 Biosynthesis of wax esters through acyl reduction pathway

The fatty acyl-ACP/CoA substrates for wax ester biosynthesis come from the process of fatty acid synthesis. These substrates are also utilized by the enzymes in Kennedy Pathway for the production of TAGs, therefore TAG biosynthesis can be a competing pathway of wax ester production. The biosynthesis of wax esters in plants requires the corporation of a vast number of enzymes. Once C₁₆ and C₁₈ fatty acyl-ACPs are synthesized by FAS, they can be reduced to fatty alcohols in plastids by acyl-ACP specified FARs (Figure 1.10). As an alternative, the C₁₆ and C₁₈ fatty acyl-CoAs are converted to generate very long-chain fatty acyl-CoAs or further desaturated in the acyl editing cycle in the ER (Figure 1.9). Then, these very long-chain or unsaturated acyl groups are reduced to primary fatty alcohols by a FAR of the acyl reduction pathway in the ER (Bart, 2013; Figure 1.10). Finally, these fatty alcohols then enter the condensation reactions with fatty acyl-CoAs to form wax esters, which is catalyzed by a membrane-associated WS. In *A. thaliana*, it is a bifunctional WS/DGAT enzyme called AtWSD1; in seeds of jojoba, it is a membrane enzyme called ScWS. Finally, the synthesized wax esters would either be transported through the cell wall and reach the cuticle of leaves and stems as the final destination (Kunst *et al.*, 2008), or enter the lipid droplet as a storage lipid as that in jojoba seeds.

1.8 *C. sativa* as an oilseed platform for metabolic engineering

In current years, the production of plant oils is mainly dominated by the food oil crops, such as soybean, sunflower, canola and palm. The oils obtained from these crops are composed of mainly five kinds of fatty acids, and the largest part of these oils is used for food with a minor part used for industrial purposes. In addition to the traditional oil crops, there are a few industrial applied oils obtained from more uncommon oil plants, including jojoba, tung tree and castor bean (Vanhercke *et al.*, 2013). However, the undesirable agronomic traits of these plants make the cultivation very difficult, and consequently keep the prices of their oils in a high level. For these reasons, novel high performance

oilseed crops need to be explored for the production of high valued industrial oils by metabolic engineering approaches.

C. sativa is also referred as gold-of-pleasure or false flax, is an emerging oilseed crop belonging to *Brassicaceae* family. *C. sativa* was first cultivated in northern Europe for food oil, and was widely cultivated in the Great Plains and Pacific Northwest as a traditional oil crop since the middle age until 1940s. However, after the World War II, *C. sativa* was largely taken place by higher-yielding oilseed crops, such as rape (*Brassica napus*). In recent years, *C. sativa* has been attracting more and more attention from the scientific community and the public as a potential platform of metabolic engineering for unusual industrial oils, due to its high content of valuable oil in seeds and considerable agronomic advantages compared with other oil crops, as well as the development of genetic manipulation technologies.

1.8.1 Oil content and composition of *C. sativa*

The oil content of *C. sativa* accounts for 30% - 49% of seed weight (Guy *et al.*, 2014; Agegnehu and Honermeier, 1997; Gehringer *et al.*, 2006), so the total oil yield of *C. sativa* can range from 403 kg ha⁻¹ to 850 kg ha⁻¹, which is comparable to that of soybean (Putnam *et al.*, 1993; Sunil *et al.*, 2016). The oil content of *C. sativa* seeds mostly depends on environment factors, including weather characteristics of cropping year, nutrition application and sowing time. For instance, the seed oil content of *C. sativa* that grown in early spring was higher than that of plants grown in late autumn (Toncea *et al.*, 2013). The seed oil content increased with the enhancement of nitrogen, but was not affected by sulfur application (Zubr, 1997; Bugnarug and Borcean, 2000; Malhi *et al.*, 2014).

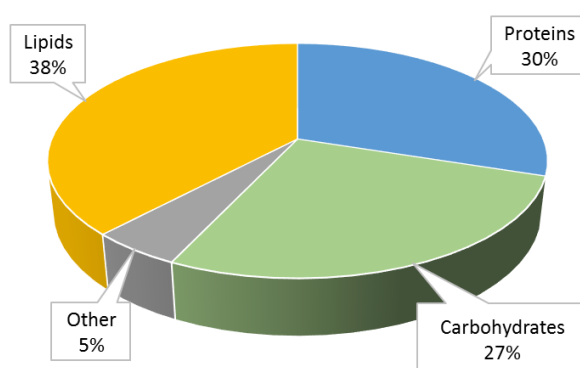


Figure 1.11 Relative distribution of nutrient components in *C. sativa* seeds. Figure is modified from Zubr (2010) and Agegnehu (1997).

The seed oil of *C. sativa* contains high percentage of polyunsaturated fatty acids (PUFAs, about 90%), including 30% - 43% of linolenic acid (18:3), 15% - 26% of linoleic acid (18:2), 11% - 18% of oleic acid (18:1) and about 11% - 18% of gondoic acid (20:1) (Bansal *et al.*, 2016; Hrastar *et al.*, 2012; Gugel *et*

al., 2006; Rodríguez *et al.*, 2013; Kirkhus *et al.*, 2013). On one hand, with the high degree of unsaturation, *C. sativa* seed oil is very interesting as a vegetable oil for food: (i) Camelia oil is a rare resource of alpha-linolenic acid, and the serum cholesterol-lowering effect of *C. sativa* oil was comparable to that of rapeseed and olive oils (Karvonen *et al.*, 2002); (ii) the concentration of erucic acid in *C. sativa* oil is relatively low for a *Brassicaceae* species. Therefore, *C. sativa* oil might be safer than other *Brassicaceae* oils for food applications, as erucic acid showed an association with increased myocardial lipidosis and heart disease in animal experiments (Food Standards Australia New Zealand 2003). On the other hand, *C. sativa* seed oil is not oxidative stable with high level of linolenic acid. So, it is less suitable for application as biodiesel and lubricant (Ciubota-Rosie *et al.*, 2013). In addition, studies revealed that growth conditions could cause a great alternation in the composition of *C. sativa* oil, but small differences were found between the cultivars (Zubr and Matthäus, 2002). For example, the concentration of linolenic acid was higher if a higher level of nitrogen-fertilizer was applied (Kirkhus *et al.*, 2013).

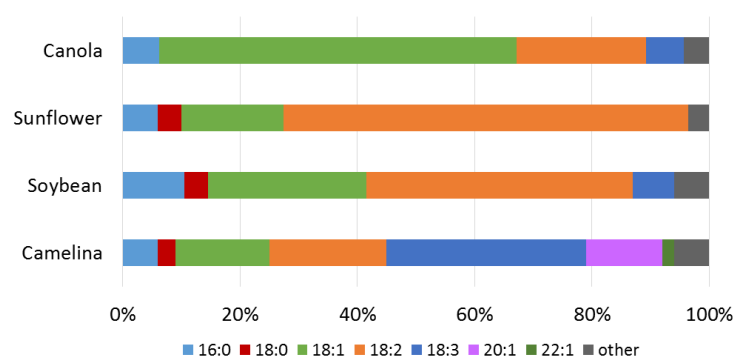


Figure 1.12 Fatty acid profile of the seed oil from canola, sunflower, soybean and *C. sativa*. Figure is modified from Puten *et al.* (1993)

1.8.2 Agronomic traits of *C. sativa*

C. sativa is a suitable oilseed crop for industrial agriculture, because it has a number of excellent agronomic traits. For example, *C. sativa* is well adapted to grow in the temperate climatic zone, and has a relatively short growing season reaching maturity in 85 - 100 days. *C. sativa* has both summer and winter varieties, so that could be grown as a rotation crop with other crops (Putnam *et al.*, 1993). The average yield of *C. sativa* was around 1100 to 1500 kg ha⁻¹ over many years of trials (Plessers *et al.*, 1962), and more recent studies showed that it could reach up to more than 1600 kg ha⁻¹ (Vollmann *et al.*, 2007; Urbaniak *et al.*, 2008). A maximum seed yield of 3 t ha⁻¹ was ever achieved by breeding for marginal, poor soil with low level of nitrogen application (Gehring *et al.*, 2006). With modern plant breeding and agriculture technologies, a dramatic yield improvement of *C. sativa* has been achieved (Gugel *et al.*, 2006; Guy *et al.*, 2014). The application of GMO is expected to improve the yield

of *C. sativa* more rapidly than the traditional breeding approaches. For instance, seed-specific expression of a G-protein or a WRI1 transcription factor of *A. thaliana* improved the seed yield and the oil content of *C. sativa* (Roy Choudhury *et al.*, 2013; An *et al.*, 2015).

Even though compared with other oilseed crops, *C. sativa* is not the highest yielding oilseed crop, it might in some conditions be the most economical crop, due to its relatively low requirements of fertilizer inputs. For instance, an optimum demand of nitrogen to 0 - 100 kg ha⁻¹ depending on annual precipitation is necessary for the growth of *C. sativa* (Zubr, 1997; Wysocki *et al.*, 2013). The increase of nitrogen application up to 120 kg ha⁻¹ significantly enhanced the seed yield to 1 - 3.3 t ha⁻¹ depending on the soil nutrition content and annual varieties (Karcauskiene *et al.*, 2014; Zubr, 1997).

Furthermore, *C. sativa* is quite capable of tolerating drought condition, and can be cultivated well on marginal lands. It may be better suited to the low rainfall regions; therefore is less dependent on irrigation than most of other oilseed crops. One two-year study conducted in western Canada showed that *C. sativa* accessions had more tolerance to drought than other three *Brassicaceae* oilseed crops (Gugel and Falk, 2006). Another study in the eastern Colorado showed that, grown in the same condition of drought stress, *C. sativa* possessed a higher yield of seeds compared to *Brassica carinata* and *Brassica juncea*, showing better adaptation to semi-arid environments (Enjalbert *et al.*, 2013). The reason why *C. sativa* has high tolerance of low water stress might be its total crop evapotranspiration (332 – 371 mm) is markedly lower than that typically needed by grain and vegetable crops (600 – 655 mm; Hunsaker *et al.*, 2011; Eynck *et al.*, 2013). Moreover, in contrast to most of *Brassicaceae* crops, *C. sativa* is resistant to black spot caused by *Alternaria brassicae* (Kolte *et al.*, 1991), stem canker or blackleg caused by *Leptosphaeria maculans* (Rouxel and Balesdent, 2005). In addition to the absolute resistance to black spot and stem canker, *C. sativa* also appears to be more resistant to other common *Brassicaceae* diseases, such as white rust, downy mildew, club root, sclerotinia stem rot and aster yellows (Sharma *et al.*, 2002; Bansal *et al.*, 2016; Vollmann and Eynck, 2015; Seguin-Swartz *et al.*, 2009; Conn *et al.*, 1994; Vollmann *et al.*, 2001). Furthermore, *C. sativa* seems to be less attractive for insect pests like flea beetles as a host compared to other *Brassicaceae* crops, due to its comparatively low level of glucosinolates (Schuster and Friedt, 1998; Lange *et al.*, 1995; Gugel and Falk, 2006). Overall, *C. sativa* could be more commercially valuable for large scale cultivation than other *Brassicaceae* oilseed crops.

C. sativa is also a suitable choice for sustainable agriculture. In an ideal situation, crops grown for biofuel production or other industrial purposes should not be competitive with other crops grown for food (Shonnard *et al.*, 2010; Bansal *et al.*, 2016). The agronomic properties of *C. sativa* reduce the worry about “food versus fuel” issue. With low water and fertilization requirements, *C. sativa* can be cultivated on undeveloped marginal lands, instead of occupying normal farming lands. Moreover, due to its low moisture and nutrient requirements, *C. sativa* can also be grown as a rotation crop during the fallow years with other crops, such as wheat and barley, without affecting the yields of these crops

(Shonnard *et al.*, 2010; Eynck *et al.*, 2013; Bansal *et al.*, 2016). *C. sativa* does not cross with any other species within the *Brassicaceae* crops because of its high number of chromosomes (Kagale *et al.*, 2014). This means it may be safe enough to grow GMO *C. sativa* in wild lands without spreading modified gene fragments to the normal crops. Overall, in comparison to other oilseed crops for the production of diesel fuels and biofuels, *C. sativa* is more environmental friendly (Bansal and Durrett, 2015).

1.8.3 Biotechnological tools of manipulating lipid metabolism in *C. sativa*

In recent years, the development of modern biotechnological tools and genetic editing methods make *C. sativa* promising to be an ideal platform of metabolism engineering for novel oil production. Importantly, *C. sativa* can be simply and rapidly transformed by *Agrobacteria*-mediated floral dip infiltration under vacuum condition, which is much quicker than tissue-culture based the method for the transformation of other oil crops (Bansal *et al.*, 2016; Liu, 2012). With this method, transgenic lines can be generated in 6 - 8 weeks after the transformation, and the transgenic seeds can be easily identified by selection markers, such as resistance to herbicides or antibiotics and fluorescence around seed coat (Bansal *et al.*, 2016). The usage of multiple selection markers makes it possible to stacking different transgenic traits (Lu and Kang, 2008). The exploration and the utilization of various seed-specific promoters and high efficient cloning methods allow the precise overexpression of multiple genes in seeds of *C. sativa* at the same time, thereby leading to the increased seed and oil production as well as the tolerance to abiotic stresses (Li *et al.*, 2014, Choudhury *et al.*, 2013).

In addition, the whole sequence of genome (Kagale *et al.*, 2014) and the seed transcriptome (Nguyen *et al.*, 2013; Liang *et al.*, 2013; Mudalkar *et al.*, 2013; Wang *et al.*, 2015; Abdullah *et al.*, 2016) of *C. sativa* have been available right now, proving that *C. sativa* has a high homology with *A. thaliana*. This allows the current and future knowledge of *A. thaliana* to be easily applied on *C. sativa*. The genomic and transcriptomic data showed that the *A. thaliana* genes involved in the lipid metabolism pathway also exist in *C. sativa*, so that the genetic and metabolic information of *A. thaliana* concerning seed oil biosynthesis can be directly transferred to *C. sativa*.

C. sativa has a highly undifferentiated hexaploid genome (Kagale *et al.*, 2014), which might be a potential disadvantage for the metabolic engineering. Former studies showed that there are always three similar homologous genes playing one enzymatic function in *C. sativa*; for instance, three copies of *C. sativa* fatty acid desaturase 2 (*CsFAD2*) were found to be expressed in developing seeds (Kang *et al.*, 2011). Therefore, if the enzymatic activity of *CsFAD2* needed to be down-regulated to block the desaturation of linoleic acid to linolenic acid, all three copies of *CsFAD2* genes should be knocked-down at the same moment. RNA interference (RNAi) has been an important method to facilitate silencing of targeted genes in post-transcriptional level in plants. The suppression of *C. sativa* fatty acid desaturase and elongase genes by RNAi resulted in the huge changes of fatty acid composition.

One single RNAi construct could target all these homologous genes of one enzyme due to the high similarity of three *C. sativa* sub-genomes (Nguyen *et al.*, 2013). However, RNAi technology has several disadvantages in gene down-regulation at the transcript level. The unmodified miRNAs or siRNAs are easily degraded by RNases, so that the transcripts with high turnover are difficult to be completely silenced. Additionally, it is too complicated to fully understand the true endogenous functions of the molecules *in vivo*; therefore, the potential unspecificity of targeting, which disturbs the functions of other enzymes, might result in undesirable phenotypes. In general, RNAi technology is costly with limited efficiency. This obviously increases difficulties of modifying endogenous metabolic fluxes, and put forward requirements to the genetic editing tools with higher efficiency.

1.8.4 Biosynthesis of unusual lipids in *C. sativa*

C. sativa has been treated as a metabolic engineering platform for production of bio-based industrial oils in the last ten years. Many researches have focused on modifying the fatty acid composition of *C. sativa* seed oil for production of unusual lipids. Fatty acids (FAs) can contain reactive functional groups, such as double bond, hydroxyl groups and carbocyclic structures, which can be good starting materials for the industrial chemistry. Three such examples of interesting FAs that researchers have managed to produce in the seeds of transgenic *C. sativa* are long chain omega-3 FAs, omega-7 FAs and hydroxyl FAs. Omega-3 long-chain polyunsaturated FAs (omega-3 LC-PUFA), containing DHA (docosahexaenoic acid, 20:5 ω 3) and EPA (eicosapentaenoic acid, 22:6 ω 3) have a lot of beneficial effects on human health. *C. sativa* transformed with microalgal fatty acid elongase and desaturase genes produced DHA-containing (6.8% of total fatty acids) TAGs with a high preference of ω 3 over ω 6 LC-PUFA (Mansour *et al.*, 2014). Similarly, transgenic *C. sativa* engineered with multiple fatty acid desaturase and elongase gene cassettes accumulated up to 31% of EPA (eicosapentaenoic acid, 22:6 ω 3) or 14% of DHA (docosahexaenoic acid, 20:5 ω 3) in seeds (Ruiz-Lopez *et al.*, 2014). Omega-7 unsaturated FAs, containing primary palmitoleic acid (16:1 Δ^9) and vaccenic acid (18:1 Δ^{11}) have a number of physical properties valuable for formulations of nutraceuticals, polyethylene and biofuels. Over 65% of omega-7 monounsaturated FAs were accumulated in the seeds of *C. sativa*, in which a plastid-localized mutant Δ 9 acyl-ACP desaturase and an ER-localized Δ 9 16:0-CoA-specific desaturase were co-expressed, and a 3-keto-acyl-ACP synthase II and a 16:0-ACP thioesterase was suppressed by RNAi (Nguyen *et al.*, 2014). The co-expression of a fatty acid hydroxylase from *Ricinus communis* (RcFAH12) with a lesquerella fatty acid elongase (LfkCS) resulted in 19% of hydroxy fatty acids accumulated in the seed oil of *C. sativa* (Snapp *et al.*, 2014).

In addition to fatty acids, there are other unusual lipids generated in seeds of *C. sativa* by metabolic engineering approaches. Poly-3-hydroxybutyrate (PHB) is a member of biodegradable materials. A bacterial PHB biosynthesis pathway was established in *C. sativa* seeds by expression of 3 genes

encoding a hybrid *Pseudomonas oleovorans*/*Zoogloea ramigera* PHA synthase, a beta-ketothiolase from *Ralstonia eutropha* and a reductase from *R. eutropha*. Levels of PHB of up to 15% of the mature seed weight were produced in transgenic *C. sativa* lines. However, the PHB biosynthesis resulted in lower level of oil accumulation and was accompanied by changes in fatty acid profile (Malik *et al.*, 2014). 3-Acetyl-1, 2-diacyl-sn-glycerols (acetyl-TAGs) are unusual TAGs with a sn-3 acetyl group instead of a fatty acyl group (Liu *et al.*, 2015). These unusual TAGs with a sn-3 acetyl group possess lower viscosity and melting temperature compared to typical TAGs (Durrettet *et al.*, 2010, Marshall *et al.*, 2014), and can therefore there be widely used as biofuels, biodegradable lubricants and food coatings. Expression of a diacylglycerol acetyltransferase from *Euonymus alatus* combined with RNAi suppression of three *C. sativa* DGAT1 homologues increased the acetyl-TAG levels up to 85 mol% of total seeds oil in transgenic plants (Liu *et al.*, 2015).

1.8.5 Biosynthesis of wax esters in *C. sativa*

Sees oil containing wax esters with long-chain monounsaturated acyl moieties are high valuable materials for lubrication applications (Iven *et al.*, 2015). The production of wax esters in seeds of plants started from introducing a wax esters biosynthesis pathway into *A. thaliana*. In principle, only a FAR and a WS need to be co-expressed to establish a wax ester synthetic pathway in plant seeds. This was first confirmed when jojoba fatty acyl reductase (ScFAR) and jojoba wax synthase (ScWS) were co-expressed in seeds of *A. thaliana*, and about 70% of seed TAGs were replaced by jojoba oil-like wax esters (Lardizabal *et al.*, 2000). In recent researches, different variants of a mouse FAR with different variants of a mouse WS were co-expressed in seeds of *A. thaliana*. In the *fad2 fae1* double mutant, co-targeted these two enzyme enabled the formation of wax esters containing over 65 mol% of 18:1/18:1, but the total yields were no more than 5% of seed dry weight (Heilmann *et al.*, 2012). Then, more combinations of FARs with WSs were tested for the wax ester production in seeds of *A. thaliana* (Iven *et al.*, 2015). Different enzyme combinations showed strong differences in the substrate preference and the wax ester synthetic activity, and later the best three combinations were transformed into seeds of *C. sativa* (Iven *et al.*, 2015). The yield of wax esters in the seeds of *C. sativa* transformed with co-targeted a mouse FAR and a mouse WS was around 33 mg g⁻¹ seeds, and the *C. sativa* plants transformed with mouse FAR and jojoba WS produced even lower amount of wax esters around 20 mg g⁻¹ in the best individual line. When a FAR from *M. aquaeolei* and the jojoba WS were co-expressed in seeds of *C. sativa*, the highest level of wax esters was achieved, yielding over 50 mg g⁻¹ in seeds (Iven *et al.*, 2013). The resulting wax esters contained 16.3 mol% oleyl - eicosenoate (18:1/20:1) and 15.6 mol% gondoyl - gondonate (20:1/20:1), which indicated that the *MaFAR/ScWS* combination preferred to use monoenoic substrates and the *ScWS* had high specificity to very long-chain acyl-CoAs. However, 18:1/18:1 accounted for only 4 mol% of total wax ester species in the transgenic *C. sativa* with the *MaFAR/ScWS* combination (Iven *et al.*, 2013).

2 OBJECTIVES

The seed oil of *C. sativa* is suitable to serve as a renewable resource of wax esters for the lubrication application. In the previous experiments, the production of wax esters in *C. sativa* were performed by introducing a transgenic wax ester pathway consisting of different combinations of FARs and WSs (Iven *et al.*, 2015; Heilmann *et al.*, 2012). Wax esters were successfully accumulated in seed oil of *C. sativa*, and the combination of *MaFAR* with *ScWS* resulted in the highest amount of wax esters among all combinations. However, the content of wax esters in the seeds of *C. sativa* was only half amount of that found in *A. thaliana* (Iven *et al.*, 2015), indicating the greater difficulty of research on a hexaploid crop plant than a model plant. More importantly, the level of 18:1/18:1 produced by *MaFAR/ScWS* in seed of *C. sativa* was only 4 mol% of the total wax esters. Overall, the total yields and the compositions of wax esters achieved in previous experiments were still far away satisfactory for industrial applications.

In the present study, the main aims are therefore to (i) further increase the overall yields of wax esters in the seed oil of *C. sativa*, and to (ii) especially elevate the level of 18:1/18:1 in all wax ester molecular species.

3 MATERIALS

3.1 Chemicals

If not especially stated, all the chemicals used in this study were purchased from Sigma-Aldrich (USA) or Carl Roth (Germany).

Table 3.1 List of chemicals

Chemical	Manufacturer
Hexane	Baker, USA
Methanol	Baker, USA
Acetonitrile	Baker, USA
Chloroform	Baker, USA
Agar	Duchefa Biochemie, Netherlands
Carbenicillin	Duchefa Biochemie, Netherlands
Rifampicin	Duchefa Biochemie, Netherlands
Ultra pure water	Sartorius arium pro system, Germany
MS Salts	Duchefa Biochemie, Netherlands
Micro Agar	Duchefa Biochemie, Netherlands

3.2 Machines and equipments

The machines and equipments used in this study are shown in Table 3.2.

Table 3.2 List of machines and equipments

Machine	Manufacturer
6890 Series GC System	Agilent, USA
LC Agilent 1100 Serie	Agilent, USA

MATERIALS

Trace gas chromatography	Thermo Finnigan, USA
Polaris Q mass selective detector	Thermo Finnigan, USA
AUTOMATIC TLC SAMPLER 4	CAMAG, Switzerland
CHROMATOGRAM IMMERSION DEVICE III	CAMAG, Switzerland
TLC PLATE HEATER III	CAMAG, Switzerland
TLC SPRAY CABINET III	CAMAG, Switzerland
ÄKTAprime™ plus GE	Healthcare, USA
Corning® Spin-X® UF Concentrators	Life Sciences (Lowell, MA, USA)
BAS-MP 2040S IMAGING PLATE	FUJI PHOTO FILM CO., LT
CARY 100 Bio UV-vis Spectrophotometer	Varian, Germany
Centrifuge 5417 R	Eppendorf, Germany
Centrifuge 5810 R	Eppendorf, Germany
CFX96 realtime PCR cycler	BioRad, Germany
UV-table 312 nm	Raytest, Germany
IDA gel documentation system	Raytest, Germany
Mastercycler personal	Eppendorf (Hamburg, Germany)
Mastercycler gradient	Eppendorf (Hamburg, Germany)
Sonifier® Cell Disruptor B15	Branson, Germany
Mini-PROTEAN3 Electrophoresis System	Bio-Rad Laboratories GmbH, Germany
Sterile bench Prettl® Telstar Bio II A	Telstar, Spain
Applied Biosystems 3200 hybrid triple quadrupole/linear ion trap mass spectrometer	ABSciex, Germany
Electric pompe VDE053	Sartorius, Germany
Growth chamber	York GmbH&Co.KG, Germany

TriVersa NanoMate	Advion BioSciences, USA
Olympus BX51 microscopy	Chromaphor, Germany

3.3 Software and web-based services

The computational work and analysis of data were done with the software and website tools shown in Table 3.3.

Table 3.3 List of software and web-based services

Name	Reference/Manufacturer	Purpose
Excel statistics	Microsoft, Deutschland GmbH	Data analysis, diagrams
WMD3-Web MicroRNA Designer	http://wmd3.weigelworld.org	Design of artificial microRNA
Geneious 7.0	Biomatters, USA	Visual sequencing, molecular cloning, sequence assembly
KEGG	http://www.kegg.jp	Searching of biosynthesis pathways, genes and chemicals
TAIR	http://www.arabidopsis.org/index.jsp	Genome database of Arabidopsis
Webcutter 2.0	Max Heiman, 1997	Map of restriction sites
ClustalX	Thompson, 1997	Construction of phylogenetic trees
Graphical Codon Usage Analyser	Fuhrmann <i>et al.</i> , 2004	Graphical codon usage analysis
Photoshop	Adobe, USA	Figures and schemes
ImageJ	Schneider <i>et al.</i> , 2012	Analysis of fluorescence microscopy signals

MATERIALS

Illustrator	Adobe, USA	Generation of figures and schemes
Origin Pro 8.5	OriginLab, USA	Statistics, data analysis, diagrams
LipidView	AB Sciex Germany	Analysis of ESI-MS/MS signaling
NIST MS Search 2.0 library	http://www.nist.gov	Identification of Mass spectra
Camelina Genomic Resources: Developing Seed Transcriptome	Nguyen <i>et al.</i> , 2013 http://www.camelinagenome.org	Database of <i>C. sativa</i> lipid related genes
<i>C. sativa</i> Genome Project	http://camelinadb.ca	Genome database of <i>C. sativa</i>
TMHMM	Sonnhammer <i>et al.</i> , 1998	Transmembrane prediction
TreeView	Page <i>et al.</i> , 1996	Construction of phylogenetic trees
Xcalibur	Thermo Electron Corp., Germany	Analysis of GC-MS-derived data
winCATS	CAMAG, Switzerland	TLC spotting operation

3.4 Kits and consumables

All the kits and consumables in this study were used according to the manufacturer's instructions.

Table 3.4 List of kits and consumables

Item	Manufacturer
NucleoSpin™ Plasmid	Macherey-Nagel, Germany
NucleoSpin® Gel and PCR Clean-up	Macherey-Nagel, Germany
Protino® Ni-NTA Agarose	Macherey-Nagel, Germany
Clone pJETPCR Cloning Kit	Thermo Scientific, USA

MATERIALS

TLC Silica gel 60	Merck, Germany
Spin-X® UF Concentrators	CORNING, USA

3.5 Standards and markers

All the standards and markers in this study were shown in Table 3.5.

Table 3.5 List of standards and markers

Item	Manufacturer
Heptadecanoyl - heptadecanoate (di-17:0)	Nu-Chek Prep, Inc. (Elysian, MN)
Tripentadecanoin (tri-15:0)	Sigma-Aldrich, Germany
Fatty acid standards	Sigma-Aldrich, Germany
Fatty alcohol standards	Sigma-Aldrich, Germany
GeneRuler - 50 bp DNA Ladder	Thermo Scientific, USA
GeneRuler - 1 kb DA Ladder	Thermo Scientific, USA
Roti®-Mark STANDARD	Carl Roth, Germany
Unstained Protein Molecular Weight Marker	Thermo Scientific, USA

3.6 Mediums, buffers and antibiotics

All media were prepared according to Ausubel *et al.* (1993), if not explicitly stated. Mediums were autoclaved at 120 °C for 20 min before use.

Table 3.6.1 The composition of LB medium

Component	Concentration
Peptone	10 g L ⁻¹
Yeast extract	10 g L ⁻¹
NaCl	5 g L ⁻¹

Table 3.6.2 The composition of ZY medium

Component	Concentration
Yeast extract	5 g L ⁻¹
N-Z-amine	10 g L ⁻¹

Table 3.6.3 Single drop-out powder without Uracil

Component	Amount	Component	Amount
Leucine	4 g	Tryptophan	3 g
Adenine hemisulfate	2 g	Methionine	2 g
Histidine	2 g	Proline	6 g
Arginine	2 g	Phenylalanine	3 g
Isoleucine	2 g	Valine	9 g
Serine	2 g	Tyrosine	2 g

Table 3.6.4 The composition of SD medium

Component	Concentration
Glucose (add after autoclaving)	20 g L ⁻¹
Galactose (filtered with sterile filter, for inducing expression)	20 g L ⁻¹
Yeast Nitro Base	6.7 g L ⁻¹
(NH ₄) ₂ SO ₄	5 g L ⁻¹
Single drop-out powder	1 g L ⁻¹

For SD-Agar, 20 g l⁻¹ of agar were added to the medium

Table 3.6.5 The composition of TBS buffer

Component	Concentration
NaCl	150 mM
Tris/HCl	50 mM
Adjust to pH = 7.6	

Table 3.6.6 The composition of 50 X TAE buffer

Component	Amount
Tris	242 g
EDTA	50 mM
Glacial acetic acid	57.1 ml

Table 3.6.7 Antibiotics

Antibiotic	Stock-solution	Concentration
Carbenicillin	100 mg ml ⁻¹ in H ₂ O	100 µg ml ⁻¹
Kanamycin	50 mg ml ⁻¹ in H ₂ O	25 µg ml ⁻¹
Rifampicin	50 mg ml ⁻¹ in Ethanol	50 µg ml ⁻¹

3.7 Columns for chromatography

All the columns used in this study are shown in Table 3.7.

Table 3.7 List of columns for chromatography

Item	Manufacturer	Purpose
DB-23 (30m x 0.25 mm; 0.25 mm coating thickness)	GC-FID / GC-MS	Agilent, USA
19091j-413 HP5 5% Phenyl Methyl Siloxane	Restek, USA	GC-FID
Restek Rxi™-5ms capillary	Restek, USA	GC-MS Nano-ESI-MS/MS
HisTrap Desalting	GE Healthcare, USA	GF
HisTrap HP	GE Healthcare, USA	IMAC
HiLoad 16/60 Superdex 200	GE Healthcare, USA	SEC

3.8 Enzymes

All enzymes used in this study were used according to the manufacturer's instructions.

Table 3.8 List of enzymes

Enzyme	Manufacturer
Phusion High Fidelity DNA Polymerase	Finnzymes, Finland

MATERIALS

GoTaq DNA Polymerase	Promega, USA
RedTag DNA Polymerase	Sigma-Aldrich, Germany
T4 DNA Ligase	Thermo Scientific, USA
Reverse Transcriptase MMLV-RT	Thermo Scientific, USA
Lysozyme	Sigma-Aldrich, Germany
Deoxribonuclease	Sigma-Aldrich, Germany
Gateway LR Clonase	Thermo Scientific, USA
Gateway LR Clonase Plus	Thermo Scientific, USA
Proteinase K	Thermo Scientific, USA
Restriction Endonucleases	NEB, USA
Restriction Endonucleases	Thermo Scientific, USA

3.9 Strains and organisms

The bacterial and yeast strains used in this study are shown in Table 3.9.

Table 3.9 List of strains and organisms.

Strain	Reference	Features
<i>E. coli</i> XL1-blue	Agilent Technologies, USA	endA1 gyrA96(nalR) thi-1 recA1 relA1 lac glnV44 F'[::Tn10 proAB+ lacIq Δ(lacZ)M15] hsdR17(rK- mK+)
<i>E. coli</i> BL21*(DE3)	Thermo Scientific, USA	F ⁻ ompT hsdSB(rB ⁻ , mB ⁻) gal dcm rne131 (DE3)
<i>S. cerevisiae</i> H1246	Sandager <i>et al.</i> , 2001	MATα are1-Δ::HIS3 are2-Δ::LEU2 dga1-Δ::KanMX4 Iro1-Δ::TRP1 ADE2
Agrobacterium EHA105	Hood <i>et al.</i> , 1993	Rifampicin resistance

MATERIALS

DH5 α TM	Thermo Scientific, USA	F- Φ 80 <i>lacZ</i> Δ M15 Δ (<i>lacZYA-argF</i>) U169 <i>recA1</i> <i>endA1</i> <i>hsdR17</i> (rK-, mK+) <i>phoA</i> <i>supE44</i> λ - <i>thi-1</i> <i>gyrA96</i> <i>relA1</i>
----------------------------	------------------------	---

3.10 Oligonucleotides

Oligonucleotides used in this study were ordered from Sigma-Aldrich (USA).

Table 3.10 List of oligonucleotides

Construct	Sequence (5' - 3')
amiOligo A	CTGCAAGGCGATTAAGTTGGGTAAC
amiOligo B	GCGGATAACAATTTACACAGGAAACAG
amiFAD2.1 I miR-s	GATATCGCATTATAATGTGGCATTCTCTCTTTTGTATTCC
amiFAD2.1 II miR-a	GAATGCCACATTATAATGCGATATCAAAGAGAATCAATGA
amiFAD2.1 III miR*s	GAATACCACATTATATTGCGATTTACAGGTCGTGATATG
amiFAD2.1 IV miR*a	GAAATCGCAATATAATGTGGTATTCTACATATATATTCCT
amiFAD2.2 I miR-s	GATATCGTAGTGAGGCAACGCATTCTCTCTTTTGTATTCC
amiFAD2.2 II miR-a	GAATGCGTTGCCTCACTACGATATCAAAGAGAATCAATGA
amiFAD2.2 III miR*s	GAATACGTTGCCTCAGTACGATTTACAGGTCGTGATATG
amiFAD2.2 IV miR*a	GAAATCGTACTGAGGCAACGTATTCTACATATATATTCCT
amiFAD3.1 I miR-s	GATAATAGTTGTTAGTCCTGCACTCTCTCTTTTGTATTCC
amiFAD3.1 II miR-a	GAGTGCAGGACTAACAACCTATTATCAAAGAGAATCAATGA
amiFAD3.1 III miR*s	GAGTACAGGACTAACTACTATTTTACAGGTCGTGATATG
amiFAD3.1 IV miR*a	GAAAATAGTAGTTAGTCCTGTACTCTACATATATATTCCT
amiFAD3.2 I miR-s	GATTATTGCCGCCCTTACATCACTCTCTCTTTTGTATTCC
amiFAD3.2 II miR-a	GAGTGATGTAAGGGCGGCAATAATCAAAGAGAATCAATGA

MATERIALS

amiFAD3.2 III miR*s	GAGTAATGTAAGGGCCGCAATATTCACAGGTCGTGATATG
amiFAD3.2 IV miR*a	GAATATTGCGGCCCTTACATTACTCTACATATATATTCCT
amiFatB I miR-s	GATTGTGAGCGACTGAACGACACTCTCTCTTTTGTATTCC
amiFatB II miR-a	GAGTGTCGTTCACTCGCTCACAATCAAAGAGAATCAATGA
amiFatB III miR*s	GAGTATCGTTCAGTCCCTCACATTACAGGTCGTGATATG
amiFatB IV miR*a	GAATGTGAGGGACTGAACGATACTCTACATATATATTCCT
amiFAE1.2_FW_Sall	TCGACTAGGTAATCATCGGTGCGCTTATGATGATCACATTCGTTA TCTATTTTTTTCGCGACCGCTGATTACCTA
amiFAE1.2_Rev_BamHI	GATCCTAGGTAATCAGCGGTGCGCAAAAAATAGATAACGAATGT GATCATCATAAGCGCACCGATGATTACCTA
amiFAE1.1_FW_Sall	TCGACTATTTATGCTGGCGAAAACACATGATGATCACATTCGTTA TCTATTTTTTGTTCGCAAGCATAAATAG
amiFAE1.1_Rev_BamHI	GATCCTATTTATGCTTGCGAAAACAAAAATAGATAACGAATGT GATCATCATGTGTTTTTCGCCAGCATAAATAG
MaFAR_FW_Sall	AGT GTCGAC ATGGCAATCCAGCAGGTCCAC
MaFAR_Rev_BamHI	AGT GGATCC TCATGCCGCTTTTTTACGTTGACG
ScWS_FW_Sall	ATG GTCGAC ATGGAGGAAATGGGAAGCATTTTAG
ScWS_Rev_BamHI	ATGGGATCCTTAGTTAAGAACGTGCTCTACGAC
AbWSD1_Rev_BamHI	AGTGGATCCTTAGTTGGCTGTCTTAATGTCCTCTT
TMMmAWAT2_Fw_Sall	AGTGTCGACATGTTCTGGCCTACTAAGAAGGAC
TMMmAWAT2_Rev	GAGATGCTGTTTTCCAATCGAATGC
AbWSD1_FW	ACAGCATCTCTAAAATGCGTCCG
PCOAbWSD1_FW_Sall	GTCGACATGAGACCACTTCATCCAATTGATTCATCTTTCTTTCTC TTGAAAAGAGACAACAACCT
AbWSD1_FW_BamHI (pYES)	ACTGGATCCATGAGACCACTTCATCCAATTGATT
AbWSD1_Rev_XhoI (pYES)	ACTCTCGAGGTTGGCTGTCTTAATGTCCTCTTG

MATERIALS

TMMmAWAT2- <i>AbWSD1_FW_BamHI</i> (pYES)	ACTGGATCCATGTTCTGGCCTACTAAGAAGGAC
TMMmAWAT2- <i>AbWSD1_Rev_XhoI</i> (pYES with TAA)	ACTCTCGAGTTAGTTGGCTGTCTTAATGTCCTCTT
<i>ScWS_FW_BamHI</i>	ACTGGATCCATGGAGGTGGAGAAGGAGCTAAAG
<i>MaFAR_Rev_XhoI</i>	ACTCTCGAGTGCCGCTTTTTTACGTTGACGGG
<i>ScWS_Rev_SalI</i>	ACTGTCGACCCACCCCAACAAACCCATCAATTT
<i>MaFAR_FW_EcoRI</i>	ACTGAATTCATGGCAATCCAGCAGGTCCACC
<i>MaFAR_Rev_NotI</i>	ACTTGCGGCCGCTGCCGCTTTTTTACGTTGACGGG
<i>ScWS-linker_Rev_EcoRI</i>	ACGGAATTCACCCCAACAAACCCATCAATTT
<i>MaFAR_FW_EcoRI</i>	ACGGAATTCATGGCAATCCAGCAGGTCCACC
<i>MaWS1_FW_HindIII</i>	ACGAAGCTTATGACGCCCTGAATCCCCTG
<i>MaWS1_Rev_XhoI</i>	ACGCTCGAGCAGACCGGCGTTGAGCTCCAG
<i>MaWS2_FW_HindIII</i>	ACGAAGCTTATGAAACGTCTCGGAACCCTGGA
<i>MaWS2_Rev_XhoI</i>	ACGCTCGAGCTTGCGGGTTCGGGCGCGCTT
<i>MaWS3_FW_HindIII</i>	ACGAAGCTTATGCGTCAGCTGTCGGAACCTGGA
<i>MaWS3_Rev_XhoI</i>	ACGCTCGAGCCTTCTGAATTTGCCAGCCAC
<i>MaWS4_HindIII</i>	ACGAAGCTTATGTCAGCAAAACGGACGGCCAT
<i>MaWS4_SacI</i>	ACGGAGCTCGGAGGCTGGCGGAAACCGC
<i>MaWS5_FW_HindIII</i>	ACGAAGCTTATGCTGCCTTCGGATTCAGCCTG
<i>MaWS5_Rev_XhoI</i>	ACGCTCGAGGTCCAGCTGATCCAGTTCCGCC
TMMmAWAT2- <i>AbWSD1_FW_SalI</i>	ACGGTCGACATGTTCTGGCCTACTAAGAAGGAC
TMMmAWAT2- <i>AbWSD1_Rev_BamHI</i> (with TAA)	ACGGGATCCTTAGTTGGCTGTCTTAATGTCCTCTT

MATERIALS

TMMmAWAT2- <i>AbWSD1_FW_NotI</i>	ACGGCGGCCGCAATGTTCTGGCCTACTAAGAAGGAC
<i>AbWSD1_NotI+a_FW</i>	ACGGCGGCCGCAATGAGACCACTTCATCCAATTGATT
<i>MaWS2_FW_XhoI</i>	ACGCTCGAGATGAAACGTCTCGGAACCTGGA
<i>MaWS2_Rev_BamHI</i>	ACGGGATCCTTACTTGCGGGTTCGGGCGCGCTT
oleosin seqa	ACCCAACAACCTCCACTTTTGC
Bata-conglycinin seqa	TATAAATAGCTGCAATCTCGG
USP seqa	TTTACATGCAACTAGTTATGC
M13_FW	GTTTTCCCAGTCACGAC
M13_Rev	CAGGAAACAGCTATGAC

3.11 DNA constructs

All the DNA constructs used in the present study are shown in Table 3.11.

Table 3.11 List of the DNA constructs

Gene	Reference	Vector	Restriction sites (5'- 3')	Resistance (bacteria)/ Auxotrophy (yeast)
<i>MaFAR</i>	Hofvander <i>et al.</i> , 2011; Wahlen <i>et al.</i> , 2009	pEntry-A pEntry-B pEntry-D	<i>Sall/BamHI</i>	Ampicillin
<i>ScWS</i>	Kathryn <i>et al.</i> , 2000	pEntry-C	<i>Sall/BamHI</i>	Ampicillin
<i>ScWS-MaFAR</i>	This study	pEntry-A pEntry-D	<i>Sall/BamHI</i>	Ampicillin
<i>AbWSD1</i>	Stöveken <i>et al.</i> , 2005	pEntry-D	<i>Sall/BamHI</i>	Ampicillin
PCO <i>AbWSD1</i>	This study	pEntry-D	<i>Sall/BamHI</i>	Ampicillin

MATERIALS

TMMmAWAT 2-AbWSD1	This study	pEntry-D	<i>Sall/BamHI</i>	Ampicillin
MaWS2 (Maqu_3067)	Holtzaple, 2007 Leman <i>et al.</i> , 2013	pEntry-D	<i>XhoI/BamHI</i>	Ampicillin
amiDGAT1.1	By Sofia Marmon	pEntry-A	<i>Sall/BamHI</i>	Ampicillin
amiDGAT1.2	By Sofia Marmon	pEntry-A	<i>Sall/BamHI</i>	Ampicillin
amiDGAT1.2	By Sofia Marmon	pEntry-A	<i>Sall/BamHI</i>	Ampicillin
amiFatB	This study	pEntry-E	<i>Sall/BamHI</i>	Ampicillin
amiFAE1.1	This study	pEntry-E	<i>Sall/BamHI</i>	Ampicillin
amiFAE1.2	This study	pEntry-E	<i>Sall/BamHI</i>	Ampicillin
amiFAD2.1	This study	pEntry-E	<i>Sall/BamHI</i>	Ampicillin
amiFAD2.2	This study	pEntry-E	<i>Sall/BamHI</i>	Ampicillin
amiFAD3.1	This study	pEntry-E	<i>Sall/BamHI</i>	Ampicillin
amiFAD3.1	This study	pEntry-E	<i>Sall/BamHI</i>	Ampicillin
MmAWAT2	Heilmann <i>et al.</i> , 2012	pYES2/NTc	<i>BamHI/XhoI</i>	Ampicillin/ Uracil
PCOAbWSD1	This study	pYES2/CT	<i>BamHI/XhoI</i>	Ampicillin/ Uracil
TMMmAWAT 2-AbWSD1	This study	pYES2/CT	<i>BamHI/XhoI</i>	Ampicillin/ Uracil
MaWS1 (Maqu_0168)	Holtzaple <i>et al.</i> , 2007 Leman <i>et al.</i> ,2013	pYES2/CT	<i>HindIII/XhoI</i>	Ampicillin/ Uracil
MaWS2 (Maqu_3067)	Holtzaple <i>et al.</i> , 2007 Leman <i>et al.</i> ,2013	pYES2/CT	<i>HindIII/XhoI</i>	Ampicillin/ Uracil
MaWS3	Holtzaple <i>et al.</i> , 2007	pYES2/CT	<i>HindIII/XhoI</i>	Ampicillin/ Uracil

MATERIALS

(Maqu_0851)				
<i>MaWS4</i>	Holtzapple <i>et al.</i> , 2007	pYES2/CT	<i>HindIII/SacI</i>	Ampicillin/ Uracil
(Maqu_3371)				
<i>MaWS5</i>	This study	pYES2/CT	<i>HindIII/XhoI</i>	Ampicillin/ Uracil
(Maqu_3411)				
<i>MaFAR</i>	Hofvander <i>et al.</i> , 2011; Wahlen <i>et al.</i> , 2009	pYES2/CT	<i>KpnI/BamHI</i>	Ampicillin/ Uracil
<i>ScWS</i>	Kathryn <i>et al.</i> , 2000	pYES2/NTc	<i>KpnI/BamHI</i>	Ampicillin/ Uracil
<i>ScWS-MaFAR</i>	This study	pYES2/CT	<i>BamHI/XhoI</i>	Ampicillin/ Uracil
<i>MaFAR/ScWS</i>	This study	pESC-URA	<i>EcoRI/ NotI</i> <i>BamHI/SalI</i>	Ampicillin/ Uracil
<i>MaWS5</i>	This study	pET-28b	<i>HindIII/XhoI</i>	Kanamycin
(Maqu_3411)				
PCOAbWSD1	This study	pUC-19- mCherry-CT	<i>SalI/XhoI</i>	Ampicillin
TMMmAWAT 2-AbWSD1	This study	pUC-19- mCherry-CT	<i>SalI/XhoI</i>	Ampicillin

3.12 Transgenic plants

All the transgenic plant lines used in this study are shown in Table 3.12.

Table 3.12 List of transgenic plant lines

Name	Host plant	Promoter	Reference	Number
<i>MaFAR/ScWS</i>	<i>C. sativa</i>	Napin	Iven <i>et al.</i> , 2013	6
<i>Atfad3/Csfad2/Csfae1</i>	<i>C. sativa</i>	--	Nguyen <i>et al.</i> , 2013	1
<i>MaFAR/ScWS</i> & HO cross	<i>C. sativa</i>	Napin	Seeds were provided by Dr. Ellen Hornung This study	6
<i>MaFAR/AbWSD1</i>	<i>C. sativa</i>	Napin	This study	12
<i>amiDGAT1.1/MaFAR/ScWS</i>	<i>C. sativa</i>	Napin	This study	21
<i>amiDGAT1.2/MaFAR/ScWS</i>	<i>C. sativa</i>	Napin	This study	19
<i>amiDGAT1.3/MaFAR/ScWS</i>	<i>C. sativa</i>	Napin	This study	6
Empty Vector	<i>C. sativa</i>	Napin	This study	13
<i>amiFatB</i>	<i>C. sativa</i>	Napin	This study	14
<i>amiFAE1.1</i>	<i>C. sativa</i>	Napin	This study	18
<i>amiFAE1.2</i>	<i>C. sativa</i>	Napin	This study	17
<i>amiFAD2.1</i>	<i>C. sativa</i>	Napin	This study	12
<i>amiFAD2.2</i>	<i>C. sativa</i>	Napin	This study	17
<i>amiFAD3.1</i>	<i>C. sativa</i>	Napin	This study	12
<i>amiFAD3.2</i>	<i>C. sativa</i>	Napin	This study	0
<i>MaFAR/AbWSD1</i>	<i>A. thaliana</i>	Napin	This study	50
<i>MaFAR/AbWSD1_fad2fae1</i>	<i>A. thaliana</i>	Napin	This study	10
<i>MaFAR/PCOAbWSD1</i>	<i>A. thaliana</i>	Napin	This study	6
<i>MaFAR/MaWS2</i>	<i>A. thaliana</i>	Napin	This study	61

MATERIALS

<i>MaFAR/TMMmAWAT2- AbWSD1</i>	<i>A. thaliana</i>	Napin	This study	56
<i>ScWS-MaFAR</i>	<i>A. thaliana</i>	β -conglycinin	This study	60
<i>MaFAR/ScWS-MaFAR</i>	<i>A. thaliana</i>	oleosin	This study	61
		β -conglycinin		
<i>ScWS-MaFAR/ScWS-MaFAR</i>	<i>A. thaliana</i>	oleosin	This study	48
		β -conglycinin		

4 METHODS

4.1 Molecular biology methods

4.1.1 Standard PCR

Standard PCR was performed following the method of Mullis *et al.* (1986). Unless otherwise stated, standard PCR was done using the Phusion-DNA polymerase (Finnzymes, Finland). The sample composition and the temperature gradient are shown below.

Table 4.1 The sample composition for standard PCR

Component	Amount		
dNTP (each 10 μ M)	0.5 μ l	98 °C 2 min	} 25 cycles
Primer A (10 μ M)	0.5 μ l	98 °C 1 min	
Primer B (10 μ M)	0.5 μ l	55 °C 30 s	
DNA template	~ 3 ng	72 °C 30 s/kb	
DNA polymerase	1 U	72 °C 10 min	
Total 25 μ l			

4.1.2 Overlap extension PCR

To generate a fusion protein, overlap extension PCR was performed. Respective fragments were at first amplified from the sequences of each part. All the forward-primers for overlap extension PCR were designed to contain a 20 bp overhang to the adjacent fragment, and the reverse primers were designed to have a 15 bp overhang to the adjacent fragment. The respective PCR fragments were purified by gel-extraction and eluted in 30 μ l H₂O. 2 μ l of the respective shorter and 3 μ l of the respective longer fragment were used for the overlap extension PCR using the Phusion DNA-Polymerase (Finnzymes, Finland) and the standard PCR protocol shown in section 4.1.1.

4.1.3 Colony PCR

In order to verify the successful ligation of a desired DNA-fragment in a respective vector, colony PCR was done according to the method of Woodman (2008). A colony PCR with primers specific for the

respective gene was performed on the basis of whole cells as DNA-templates. A single *E. coli* colony was picked from an agar plate with a sterile toothpick. The *E. coli* cells were re-suspended in a single PCR-sample and furthermore spread out on an LB-Agar plate supplemented with respective antibiotics for later use. GoTaq-DNA Polymerase (Promega, USA) was used. The colony PCR sample composition and the temperature gradient were described as below.

Table 4.2 The sample composition of colony PCR

Component	Amount		
GoTag buffer	4 μ l	98 °C 4 min	} 25 cycles
Primer A (10 μ M)	0.5 μ l	98 °C 1 min	
Primer B (10 μ M)	0.5 μ l	58 °C 30 s	
dNTPs	0.2 μ l	72 °C 1 min/kb	
GoTag - DNA Polymerase	1 μ l	72 °C 10 min	

4.1.4 Restriction of DNA

Restriction of DNA was done as described by Boyer (1971). The DNA-restriction endonucleases (Thermo Scientific) were utilized in the buffer recommended by the respective manufacturer and according to the manufacturer's protocol.

4.1.5 Separation of DNA by agarose gel-electrophoresis

This method is based on a principle published by Aaij and Borst (1972). DNA sample was mixed with an appropriate volume of 6 x loading dye. Preparation of agarose gel was done by boiling 1% agarose (*w/v*) in TAE-buffer. Electrophoresis was performed for approximately 25 min, until the bromophenol-blue running front left the agarose gel. Afterwards, the agar gel was incubated in TAE supplemented with 2 μ g ml⁻¹ of ethidium bromide. DNA binds were visualized in UV-light. For DNA extraction from the agarose gel, the DNA fragment was cut off from the agarose gel in minimize UV exposure. The DNA fragment was prepared using the NucleoSpin™ Gel and PCR Clean-up Kit according to the instructions provided by the manufacturer.

Table 4.3 The composition of TAE buffer

Component	Concentration
Tris/HCl, pH 7.0	40 mM
Acetic acid	20 mM
EDTA	1 mM

Table 4.4 The composition of 6 X loading buffer

Component	Concentration
Tris/acetate pH 8.5	40 mM
EDTA	100 mM
SDS	0.1% (w/v)
Glycerol	50% (v/v)
Xylencyanol blue	0.25% (w/v)
Bromophenol blue	0.25% (w/v)

4.1.6 Ligation of DNA

Ligation of DNA was performed by utilization of the T4-ligase (Weiss and Richardson, 1967). For cloning of blunt-end PCR products generated by the Phusion-DNA polymerase into pJET vector, the blunt-end ligation reaction was performed with the instructions provided by the manufacturer. Then, the ligation mixture was briefly vortexed and incubated at room temperature for 30 min before directly using for bacterial transformation. In case of the PCR products with 3'-dA overhangs generated by Red-Tag-DNA-Polymerase, the blunting reaction of sticky-end cloning was first performed to remove 3' overhangs and fill-in 5' overhangs. The reaction mixture was incubated at 70 °C for 5 min and then chilled briefly on ice for ligation reaction.

Table 4.5 The Composition of blunt-end ligation reaction

Component	Amount
2x Reaction Buffer	5 µl
PCR products	1 µl
pJET1.2/blunt cloning vector (50 ng µl ⁻¹)	0.5 µl
T4 DNA ligase	0.5 µl
Water, nuclease-free	3 µl

METHODS

Table 4.6 Blunting reaction

Component	Amount
2x Reaction Buffer	5 μ l
PCR products	3.5 μ l
DNA blunting enzyme	0.5 μ l

Table 4.7 Ligation reaction of sticky-end cloning

Component	Amount
pJET1.2/blunt cloning vector	0.5 μ l
T4 DNA ligase	0.5 μ l

4.1.7 Cloning of artificial microRNAs

The artificial microRNAs were designed according to the guide offered by WMD3-Web MicroRNA Designer (<http://wmd3.weigelworld.org>). The 21 bp amiRNAs were designed to target all three homologous genes of *CsFAD2*, *CsFAD3*, *CsFAE1* and *CsFatB*, respectively. The amiRNA candidates targeting the 3' end of coding region, having no mismatch between positions 2 - 12 of amiRNAs for all targets, with absolute hybridization energy is between -35 and -38 kcal/mole, were finally selected and used in this study. The cloning of artificial microRNAs of *CsFAD2*, *CsFAD3* and *CsFatB* was performed according to the protocol by Schwab (2006). Four oligonucleotide sequences (I to IV) delivered by WMD were used to engineer artificial microRNA into the endogenous miR319a precursor by sit-directed mutagenesis. The plasmid pRS300 that contains the miR319 precursor in pBSK, was used as a template for PCR. The amiRNAs containing precursor were generated by overlapping PCR. The cloning of artificial microRNAs of *CsFAE1* was conducted as the method described by Carnonell (2014), 2 μ l of each of the two overlapping and complementary oligonucleotides with restriction sites were annealed in 46 μ l Oligo Annealing Buffer by heating the reaction at 94 °C for 5 min and then cooling to room temperature. The annealed oligonucleotide pair was then diluted and cloned into pEntry vector by DNA-ligation reaction.

Table 4.8 Cloning strategy of artificial microRNAs

Fragment	Forward oligo	Reverse oligo	Template
(a)	amiOligo A	IV miR+a (microRNA* reverse)	pRS300
(b)	III miR*s (microRNA* forward)	II miR-a (microRNA reverse)	pRS300
(c)	I miR-s (microRNA forward)	amiOligo B	pRS300
(d)	amiOligo A	amiOligo B	(a)+(b)+(c)

Table 4.9 Site-directed PCR reaction (a) (b) (c)

Component	Amount		
H ₂ O	28.5 µl		
10x PCR buffer	5 µl	98 °C 30s	} 30 cycles
1 mM dNTPs	10 µl	98 °C 30 s	
10 µM each oligo	2 µl	55 °C 30 s	
Plasmid DAN (1:100)	2 µl	72 °C 30s	
Phusion- DNA polymerase	0.5 µl	72 °C 10 min	
Total 50 µl			

Table 4.10 Overlapping PCR reaction (d)

Component	Amount		
H ₂ O	29.5 µl		
10x PCR buffer	5 µl		
1 mM dNTPs	10 µl	98 °C 30s	} 30 cycles
10 µM amiOligo A	2 µl	98 °C 30 s	
10 µM amiOligo B	2 µl	55 °C 30 s	
PCR (a)	0.5 µl	72 °C 1 min 30 s	
PCR (b)	0.5 µl	72 °C 10 min	
PCR (c)	0.5 µl		
Phusion- DNA polymerase	0.5 µl		
Total 50 µl			

Table 4.11 The composition of oligo annealing buffer

Component	Concentration
Tris-HCl (pH 7.5)	60 mM
NaCl	500 mM
MgCl ₂	60 mM
DTT	10 mM

4.1.8 Gateway technology

Gateway Reaction is conducted according to the manufacturer's protocol (Thermos Scientific). 10 fmol of each pEntry vector, 20 fmol of destination vector (pCAMBIA 33.0 with kanamycin resistance gene) and TE buffer were mixed together to a total volume of 9 μ l. In case of only one pEntry vector, the LR Clonase II Enzyme Mix was taken out of -20 °C freezer and vortexed for approximately 1 min, then 1 μ l LR Clonase II Enzyme Mix was pipetted into the reaction mix and briefly vortexed for 1 min. In case of multiple cassettes, 1 μ l LR Clonase II Plus Enzyme Mix was used. The 10 μ l reaction mixture was incubated at 25 °C overnight. On the next day, 1 μ l Proteinase K was added to reaction mixture and incubated for 10 min at 37 °C to stop Gateway Reaction, then the mixture was heated at 70 °C for 10 min to inactive Proteinase K. Finally, the plasmid was transformed into DH5 α cells according to the manufacturer's protocol.

4.1.9 Preparation of competent *E. coli* cells

One 5 ml overnight culture of LB was inoculated directly from the respective agar plate. After 16 h, 125 ml of LB-medium was mixed with the cell culture, incubated at 37 °C, shaken at 180 rpm until the culture reached OD₆₀₀ = 0.4 - 0.75. Cell culture was then transferred to sterile 50 ml centrifugation tubes and incubated on ice for 10 min. Then, cells were centrifuged at 4 °C 1000 g for 10 min. The supernatant was removed and the pellet was re-suspended with 20 ml TFB buffer (pH 6.7) per tube. After 10 min of incubation on ice, the tube was centrifuged again at 4 °C and 1000 g for 10 min. The supernatant was discarded and the pellets were re-suspended with 4 ml of TFB-buffer and all combined in one tube. After the addition of DMSO to a final concentration of 7% (v/v), the cells were further incubated on ice for 10 min. Finally, the cells were divided into 200 μ l aliquots and flash-frozen in liquid nitrogen. Aliquots were stored at -80 °C.

Table 4.12 The composition of TFB buffer

Component	Concentration	Amount
PIPES	10 mM	0.605 g
CaCl ₂ x 2H ₂ O	15 mM	0.441 g
KCl	250 mM	3.728 g
MnCl ₂ x 4H ₂ O	55 mM	2.18 g

4.1.10 Transformation of *E. coli*

A volume of 100 µl competent *E. coli* cells was mixed with up to 10 µl DNA. The cell-DNA mixture was incubated on ice for 20 min. Then, a heat shock was performed at 42 °C for 45 s. After further incubation on ice for 5 min, 900 µl of LB medium was added. The sample was then incubated at 37 °C for 1 h in case of plasmids having a kanamycin resistance, and for 30 min in case of plasmids having an ampicillin resistance. In case of retransformations, 100 µl of the sample was plated out on LB-plates containing the respective antibiotics. In all other cases, the complete sample was pelleted via centrifugation at 200 g for 1 min, and then the supernatant was removed and the remaining pellet was plated out. Plates were incubated overnight at 37 °C.

4.1.11 Plasmid preparation

For plasmid preparation, one 5 ml of *E. coli* overnight culture was inoculated with one single colony and supplemented with suitable antibiotics. After 16 h of incubation, the plasmid-DNA was prepared using the NucleoSpin™ Plasmid-Kit according to the instructions provided by the manufacturer. The protocol is based on a publication of Birnboim and Doly (1979).

4.1.12 Preparation of competent *S. cerevisiae* cells

For preparation of competent yeast cells, 50 ml of YPD medium was inoculated with a single colony of the respective strain and incubated overnight at 30 °C, shaken at 180 rpm. 5 ml of this culture was used for further inoculation in 100 ml of YPD medium. The resulting culture was grown at 30 °C for about 4 h until OD₆₀₀ = 0.6 - 0.7. Yeast cells were pelleted via centrifugation at 500 g for 5 min and washed with 20 ml of solution A. Then, cells were re-suspended in 4 ml solution A. Subsequently, 100

μl of a 10 mg ml^{-1} heat-denatured Fisch sperm-DNA solution and $100 \mu\text{l}$ of a 1 M histamine solution were added and mixed. Finally cells were divided in $200 \mu\text{l}$ aliquots (2 ml tubes) and frozen at $-80 \text{ }^{\circ}\text{C}$.

Table 4.13 The composition of YPD medium

Component	Amount
Yeast extract	10 g L^{-1}
Peptone	10 g L^{-1}
Glucose (autoclaved)	20 g L^{-1}

Table 4.14 The composition of solution A

Component	Concentration
Sorbit	1 M
Tricine	10 mM
Ethylene glycol	$3\% \text{ (w/v)}$

4.1.13 Transformation of *S. cerevisiae*

Transformation of *S. cerevisiae* was done according to the method described by Gietz and Schiestl (2007) and Ito *et al.* (1983). $5 \mu\text{g}$ of plasmid-DNA was added to a $200 \mu\text{l}$ aliquot of frozen *S. cerevisiae* cells. The sample was incubated in a thermos shaker at $37 \text{ }^{\circ}\text{C}$ and at a medium speed for 5 min . Then, the sample was diluted in 1.2 ml solution B and further incubated at $30 \text{ }^{\circ}\text{C}$ for 1 h . Subsequently, the sample was pelleted via centrifugation at 4000 g for 1 min , and washed three times with solution C. Then, cells were finally re-suspended in $300 \mu\text{l}$ solution C and plated out on respective SD-agar-plates.

Table 4.15 The composition of solution B

Component	Concentration
PEG3350	40%
Tricine-NaOH	200 mM

Table 4.16 The composition of solution C

Component	Concentration
NaCl	0.15 mM
Tricine-NaOH	10 mM

4.1.14 Cultivation of *S. cerevisiae*

Cultivation of *S. cerevisiae* expression cultures was done in accordance to Heilmann *et al.* (2012). At first, an overnight pre-culture was prepared, 5 ml of SD-URA-medium with 2% glucose and Dropout was inoculate with yeast clone, then incubated at $30 \text{ }^{\circ}\text{C}$ and shaking 180 rpm overnight to obtain $\text{OD}_{600} = 2$. Afterwards, 25 ml of SD-URA-medium plus 2% galactose were incubated to an $\text{OD}_{600} = 0.05$ from the pre-culture. In case of different purposes, fatty alcohols ($16:0\text{-OH}$ or $18:1\text{-OH}$) were dissolved in ethanol and added into expression cultures to a final concentration of 1 mM . Then, the expression culture was incubated at $30 \text{ }^{\circ}\text{C}$ and 180 rpm for $3 - 5 \text{ days}$. Then, the cells were harvested by centrifugation at 3200 g for 10 min for lipid analysis or for storage.

4.1.15 Preparation of competent *A. tumefaciens* cells

For preparation of competent *Agrobacterium* cells, one 5 ml pre-culture was prepared by inoculating single colony into LB medium with Rifampicin, and the pre-culture was incubated overnight at 28 °C, shaken at 180 rpm. Then, 50 ml LB medium was inoculated with 2 ml of pre-culture, and incubated at 28 °C for 3 - 4 h until OD₆₀₀ = 0.5. Then, cells were pelleted via centrifugation at 4 °C 3200 g for 15 min and washed with 0.15 M cold NaCl. After centrifugation, cells were dissolved in 1 ml cold 75 mM CaCl₂. Finally, cells were divided in 200 µl aliquots (2 ml tubes), frozen in liquid nitrogen, and stored at -80 °C.

4.1.16 Transformation of *A. tumefaciens*

One aliquot of frozen competent cells for each transformation was taken out of -80 °C and quickly warmed by 37 °C. Then, 3 µl plasmid-DNA was mixed with each aliquot of cells and incubated on ice for 30 min. The cell-DNA mix was frozen at -80 °C for 2 min and then warmed immediately at 37 °C after freezing. Afterwards, 800 µl of LB medium was added, the mixture was incubated at 28 °C for 3 - 4 h while shaking. Subsequently, cells were centrifuged to pellet at 1800 g for 1 min, the supernatant was removed and the pellet in remaining medium was plate on agar plate with Rifampicin and Kanamycin. The plates were incubated at 28 °C for 2 days.

4.1.17 Transformation of *A. thaliana*

A. thaliana plants were transformed via *Agrobacterium*-mediated floral dipping method (Clough *et al.*, 1998). 5 ml of pre-culture was inoculated with single *agrobacterium* colony and supplemented with Rifampicin and Kanamycin. After incubation at 28 °C overnight, 500 ml LB medium with antibiotics were inoculated with the pre-culture, and shaken again overnight at 28 °C. Hereafter, the *agrobacterium* cells were pelleted via centrifugation at 4 °C 3200 g for 20 min, and then the pellet was re-suspended in 300 ml of 5% sucrose with 70 µl Sylvet. After dipping flowers in the *agrobacterium*-sucrose solution for at least 30 s, *Arabidopsis* plants were covered with a lid onto their plant tray for one day and cultivated in the green house. To increase the yield of transgenic plants, the transformation could be repeated after one week.

4.1.18 Transformation of *C. sativa* via vacuum floral dipping

C. sativa plants were transformed via *Agrobacterium*-mediated vacuum floral dipping method described by Lu and Kang (2008). At least 6 wild type plants were used for transformation of each gene construct and cultivated in growth chamber. The cultivation of harvest of *Agrobacterium* were done

according to the steps described in section 4.1.17. Then, the *Agrobacterium* pellets were re-suspended in 500 - 700 ml Mix A solution. Three *C. sativa* plants were put into an exicator together with the solution containing agrobacterium. Then, the exicator was closed and vacuum was applied to minus 0.6 bar. The vacuum condition was hold for 5 min and then slowly released during 15 min. Then, the transformed plants were put into their tray with plastic cover and keep in dark for one day. The plants were finally cultivated in the growth chamber until the seeds get mature. The T1 seeds were harvested and grown on soil, the selection of transgenic lines was performed by spraying phosphinothricin on seedlings.

Table 4.17 The composition of Mix A solution

Component	Amount
½ MS-stock	2.2 g
Sucrose	50 g
0.05% Silvet 77	500 µl
H ₂ O	1 L

4.1.19 Sterilization of seeds of *C. sativa* for germination experiment

More than 20 seeds of *C. sativa* were selected and transferred into 2 ml tubes. Then, 1 ml 70% ethanol was added and shaken for 1 min. Then, the supernatant was discarded, 1 ml 1% sodium hypochlorite was added to the tube and gently shaken for 20 min. Afterwards, the seeds were washed 4 times with sterile water and kept cool at 4 °C for 2 days. The sterilized seeds were plated on a sterile filter paper in a petri dish. Seeds germinated in 1 - 2 days in the condition of 25 °C with light intensity 60%, 16 h.

4.1.20 Cultivation of *E. coli* expression culture for protein purification

For cultivation of *E. coli* expression culture, 50 ml pre-culture of LB medium supplemented with the antibiotics was inoculated with a single colony and incubated at 37 °C shaking at 200 rpm overnight. On the next day, 1 L of auto-induction medium, supplemented with appropriate antibiotics, was inoculated with 50 ml of the pre-culture. The culture was incubated at 37 °C, shaking in 2 L flasks at 200 rpm for 60 - 120 min, until the culture reached an OD₆₀₀ = 0.4 - 0.8. Afterwards, the culture was further incubated at 200 rpm and 16 °C for 48 h. Then, the culture was harvested by centrifugation at 3000 g, and the resulting pellet was flash frozen in liquid nitrogen and stored at -20 °C until using for protein purification.

METHODS

Table 4.18 The composition of 1000 x metal mix

Component	Concentration
FeCl ₃	50 mM
CaCl ₂	20 mM
MnCl ₂	10 mM
ZnSO ₄	10 mM
CoCl ₂	2 mM
CuCl ₂	2 mM
NiCl ₂	2 mM

Table 4.19 The composition of 50 x 5052

Component	Amount
Glycerol	25 g
Glucose	2.5 g
Alpha-lactose	10 g
H ₂ O	73 ml
Total volume 100 ml	

Table 4.20 The composition of 20 x NPS

Component	Amount
(NH ₄) ₂ SO ₄	6.6 g
KH ₂ PO ₄	13.6 g
NaH ₂ PO ₄	14.2 g
H ₂ O	80 ml
Total volume 100 ml	

Table 4.21 Auto-induction medium

Component	Amount
ZY Medium	928 ml
1 M MgSO ₄	1 ml
1000 x Metal Mix	1 ml
50 x 5052	20 ml
20 x NPS	50 ml
Total volume 1 L	

4.2 Biochemical methods

4.2.1 Preparation of cell pellets for protein purification

5 g pellets of frozen *E. coli* cells were diluted with 50 ml of buffer A (running buffer for HisTrap) and re-suspended by vortexing. Small amounts of DNase and lysozyme were added. The pellets were incubated at 4 °C shaking for 30 min. Then, the resuspension was applied to sonication for 15 x 1 min, with 1 min of break between the cycles. During sonication, the cell resuspension was incubated on ice. Subsequently, the sample was centrifuged at 15000 g for 20 min to pellet cell debris. Then, the supernatant was collected and used for loading of a respective affinity-chromatography column.

4.2.2 Protein purification

For purification of heterologously produced protein from *E. coli*, the principle of nickel affinity chromatography (NAC) was used in this study. The coding sequence of the protein was cloned into *E. coli* expression vector (pET-28b), resulting in the production of the protein fused to 6xHis- tags. The 6xHis-tagged protein was immobilized at Ni²⁺-NTA-agarose resin. The protein purification steps were either conducted on an ÄKTAprime™ plus or an ÄKTAFPLC™ system (GE Healthcare, USA). The protein sample was loaded onto the NAC column with a flow rate of 1.5 ml min⁻¹, and washed with 5% of buffer B (elution buffer) in a volume of 20 ml. Then, the column was washed with 40% of buffer B, and finally with 100% of buffer B. The compositions of buffers used are shown below.

Table 4.22 Buffer A for HisTrap

Component	Concentration
Tris	0.02 M
NaCl	0.15 M
PMSF	1 ml
pH=8	

Table 4.23 Buffer B for HisTrap

Component	Concentration
Tris	0.02 M
NaCl	0.15 M
Imidazole	0.5 M
pH=8	

4.2.3 Size exclusion chromatography (SEC)

Further purification of affinity chromatography-derived proteins and determination of the enzymes' multimeric states were achieved by size exclusion chromatography (SEC). The SEC column was firstly washed with one column volume of H₂O and then with one column volume of SEC buffer. The protein sample was loaded onto the SEC column with a flow rate of 1 ml min⁻¹. Then, fractions were collected in a size of 5 ml, starting at an elution-volume of 90 ml after sample injection. Molecular weight of eluted protein was determined according to the equation shown in Figure 4.1. In this study, for protein purification, two kinds of buffer were used as the SEC buffer. Their compositions are shown below.

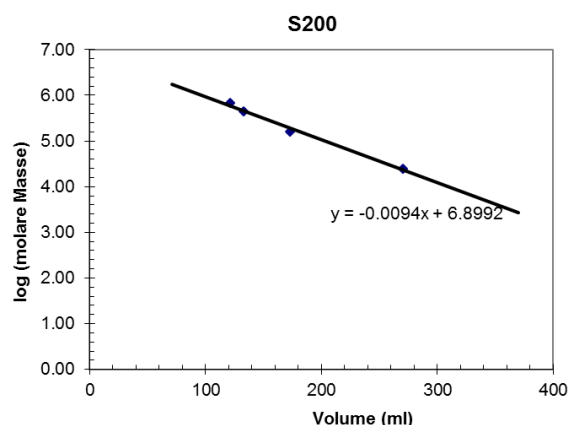


Figure 4.1 Standard curve for determination of molecular weights according to SEC. Standard curve was determined by Dr. Florian Brodhun (Department of Plant Biochemistry, University of Göttingen, Germany) according to elution volumes of HiLoad 26/60 Superdex S200 SEC-column.

Table 4.24 Tris-HCl buffer for SEC

Component	Concentration
Tris	0.05 M
NaCl	0.15 M
Glycerol	2%

pH=7

Table 4.25 Phosphate buffer for SEC

Concentration	Component
0.05 M	Phosphate buffer = 39 ml 1 M NaH ₂ PO ₄ + 61 ml 1 M Na ₂ HPO ₄
0.15 M	NaCl
30 mg	3-[(3-cholamidopropyl) dimethylammonio]-1-propanesulfonate (CHAPS)

pH=7

4.2.4 Desalting chromatography

The protein purified from affinity chromatography was load onto HisTrap Desalting Column (GE Healthcare, USA) to remove imidazole according to the manual provided by the manufacturer, protein was eluted in TBS buffer for further assay.

4.2.5 SDS polyacrylamide gel electrophoresis (SDS-PAGE)

SDS-PAGE was performed according to the method described by Weber (1977). For SDS-PAGE, protein samples were mixed with 4 x sample loading buffer and water, denatured at 95 °C for 5 min. 5 µl of denatured protein samples and 5 µl of a MW marker were loaded onto the SDS gel. SDS-PAGE was run on Mini-PROTEAN3 electrophoresis Systems at 35 mA and 300 V until the bromophenol-blue front migrated out of the gel. Proteins were stained in Coomassie-staining solution at room temperature for 2 h while shaking, then the gel was unstained with Destaining Buffer. Additionally, the SDS gel was supplemented with 2,2,2-trichloroethanol (TCE) according to Ladner *et al.* (2004) in order to achieve first, fast visualization of the separated proteins on the gel. Respective gel was developed for 2 min under UV-radiation at 312 nm. Afterwards, the gel was exposed to UV-light for 20 s while the image was recorded upon utilization of the SybrGreen-filter in a Diana machine.

Table 4.26 Stacking gels (4%) for SDS-PAGE

Component	Amount
ddH ₂ O	6.12 ml
0.5 M Tris/HCl, pH = 6.8	2.5 ml
Acrylamide bis-acrylamid (30% of acrylamid, w/v)	1.3 ml
APS (25%, w/v)	400 µl
TEMED	100 µl

Table 4.27 Separation gels (12%) for SDS-PAGE

Component	Amount
ddH ₂ O	5.52 ml
Acrylamide bis-acrylamid (30% of acrylamid, w/v)	6.4 ml
0.5 M Tris/HCl, pH = 8.8	4.00 ml
APS (25%, w/v)	64 µl
TEMED	16 µl

Table 4.28 The composition of 10 x gel running buffer

Concentration	Component
200 mM	Glycine
25 mM	Tris/HCl, pH = 8.0
0.1% (w/v)	SDS

Table 4.29 The composition of 4 X sample loading buffer

Component	Amount
1 M Tris HCl pH 6.8	1.5 ml
1 M DTT (dithiothreitol)	3 ml
SDS	0.6 g
Bromophenol blue	0.03 g
Glycerol	2.4 ml

Table 4.30 The composition of staining buffer

Component	Concentration
H ₂ O	50% (v/v)
Ethanol	40% (v/v)
Acetic acid	10% (v/v)
Coomassie Brilliant Blue G250	0.5% (w/v)

Table 4.31 The composition of destaining buffer

Component	Concentration
H ₂ O	60% (v/v)
Ethanol	30% (v/v)
Acetic acid	10% (v/v)

4.2.6 Measurement of protein concentration

The concentrations of protein were determined using the method described by Bradford (1976). A respective calibration curve was prepared with BSA as the standard in a linear range of 20 $\mu\text{g ml}^{-1}$ to 1000 $\mu\text{g ml}^{-1}$. For preparation of the calibration curve as well as for determination protein

concentration of unknown samples, 1 ml of Bradford-Reagent was mixed with 20 μ l protein sample and briefly vortexed. After incubation in the dark for 10 min, the absorption of sample was measured at 595 nm in a spectrophotometer. 1 ml of Bradford-Reagent without any sample was used as a blank-value.

Table 4.32 The composition of bradford-reagent

Component	Amount
Serva Blue G	35 g
Ethanol	25 ml
85% Phosphoric acid	50 ml
H ₂ O	425 ml

4.2.7 DTNB-based *in vitro* test of acyltransferase activity

The activity of WS was tested according to the method described by Willis *et al.* (2008). DTNB-based *in vitro* assay was used to monitor the enzyme-mediated cleavage of acyl-CoA-derived thioester-bonds. The enzyme catalyzes the cleavage of acyl-CoA resulting in the liberation of free CoA-SH molecule. Free CoA-SH reacts with the intramolecular disulfide bond of a DTNB molecule, therefore the disulfide bond is cleaved. As a result, a disulfide consisting of a CoA and a 5-thio-2-nitrobenzoic acid (TNB) is generated. At the same moment, a free TNB²⁻-ion is released, which absorbs at 412 nm and appears yellow.

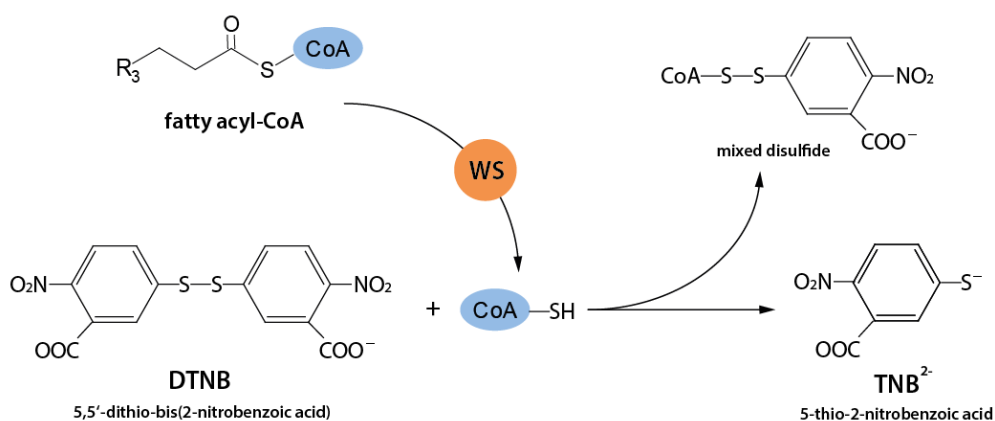


Figure 4.2 Reaction scheme of the DTNB-reaction. DTNB is cleaved, forming a mixed disulfide with free CoA molecules and a TNB²⁻ ion which absorbs at 412 nm.

The reaction sample contained 0.2 mg ml⁻¹ DTNB, the same amount of fatty alcohol and fatty acyl-CoA in a total volume of 1 ml TBS. The sample was pipetted in polystyrene cuvettes without enzymes and vortexed for 5 s. Cuvettes were placed in a Cary 100 Bio spectrophotometer (Varian, Germany) and the measured absorbance was taken as a blank-value. After absorbance stabilized to a continuous baseline, the enzyme was added, then the reaction sample was vigorously mixed and the increased absorbance was continuously recorded at 412 nm.

4.3 Imaging methods

4.3.1 Gold particle preparation for bombardment

Gold particles for DNA coating were prepared according to the method described by Sanford *et al.* (1993). 10 mg of 1 µm gold particles was suspended in 500 µl 100% ethanol. After centrifugation for 30 s at 4000 g, the supernatant was removed and the pellets were re-suspended in 250 µl 100% ethanol. The gold particles were vortexed for 1 min, and centrifuged for 30 s. After removing the supernatant, the pellets were washed 3 times with 250 µl sterile water. The gold particles were suspended in 150 µl water after the final centrifugation. Then, the suspension was divided in 50 µl aliquots and kept on ice. To precipitate plasmids with gold particles, 5 - 8 µg of plasmids were added to one aliquot gold particles, and vortexed for 10 s and incubated on ice for 5 min. After 50 µl 2.5 M CaCl₂ was added, the sample was vortexed for 10 s and incubated on ice for 1 min. Afterwards, 20 µl 0.1 M spermidine was added, the sample was vortexed and incubated on ice for 1 min and vortexed again for 3 min. Then, the supernatant was removed after centrifugation for 5 s. Subsequently, the pellets were re-suspended in 250 µl 96% pure ethanol, and vortexed for 1 min. After centrifugation for 15 s, the pellets were washed 2 times with 50 µl 96% pure ethanol, and finally dissolved in 60 µl ethanol, kept at -20 °C until use.

4.3.2 Particle bombardment

The bombardment with plasmid-coated gold particles was used to transform onion epidermal cells. A helium-driven particle accelerator (PDS-1000/he; Bio-Rad), a vacuum of 27 inches of mercury and 1350 psi rupture discs were used. After particle bombardment, the onion epidermal cells were kept in a humid condition and incubated for 20 h.

4.3.3 Microscopy

Images were recorded using an Olympus-U-RFL-T fluorescence microscope with an ORCA-Flash 4.0 digital camera. Images of onion epidermal cells were analyzed and overlay by ImageJ.4.4 Analytical methods.

4.4 Analytical methods

4.4.1 Wax ester extraction from *S. cerevisiae*

Extraction of wax esters from *S. cerevisiae* was done similar as described by Kawelke and Feussner (2015). In detail, cells corresponding to 50 OD₆₀₀ units were harvested by centrifugation at 1000 g for 10 min. After centrifugation, 1 ml methanol was added to the cell-pellets together with 0.5 mm glass beads. Then, the samples were vortexed for 15 min at room temperature (RT). Subsequently, 2 ml hexane was added, samples were vortexed for another 15 min at RT. The upper phase was removed, evaporated under nitrogen stream and resolved in 200 µl of *n*-hexane. The sample was transferred to GC-vials and stored at -20 °C for further analysis.

4.4.2 Wax ester extraction from seeds of *C. sativa* and *A. thaliana*

Extraction of wax esters from seeds was done according to the method described by Iven *et al.* (2013). 5 mg seeds for *A. thaliana* or 10 mg dry seeds for *C. sativa* were used. Seeds were homogenized in an 8 ml screw lid glass tube with some sea sand (Carl Roth GmbH, Karlsruhe, Germany). Then, 2 ml of chloroform: methanol (1:1, v/v) was added, and 5 nmol of heptadecanoyl - heptadecanoate (di-17:0) was added as an internal standard. The sample was shaken at 4 °C for 20 min. After centrifugation at 450 g for 5 min, the supernatant was transferred into a new glass tube, and the pellet was re-extracted with 1 ml of *n*-hexane: diethyl ether: glacial acetic acid (65:35:1, v/v/v). The sample was pelleted again by centrifugation at 450 g for 5 min. The supernatants from two steps of extraction were combined, and evaporated under streaming nitrogen. Finally, the lipid extract was dissolved in 100 µl chloroform.

4.4.3 Thin layer chromatography analysis

Thin layer chromatography (TLC) analysis of wax esters and TAGs was done as described previously (Heilmann *et al.*, 2012). For TLC analysis of lipid extracts, 40 µl sample for seed lipid extraction, or 50 µl sample for yeast lipid extraction were applied on silica gel glass TLC plates (Merck, Darmstadt, Germany) with the assistance of an AUTOMATIC TLC SAMPLER 4 (Camag, Muttenz, Switzerland). The

TLC plate was developed in a glass chamber containing hexane: diethyl ether: acetic acid (80:20:1, v/v/v) as a running solvent. Separated bands of lipids were visualized by incubating dry TLC plates in CuSO₄ solution. After drying, the plates were heated up to 190 °C on a CAMAG TLC Heater. Bands were assigned to different lipid classes according to their migration behavior in comparison to respective standard substances. Standard-substances were applied at amounts of 50 µg each. For analysis of wax esters, di-17:0 was used as standard, hexadecanoyl alcohol (17:0-OH) for fatty alcohols, and olive oil for TAGs were applied as standards on respective TLC plate.

4.4.4 Transesterification of *C. sativa* cotyledons

For analysis of fatty acid profile of *C. sativa* cotyledons, total lipids of one cotyledon of seedlings were first extracted as described in section 4.4.2. Then, 6 µl cotyledon extract of each sample was dried under nitrogen stream. Afterwards, 330 µl methanol and 170 µl 0.5 M sodium methoxide were added, and the sample was shaken for 20 min at room temperature. After 500 µl saturated NaCl solution was added, the sample was extracted twice with 1 ml *n*-hexane. Then, the hexane phases were transferred into a new eppendorf tube, and the combined upper phases were evaporated under nitrogen stream. Finally, the extract was dissolved in 100 µl methanol and stored at -20 °C for gas chromatograph-flame ionization (GC-FID) analysis.

4.4.5 GC-FID analysis of fatty acid profile of *C. sativa* seed oil

To analyze the fatty acid profile of *C. sativa* seed oil, acidic methanolysis and GC-FID detection of the fatty acid methyl esters were performed as described previously (Miquel and Browse, 1992). 10 mg seeds were homogenized to powder. Then, 2 ml FAME solution was directly added.

Table 4.33 The composition of FAME Solution

Component	Concentration
H ₂ SO ₄	25 ml
Dimethoxypropan	20 ml
Methano/Toluol (2:1, v/v)	660 ml/330 ml

The sample was incubated at 80 °C for 1 h. Afterwards, 400 µl saturated NaCl solution was added, and the sample was vortexed vigorously. Then, the sample was extracted with 3 ml *n*-hexane 2 times. The hexane upper phases were combined and evaporated under nitrogen steaming. The sample was re-

suspend in 2 ml *n*-hexane and 2 ml dest H₂O was added. After centrifugation of the sample at 450 g for 10 min, the upper phase was transferred into a new Kimble-Glass tube. The hexane was then evaporated and the sample was dissolved in 100 µl acetonitrile for GC-FID detection.

4.4.6 Wax ester analysis via GC-MS

Analysis of wax esters via GC-MS was done according to Heilmann *et al.* (2012), Kawelke and Feussner (2015), to confirm the signals of wax ester fractions. Lipid extracts were prepared according to section 4.4.2. Of these samples, 2 µl sample was injected into a Trace gas chromatograph (Thermo Finnigan, Austin, TX, USA) with a Restek Rxi™ - 5ms capillary column (15 m x 0.25 mm, 0.25 µm film thickness; Restek, Bellefonte, PA, USA), and connected with a Polaris Q mass selective detector. The carrier gas was helium at a flow rate of 1.5 ml min⁻¹. The temperature gradient was 60 °C for 2 min, 40 K min⁻¹ at 60 °C - 200°C, 200 °C for 2 min at, 3 K min⁻¹ at 200 °C - 340 °C and finally 340 °C for 16 min. The wax esters were detected by the electron impact ionization (Aux-line 350 °C, ion source 200 °C, -70 eV) in a mass range of 50 - 730 amu.

4.4.7 GC-FID analysis of wax esters and TAGs

To determine the yield and profile of wax esters and TAGs, GC-FID detection was performed. Lipid extracts were prepared according to section 4.4.2. 50 µl of 1 µg µl⁻¹ di-17:0 and 50 µl of 2 µg µl⁻¹ tripentadecanoate (tri-15:0) were added to the sample as internal standards. The crude seed oil extract was spotted on a TLC plate and developed as described in section 4.4.3. The TLC plate was sprayed with 8-anilino-1-naphthalenesulfonic acid (0.2%, w/v), and the lipid bands of wax esters and TAGs were marked under UV light. Then, the silica containing wax esters or TAGs were scraped from the TLC plate and transferred into a glass tube. The silica powder with lipids were extracted twice using 1 ml *n*-hexane. After centrifugation at 450 g for 5 min, the solvent supernatants of two extractions were combined and evaporated under streaming nitrogen. The acidic methanolysis process was then done according to section 4.4.5.

For GC-FID detection, 10 µl methanolysed of wax ester or TAG fraction were transferred to a GC-vial with glass inlet. To measure wax esters, the GC running program with long retention time (30 min) was used. In order to completely separate the overlaid peaks of FAMES and OHs, and 5 µl *N,O*-Bis(trimethylsilyl) trifluoroacetamide (BSTFA) was added to the methanolysed wax ester fraction. The silylated fatty alcohols deriving from steryl esters also exist in the wax ester fractions. So the alcohol profiles of wild type plants were also measured, used as a negative control and subtracted from the alcohol profiles of transgenic lines.

4.4.8 Nano-ESI-MS/MS analysis of wax ester molecular species

The molecular species of wax esters were measured by nano-electrospray ionization tandem mass spectrometry (nano-ESI-MS/MS) according to the protocol described in previous studies (Iven *et al.*, 2013; Iven *et al.*, 2015). Briefly, the crude lipids of 5 mg seed were extracted according to the steps in section 4.4.2, and 5 nmol di-17:0 was added as internal standard. Wax esters were separated by preparative TLC from the crude lipid extraction, especially from TAGs. As steryl esters and wax esters cannot be completely separated by the TLC, the analytical samples for nano-ESI-MS/MS also contained steryl esters. Wax esters were recovered from silica-plate and extracted with 1 ml *n*-hexane twice, then the solvent was dried under streaming nitrogen. The wax ester extract was dissolved in 2 ml methanol: chloroform (2:1, v/v) with 5 mM ammonium acetate for nano-ESI-MS/MS.

In general, an Applied Biosystems 3200 hybrid triple quadrupole/linear ion trap mass spectrometer (ABSciex, Germany) was used to perform the analysis. 10 µl wax ester extract was directly injected into the nano-ESI with a chip ion source (TriVersa NanoMate; Advion BioSciences, Ithaca, USA), in the backpressure of 0.4 psi and in the positive ionization mode (1.5 kV). In the present study, peak intensities of 485 MRM transitions, corresponding to even chain wax ester molecular species with acyl moieties of C₁₆ - C₂₄ containing 0 - 3 double bonds and C₂₆ with 0 - 1 double bond, were collected with the software of Analyst 1.5.1 (AB Sciex, Germany). Signal intensities were extracted with the software of LipidView (AB Sciex, Germany), and the signals below 50 counts per second were treated as background and deleted during calculation. The profiles of wax ester molecular species and calculating the total amounts of wax esters were performed using the Excel 2007 software (Microsoft Deutschland GmbH, Germany).

4.5 Statistical methods

The data obtained in this study were calculated with the Excel 2007 software (Microsoft Deutschland GmbH, Germany). Student's t-tests were performed to compare the significant differences between the different constructs. All the tests were two-sided type 3 tests.

5 RESULTS

To expand the natural resource of wax esters for lubrication application, a wax ester biosynthesis pathway was established in seeds of *C. sativa* in a previous study. Wax esters were successfully accumulated in seeds of *C. sativa*, but the amount of wax esters need to be enhanced for industrial application. In order to further increase the overall yield of wax esters, and especially to enhance the formation of 18:1/18:1 in the seed oil of *C. sativa*, several approaches were conducted in the present study. In general, there were two strategies applied in this thesis. On one aspect, the production of wax esters is determined by the activities and substrate specificities of FARs and WSs. Thus, one strategy is the optimization of the wax ester production enzymes. On the other hand, since the content and composition of wax esters are highly influenced by the acyl-CoA pool of host cells, the second strategy is to adjust the substrate pool of wax ester biosynthesis by modification of the lipid metabolic pathways of *C. sativa*.

The first part of the results focus on the utilization of new enzyme combinations, the re-localization of FARs or WSs and the enhancement of the enzyme activity. The second part of the results are about metabolic engineering of the formation of fatty acyl-CoAs in *C. sativa* seeds.

5.1 Fusion of *MaFAR* with *ScWS* to locate *MaFAR* to the ER

In a previous study, co-expression of *MaFAR* and *ScWS* resulted in high yields of 18:1/20:1 in seeds of *A. thaliana* and *C. sativa*, indicating this combination of enzymes is beneficial for the formation of monounsaturated wax esters. As it is known that the localization of an enzyme has important effects on its activity and substrate preference, so the re-localization of wax ester production enzymes might be an approach to increase the amount of 18:1/18:1. According to TMHMM analysis, *ScWS* is predicted to contain seven transmembrane domains (Supplementary Material 1. A), and localizes to the ER membrane (Figure 5.1.1). Whilst, *MaFAR* (Maqu_2220) is predicted to be a cytosolic protein (Supplementary Material 2), which may use both acyl-CoAs and acyl-ACPs as substrates to produce fatty alcohols. Hence, in consideration of the different subcellular localizations of *MaFAR* and *ScWS*, it might be an optimization for *MaFAR* to re-localize it to the ER, so that *MaFAR* can access the membrane-localized substrates, as well as interact with *ScWS* as a dimeric protein. Therefore, a *ScWS-MaFAR* fusion protein was generated by fusing *MaFAR* to the C-terminal end of *ScWS* with a small linker (Figure 5.1.1), to produce a bifunctional enzyme which might display enhanced catalytic activity.

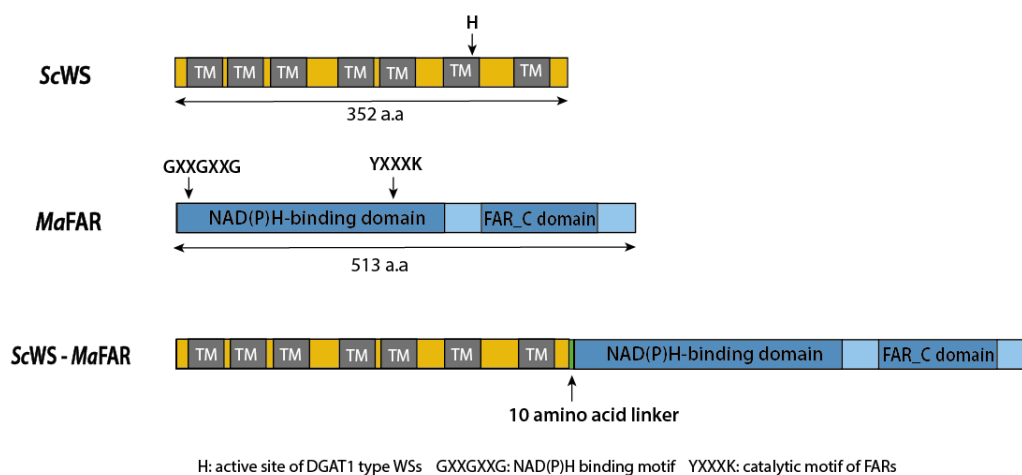


Figure 5.1.1 Domain structure of the ScWS-MaFAR fusion protein. The sequence of ScWS is predicted to contain seven transmembrane domains, and the protein localizes to the ER according to the TMHMM analysis (Supplementary Material 1. A). The sequence of MaFAR contains no transmembrane domains and this protein is predicted to be localized in the cytosol (Supplementary Material 2). MaFAR was fused to the C-terminal end of ScWS with a 10 amino acid linker. H: a histidine residue is believed as the active site of DGAT1/plant type WS. GXXGXXG: NAD(P)H motif of FAR. YXXXX: catalytic motif of FAR. TMHMM analysis was performed according to the method of Sonnhammer *et al.* (1998).

5.1.1 Expression of ScWS-MaFAR in *S. cerevisiae*

The ability of the ScWS-MaFAR fusion protein to produce wax esters was first tested in a quadruple mutant *S. cerevisiae* strain (H1246), in which four genes contributing to the biosynthesis of neutral lipids are knocked out (Sandager *et al.*, 2002). The ScWS-MaFAR fusion protein, as well as MaFAR and ScWS as single construct were expressed in yeast, MaFAR and ScWS were also co-expressed as separate peptides in yeast. The yeast cells were cultivated with or without fatty alcohol (18:1-OH), and total lipids were extracted and analyzed with TLC (Figure 5.1.2).

Expression of an empty vector with feeding fatty alcohol did not result in the accumulation of any neutral lipids (neither steryl esters, wax esters nor TAGs). Expression of MaFAR without fatty alcohol and ScWS with fatty alcohol were used as controls to check whether the single enzymes display activities in yeast, and if therefore the ScWS-MaFAR fusion protein has activity to produce fatty alcohols and wax esters. Without feeding fatty alcohol, the accumulation of fatty alcohols were found in the yeast cells with ScWS-MaFAR, similar as MaFAR and MaFAR/ScWS co-expression, indicating that the ScWS-MaFAR fusion protein has a FAR activity. Meanwhile, the accumulation of wax esters was observed in the yeast cells transformed with ScWS-MaFAR as well as MaFAR/ScWS, proving that the fusion protein was also active as a WS. With feeding fatty alcohol, the yeast cells transformed with ScWS, ScWS-MaFAR and MaFAR/ScWS seem to accumulate higher amounts of wax esters compared

with those of feeding no fatty alcohols (Figure 5.1.2).

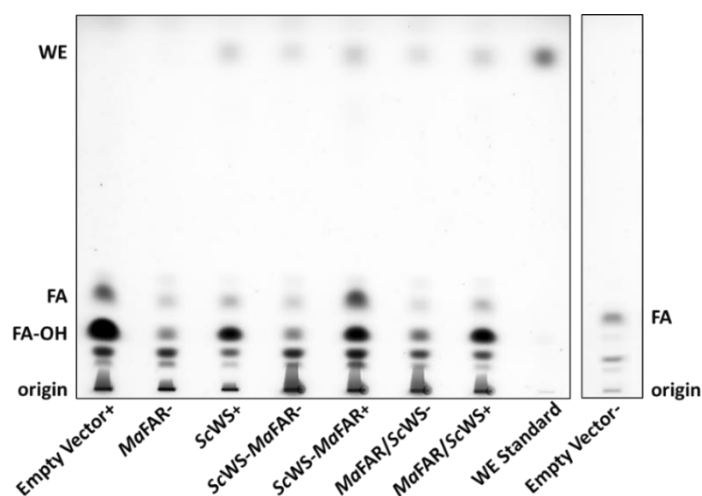


Figure 5.1.2 Accumulation of neutral lipids in *S. cerevisiae* transformed with empty vector, *MaFAR*, *ScWS*, *ScWS-MaFAR* fusion protein, *MaFAR/ScWS* co-expression. The yeast strain (H1246) is deficient in neutral lipid production, no wax esters, TAGs or steryl esters were accumulated in the yeast cells transformed with empty vector. + means the yeast cells were fed with fatty alcohol (18:1-OH). – means the yeast cells were not fed with fatty alcohol. Yeast cells were cultivated for 3 days, before the total lipids were extracted from OD₆₀₀ 50 cells. Thin layer chromatography (TLC) was performed with hexane: diethyl ether: acetic acid (80:20:1, v/v/v) as a running solvent, after incubating dry TLC plates in CuSO₄ solution, the plate was heated at 190 °C till to the appearance of lipid spots. This is representative for two experiments. WE, wax ester; FA, fatty acid; FA-OH, fatty alcohol.

5.1.2 Expression of *ScWS-MaFAR* in seeds of *A. thaliana*

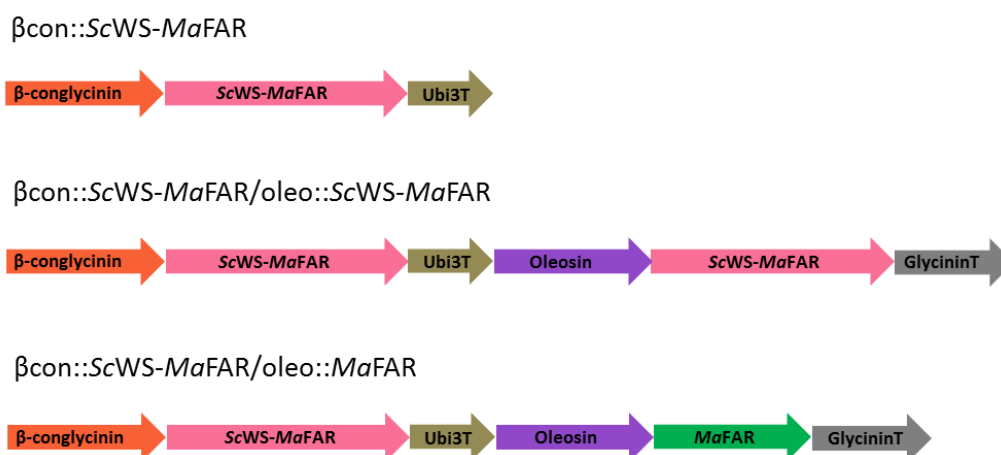


Figure 5.1.3 DNA constructs used for the seed-specific expression of the *ScWS-MaFAR* fusion protein. The *ScWS-MaFAR* fusion protein was expressed under the β -conglycinin promoter (β con) or the oleosin promoter (oleo) from soybean. *MaFAR* was expressed under the soybean oleosin promoter. The DNAs of the promoters to generate the respective vectors was provided by Prof. Edgar Cahoon (UNL, NE, USA).

The ScWS-*MaFAR* fusion protein was tested to be active as both FAR and WS (Figure 5.1.2). Then, this fusion protein was expressed in the seeds of *A. thaliana*, where the resulting transgenic lines could be compared with the existing *MaFAR/ScWS* co-expression lines. The ScWS-*MaFAR* was expressed in *A. thaliana* as single copy under the seed specific β -conglycinin promoter from soybean with Ubi3 terminator. To increase the total yield of wax esters as high as possible, two copies of ScWS-*MaFAR* were expressed under β -conglycinin promoter with the Ubi3 terminator and soybean oleosin promoter with the glycinin terminator, respectively. Additionally, one copy of ScWS-*MaFAR* was co-expressed together with *MaFAR* to offer more fatty alcohol substrates to the fusion protein (Figure 5.1.3).

Table 5.1.1 Numbers of harvested T2 *A. thaliana* transgenic lines transformed with β con::*ScWS-MaFAR*, β con::*ScWS-MaFAR/oleo::ScWS-MaFAR* and β con::*ScWS-MaFAR/oleo::MaFAR*, numbers of transgenic lines analyzed by TLC and GC-FID.

Construct	Number of T2 lines	TLC analysis	GC-FID analysis
β con:: <i>ScWS-MaFAR</i>	60	40	3
β con:: <i>ScWS-MaFAR/oleo::ScWS-MaFAR</i>	61	40	3
β con:: <i>ScWS-MaFAR/oleo::MaFAR</i>	48	40	3

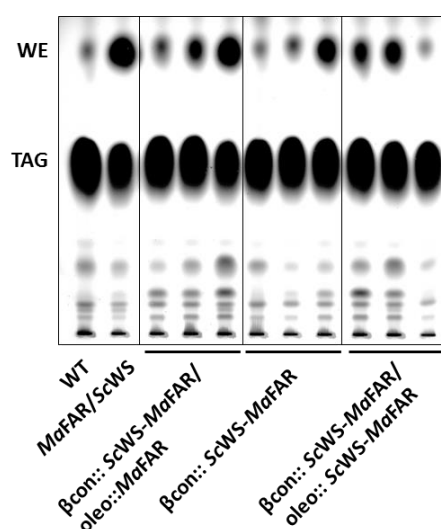


Figure 5.1.4 Neutral lipid accumulation in seeds of wild-type, *A. thaliana* transformed with *MaFAR/ScWS*, β con::*ScWS-MaFAR*, β con::*ScWS-MaFAR/oleo::ScWS-MaFAR* and β con::*ScWS-MaFAR/oleo::MaFAR*. Neutral lipids of T2 transgenic seeds were extracted according to the method described in section 4.4.2. Thin layer chromatography (TLC) was performed with hexane: diethyl ether: acetic acid (80:20:1, v/v/v) as a running solvent, after incubating dry TLC plates in CuSO_4 solution, the plate was heated at 190 °C till to the appearance of lipid spots. TLC plate showing the spots of triacylglycerols (TAGs) and wax esters (WEs). The selected three individuals for each construct are shown as three representative.

The DNAs of $\beta\text{con}::\text{ScWS-MaFAR}$, $\beta\text{con}::\text{ScWS-MaFAR/oleo}::\text{ScWS-MaFAR}$ and $\beta\text{con}::\text{ScWS-MaFAR/oleo}::\text{MaFAR}$ were cloned into the pCAMBIA 33.0 destination vector with a phosphinothricin resistance gene. After phosphinothricin selection, more than one hundred heterozygous *A. thaliana* T2 transgenic lines containing $\beta\text{con}::\text{ScWS-MaFAR}$, $\beta\text{con}::\text{ScWS-MaFAR/oleo}::\text{ScWS-MaFAR}$, or $\beta\text{con}::\text{ScWS-MaFAR/oleo}::\text{MaFAR}$ were generated (Table 5.1.1). Forty transgenic lines for each combination were first analyzed by running the neutral lipid extracts of their seeds via TLC as shown in Figure 5.1.4, then the best three performing individual lines of each combination were analyzed by GC-FID to determine the total yields of wax esters and TAGs in seeds.

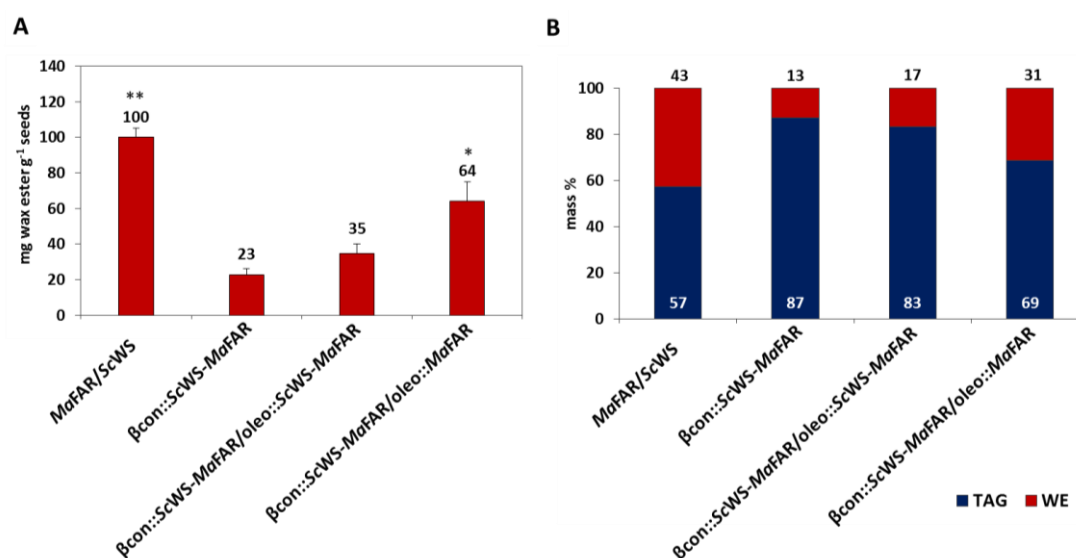


Figure 5.1.5 Quantification of wax esters in seeds of *A. thaliana* transformed with *MaFAR/ScWS*, $\beta\text{con}::\text{ScWS-MaFAR}$, $\beta\text{con}::\text{ScWS-MaFAR/oleo}::\text{ScWS-MaFAR}$ and $\beta\text{con}::\text{ScWS-MaFAR/oleo}::\text{MaFAR}$. (A) Absolute quantification of wax esters in mg g⁻¹ seeds. *means significantly different from $\beta\text{con}::\text{ScWS-MaFAR}$, $p \leq 0.05$; **means significantly different from $\beta\text{con}::\text{ScWS-MaFAR}$, $p \leq 0.01$. (B) The relative quantification of total neutral lipids (WE, wax ester; TAG, triacylglycerol) in mass% are calculated according to the absolute quantification of each lipid class. The data shown is an average of three individual heterozygous T2 lines for each enzyme combination with two extraction replicates for each individual line. βcon , β -conglycinin promoter; oleo, oleosin promoter.

Expression of a single copy of *ScWS-MaFAR* resulted in an average accumulation of 23 mg g⁻¹ wax esters in the seeds of *A. thaliana* (Figure 5.1.5 A). The second copy of *ScWS-MaFAR* expressed under a different promoter further increased the yield of wax esters up to around 35 mg g⁻¹, but it was not remarkably different from that of the $\beta\text{con}::\text{ScWS-MaFAR}$ line. Co-expression of *ScWS-MaFAR* together with one copy of *MaFAR* under different promoters led to a significant enhancement of wax ester content up to 64 mg g⁻¹ in the seeds of *A. thaliana*, which was more than the double amount of the wax esters produced by the $\beta\text{con}::\text{ScWS-MaFAR}$ line. However, this result was still much lower than the 100 mg g⁻¹ of wax esters that accumulated in the seeds of the *MaFAR/ScWS* line (Figure 5.1.5 A). As consequence, the wax ester to TAG ratio was 13% for the $\beta\text{con}::\text{ScWS-MaFAR}$ line, 17% for

β con::*ScWS-MaFAR/oleo*::*ScWS-MaFAR* line and 31% for the β con::*ScWS-MaFAR/oleo*::*MaFAR* line, being lower than the 43% of the *MaFAR/ScWS* line (Figure 5.1.5 B).

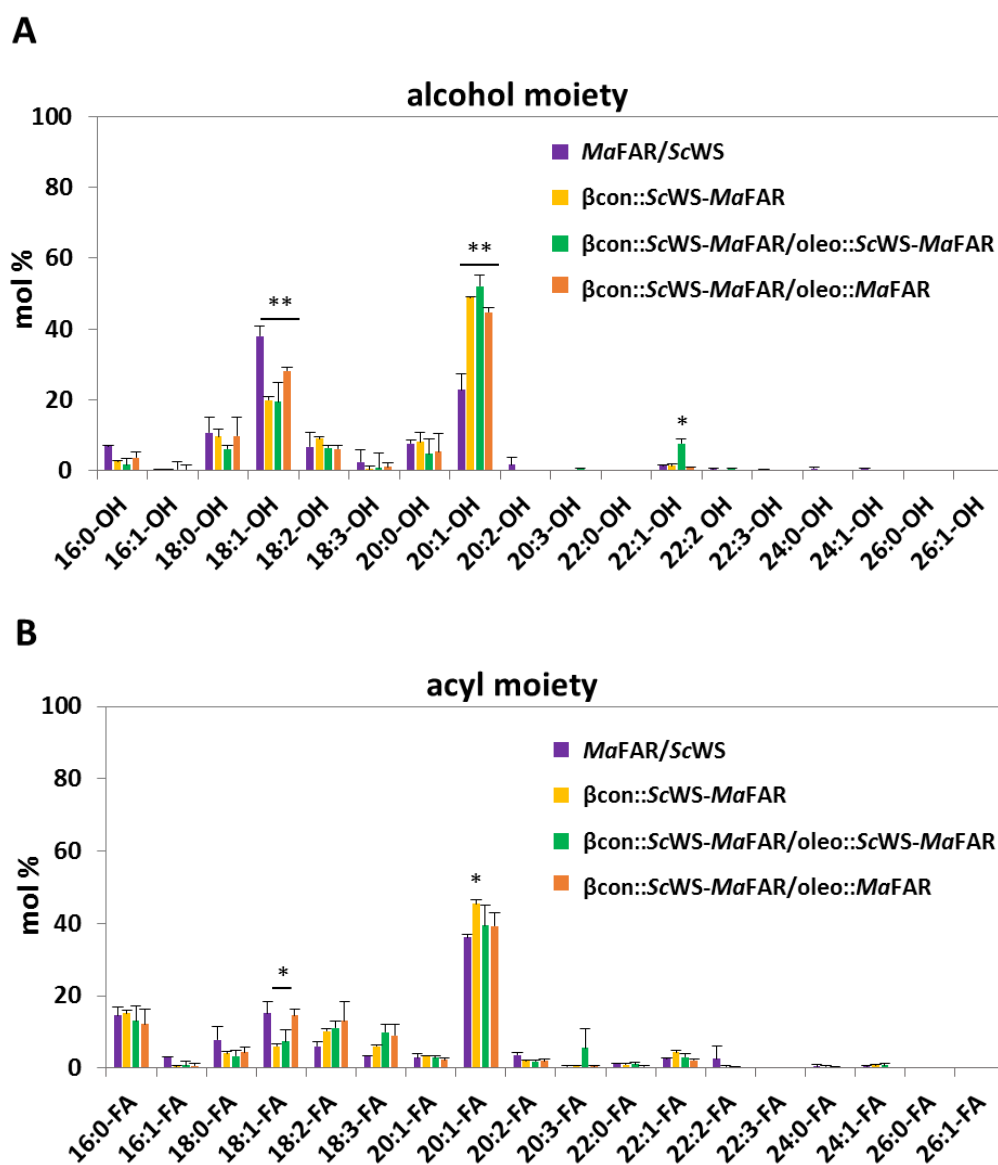


Figure 5.1.6 Alcohol and acyl moieties of wax esters in seeds of *A. thaliana* transformed with *MaFAR/ScWS*, β con::*ScWS-MaFAR*, β con::*ScWS-MaFAR/oleo*::*ScWS-MaFAR* and β con::*ScWS-MaFAR/oleo*::*MaFAR*. (A) Relative abundance of alcohol moieties in mol%. (B) Relative abundance of acyl moieties in mol%. The data shown is an average of three individual heterozygous T2 lines for each enzyme combination with two extraction replicates for each individual line. *means significantly different from *MaFAR/ScWS*, $p \leq 0.05$; **means significantly different from *MaFAR/ScWS*, $p \leq 0.01$.

The compositions of wax esters accumulated in the seeds of *A. thaliana* transformed with *ScWS-MaFAR* differed remarkably from that in the *MaFAR/ScWS* co-expression line (Figure 5.1.6). In the wax esters accumulated in the seeds of the *MaFAR/ScWS* line, oleic alcohol (18:1-OH) was the most abundant alcohol species (almost 40 mol%), followed by gondoic alcohol (20:1-OH, 23 mol%). However,

the wax esters produced by the $\beta\text{con}::\text{ScWS-MaFAR}$, $\beta\text{con}::\text{ScWS-MaFAR/oleo}::\text{ScWS-MaFAR}$ and $\beta\text{con}::\text{ScWS-MaFAR/oleo}::\text{MaFAR}$ lines predominantly consisted of 20:1-OH, accounting for 45 mol% - 52 mol% of total fatty alcohols, which were significantly higher than that of *MaFAR/ScWS* line. Meanwhile, a significantly lower abundance of 18:1-OH (20 mol% - 28 mol%) as observed in the three lines with *ScWS-MaFAR*, compared with the *MaFAR/ScWS* line (Figure 5.1.6 A).

The wax esters produced by the *MaFAR/ScWS* line consist of 40 mol% gondoic acid (20:1-FA) in all fatty acid species (Figure 5.1.6 B). The wax esters produced by the $\beta\text{con}::\text{ScWS-MaFAR}$ line composed of significantly higher levels of 20:1-FA compared with *MaFAR/ScWS*. Furthermore, expression of one or two copies of *ScWS-MaFAR* resulted in significantly decreased mol% of oleic acid (18:1-FA) in comparison to *MaFAR/ScWS*. The increased levels of gondoyl alcohol and acyl moieties in the wax esters of the three *ScWS-MaFAR* lines indicated the preference of the *ScWS-MaFAR* fusion protein to $\text{C}_{20:1}$ substrates.

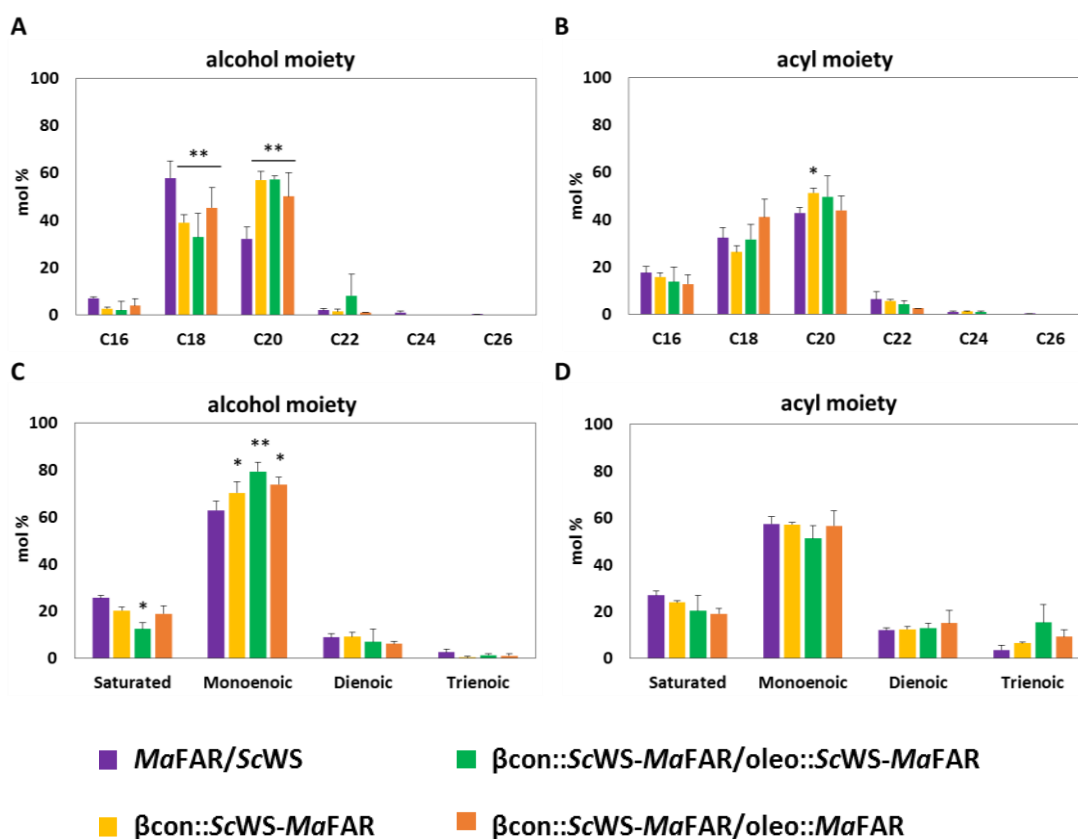


Figure 5.1.7 Relative abundance of alcohol and acyl moieties of wax esters in seeds of *A. thaliana* transformed with *MaFAR/ScWS*, $\beta\text{con}::\text{ScWS-MaFAR}$, $\beta\text{con}::\text{ScWS-MaFAR/oleo}::\text{ScWS-MaFAR}$ and $\beta\text{con}::\text{ScWS-MaFAR/oleo}::\text{MaFAR}$. **(A)** Alcohol moiety calculated by total carbon number. **(B)** Acyl moiety calculated by total carbon number. **(C)** Alcohol moiety calculated by desaturation degree. **(D)** Acyl moiety calculated by desaturation degree. The data is calculated according to the wax ester composition shown in Figure 5.1.6, and is an average of three individual heterozygous T2 lines of each enzyme combination with two extraction replicates for each

individual line. *means significantly different from *MaFAR/ScWS*, $p \leq 0.05$; **means significantly different from *MaFAR/ScWS*, $p \leq 0.01$.

With regard to the chain length of the substrates incorporated into wax esters, the three transgenic lines containing *ScWS-MaFAR* showed an obvious preference for C_{20} alcohols instead of C_{18} alcohols in comparison to *MaFAR/ScWS* (Figure 5.1.7 A). The β con::*ScWS-MaFAR* also showed higher specificity to C_{20} acyl-CoAs compared with *MaFAR/ScWS* (Figure 5.1.7 B). The three transgenic lines with *ScWS-MaFAR* also had higher preference for monounsaturated alcohols compared with the *MaFAR/ScWS* co-expression (Figure 5.1.6 C). While, no significant differences were observed on the saturation degree of acyl-CoAs utilized by *ScWS-MaFAR* and *MaFAR/ScWS* (Figure 5.1.6 D).

In summary, the introduction of a fusion protein containing the catalytic domains of both *MaFAR* and *ScWS* expressed as a single polypeptide led to the formation of wax esters. But unfortunately, upon expression in seeds of *A. thaliana*, lower amounts of wax esters were produced by the three lines with the *ScWS-MaFAR* fusion protein, in comparison to the expression of *ScWS* and *MaFAR* as separate polypeptides. Furthermore, the *ScWS-MaFAR* fusion protein showed higher substrate preference for C_{20} acyl-CoAs and C_{20} alcohols than the co-expression of *ScWS* and *MaFAR*, which was a negative effect on the formation of 18:1/18:1. Thus, the *ScWS-MaFAR* fusion protein was not expressed in seeds of *C. sativa*.

5.2 Bifunctional enzyme *AbWSD1* from *A. baylyi* ADP1

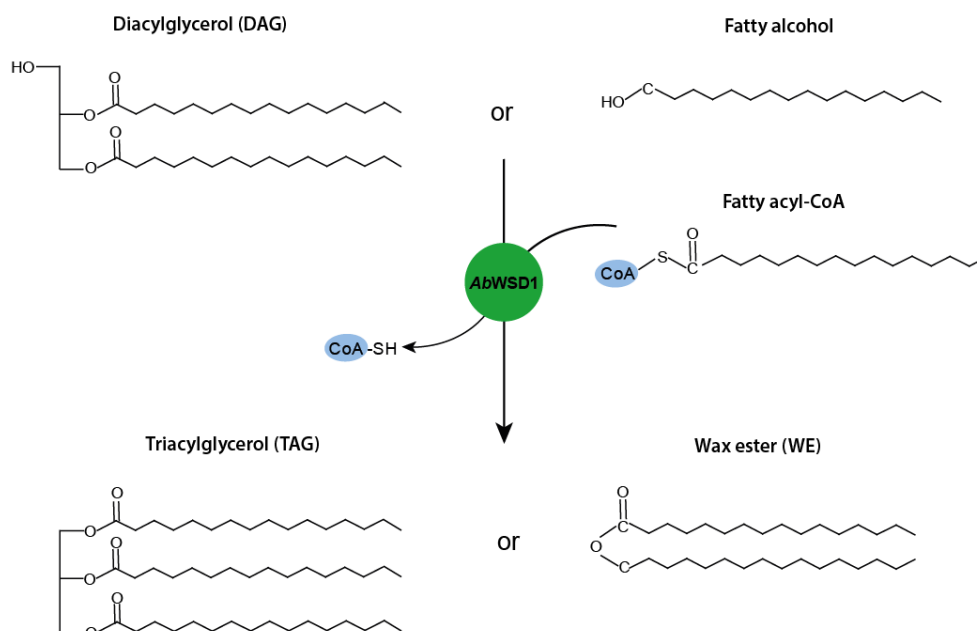


Figure 5.2.1 *AbWSD1* catalyzes the synthesis of TAGs or wax esters from fatty acyl-CoAs and diacylglycerols or fatty alcohols, respectively.

The long-chain wax esters containing one double bond in either alcohol or acyl moiety are favorite for lubrication purpose. In a previous research, the jojoba wax synthase (*ScWS*) was proved to harbor specificity to the substrates with 20 carbons (Iven *et al.*, 2015). To optimize the composition of wax esters, utilizing enzymes exhibiting higher specificity to $C_{18:1}$ substrates would be helpful to increase the level of 18:1/18:1 in the produced wax esters. The enzyme from *A. baylyi ADP1* (*AbWSD1*) is a bifunctional WS/DGAT enzyme. *AbWSD1* catalyzes the synthesis of wax esters or TAGs from fatty acyl-CoAs with fatty alcohols or DAGs (Figure 5.2.1). It was observed to exhibit 10-fold-higher WS activity than DGAT activity and has preference forwards the substrates with 18 carbons (Röttig and Steinbüchel; 2013; Stöveken *et al.*, 2005). It was interesting to utilize *AbWSD1* for wax ester production in seeds of *C. sativa*.

5.2.1 Co-expression of *MaFAR* with *AbWSD1* in seeds of *A. thaliana*

To check the wax ester production activity of *AbWSD1* in plants, this enzyme was first co-expressed with *MaFAR* under the seed-specific promoter (*napin*) in both *A. thaliana* Col._0 background and a high oleic background (*fae1 fad2* double mutant). Over fifty T2 transgenic lines containing *MaFAR/AbWSD1* were generated (Table 5.2.1). The seed oil of more than thirty T2 transgenic lines were screened by TLC. Then, the molecular species of wax esters in the seeds of *A. thaliana* containing *MaFAR/AbWSD1* were determined by nano-ESI-MS/MS, and the ten most abundant species were shown in Figure 5.2.2.

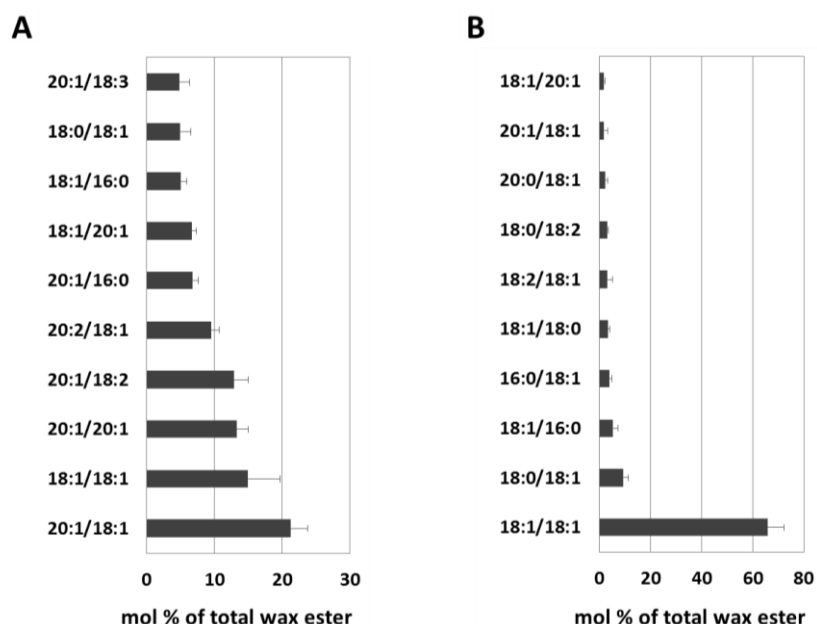


Figure 5.2.2 Molecular species of wax esters in seeds of *A. thaliana* transformed with *MaFAR/AbWSD1*. (A) In Col._0 background. (B) In *fad2 fae1* double mutant. Wax ester molecular species were determined by nano-ESI-MS/MS. The relative abundance of the top ten wax ester molecular species (alcohol moiety/acyl moiety) in mol%

are shown. The data shown is an average of ten individual T2 heterozygous transgenic lines resulting from the transformation of *MaFAR/AbWSD1* in the two backgrounds.

Expression of *MaFAR/AbWSD1* in Col._0 background led to the accumulation of 21 mol% gondoyl - oleate (20:1/18:1; Figure 5.2.2 A), indicating that *MaFAR/AbWSD1* had high ability to combine 20:1-OH with 18:1-FA. This result was different from *MaFAR/ScWS* that preferred to combine 18:1-OH with 20:1-FA, forming 18 mol% oleyl - gondoate (18:1/20:1; Iven *et al.*, 2015). In addition, in Col._0 background, *MaFAR/AbWSD1* accumulated 16 mol% 18:1/18:1 in all wax ester molecular species, which was higher than the 10 mol% produced by *MaFAR/ScWS* (Figure 5.2.2 A; Iven *et al.*, 2015). When *MaFAR/AbWSD1* was expressed in *A. thaliana fae1 fad2* double mutant, 18:1/18:1 became the most abundant wax ester species, accounting for around 65 mol% of all wax ester molecular species (Figure 5.2.2 B), indicating the strong activity of *MaFAR/AbWSD1* to produce 18:1/18:1 in a high oleic background.

The total yields of wax esters of the most promising *A. thaliana* individual lines were measured by GC-FID. However, the co-expression of *AbWSD1* with *MaFAR* resulted in low amounts of wax esters in seeds of *A. thaliana* up to 4 mg g⁻¹ in Col._0 background and 5 mg g⁻¹ in *fae1 fad2* double mutant, respectively (Figure 5.2.5). *AbWSD1* with *MaFAR* was also co-expressed in seeds of *C. sativa*. Analysis of T2 transgenic *C. sativa* lines expressing *MaFAR/AbWSD1* by TLC displayed comparable results to the corresponding *A. thaliana* lines. The first group of T2 transgenic *C. sativa* lines with *MaFAR/AbWSD1* also accumulated only small amounts of wax esters in seeds (Supplementary Material 5).

5.2.2 Optimization of *AbWSD1*

The *MaFAR/AbWSD1* combination showed a higher preference for the formation of 18:1/18:1 in comparison to *MaFAR/ScWS*, but *MaFAR/AbWSD1* did not produce much wax esters in the seeds of *A. thaliana* and *C. sativa*. Thus, different approaches to improve the yield of wax esters produced by *AbWSD1*: (i) optimization of *AbWSD1* for plant codon usage and (ii) re-localization of *AbWSD1* to the ER membrane by transmembrane fusion were tried.

5.2.2.1 Optimization of *AbWSD1* for plant codon usage

The *AbWSD1* was codon optimized for expression in *E. coli* for previous experiments. The codon usage frequency values of some amino acids, especially arginine, were very low for expression in *A. thaliana* (Supplementary Material 6). Thus, the first 20 AA of the *AbWSD1* were optimized for plant codon usage to increase the level of *AbWSD1* expressed in a plant cell. The plant codon optimized *AbWSD1* (PCO*AbWSD1*) was generated by standard PCR using a long (60 bp) forward primer.

5.2.2.2 Fusion of AbWSD1 with transmembrane domain of *Mus musculus* WS

The WS/DGAT enzyme from *Mus musculus* (*MmAWAT2*) showed higher activity than *AbWSD1* in *A. thaliana*, and had a strong preference for C₁₈ substrates, but showed a poor specificity to 18:1/18:1 (Heilmann *et al.*, 2012; Iven *et al.*, 2015). On the contrary, *AbWSD1* showed a high specificity for the formation of 18:1/18:1 (Figure 5.2.2), but a low WS activity in a plant cell. This may be due to the fact that *AbWSD1* is an enzyme from bacteria and contains no transmembrane domain (Supplementary Material 1. C), so that it cannot access the fatty acyl-CoA substrates within the ER of a plant cell. *MmAWAT2* was predicted to contain three transmembrane domains and to localize to the ER membrane (Supplementary Material 1.B; Heilmann *et al.*, 2012). In a previous experiment, *MmAWAT2* was analyzed by expressing in yeast, the activity towards wax ester formation showing that the two transmembrane domains in its N-terminus are essential for the catalytic activity and substrate specificity of the enzyme (Kawelke and Feussner; 2015). Thus, for re-localization of *AbWSD1* to the ER membrane as well as for a potential enhancement of its enzymatic activity, a fusion version of *AbWSD1* with the first two transmembrane domains of *MmAWAT2* was generated. This fusion protein (*TMMmAWAT2-AbWSD1*) harbors the first sixty amino acids of *MmAWAT2* connected to the N-terminal end of *AbWSD1* (Figure 5.2.3).

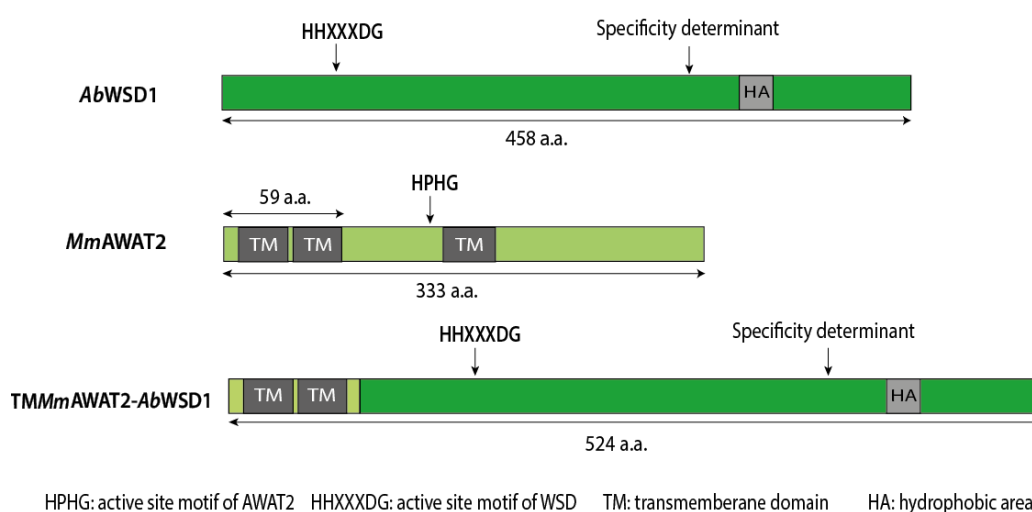


Figure 5.2.3 Domain structure of the TMMmAWAT2-AbWSD1 fusion protein. The sequence of *MmAWAT2* contains three transmembrane domains and this protein localizes to the ER. The sequence of *AbWSD1* contains no transmembrane domain. The first sixty amino acids of *MmAWAT2* were fused to the N-terminal end of *AbWSD1*, and a *TMMmAWAT2-AbWSD1* fusion protein was generated. HPHG, predicted active site motif of *MmAWAT2*; HHXXXDG, catalytic motif of *AbWSD1*; HA, hydrophobic area.

5.2.2.3 Expression of PCOAbWSD1 and TMMmAWAT2-AbWSD1 in *S. cerevisiae*

To test whether PCOAbWSD1 and TMMmAWAT2-AbWSD1 have a strong activities with respect to wax ester production upon heterologous expression, *MmAWAT2*, PCOAbWSD1, and TMMmAWAT2-AbWSD1 as well as an empty vector as negative control, were first expressed in the quadruple mutant *S. cerevisiae* strain as described before (section 5.1.1). The yeast cells were cultivated for 3 days with feeding fatty alcohol to provide these substrates for the wax ester biosynthesis. Afterwards, the neutral lipids of the yeast cells were extracted and analyzed applying TLC. Wax esters as well as fatty alcohols are not naturally accumulated in yeast. With feeding fatty alcohol, *MmAWAT2* only showed the ability of wax ester biosynthesis, though *MmAWAT2* might be a bifunctional enzyme harboring both WS and DGAT activity. PCOAbWSD1 only produced wax esters in yeast, while the AbWSD1 with transmembrane domains of *MmAWAT2* (TMMmAWAT2-AbWSD1) showed a bifunctional enzyme activity, producing both wax esters and TAG in yeast. Moreover, the wax ester signal of TMMmAWAT2-AbWSD1 on TLC was stronger than those of *MmAWAT2* and PCOAbWSD1 (Figure 5.2.4).

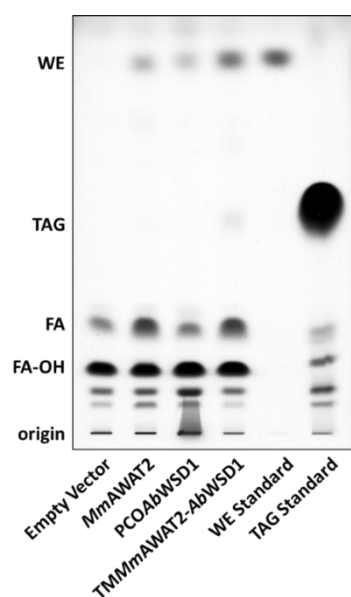


Figure 5.2.4 Accumulation of neutral lipids in *S. cerevisiae* transformed with empty vector, *MmAWAT2*, PCOAbWSD1 and TMMmAWAT2-AbWSD1. The yeast strain (H1246) is deficient in neutral lipid production, no wax ester, TAG or fatty alcohol were accumulated in yeast cells with empty vector. Yeast cells were fed with fatty alcohol (18:1-OH) and cultivated for 3 days. The total lipids were extracted from OD₆₀₀ 50 cells. Thin layer chromatography (TLC) was performed with hexane: diethyl ether: acetic acid (80:20:1, v/v/v) as a running solvent, after incubating dry TLC plates in CuSO₄ solution, the plate was heated at 190 °C till to the appearance of lipid spots. This is representative for three experiments. WE, wax ester; TAG, triacylglycerol; FA, fatty acid; FA-OH, fatty alcohol.

5.2.2.4 Localization of PCOAbWSD1 and TMMmAWAT2-AbWSD1

To check the localization of PCOAbWSD1 and TMMmAWAT2-AbWSD1, they were fused to mCherry and then transiently expressed in onion epidermal cells. The fluorescence-tagged TMMmAWAT2-AbWSD1 fusion protein decorated punctate structures that coincided with the CFP-labeled ER marker, suggesting the localization of TMMmAWAT2-AbWSD1 to the ER (Figure 5.2.5 A). Unexpectedly, PCOAbWSD1 was also found to be ER localized when it was transiently expressed in onion epidermal cells (Figure 5.2.5 B). According to the TMHMM analysis, AbWSD1 has no transmembrane domain, but containing a hydrophobic area in its C-terminus (Supplementary Material 1. C).

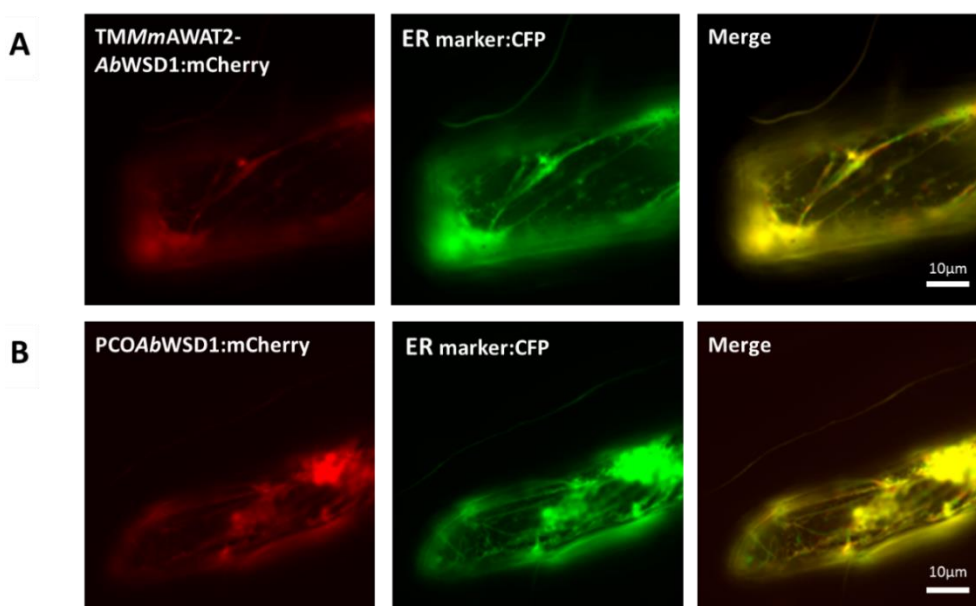


Figure 5.2.5 Localization of mCherry-tagged TMMmAWAT2-AbWSD1 and PCOAbWSD1 in onion epidermal cells. (A) Co-expression of TMMmAWAT2-AbWSD1: mCherry and the ER marker: CFP, as indicated. Right panel, merged image. (B) Co-expression of PCOAbWSD1: mCherry and the ER marker: CFP, as indicated. Right panel, merged image. The image is representative for five transformed cells that showed the same localization.

5.2.3 Co-expression of MaFAR with optimized AbWSD1 in seeds of *A. thaliana*

Even though the attempt of re-localization of AbWSD1 by transmembrane fusion was an exercise in futility, it is still interesting to check whether the two optimized AbWSD1 enzymes would perform better regarding enzymatic activity and substrate specificity for wax ester biosynthesis. So, PCOAbWSD1 and TMMmAWAT2-AbWSD1 were seed-specific co-expressed with MaFAR in *A. thaliana* Col._0 background.

Table 5.2.1 Numbers of T2 transgenic lines with *MaFAR/AbWSD1*, *MaFAR/PCOAbWSD1* and *MaFAR/TMMmAWAT2-AbWSD1* in Col._0 background, lines with *MaFAR/AbWSD1* in *fad2 fae1* dpuble mutant; numbers of transgenic lines analyzed by TLC and GC-FID.

Construct	Number of T2 lines	TLC analysis	GC-FID analysis
<i>MaFAR/AbWSD1</i>	50	30	3
<i>MaFAR/PCOAbWSD1</i>	10	6	3
<i>MaFAR/TMMmAWAT2-AbWSD1</i>	56	30	3
<i>MaFAR/AbWSD1_fad2fae1</i>	10	10	3

The numbers of T2 transgenic lines with *MaFAR/AbWSD1*, *MaFAR/PCOAbWSD1* and *MaFAR/TMMmAWAT2-AbWSD1* in Col._0 background, and the lines with *MaFAR/AbWSD1* in the *fad2 fae1* double mutant (*MaFAR/AbWSD1_fad2fae1*) are shown in Table 5.2.1. Three individual lines with strong wax ester signal on TLC were selected and their wax ester contents were measured by GC-FID (Figure 5.2.6).

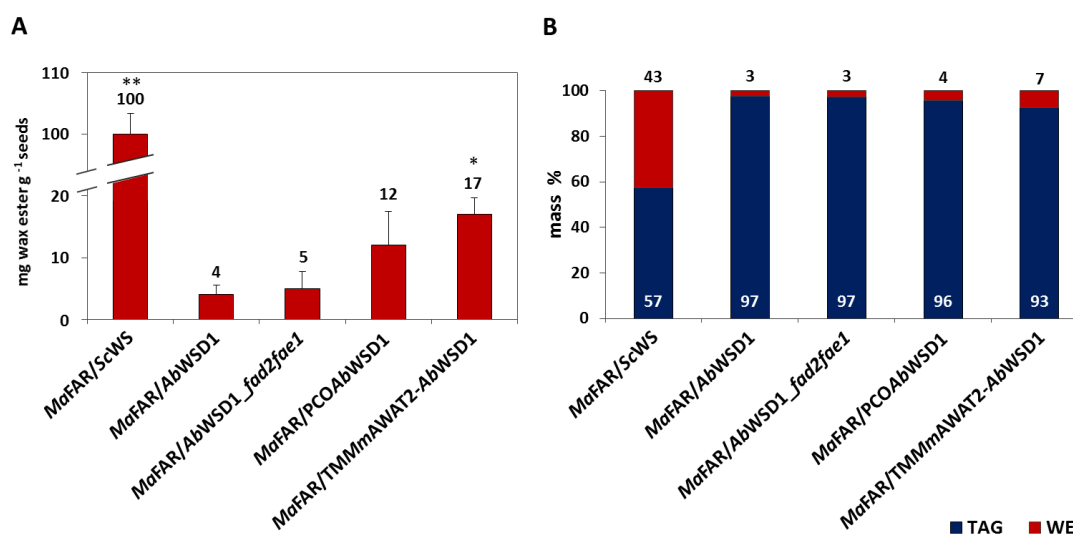


Figure 5.2.6 Quantification of wax esters in seeds of *A. thaliana* Col._0 transformed with *MaFAR/ScWS*, *MaFAR/AbWSD1*, *MaFAR/PCOAbWSD1* and *MaFAR/TMMmAWAT2-AbWSD1*, *A. thaliana fad2 fae1* double mutant transformed with *MaFAR/AbWSD1*. **(A)** Absolute quantification of wax esters in mg g⁻¹ seeds. *means significantly different from *MaFAR/AbWSD1*, $p \leq 0.05$; **means significantly different from *MaFAR/AbWSD1*, $p \leq 0.01$. **(B)** The relative quantification of total neutral lipids (WE, wax ester; TAG, triacylglycerol) in mass% are calculated according to the absolute quantification of each lipid class. The data shown is an average of three individual heterozygous T2 lines for each enzyme combination with two extraction replicates for each individual line.

RESULTS

In comparison to the *MaFAR/AbWSD1* combination, *MaFAR/PCOAbWSD1* and *MaFAR/TMMmAWAT2-AbWSD1* combinations enabled to increase the formation of wax esters up to 12 mg g⁻¹ and 17 mg g⁻¹ in the seeds of *A. thaliana*, respectively, which were three times than the wax esters produced by *MaFAR/AbWSD1* (Figure 5.2.6 A); however, these were still much lower than that of *MaFAR/ScWS* (100 mg g⁻¹ seeds). The wax esters produced by *MaFAR/PCOAbWSD1* and *MaFAR/TMMmAWAT2-AbWSD1* accounted for 4% and 7% of total neutral lipids, much lower than the 43 mol% of *MaFAR/ScWS* (Figure 5.2.6 B).

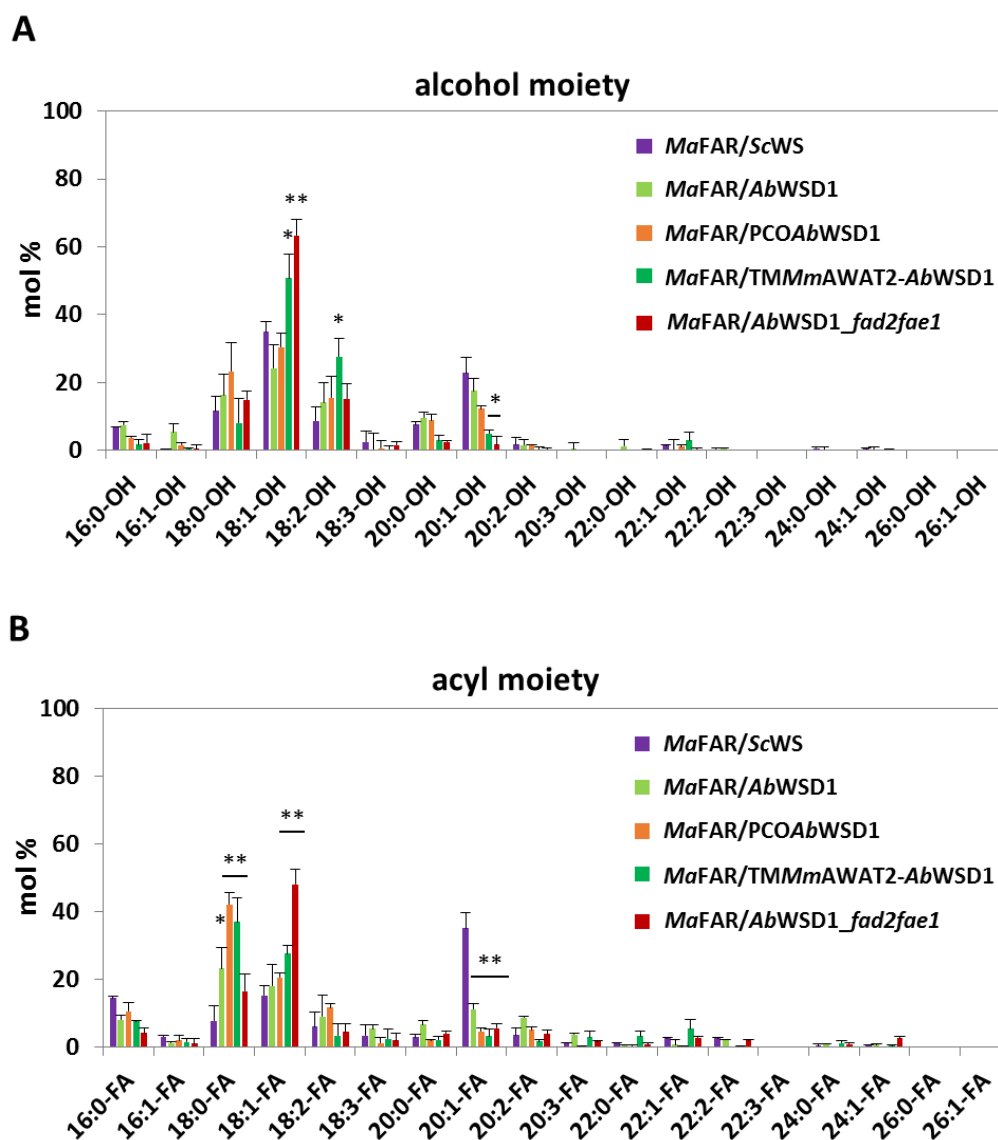


Figure 5.2.7 Alcohol and acyl moieties of wax esters in seeds of *A. thaliana* Col.₀ background transformed with *MaFAR/ScWS*, *MaFAR/AbWSD1*, *MaFAR/PCOAbWSD1* and *MaFAR/TMMmAWAT2-AbWSD1*, *A. thaliana fad2 fae1* double mutant background transformed with *MaFAR/AbWSD1*. (A) Relative abundance of alcohol moieties in mol%. (B) Relative abundance of acyl moieties in mol%. The data shown is an average of three individual heterozygous T2 lines for each enzyme combination with two extraction replicates for each individual line. *means significantly different from *MaFAR/ScWS*, $p \leq 0.05$; **means significantly different from *MaFAR/ScWS*, $p \leq 0.01$.

Interestingly, the compositions of wax esters produced by co-expression of *MaFAR* with *AbWSD1*, *PCOAbWSD1* or *TMMmAWAT2-AbWSD1* were observed to be different from those produced by the *MaFAR/ScWS* combination (Figure 5.2.7). With regard to the fatty alcohol moieties, the levels of 18:1-OH and 20:1-OH incorporated into the wax esters of *MaFAR/AbWSD1* and *MaFAR/PCOAbWSD1* were not significantly different from that of *MaFAR/ScWS* (Figure 5.2.7 A). Interestingly, in comparison to *MaFAR/ScWS* as well as *MaFAR/AbWSD1*, a significantly higher level of 18:1-OH (more than 50 mol%) and remarkably lower level of 20:1-OH were utilized by the *MaFAR/TMMmAWAT2-AbWSD1* combination (Figure 5.2.7 A). When *MaFAR/AbWSD1* was expressed in a high oleic background (*fad2 fae1* double mutant), over 60 mol% of all fatty alcohols incorporated into wax esters was 18:1-OH.

In term of the fatty acyl moieties incorporated into wax esters, upon expression in Col._0 background, the *MaFAR/AbWSD1*, *MaFAR/PCOAbWSD1* and *MaFAR/TMMmAWAT2-AbWSD1* combinations incorporated no more than 10 mol% 20:1-FA into wax esters, significantly lower than *MaFAR/ScWS* utilizing 38 mol% 20:1-FA (Figure 5.2.7 B). Furthermore, in Col._0 background these three combinations utilized stearic acid (18:0-FA) as the predominant fatty acyl moiety for wax ester synthesis, which was significantly higher than that of *MaFAR/ScWS*. The *MaFAR/AbWSD1* and *MaFAR/PCOAbWSD1* combinations did not utilize much higher level of 18:1-FA in comparison to *MaFAR/ScWS*; however, significantly higher levels of 18:1-FA were used by *MaFAR/TMMmAWAT2-AbWSD1*. When *MaFAR/AbWSD1* was expressed in the *fad2 fae1* double mutant, the level of 18:1-FA in wax esters was as high as 50 mol%, followed by 17 mol% stearic acyl moiety (Figure 5.2.7 B).

With regard to the preference for substrate chain length, *AbWSD1*, *PCOAbWSD1* and *TMMmAWAT2-AbWSD1* showed less preference for longer-chain substrates (Figure 5.2.8 A and B). The *MaFAR/PCOAbWSD1* and *MaFAR/TMMmAWAT2-AbWSD1* combinations utilized much lower levels of C₂₀ alcohols compared with *MaFAR/ScWS*. In comparison to *MaFAR/AbWSD1* as well as *MaFAR/ScWS*, the *MaFAR/TMMmAWAT2-AbWSD1* combination showed much higher preference for C₁₈ alcohols (Figure 5.2.8 A). In *fad2 fae1* double mutant, *MaFAR/AbWSD1* incorporated over 90 mol% C₁₈ alcohols into wax esters (Figure 5.2.8 A). In *A. thaliana* Col._0 background, *AbWSD1* and its optimized enzymes utilized over 60 mol% C₁₈ acyl substrates for wax ester synthesis, significantly higher than the 35 mol% of *ScWS*. Moreover, these enzymes showed obvious less specificity to C₂₀ acyl substrates compared with *ScWS*. In *fad2 fae1* double mutant, *AbWSD1* predominantly utilized C₁₈ acyl substrates for wax ester production (Figure 5.2.8 B).

In *A. thaliana* Col._0 background, *MaFAR/AbWSD1* and *MaFAR/PCOAbWSD1* preferred to use much less monoenoic alcohols but more saturated alcohols compared with *MaFAR/ScWS*. While, *MaFAR/TMMmAWAT2-AbWSD1* tend to incorporate more unsaturated alcohols instead of saturated alcohols compared with *MaFAR/AbWSD1* (Figure 5.2.8 C). Similarly, significantly lower levels of monoenoic acyl substrates but higher level of saturated acyl substrates were utilized by *AbWSD1*, *PCOAbWSD1* and *TMMmAWAT2-AbWSD1* in comparison to *ScWS* (Figure 5.2.8 D). Additionally,

AbWSD1 and *PCOAbWSD1* utilized more dienoic acyl substrates than *ScWS*. In *fad2 fae1* double mutant, *MaFAR/AbWSD1* incorporated over 60 mol% monounsaturated alcohols and acyl substrates for wax ester production (Figure 5.2. 8 C and D).

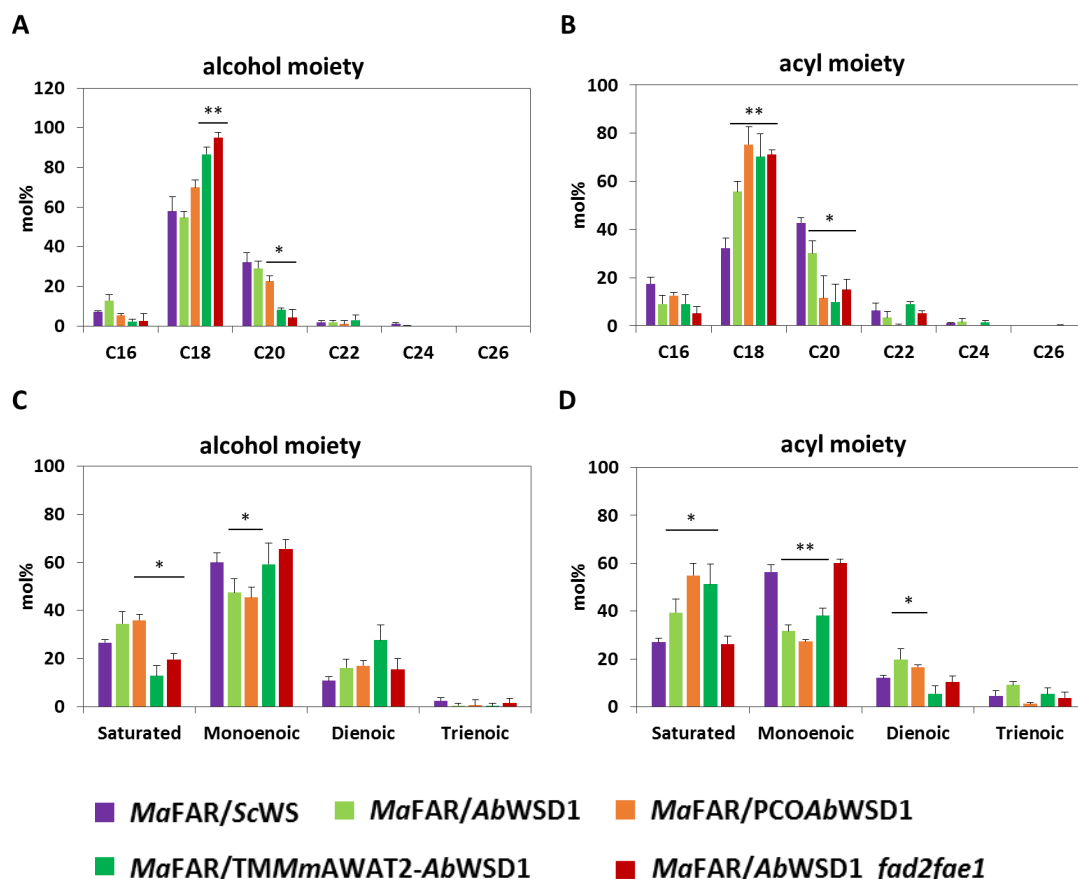


Figure 5.2.8 Relative abundance of alcohol and acyl moieties of wax esters in seeds of *A. thaliana* Col_0 background transformed with *MaFAR/ScWS*, *MaFAR/AbWSD1*, *MaFAR/PCOAbWSD1* and *MaFAR/TMMmAWAT2-AbWSD1*, *A. thaliana fad2 fae1* double mutant background transformed with *MaFAR/AbWSD1*. (A) Alcohol moiety calculated by total carbon number. (B) Acyl moiety calculated by total carbon number. (C) Alcohol moiety calculated by desaturation degree. (D) Acyl moiety calculated by desaturation degree. The data is calculated according to the wax ester composition shown in Figure 5.2.7, and is an average of three individual heterozygous T2 lines for each enzyme combination with two extraction replicates for each individual line. * means significantly different from *MaFAR/ScWS*, $p \leq 0.05$; ** means significantly different from *MaFAR/ScWS*, $p \leq 0.01$.

In summary, co-expression of *AbWSD1* with *MaFAR* led to increased formation of 18:1/18:1, due to the preference of *AbWSD1* for C₁₈ acyl substrates. However, the activity of *AbWSD1* in plant cells was low, so that the *MaFAR/AbWSD1* combination resulted in low amounts of wax esters in seeds of *A. thaliana* and *C. sativa*. Co-expression of *MaFAR* with optimized *AbWSD1* increased the amount of wax esters, but the yield of these combinations were still lower than the *MaFAR/ScWS* combination. The transmembrane domains of *MmAWAT2* affected the formation of molecular specificities of *AbWSD1*,

so that TMM*m*AWAT2-*Ab*WSD1 showed higher preference for C₁₈ alcohol and acyl substrates compared with *Ab*WSD1.

5.3 Wax synthases from *M. aquaeolei* VT8

The gram-negative marine bacterium *M. aquaeolei* VT8 was reported to synthesize isoprenoid wax esters as carbon source and for energy storage (Barney *et al.*, 2012). There were two genes coding for putative FAR and four genes for putative WS identified in the genome of *M. aquaeolei* VT8 (Holtzapple and Schmidt-Dannert, 2007; Wahlen *et al.*, 2009; Willis *et al.*, 2011). One of FARs from *M. aquaeolei* VT8, *Ma*FAR (Maqu_2220) was used in the present study. It is the major enzyme to provide fatty alcohols for the wax ester biosynthesis *in vivo* of *M. aquaeolei* VT8 (Lenneman *et al.*, 2013). It also showed higher activity than *Ma*FAR2 (Maqu_2507) for fatty alcohol production in *E. coli* (Liu *et al.*, 2013). Among the four WSs from *M. aquaeolei* VT8, three enzymes (*Ma*WS1, *Ma*WS2 and *Ma*WS3) were successfully purified and tested *in vitro*. Only *Ma*WS1 and *Ma*WS2 showed WS activities, with a preference for long-chain acyl-CoAs with a broad range of linear-chain fatty alcohols (Holtzapple and Schmidt-Dannert, 2007). In addition, *Ma*WS1 also exhibited DGAT activity, while *Ma*WS3 did not show any activity *in vitro*. Considering that *Ma*FAR showed preferred preference for C_{18:1} acyl-CoA, it was reasonable to assume that the WSs from *M. aquaeolei* VT8 might have a similar substrate specificity with *Ma*FAR. In addition, being from the same bacterium, a *Ma*WS and *Ma*FAR could possibly better function together, thereby increasing the yields of wax esters in seeds of *A. thaliana* and *C. sativa*. Therefore, WSs from *M. aquaeolei* VT8 were further studied in the present thesis.

5.3.1 Identification of a fifth putative wax synthase in *M. aquaeolei* VT8

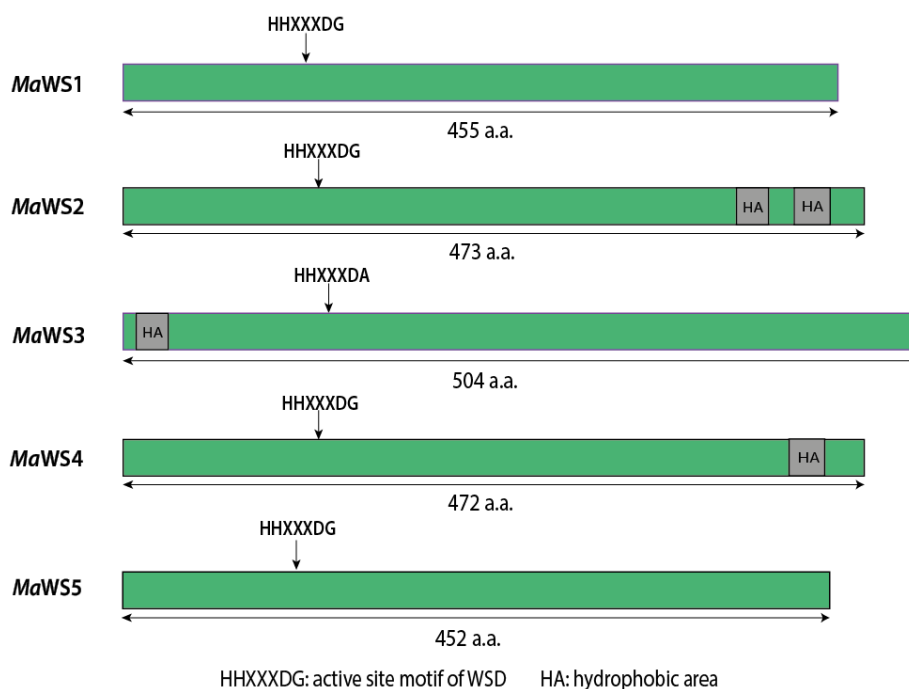


Figure 5.3.1 Domain structure of 5 five putative WSs from *M. aquaeolei* VT8. According to TMHMM analysis, *MaWS1* and *MaWS5* were predicted to be soluble proteins with no hydrophobic area in their amino acid sequence. Two hydrophobic areas were found in C-terminus of *MaWS2*, one hydrophobic area was found in N-terminus of *MaWS3*, and *MaWS4* contains one hydrophobic area in its C-terminus. HHXXDG, catalytic motif of *MaWSs*; HA, hydrophobic area.

Interestingly, when a BLAST homology search of the genome of *M. aquaeolei* VT8 was done using the amino acid sequence of *AbWSD1*, except for the four known WS genes identified by Holtzapfle and Schmidt-Dannert (2007), a new putative WS gene was found (Figure 5.3.1). The peptide sequence identity of this WS homologues to *AbWSD1* was 19%, sharing the lowest identity among the five WS genes (Supplementary Material 7.B). *MaWS5* is not very similar to the other four *MaWSs*, with the peptide sequence identities ranging from 23% to 33% (Supplementary Material 7.B). Similar with the other four *MaWSs* and *AbWSD1*, *MaWS* was found to contain the catalytic motif HHXXDG(A), which is found in the acyltransferases. In addition, some other conserved motifs such as PL(M/R)W, ND and NVP were also found in the peptide sequence of *MaWS5* (Supplementary Material 7. A).

5.3.2 Expression of five putative *MaWSs* in *S. cerevisiae*

To test whether these five putative *MaWSs* can show WS or DGAT activity in an eukaryotic host, the five putative *MaWSs* were amplified from the genome of *M. aquaeolei* VT8 and expressed in a quadruple mutant *S. cerevisiae* strain (H1246). The yeast cells were cultivated for 3 days fed with or without fatty alcohol (18:1-OH), afterwards, total neutral lipids were extracted and analyzed by TLC (Figure 5.3.2).

The reaction products of the five *MaWSs* expressed in yeast in the presence of the fatty alcohol were shown in Figure 5.3.2 A. Expression of *MaWS1* resulted in the accumulation of both wax esters and TAGs, as well as three unknown compounds (Spot 1, 3 and 4). *MaWS2* only showed WS activity, producing high levels of wax esters. *MaWS3* and *MaWS4* did neither show WS nor DGAT activity. *MaWS5* was observed to have strong WS activity, resulting in the accumulation of wax esters even more than that produced by *MaWS2* (Figure 5.3.2 A). Without feeding fatty alcohol, *MaWS1* did not produce wax esters in yeast cells, but still accumulated TAG and the other three unknown compounds (Figure 5.3.2 B). Unexpectedly, *MaWS4* was active and produced a small amount of an unknown compound which migrated like spot 4 from *MaWS1*. No activity again was detectable for *MaWS3*. There were no wax esters or TAG to be detected by *MaWS5* as well as by *MaWS2*, suggesting that these two enzymes only have WS activity instead of being bifunctional WS/DGAT enzymes (Figure 5.3.2 B).

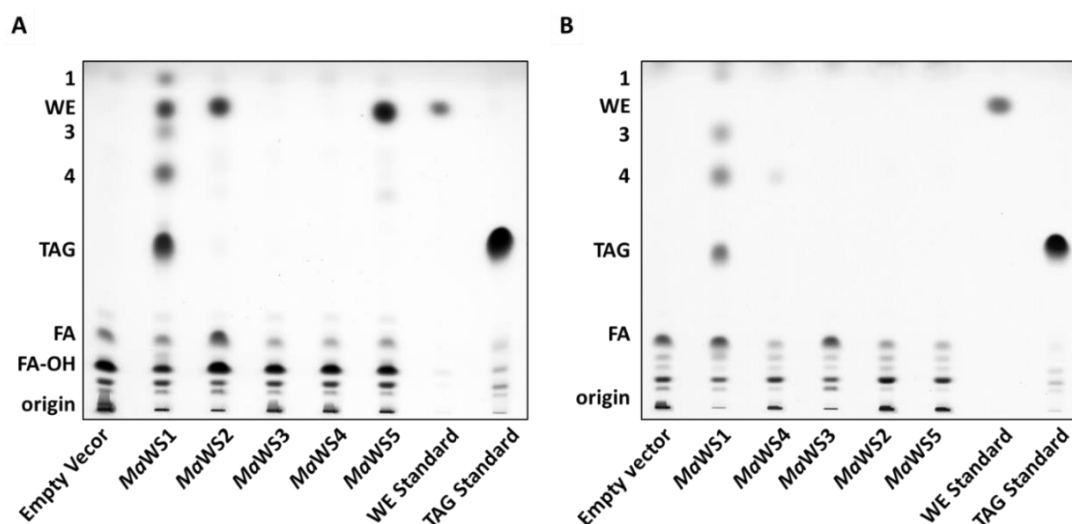


Figure 5.3.2 Accumulation of neutral lipids in *S. cerevisiae* H1246 strain transformed with either empty vector or one of the 5 five putative Ws from *M. aquaeolei* VT8. (A) The yeast cells were fed with fatty alcohol (18:1-OH). **(B)** The yeast cells were not fed with fatty alcohol. Yeast cells were cultivated for 3 days. The total lipids were extracted from OD₆₀₀ 50 cells. Thin layer chromatography (TLC) was performed with hexane: diethyl ether: acetic acid (80:20:1, v/v/v) as a running solvent, after incubating dry TLC plates in CuSO₄ solution, the plate was heated at 190 °C till to the appearance of lipid spots. WE, wax ester; TAG, triacylglycerol; FA, fatty acid; FA-OH, fatty alcohol. Spot 1, 3 and 4 are unknown compounds produced by *MaWS1* in yeast cells. This is representative of three experiments.

5.3.3 Co-expression of *MaFAR* with *MaWS2* in seeds of *A. thaliana*

Among the three enzymes showing activities of wax ester biosynthesis, little information about *MaWS5* had been known yet; *MaWS1* seems to be quite similar with *AbWSD1*, sharing 46% of amino acid identity (Supplementary Material 7. B), and having similar substrate preference (Holtzapfle and Schmidt-Dannert, 2007). *MaWS2* was reported to be significantly more active than *MaWS1* and *AbWSD1* for the formation of linear-chain wax esters, and it appeared to also exhibit a broader substrate range, with a higher specificity to long-chain alcohols compared with *MaWS1* (Holtzapfle and Schmidt-Dannert, 2007). Hence, *MaWS2* (*Maqu_3067*) was selected to be co-expressed with *MaFAR* in seeds of *A. thaliana*, to check whether these two enzymes from the same organism could function well together in plant cells and produce more wax esters than the *MaFAR/ScWS* combination.

Table 5.3.1 Number of harvested T2 *A. thaliana* transgenic lines transformed with *MaFAR/MaWS2*, number of transgenic lines analyzed by TLC and GC-FID.

Construct	Number of T2 lines	TLC analysis	GC-FID analysis
<i>MaFAR/MaWS2</i>	61	30	3

Thirty individual T2 lines of the *MaFAR/MaWS2* combination were screened by TLC. Three lines with relatively strong wax ester signals on TLC were measured to determine the total yields of wax esters in seeds. Co-expression of *MaFAR* with *MaWS2* resulted in the accumulation of wax esters up to approximately 14 mg g⁻¹ in seeds of *A. thaliana*, accounting for only 6% of total neutral lipids (Figure 5.3.3). This yield was significantly lower than the *MaFAR/ScWS* combination.

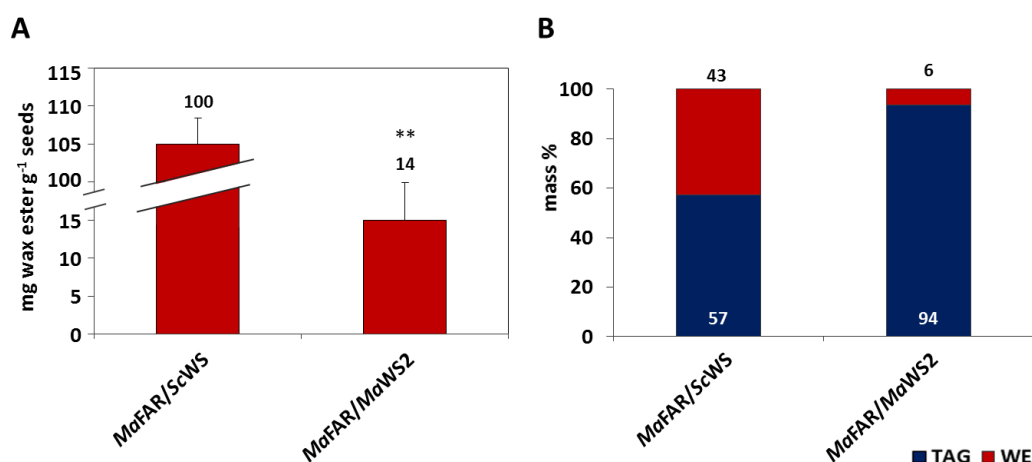


Figure 5.3.3 Quantification of wax esters in seeds of *A. thaliana* transformed with *MaFAR/ScWS* and *MaFAR/MaWS2*. (A) Absolute quantification of wax esters in mg g⁻¹ seeds. **means significantly different from *MaFAR/ScWS*, $p < 0.01$. (B) The relative quantification of total neutral lipids (WE, wax ester; TAG, triacylglycerol) in mass% are calculated according to the absolute quantification of each lipid class. The data shown is an average of three individual heterozygous T2 lines for each enzyme combination with two extraction replicates for each individual line.

In regard to the profile of wax esters produced by the *MaFAR/MaWS2* combination, a significantly higher level of 18:1-OH was observed compared with *MaFAR/ScWS*. Meanwhile, *MaFAR/MaWS2* utilized only a little amount of 20:1-OH, which was significantly lower than the 23 mol% of *MaFAR/ScWS* (Figure 5.3.4 A). Different from *MaFAR/ScWS* having high preference for 20:1, the *MaFAR/MaWS2* combination did not use much of 20:1, instead, preferred to incorporate more 18:0 (over 60 mol%) as well as 18:1 (over 20 mol%) into wax esters (Figure 5.3.4 B).

Expressed together *MaFAR* and *MaWS2* showed significantly higher preference for C₁₈ alcohols and acyl-CoAs compared with *ScWS*, and had little activity towards very long-chain substrates (Figure 5.3.5 A and B). Furthermore, the *MaFAR/MaWS2* combination tend to utilize more dienoic alcohols instead of saturated alcohols compared with *MaFAR/ScWS* (Figure 5.3.5 C). While, in comparison to *ScWS*, *MaWS2* showed high specificity to saturated acyl-CoAs, and took significantly lower level of monoenoic acyl-CoAs for wax esters production (Figure 5.3.5 D).

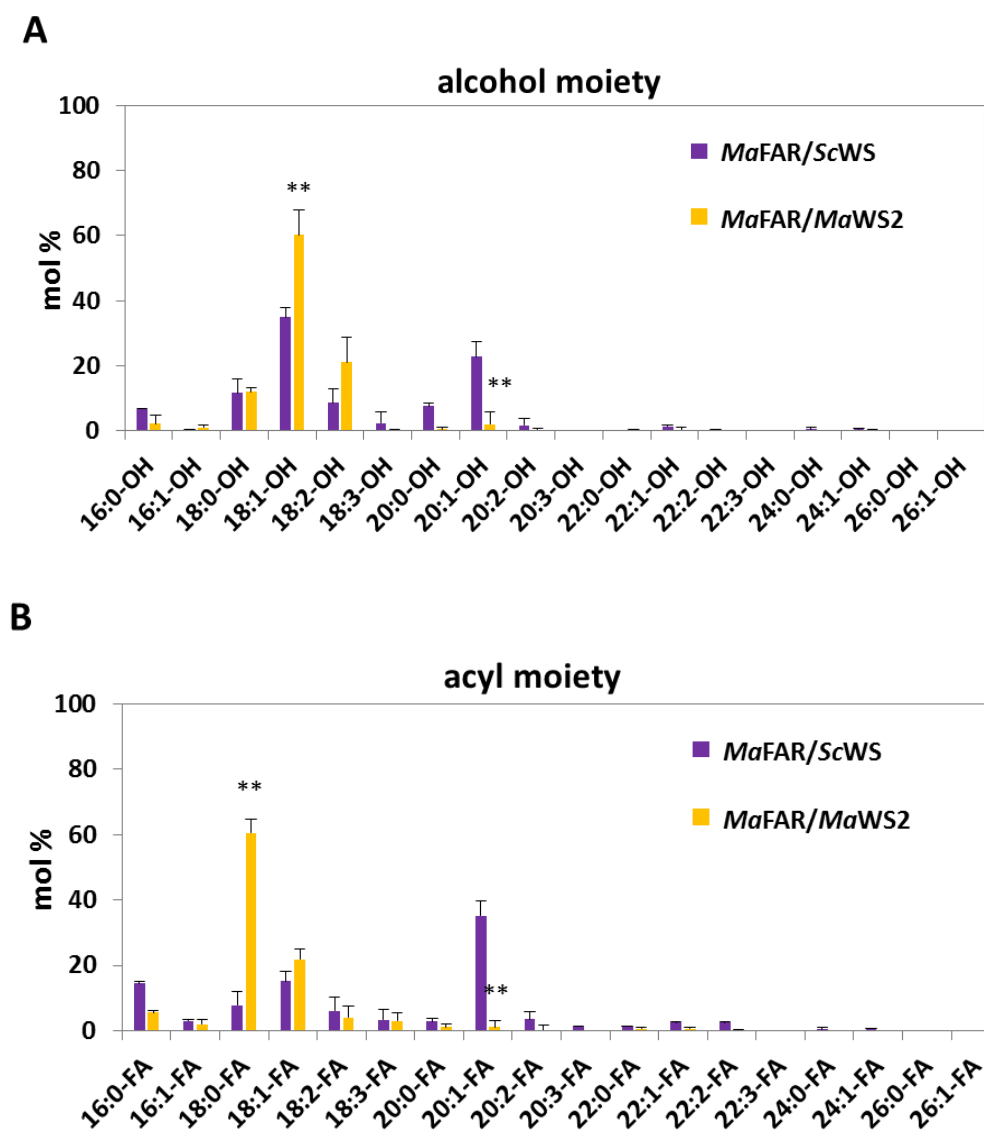


Figure 5.3.4 Alcohol and acyl moieties of wax esters in seeds of *A. thaliana* transformed with *MaFAR/ScWS* and *MaFAR/MaWS2*. (A) Relative abundance of alcohol moieties in mol%. (B) Relative abundance of acyl moieties in mol%. The data shown is an average of three individual heterozygous T2 lines for each enzyme combination with two extraction replicates for each individual line. *means significantly different from *MaFAR/ScWS*, $p \leq 0.05$; **means significantly different from *MaFAR/ScWS*, $p \leq 0.01$.

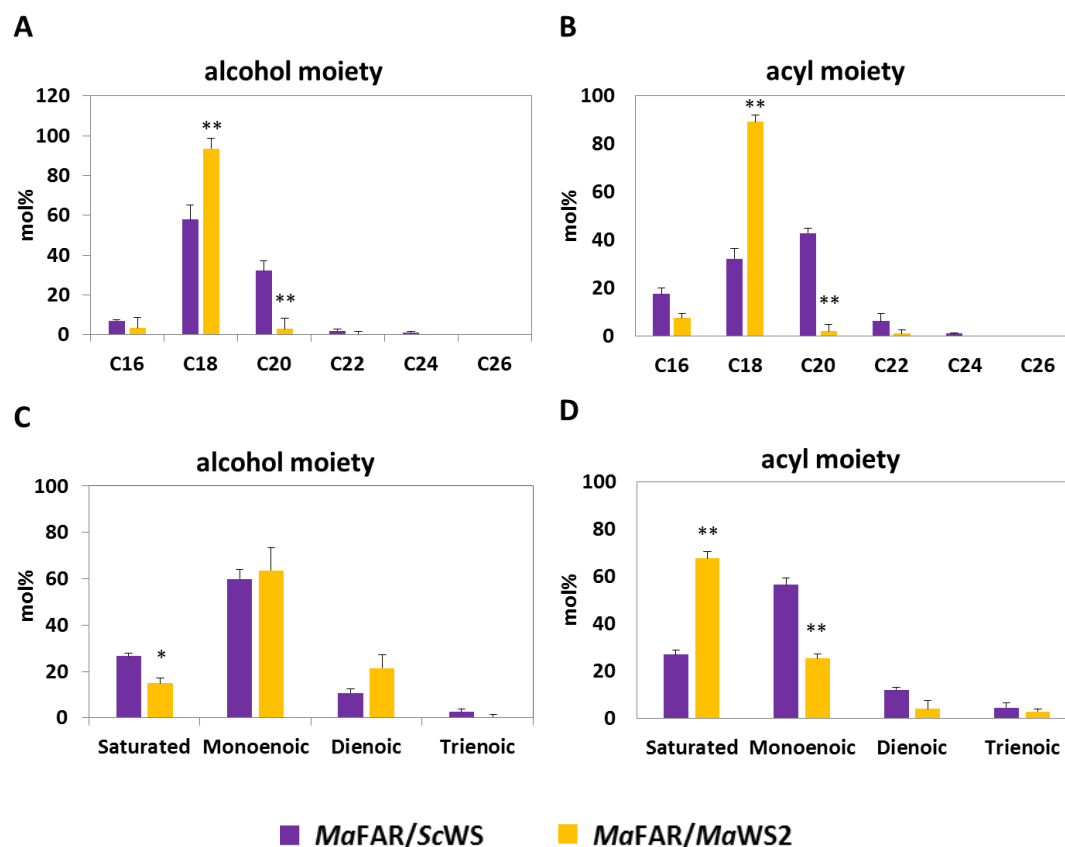


Figure 5.3.5 Relative abundance of alcohol and acyl moieties of wax esters in seeds of *A. thaliana* transformed with *MaFAR/ScWS* and *MaFAR/MaWS2*. **(A)** Alcohol moiety calculated by total carbon number. **(B)** Acyl moiety calculated by total carbon number. **(C)** Alcohol moiety calculated by desaturation degree. **(D)** Acyl moiety calculated by desaturation degree. The data is calculated according to the wax ester composition shown in Figure 5.3.4, and is an average of three individual heterozygous T2 lines for each enzyme combination with two extraction replicates for each individual line. *means significantly different from *MaFAR/ScWS*, $p \leq 0.05$; **means significantly different from *MaFAR/ScWS*, $p \leq 0.01$.

5.3.4 Purification of heterologously expressed *MaWS5*

Analysis of the hydrophobicity of *MaWS5* sequence by the TMHMM online service (Sonnhammer *et al.*, 1998) indicated that no putative transmembrane domain or hydrophobic area exist within the enzyme, which is similar with *MaWS1* but different from *MaWS2* containing a small hydrophobic area in C-terminus (Supplementary Material 1). This result supports the anticipated soluble nature of *MaWS5*, suggesting that this enzyme could be efficiently purified from *E. coli* expression cultures. Therefore, study on *MaWS5* should be relatively easy compared with other WSs containing transmembrane domains or hydrophobic areas. Being a soluble protein, *MaWS5* was also considered to be a promising candidate for 3D structural analysis. Hence, the DNA of *MaWS5* was also cloned into

pET28b vector and expressed in *E. coli* in order to purify the heterologously produced enzyme for activity tests *in vitro*.

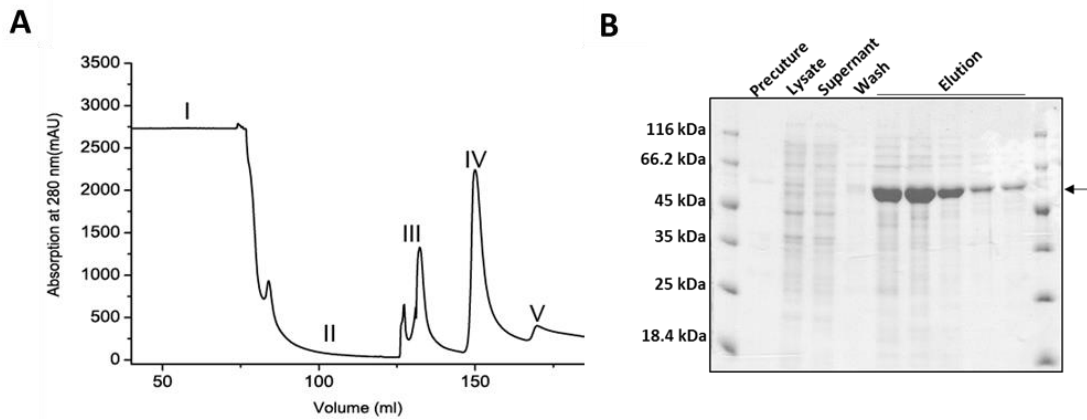


Figure 5.3.6 Nickel affinity chromatography (NAC) purification of heterologously produced *MaWS5* from *E. coli*.

(A) Representative example for affinity chromatography purification of *MaWS5*-6xHis. (I) Protein loading. (II) Washed with 0% of imidazole. (III) Washed with 5% of buffer B (with 25 mM imidazole). (IV) Elution of bound protein from the column with 40% of buffer B (with 200 mM imidazole). (V) Washed with 100% of buffer B (with 500 mM imidazole). **(B)** SDS-PAGE showing the purification of *MaWS5*-6xHis fusion protein from nickel affinity chromatography. The position of *MaWS5*-6xHis is indicated by a black arrow. SDS-PAGE was performed according to the method described in section 4.2.5, 5 μ l protein samples were mixed with 4x loading buffer and 5 μ l of the mixture were loaded onto 12% SDS gel. This is representative for three experiments.

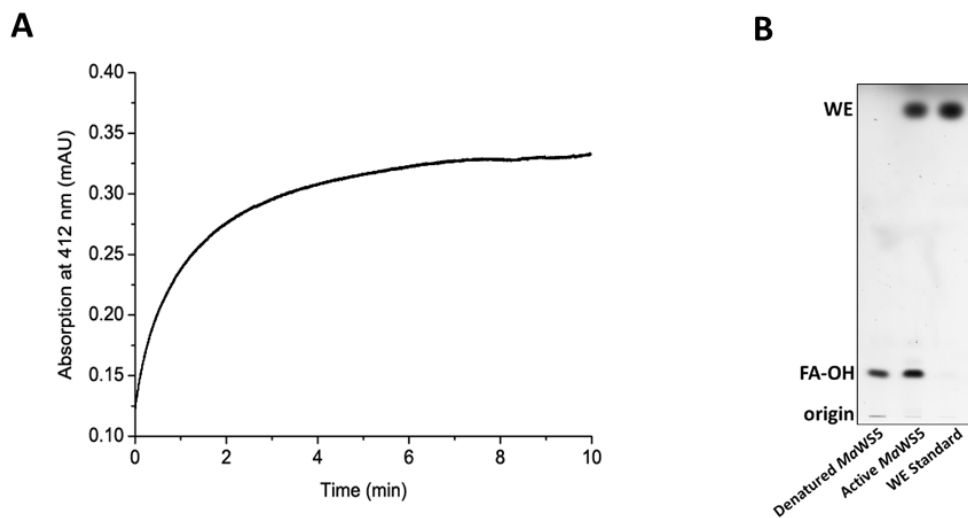


Figure 5.3.7 *In vitro* activity test of purified *MaWS5*-6xHis. **(A)** Activity monitored photometrically by the DTNB assay. The assay solution contained 0.2 mg DTNB/ml, 20 μ M of 18:1-OH, 10 μ M of 18:1-CoA and 15 μ l (about 5 μ g) of purified protein solution in a total volume of 1 ml of TBS buffer (pH 7.0). The reaction was observed for 10 min. **(B)** TLC plate showing the wax esters produced by *MaWS5* *in vitro*. The samples for TLC analysis were collected solution of the DTNB assay, and the reaction products were extracted twice using 1 ml n-hexane, then evaporated under streaming nitrogen, solved in 100 μ l chloroform, and 50 μ l sample was applied for TLC. Data shown are representative for three experiments.

The size of the *MaWS5-6xHis* fusion protein was calculated to be about 50.9 kDa. Purification of cell lysates from *E. coli* expressing the *MaWS5-6xHis* fusion protein through NAC resulted in a high amounts of the protein (Figure 5.3.6A). The eluted protein at 40% of 500 mM imidazole was quite pure with only minor contaminants. The eluted protein sample ran at about 50 kDa on SDS-PAGE, thus matching the calculated size of *MaWS5-6xHis* fusion protein (Figure 5.3.6B).

The *in vitro* activity of purified *MaWS5-6xHis* was tested by a DTNB-based assay immediately after the protein was eluted from Ni-NTA agarose column. The activity of *MaWS5-6xHis* enzyme was photometrically observed for 10 minutes. The active *MaWS5-6xHis* enzyme catalyzed the esterification reaction at a relatively high initial speed, and then the speed of reaction slowed down with the consumption of the substrates (Figure 5.3.7 A). TLC analysis confirmed that the reaction products of active *MaWS5-6xHis* was wax ester, while mixing denatured enzyme with fatty acyl-CoA and excessive fatty alcohol did not result in the formation of wax esters (Figure 5.3.7 B).

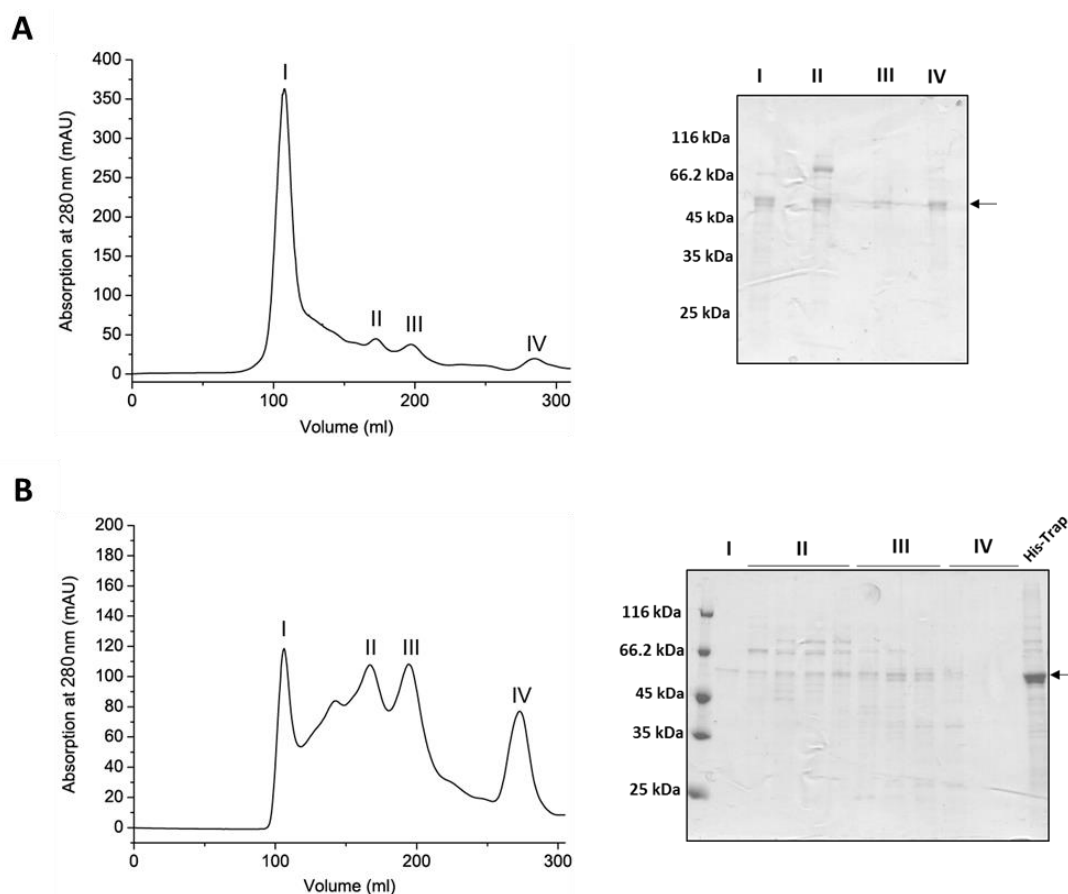


Figure 5.3.8 Size exclusion chromatography (SEC) of the *MaWS5-6xHis*. (A) SEC of *MaWS5-6xHis* eluted with TBS buffer without detergent. Peak I refers to the void volume of the SEC column and thus represents the aggregate peak. Peak II refers to a calculated molecular weight of about 220 kDa, while peak III corresponds to about 116 kDa and peak IV corresponds to about 23 kDa. All fractions were analyzed by SDS-PAGE. Position of *MaWS5-6xHis* in the SDS-PAGE is indicated by a black arrow. (B) SEC of *MaWS5-6xHis* eluted with potassium phosphate buffer containing detergent. Position of *MaWS5-6xHis* is indicated by a black arrow. SDS-PAGE was performed according

to the method described in section 4.2.5, 5 μ l eluted protein samples were mixed with 4x loading buffer and 10 μ l of the mixture were loaded onto 12% SDS gel. Data shown are representative for one experiment.

The *MaWS5*-6xHis was further purified by size exclusion chromatography (SEC). Utilization of TBS buffer (pH 7.6) as the elution buffer resulted in a huge signal beside three tiny signals (Figure 5.3.8 A). The elution volumes of these four peaks corresponded to the aggregated protein in the void volume of the column (peak I), a tetramer of about 220 kDa (peak II), a dimer of about 116 kDa (peak III) and a monomer of about 23 kDa (peak IV). According to the SDS-PAGE analysis, the proteins eluted from these four peaks had the same molecular weight at about 50 kDa. The protein concentrations of peak II-IV were very low, suggesting that most of the purified proteins were not stable and tend to aggregate in TBS buffer.

In order to increase the stability of *MaWS5*-6xHis during SEC, phosphate buffer (pH 7.0) containing detergent (details shown in section 4.2.4) was used as SEC elution buffer. Four peaks of aggregated proteins, 220 kDa elution, 116 kDa elution and 23 kDa elution were observed at about similar level (Figure 5.3.8B), indicating that phosphate buffer with detergent was helpful for disturbing the hydrophobic interactions of proteins, thereby decreasing the amount of aggregates during SEC.

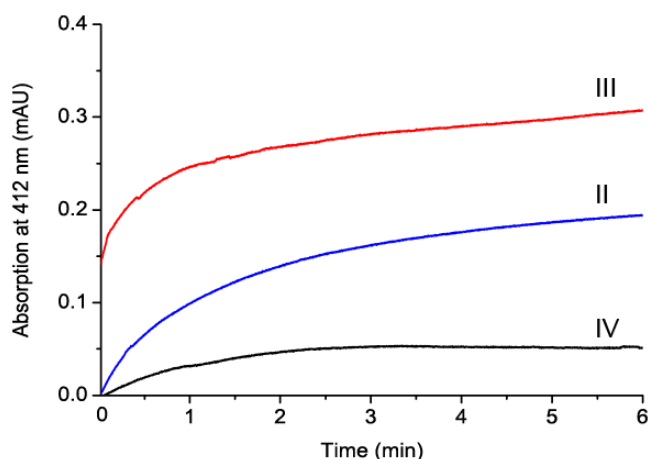


Figure 5.3.9 *In vitro* activity test of purified *MaWS5*-6xHis eluting from SEC. Activity monitored by the DTNB assay. The assays contained 0.2 mg DTNB/ml, 10 μ M of 18:1-OH, 10 μ M of 18:1-CoA and 15 μ l of purified protein solution in a total volume 1 ml of TBS buffer (pH 7.0). II refers to the protein solution from peak II (220 kDa), III refers to the protein solution from peak III (116 kDa), and IV refers to the protein solution from peak IV (23 kDa) shown in Figure 5.3.8B. Data shown is representative of two experiments.

The DNTB assay showed again that the proteins eluting from peak II-IV were active as WS (Figure 5.3.9). The 15 μ l of protein solution from peak II and III showed relatively higher activity compared with that of peak IV (Figure 5.3.9), perhaps because the protein concentrations were higher (data not shown).

In summary, among the five WS homologous genes found in genome of *M. aquaeolei* VT8, *MaWS1*, *MaWS2* and *MaWS5* showed WS activity in *S. cerevisiae*. *MaWS5* was successfully purified and also

showed WS activity *in vitro*. The combination of *MaWS2* with *MaFAR* preferred to use C₁₈ substrates for wax ester biosynthesis, while resulting in low amounts of wax esters in seeds of *A. thaliana*.

5.4 Down-regulation of TAG biosynthesis in seeds of *C. sativa*

TAGs are the dominant storage lipids in the seeds of most plant species. Acyl-CoA: diacylglycerol O-acyltransferase (DGAT) catalyzes the last step of TAG biosynthesis, esterifying fatty acyl-CoAs to the *sn*-3 OH group of DAGs. In the final step of wax ester biosynthesis, fatty acyl-CoAs are esterified to the primary OH group of fatty alcohols. Thus, the introduced wax ester biosynthesis pathway in seeds of *C. sativa* is a competitive pathway with the endogenous TAG biosynthesis pathway. To enhance the total yield of wax esters accumulating in the seeds of *C. sativa*, a major aim was to down-regulate an enzyme of TAG biosynthesis in *C. sativa*, *CsDGAT1*, using artificial microRNA (amiRNA), so that it was expected that higher levels of fatty acyl-CoAs would be available for wax ester biosynthesis instead of the formation of TAG.

Three amiRNAs for targeting different parts of the *CsDGAT1* sequence (amiDGAT1) were designed in a previous project by Dr. Sofia Marmon (Supplementary Material 9). Each amiDGAT1 was co-expressed together with *MaFAR* and *ScWS* to establish an exogenous wax ester synthesis pathway and synchronously block the formation of TAG. Each amiDGAT1, *MaFAR* and *ScWS* were cloned into one destination vector with phosphinothricin (Basta) resistance gene, and co-expressed under the napin promoter in the seeds of *C. sativa*.

Table 5.4.1 Numbers of harvested T2 *C. sativa* transgenic lines transformed with amiDGAT1.1/*MaFAR/ScWS*, amiDGAT1.2/*MaFAR/ScWS*, amiDGAT1.3/*MaFAR/ScWS*, numbers of transgenic lines analyzed by TLC and GC-FID.

Construct	Number of T2 lines	TLC analysis	GC-FID analysis
amiDGAT1.1/ <i>MaFAR/ScWS</i>	21	21	2
amiDGAT1.2/ <i>MaFAR/ScWS</i>	19	19	11
amiDGAT1.3/ <i>MaFAR/ScWS</i>	6	6	2

After Basta selection, a total of 43 T2 transgenic *C. sativa* lines were generated, 21 lines for the amiDGAT1.1/*MaFAR/ScWS* combination, 19 lines for amiDGAT1.2/*MaFAR/ScWS*, and 6 lines for amiDGAT1.3/*MaFAR/ScWS* (Table 5.4.1). All T2 transgenic lines were first analyzed by spotting neutral lipid extractions of seed oil on TLC-plates (Figure 5.4.1; Supplementary Material 10). Most of amiDGAT1.1/*MaFAR/ScWS* and amiDGAT1.3/*MaFAR/ScWS* lines accumulated low amounts of wax esters, and 11 amiDGAT1.2/*MaFAR/ScWS* lines accumulated relatively high levels of wax esters in the seeds (Supplementary Material 11). The individual lines showing a strong wax ester signal on TLC-

plates were selected for measurement of total wax esters by GC-FID. The total wax ester contents in seed of the best two performing individual lines for each combination are shown in Figure 5.4.2 A.

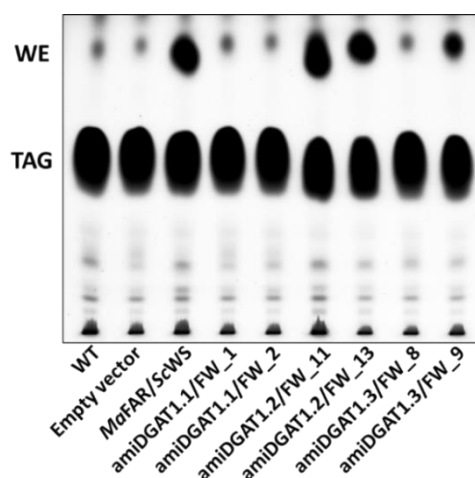


Figure 5.4.1 Neutral lipid accumulation in seeds of wild-type, *C. sativa* transformed with empty vector, *MaFAR/ScWS*, *amiDGAT1.1/MaFAR/ScWS*, *amiDGAT1.2/MaFAR/ScWS*, *amiDGAT1.3/MaFAR/ScWS*. Thin layer chromatography (TLC) was performed with hexane: diethyl ether: acetic acid (80:20:1, v/v/v) as a running solvent, after incubating dry TLC plates in CuSO_4 solution, the plate was heated at 190 °C till to the appearance of lipid spots. TLC plate showing the spots of TAG and WE. FW is the abbreviation of *MaFAR/ScWS*.

The three *amiDGAT1/MaFAR/ScWS* combinations accumulated from 3 mg g⁻¹ to 49 mg g⁻¹ wax esters in the seeds of *C. sativa*. Among all transgenic lines with *amiDGAT1*, only two individual lines of the *amiDGAT1.2/MaFAR/ScWS* combination (*amiDGAT1.2/MS_11* and *_13*) produced 42 mg g⁻¹ and 49 mg g⁻¹ wax esters in seeds, respectively, which were similar with the 41 mg g⁻¹ of the *MaFAR/ScWS* combination (Figure 5.4.2 A). In addition, the cotyledons of these two individual lines had white cotyledons (Supplementary Material 3), and their seedlings developed slower during the first two weeks compared with the seedlings of *C. sativa* wild-type.

The total amounts of TAG in the seeds of all *amiDGAT1/MaFAR/ScWS* lines were not significantly lower than that of *MaFAR/ScWS*, some of the individual lines even contained higher levels of TAG (Figure 5.4.2 B). As consequence, the wax ester to TAG ratio of *amiDGAT1/MaFAR/ScWS* lines ranged from 3% to 20.7%, only the two best performing lines of the *amiDGAT1.2/MaFAR/ScWS* combination accumulated around 20% wax esters in total neutral lipids, which were similar with that of the *MaFAR/ScWS* combination (Figure 5.4.2 C).

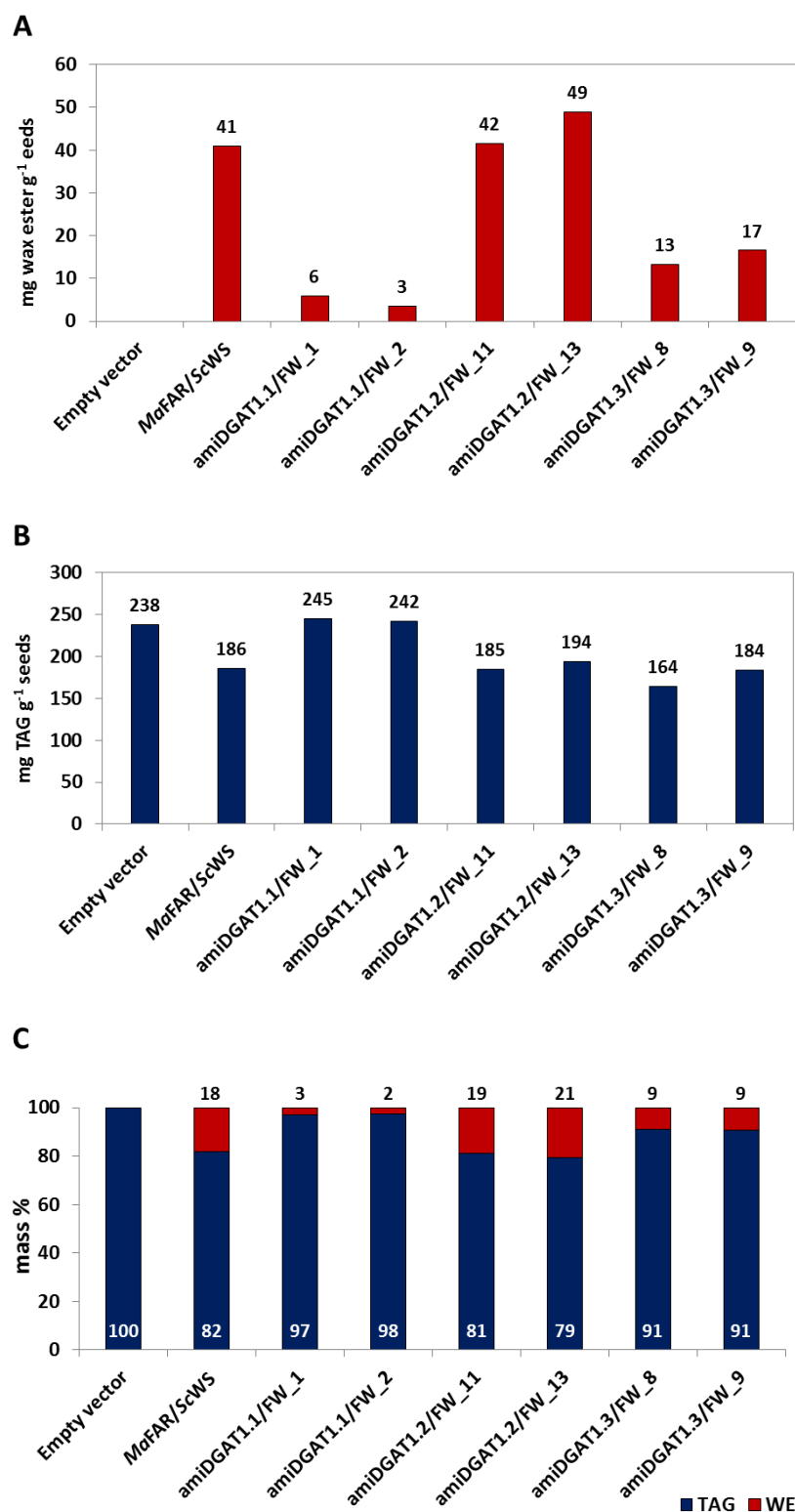


Figure 5.4.2 Wax ester and TAG accumulation in seeds of *C. sativa* transformed with empty vector, *MaFAR/ScWS*, *amiDGAT1.1/MaFAR/ScWS*, *amiDGAT1.2/MaFAR/ScWS*, *amiDGAT1.3/MaFAR/ScWS*. (A) Absolute quantification of wax esters in mg g⁻¹ seeds. (B) Absolute quantification of TAG in mg g⁻¹ seeds. (C) The relative quantification of total neutral lipids (WE, wax ester; TAG, triacylglycerol) in mass% are calculated according to the absolute quantification of each lipid class. The data shown is an average of three individual

heterozygous T2 lines for each enzyme combination with two extraction replicates for each individual line. FW is the abbreviation of *MaFAR/ScWS*.

Even though there was no significant difference in the total TAG content between the three *amiDGAT1/MaFAR/ScWS* combinations and the *MaFAR/ScWS* combination, it was interesting to observe that the fatty acid profile of TAG in *Camelina* seeds was altered with the existence of the *amiDGAT1.2* or *amiDGAT1.3* (Figure 5.4.3). In the seed oil of plants transformed with empty vector, *MaFAR/ScWS* and *amiDGAT1.1/MaFAR/ScWS* lines, linolenic acid (18:3-FA) accounted for around 40 mol% of total fatty acids esterified into TAG. However, in the *amiDGAT1.2/MaFAR/ScWS* lines, the percentage of 18:3-FA in TAG increased up to 50 mol% of total acyl moieties, accompanied by a small increase of palmitic acid (16:0-FA). Whereas, the levels of 18:1, linoleic acid (18:2-FA) and 20:1 in the TAG produced by *amiDGAT1.2/MaFAR/ScWS* displayed 3 mol% - 6 mol% decreases compared with those in the *MaFAR/ScWS* line. In addition, a slight (4 mol%) enhancement of linolenic acid (18:3) was also observed in TAG in the *amiDGAT1.3/MaFAR/ScWS* lines (Figure 5.4.3).

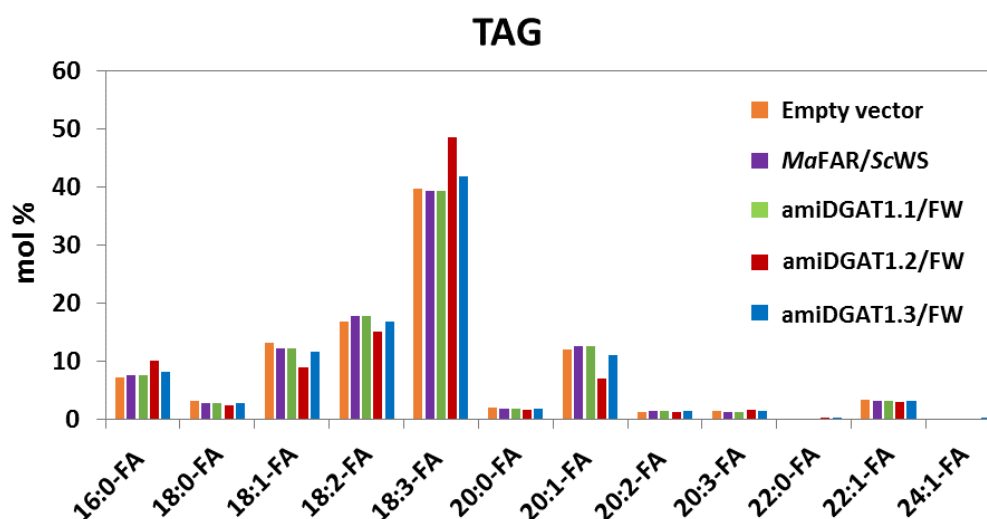


Figure 5.4.3 Fatty acid profile of TAG in seeds of *C. sativa* transformed with empty vector, *MaFAR/ScWS*, *amiDGAT1.1/MaFAR/ScWS*, *amiDGAT1.2/MaFAR/ScWS*, *amiDGAT1.3/MaFAR/ScWS*. The relative abundance of fatty acid in TAG is shown in mol%. The data shown is an average of three individual heterozygous T2 lines for each enzyme combination with two extraction replicates for each individual line. FW is the abbreviation of *MaFAR/ScWS*.

Unexpectedly, the three *amiRNAs* targeting *CsDGAT1* also resulted in changes in the alcohol and acyl moieties incorporated in wax esters (Figure 5.4.4). The wax esters accumulating in seeds of *C. sativa* with *MaFAR/ScWS* mainly consist of 43 mol% 18:1-OH and 18 mol% 20:1-OH. In comparison to *MaFAR/ScWS*, the three *amiDGAT1/MaFAR/ScWS* lines incorporated higher levels of gondoic alcohol (21 mol% - 26 mol%) into wax esters. Furthermore, the *amiDGAT1.3/MaFAR/ScWS* combination utilized slightly higher levels of 18:1-OH compared with the *MaFAR/ScWS* combination (Figure 5.4.4 A). Additionally, in the wax esters produced by *amiDGAT1.1/MaFAR/ScWS* and

amiDGAT1.2/*MaFAR/ScWS*, linoleic alcohol (18:2-OH) accounted for 17.5 mol% and 19.5 mol%, respectively, which were higher than that of *MaFAR/ScWS*; in contrast, a decreased level of 18:2-OH (7 mol%) was observed in the wax esters produced by amiDGAT1.3/*MaFAR/ScWS* (Figure 5.4.4 A).

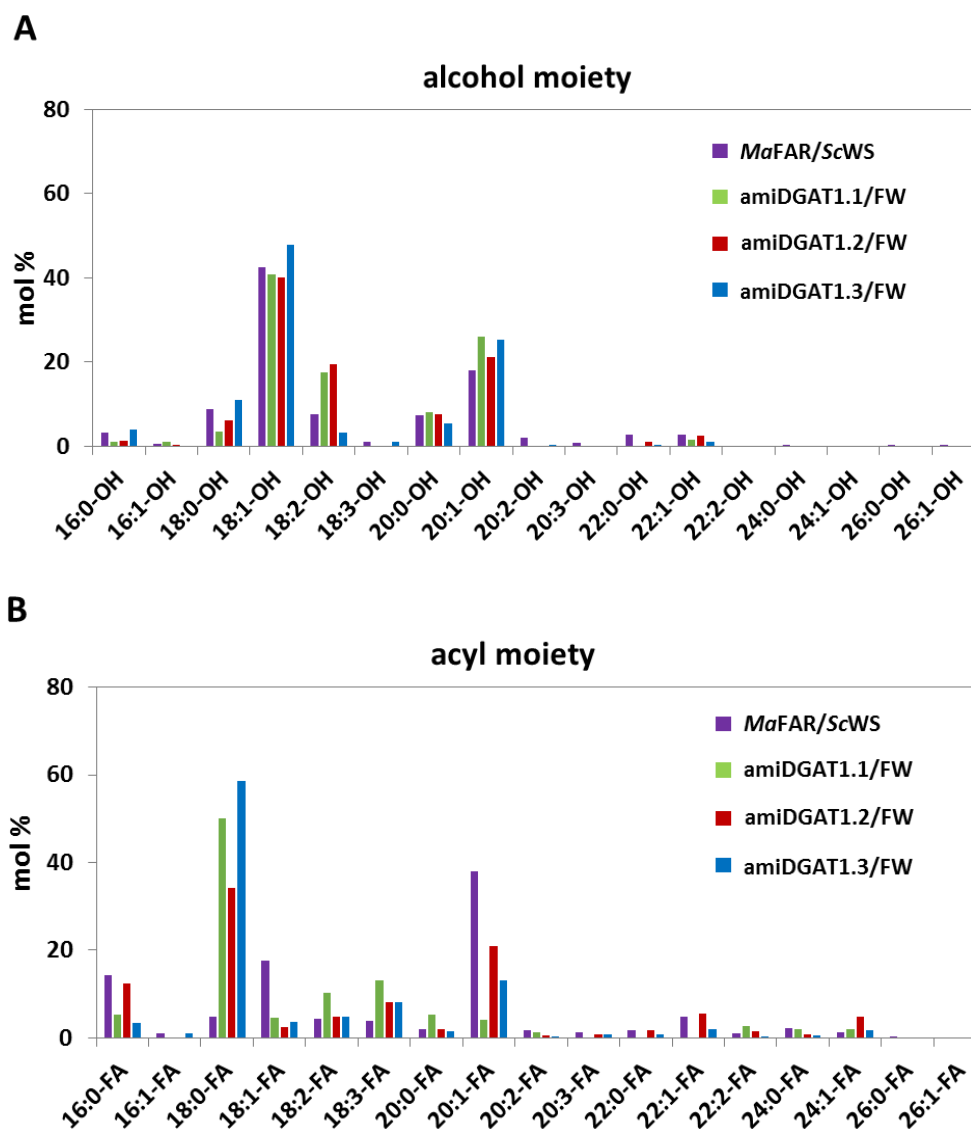


Figure 5.4.4 Alcohol and acyl moieties of wax esters in seeds of *C. sativa* transformed with empty vector, *MaFAR/ScWS*, amiDGAT1.1/*MaFAR/ScWS*, amiDGAT1.2/*MaFAR/ScWS*, amiDGAT1.3/*MaFAR/ScWS*. **(A)** Relative abundance of alcohol moieties in mol%. **(B)** Relative abundance of acyl moieties in mol%. The data shown is an average of three individual heterozygous T2 lines for each enzyme combination with two extraction replicates for each individual line. FW is the abbreviation of *MaFAR/ScWS*.

The most abundant fatty acid moiety in the wax esters produced by *MaFAR/ScWS* was 20:1, accounting for almost 39 mol% of all fatty acid moieties. However, 20:1-FA only accounted for 4 mol%, 20 mol% and 13 mol% in the three amiDGAT1/*MaFAR/ScWS* combinations, which were obvious lower than the *MaFAR/ScWS* combination (Figure 5.4.4 B). Stearic acid (18:0; over 30 mol%) was the predominant fatty acid moiety found in the wax esters produced by the three

amiDGAT1/*MaFAR/ScWS* combinations, accounting for 34 mol% in the amiDGAT1.2/*MaFAR/ScWS* combination, and over 50 mol% in the amiDGAT1.1/*MaFAR/ScWS* and amiDGAT1.3/*MaFAR/ScWS* combinations. Furthermore, only 2 mol% - 5 mol% 18:1 were utilized by the three amiDGAT1/*MaFAR/ScWS* combinations for wax ester production, which were much lower than the 18 mol% of *MaFAR/ScWS*. In addition, higher levels of 18:3 (8 mol% - 13 mol%) were incorporated into the wax esters by three amiDGAT1/*MaFAR/ScWS* combinations, which means double amount of the yield of the *MaFAR/ScWS* combination (Figure 5.4.4 B).

There were no significant differences on the chain length of fatty alcohol moieties between *MaFAR/ScWS* and three amiDGAT1/*MaFAR/ScWS* combinations (Figure 5.4.5 A). Meanwhile, in comparison to *MaFAR/ScWS*, amiDGAT1.3/*MaFAR/ScWS* tend to utilize more monoenoic alcohols instead of dienoic alcohols for wax ester synthesis; while, amiDGAT1.1/*MaFAR/ScWS* and amiDGAT1.2/*MaFAR/ScWS* took higher levels of dienoic alcohols as substrates (Figure 5.4.5 C). Different from *MaFAR/ScWS* predominantly taking C₂₀ acyl substrates for wax ester production, the three amiDGAT1/*MaFAR/ScWS* combinations showed obvious less preference for C₂₀ acyl substrates and higher specificity to C₁₈ acyl substrates (Figure 5.4.5 C). Moreover, the three amiDGAT1/*MaFAR/ScWS* combinations showed higher preference for saturated acyl substrates instead of monoenoic acyl substrates compared with the *MaFAR/ScWS* combination (Figure 5.4.5 D).

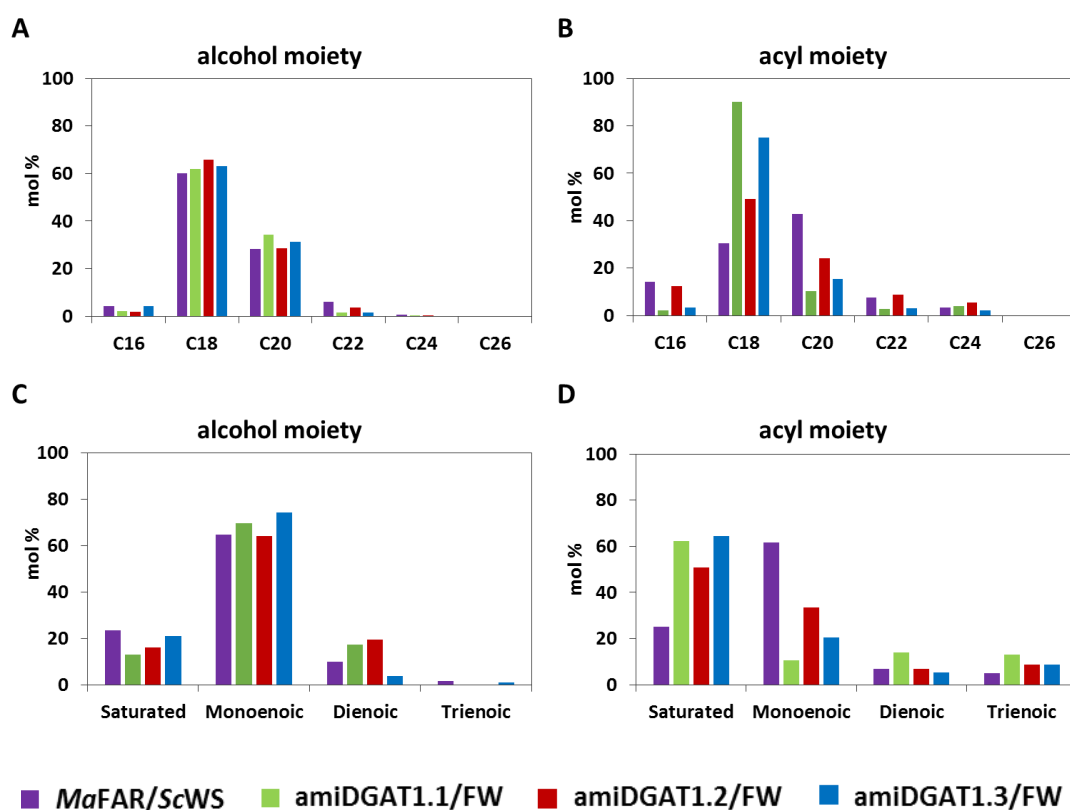


Figure 5.4.5 Relative abundance of alcohol and acyl moieties of wax esters in seeds of *C. sativa* transformed with *MaFAR/ScWS*, amiDGAT1.1/*MaFAR/ScWS*, amiDGAT1.2/*MaFAR/ScWS*, amiDGAT1.3/*MaFAR/ScWS*. (A)

Alcohol moiety calculated by total carbon number. **(B)** Acyl moiety calculated by total carbon number. **(C)** Alcohol moiety calculated by desaturation degree. **(D)** Acyl moiety calculated by desaturation degree. The data shown is calculated according to the wax ester composition shown in Figure 5.4.4. FW is the abbreviation of *MaFAR/ScWS*.

In summary, co-expression of *amiDAGT1* with *MaFAR* and *ScWS* did not significantly reduce the TAG content or further increase the amount of wax esters in seeds of *C. sativa*. However, the existence of *amiDGAT1.2* and *amiDGAT1.3* altered the fatty acyl profile of TAG and the compositions of wax esters in seeds of *C. sativa*.

5.5 Optimization of wax ester composition in the seeds of *C. sativa*

For the application in lubrication, it is better to produce those wax esters that mainly are composed of 18:1/18:1 (Iven *et al.*, 2015). However, the seed oil of *C. sativa* wild-type is rich in polyunsaturated fatty acids, including 15% - 25% linoleic acid (18:2) and 30% - 40% linolenic acid (18:3), making the seed oil oxidative unstable and inappropriate as a source for lubrication. Oleic acid (18:1) accounts for only 10% - 15% of total fatty acids in the seed oil of *C. sativa*, which is not sufficient for producing high levels of 18:1/18:1. Therefore, there is a need to increase the level of 18:1 in the seed oil of *C. sativa* for the formation of 18:1/18:1.

In a previous study, the seeds of more than 200 *C. sativa* wild-type lines from the Genebank in Gartersleben were ever grown in the green house. The fatty acid profiles of these seeds were analyzed and ten lines were finally selected for a higher percentage of 18:1. The selected ten wild-type lines then were grown in a climate chamber at the same time. The fatty acid profile of the resulting seeds for these ten lines were re-analyzed. However, the percentage of 18:1 ranged from 9.5% to 12.6% of total fatty acids, and was not significantly different from each other (Supplementary Material 12). In addition, no obvious differences in the fatty acid content were found among these wild-type lines (Supplementary Material 13). These results suggested that the natural variation has limited effects on the fatty acid profile and total oil content of *C. sativa* seeds. To increase the level of 18:1 in seed oil of *C. sativa*, it is therefore necessary to re-engineering fatty acid profile by biotechnological approaches.

5.5.1 Modification of fatty acid profile of *C. sativa* seeds

In order to improve the available wax ester quality, a major step is to tailor the substrate pool for the wax ester biosynthesis pathway by changing the fatty acid profile of the seed oil. In higher plants, *de novo* fatty acid biosynthesis occurs in the plastid and is catalyzed by the fatty acid synthase complex (FAS) yielding medium and long chain fatty acyl-CoAs (C_{16} and C_{18}). Then, these fatty acyl-CoAs are transported to the ER for further elongation and desaturation or they stay in the plastids. To reach a high oleic acid background, three enzymes need to be knocked-down at the same time. To block the

desaturation of 18:1-PC to polyunsaturated acyl-PC (such as 18:2-PC and 18:3-PC) in the seeds of *C. sativa*, two amiRNAs for down-regulating of *C. sativa* fatty acid desaturase 2 (CsFAD2), and two amiRNAs for targeting *C. sativa* fatty acid desaturase 3 (CsFAD3) were generated. For down-regulation of *C. sativa* fatty acid elongase 1 (CsFAE1), two amiRNAs were also created, so that oleic acyl-CoA could not be elongated to very long-chain acyl-CoAs (such as 20:1-CoA). In addition, palmitic acid (16:0) is another major fatty acid species in the seed oil of *C. sativa*. Palmitoyl-ACP (16:0-ACP) synthesized by the FAS might be further elongated to stearyl-ACP (18:0-ACP), and then desaturated to yield oleoyl-ACP (18:1-ACP) in the plastids. Fatty acyl-ACP thioesterase B (FatB) releases preferentially 16:0-ACP, so that it is transported out of the plastid instead of generating more 18:1-ACP. Therefore, down-regulation of FatB can also elevate the level of 18:1 for wax ester production, and one amiRNA for targeting *C. sativa* fatty acyl-ACP thioesterase B (CsFatB) was created.

Table 5.5.1 Numbers of harvested T2 *C. sativa* transgenic lines transformed with empty vector, amiFAD2.1, amiFAD2.2, amiFAD3.1, amiFAE1.1, amiFAE1.2 and amiFatB.

Construct	Number of T2 lines	GC-FID analysis
Empty vector	13	5
amiFAD2.1	12	12
amiFAD2.2	17	17
amiFAD3.1	12	12
amiFAD3.2	0	0
amiFAE1.1	18	18
amiFAE1.2	16	16
amiFatB	14	14

The efficiency of each amiRNA needed to be tested, and the best performing amiRNA for targeting each enzyme should be selected and then combined for the generation of a high oleic line. All amiRNAs against CsFAE1, CsFAD2, CsFAD3 and CsFatB were first cloned as a single construct under the napin promoter and transformed into *C. sativa*. The resulting transgenic lines were grown in a climate chamber and rotated every two days to make sure the plants got the same intensity of light. The single amiRNA lines were expected to have altered fatty acid profiles of the seed oil compared with those of control lines.

A total of 12 transgenic T2 lines for amiFAD2.1 and 17 lines for amiFAD2.2 were generated (Table 5.5.1). The two amiFAD2 were expected to target *C. sativa* fatty acid desaturase 2 (CsFAD2), so that the levels of 18:1 would be increased whilst the levels of 18:2 and 18:3 would decrease. However, the

effects of amiFAD2 were not obviously observed in all transgenic lines (Figure 5.5.1). 18:1 accounted for 12 mol% - 16 mol% of total fatty acids in negative controls (black spots in Figure 5.5.1), and only two individual lines with amiFAD2.2 (amiFAD2.2_3 and amiFAD2.2_15) contained a slight increase (over 16 mol%) of 18:1 (red spots in Figure 5.5.1). Meanwhile, there were two individual lines (amiFAD2.1_1 and amiFAD2.2_15) that had decreased levels of 18:2 plus 18:3 (around 50 mol%) compared with the 52 mol% - 55 mol% of negative controls (Figure 5.5.1). In addition, the individual line amiFAD2.1_1 interestingly contained 24 mol% 18:3, which was 10 mol% lower than those of negative control (Supplementary Material 16).

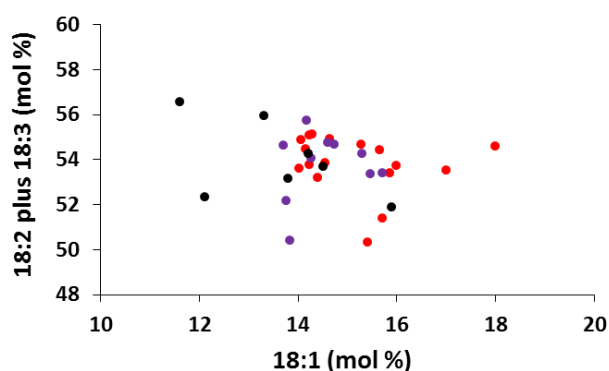


Figure 5.5.1 Mol% of oleic acid, linoleic acid plus linolenic acid of seed oil of *C. sativa* wild-type, transformed with empty vector, amiFAD2.1 and amiFAD2.2. Black spots are wild-type and empty vector individual lines used as negative control. Purple spots are individual lines with amiFAD2.1. Red spots are individual lines with amiFAD2.2. The data shown represent the mean value of each individual line determined with two extraction replicates of seed oil by GC-FID.

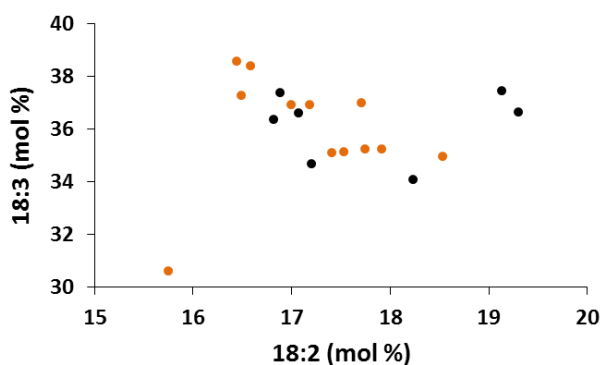


Figure 5.5.2 Fatty acid profile of seed oil of *C. sativa* wild-type, transformed with empty vector and amiFAD3.1. Black spots are wild-type and empty vector individual lines used as negative control. Orange spots are individual lines with amiFAD3.1. The data shown represent the mean value of each individual line determined with two extraction replicates by GC-FID.

The T2 seeds of in total 12 transgenic lines for amiFAD3.1 were harvested, but no transgenic lines for amiFAD3.2 were successfully created (Table 5.5.1). The amiFAD3 was expected to down-regulate CsFAD3, so that transgenic lines would contain decreased level of 18:3 and increased level of 18:2. In comparison to the 35 mol% - 37 mol% of negative controls, only one individual line of amiFAD3.1 had

a lower level of 18:3 (around 30 mol%; orange spot in Figure 5.5.2). No individual lines with amiFAD3.1 contained higher level of 18:2 than the negative controls. Additionally, several amiFAD3.1 transgenic lines had higher levels of 18:1 (about 16 mol%), but not significantly different from negative controls (Supplementary Material 16). In conclusion, the amiFAD3 did not significantly affect the fatty acid profile of *C. sativa* seed oil.

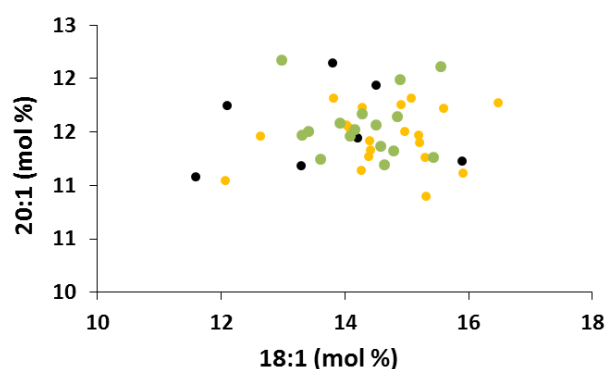


Figure 5.5.3 Mol% of oleic acid, gondoic acid of *C. sativa* wild-type, transformed with empty vector, amiFAE1.1 and amiFAE1.2. Black spots are wild-type and empty vector individual lines, yellow spots are amiFAE1.1 individual lines, green spots are individual lines with amiFAE1.2. The data shown represent the mean value of each individual line determined with two extraction replicates by GC-FID.

In total 18 T2 transgenic lines for amiFAE1.1 and 16 lines for amiFAE1.2 were generated. The transgenic lines with amiFAE1 were expected to contain lower levels of gondoic acid (20:1) as well as higher levels of 18:1. However, the levels of 20:1 in all amiFAE1 lines were around 11 mol% - 13 mol% (green and yellow spots in Figure 5.5.3), obvious different from those of negative controls (black spots in Figure 5.5.3). The highest level of 18:1 found in one amiFAE1 transgenic line (amiFAE1.1_6) was over 16 mol%, which was not significantly higher than the negative controls (Figure 5.5.3). In summary, the influences of the two amiFAE1 on the fatty acid profile of *C. sativa* seed oil were very limited.

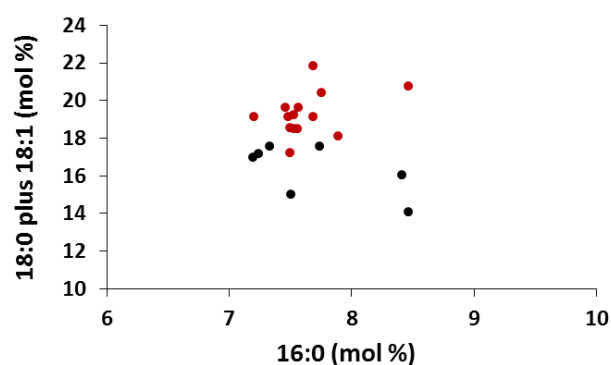


Figure 5.5.4 Mol% of palmitic acid, stearic acid plus oleic acid of seed oil of *C. sativa* wild-type, transformed with empty vector and amiFatB. Black spots are wild-type and empty vector individual lines, dark red spots are individual lines with amiFatB. The data shown represent the mean value of each individual line determined with two extraction replicates by GC-FID.

If CsFatB was successfully down-regulated by amiFatB, the level of 16:0 was expected to be decreased in the transgenic lines. However, in the generated 14 T2 transgenic lines with amiFatB, 16:0 accounted for over 7 mol%, which was not significantly different from the negative controls (Figure 5.5.4). Most of amiFatB individual lines contained slightly higher levels of 18:0 plus 18:1 than the negative controls. There were three individual lines (amiFatB_2, amiFatB_10 and amiFatB_13) containing relatively high level of 18:0 plus 18:1 (over 20 mol%), which were about 5 mol% higher than those of the negative controls (Figure 5.5.4).

Overall, as expression of the amiRNAs as single construct targeting CsFAD2, CsFAD3, CsFAE1 and CsFatB did not significantly influence the fatty acid profile of *C. sativa* seed oil, it was uncertain that the designed amiRNAs did efficiently knock-down the enzymes in the fatty acid desaturation and elongation pathway. Therefore, we decided not to co-express these amiRNAs with wax ester synthesizing enzymes.

5.5.2 Crossing wax ester producing lines with a high oleic line

In parallel to the attempts to generate high oleic lines using artificial microRNAs in the background of *C. sativa* suneson, I got an existing high oleic line (HO line) generated by the group of Prof. E. Cahoon (UNL, NE, USA). In order to change the unfavorable fatty acid composition of *C. sativa* seed oil, the *C. sativa* wild-type plants were transformed with the gene construct AtFAD2-RNAi+CsFAD3-RNAi+CsFAE1-RNAi to block the elongation and desaturation of C_{18:1} acyl-CoA. The seed oil of this *Atfad3/Csfad2/Csfae1* line contains around 65% 18:1 in total fatty acids (Nguyen *et al.*, 2013).

To optimize the composition of wax esters accumulating in seeds of *C. sativa*, six *MaFAR/ScWS* lines with high wax ester content were crossed with the HO line (mother line). The seeds of individual heterozygous plants resulting from the six crosses were germinated on steril filter papers. One of the two cotyledons of the individual seedlings were cut off and their wax ester contents were analyzed applying TLC (Supplementary Material 17), the seedlings with relatively high amounts of wax esters were planted on soil to propagate seeds of the next generation. Then, the resulting seeds of six independent *MaFAR/ScWS* & HO crosses were analyzed by GC-FID for the total wax ester content, and by ESI-MS/MS for the molecular species of wax esters.

The total yields of wax esters in seeds of the six *MaFAR/ScWS* & HO crosses ranged from 13 mg g⁻¹ seeds to 44 mg g⁻¹ seeds (Figure 5.5.5 A). L4 *MaFAR/ScWS* & HO and L5 *MaFAR/ScWS* & HO lines resulted in the highest wax ester accumulation up to the similar level found in seeds of the parental *MaFAR/ScWS* line (over 40 mg g⁻¹ seeds). But the amounts of wax esters produced by L13 *MaFAR/ScWS* & HO and L26 *MaFAR/ScWS* & HO lines were significantly lower than that of the *MaFAR/ScWS* lines (Figure 5.5.5 A).

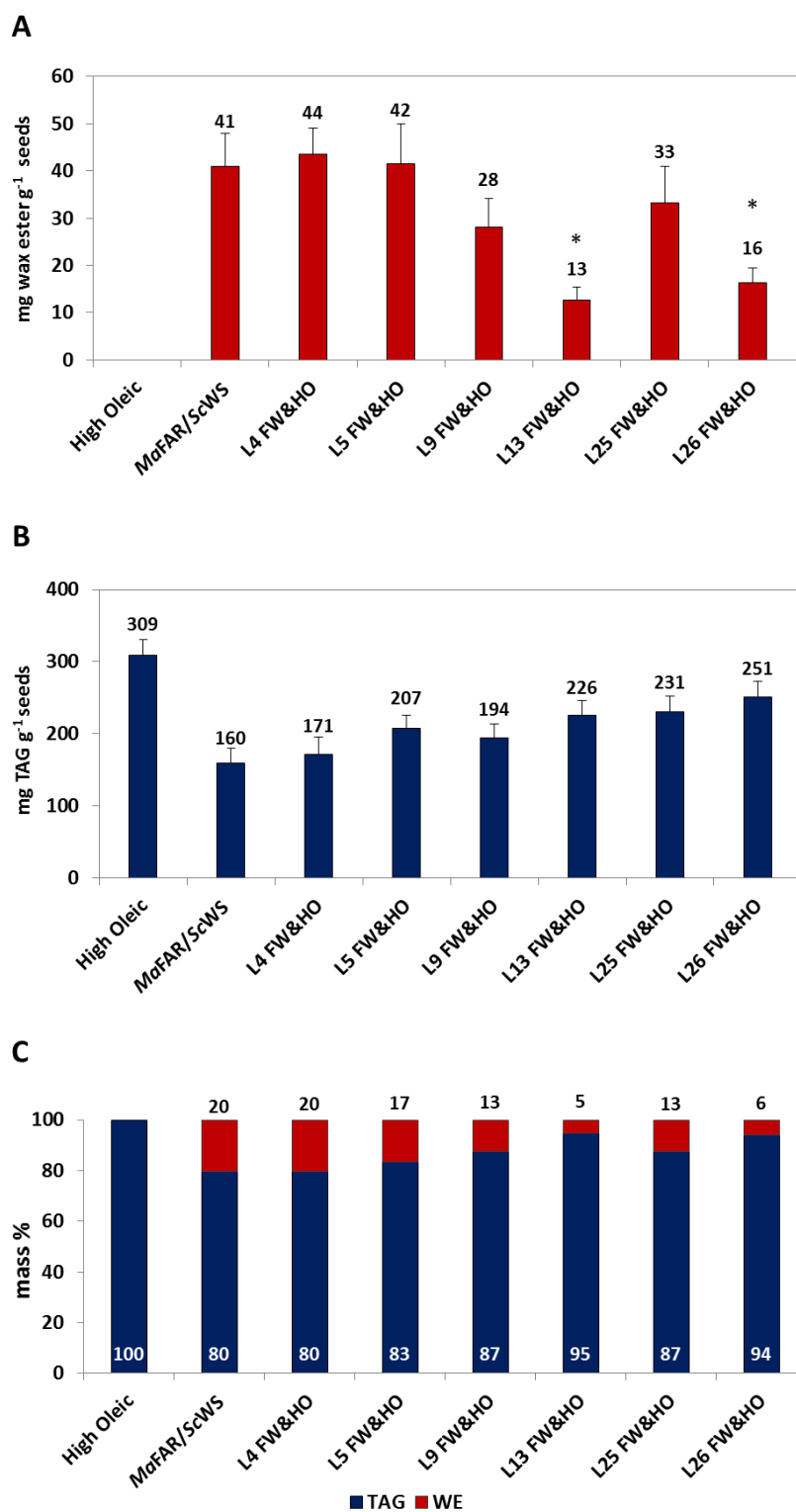


Figure 5.5.5 Wax ester and TAG accumulation in seeds of *C. sativa* containing high levels of oleic acid (HO), transformed with *MaFAR/ScWS* (FW), six crosses of *MaFAR/ScWS* with the HO line (FW/HO). (A) Absolute quantification of wax esters in mg g⁻¹ seeds. *means significantly different from *MaFAR/ScWS*, $p \leq 0.05$. (B) Absolute quantification of TAG in mg g⁻¹ seeds. (C) The relative quantification of total neutral lipids (WE, wax ester; TAG, triacylglycerol) in mass% are calculated according to the absolute quantification of each lipid class. The data

shown is an average of three individual heterozygous lines for each independent cross with two extraction replicates for each individual line. FW is the abbreviation of *MaFAR/ScWS*.

The TAG amounts in seeds of six *MaFAR/ScWS* & HO crosses ranged from 171 mg g⁻¹ seeds to 251 mg g⁻¹ seeds, which were lower than that of HO line. But these were not significantly higher than the 160 mg g⁻¹ seeds of the *MaFAR/ScWS* lines (Figure 5.5.5 B). As consequence, the wax ester to TAG proportion of the six *MaFAR/ScWS* & HO crosses ranged from 5% to 20%, with the best performing cross (L4 *MaFAR/ScWS* & HO) displaying a similar percentage of wax esters in the total neutral lipids compared with the *MaFAR/ScWS* lines (Figure 5.5.5 C).

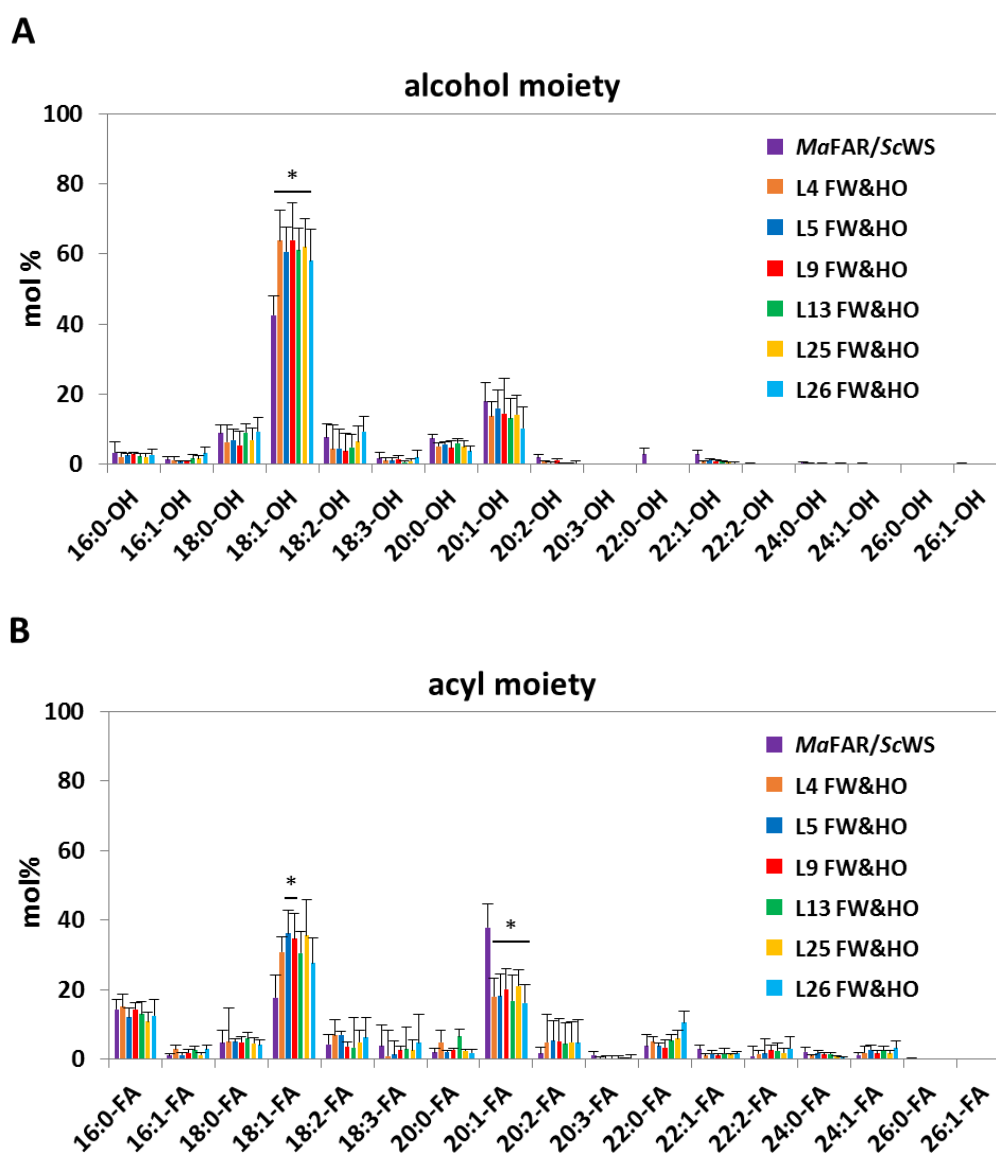


Figure 5.5.6 Alcohol and acyl moieties of wax esters in seeds of six *C. sativa* *MaFAR/ScWS* & HO cross lines. (A) Relative abundance of alcohol moieties in mol%. **(B)** Relative abundance of acyl moieties in mol%. The data shown is an average of three individual heterozygous lines for each independent cross with two extraction replicates for each individual line. *means significantly different from *MaFAR/ScWS*, $p \leq 0.05$. FW is the abbreviation of *MaFAR/ScWS*.

The compositions of wax esters produced by the six *MaFAR/ScWS* & HO crosses were obviously distinct from the *MaFAR/ScWS* lines (Figure 5.5.6). When *MaFAR* and *ScWS* were expressed in a high oleic background, the predominant alcohol species incorporated into wax esters was 18:1-OH, accounting for over 60 mol% of all fatty alcohol moieties, which was significantly higher than that in the *MaFAR/ScWS* lines. Additionally, less than 20 mol% 20:1-OH was utilized by the six *MaFAR/ScWS* & HO crosses, while the other fatty acids were not significantly different from that of the *MaFAR/ScWS* lines (Figure 5.5.6 A).

In regard to the fatty acyl moieties in wax esters, the six *MaFAR/ScWS* & HO crosses were different from the almost 40 mol% 20:1-FA found in the *MaFAR/ScWS* lines, incorporating significantly decreased levels of 20:1 (18 mol% - 20 mol%). However, 18:1 was predominantly utilized for wax ester production by the six *MaFAR/ScWS* & HO crosses, accounting for 30 mol% - 37 mol% of all fatty acyl moieties (Figure 5.5.6 B). In conclusion, high levels of C_{18:1} substrates were incorporated into wax esters by the six *MaFAR/ScWS* & HO crosses.

The molecular species of wax esters in seeds of the six *MaFAR/ScWS* & HO crosses were analyzed by ESI-MS/MS. In general, high levels of 18:1/18:1 were accumulated in the seeds of all tested individual lines resulting from the six *MaFAR/ScWS* & HO crosses (Figure 5.5.7). The six *MaFAR/ScWS* & HO crosses resulted in a much higher accumulation of 18:1/18:1 in seeds, compared with *MaFAR/ScWS* lines, which only accumulated 4.7 mol% 18:1/18:1 in all wax ester species (Figure 5.5.7; Iven *et al.*, 2015). Importantly, the major wax ester species is 18:1/18:1 for all six *MaFAR/ScWS* & HO crosses, with the highest level of 49% for the L25 *MaFAR/ScWS* & HO line, and the lowest level of 32% for the L26 *MaFAR/ScWS* & HO line (Figure 5.5.3 E and F). Furthermore, the *MaFAR/ScWS* combination accumulated large amounts of very long-chain wax esters (C₃₈ - C₄₀), with 17.7 mol% oleyl - gondonate (18:1/20:1) and 10 mol% gondoyl - gondonate (20:1/20:1). However, in the wax esters produced by the six *MaFAR/ScWS* & HO crosses, the level of 18:1/20:1 decreased to 8 mol% - 13 mol%, and the amount of 20:1/20:1 decreased to around 7 mol%. In contrary, more wax esters with shorter chain length (C₃₄ - C₃₆) were accumulated in the seeds of *MaFAR/ScWS* & HO crosses, with the levels of oleyl - palmitate (18:1/16:0) increased up to around 16 mol% of all wax ester species (Figure 5.5.7).

In conclusion, expression of *MaFAR* and *ScWS* in a HO background of *C. sativa* resulted in an increased level of 18:1/18:1 up to around 40 mol% of all wax ester species; meanwhile, the total amounts of wax esters and TAG accumulated in seeds of *C. sativa* were not negatively affected.

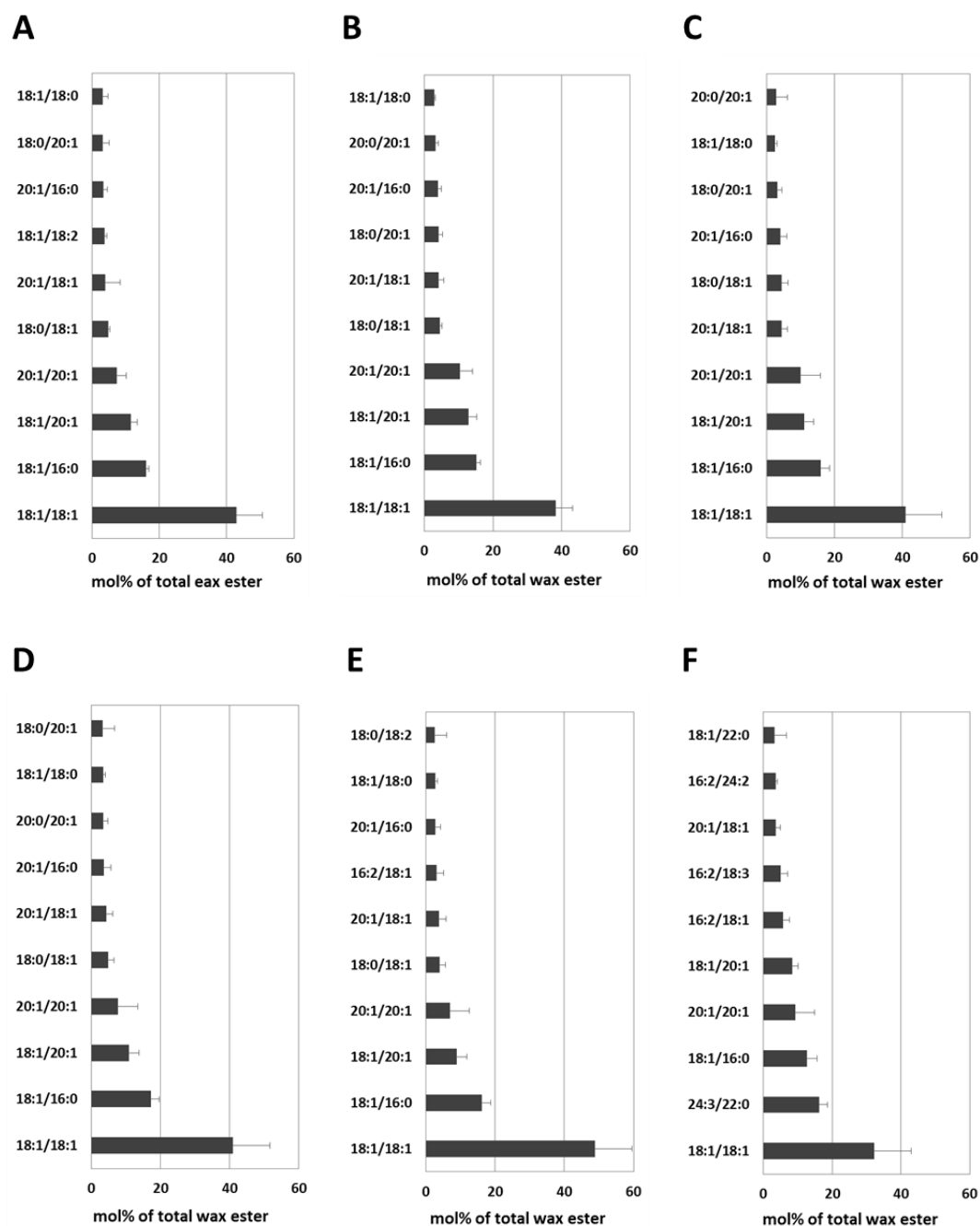


Figure 5.5.7 Wax ester profiles of six *C. sativa* MaFAR/ScWS &HO cross lines. (A) L4 FW&HO line; (B) L5 FW&HO line; (C) L9 FW&HO line; (D) L13 FW&OH line; (E) L25 FW&HO line; (F) L26 MA&HO line. Wax ester compositions were determined by nano-ESI-MS/MS. The relative abundance of the top ten wax ester molecular species (alcohol moiety/acyl moiety) are shown. The data shown is an average of ten individual heterozygous transgenic lines resulting from the six independent cross lines with two extraction replicates for each individual line. FW is the abbreviation of MaFAR/ScWS.

6 DISCUSSION

Overall, this study tested four different strategies: (i) trying to co-localize heterologous enzymes, (ii) identifying WSs with better substrate specificities, (iii) down-regulating competing pathway, and (iv) optimizing the substrate pool for the wax synthesis pathway. In this study, the abilities to produce wax esters of different combinations of WSs in combination with the FAR from *Marinobacter aqualeolei* VT8 were tested in yeast and *A. thaliana*. These combinations showed differences in the biosynthetic performance and composition of wax esters. Moreover, the catalytic activities of WSs were shown to be heavily affected upon expression in different hosts. Furthermore, down-regulation of a single enzyme on TAG biosynthesis was insufficient for blocking this competing pathway and thus promoting the biosynthesis of wax esters as demonstrated in *C. sativa*. However, producing wax esters in a high oleic background in *C. sativa* led to an increase in the formation of 18:1/18:1 as the composition of wax esters was closely related to the fatty acid profile of the seed oil.

6.1 Fusion of *MaFAR* with *ScWS* to locate *MaFAR* to the ER

6.1.1 Enzymatic activities of the *ScWS-MaFAR* fusion protein

For localization of *MaFAR* to the ER, a *ScWS-MaFAR* fusion protein was generated by fusing *MaFAR* to the C-terminal end of *ScWS*. The *ScWS-MaFAR* fusion protein was proved to harbor both FAR and WS activities as expected (Figure 5.1.2). However, the *ScWS-MaFAR* fusion protein as well as *MaFAR/ScWS* co-expression produced only low amounts of wax esters in *S. cerevisiae* (Figure 5.1.2); in contrast, expression of *MaFAR/ScWS* or the *ScWS-MaFAR* fusion protein in seeds of *A. thaliana* resulted in relatively high levels of wax ester accumulation (Figure 5.1.5 A). This is hard to interpret, since yeast only synthesizes C₁₆ – C₁₈ fatty acids (Sandager *et al.*, 2002), which should be the preferred substrates. *MaFAR* and *ScWS* are plant-type FAR and WS, respectively (Figure 1.4; Figure 1.6), and were heterologously expressed; therefore, they probably had low activities in *S. cerevisiae*, because of their low protein abundances. The codon usage values of *MaFAR* and *ScWS* indicated that these two proteins might have problems to be expressed in *S. cerevisiae* (Supplementary Material 20 and 21), thereby producing only small amount of wax esters.

The *A. thaliana* transgenic lines with β con::*ScWS-MaFAR* produced less wax esters in seeds compared with *MaFAR/ScWS* co-expression lines (Figure 5.1.5 A). There are several possibilities why the wax ester production of the *ScWS-MaFAR* fusion protein is lower than that of the *MaFAR/ScWS* co-expression. On one hand, the *ScWS-MaFAR* fusion protein was expressed under the soybean β -conglycinin promoter or the oleosin promoter, while the *MaFAR/ScWS* was expressed under the napin promoter. Therefore, the expression levels of the wax synthesizing enzymes and when these enzymes

are expressed in seeds of *A. thaliana* could be different. On the other hand, the optimal localization of *MaFAR* might be in the cytosol, where it catalyzes the reduction of C_{16} and C_{18} acyl-CoAs to fatty alcohols when these fatty acyl-CoAs are transported from plastids into the ER. Localization of *MaFAR* to the ER by fusing it to the C-terminal end of *ScWS* might have negatively influenced the biosynthesis of fatty alcohols, thereby decreasing the accumulation of wax esters. In addition, no free fatty alcohols were accumulated in the seeds of $\beta\text{con}::\text{ScWS-}MaFAR$ or co-expression *MaFAR/ScWS* transgenic lines, while there were several transgenic lines with $\beta\text{con}::\text{ScWS-}MaFAR/\text{oleo}::MaFAR$ that accumulated free fatty alcohols in *A. thaliana* seeds (Supplementary Material 3), illustrating that fatty alcohols synthesized by the separate polypeptide of *MaFAR* in the cytosol were not fully utilized by the *ScWS-MaFAR* fusion protein at the ER. It means that the enzymatic activity in the *ScWS-MaFAR* fusion protein might be compromised, and the activities of both the FAR and the WS were negatively affected by fusing them together. This could explain why the $\beta\text{con}::\text{ScWS-}MaFAR/\text{oleo}::MaFAR$ combination led to higher amounts of wax esters compared with the $\beta\text{con}::\text{ScWS-}MaFAR$ combination that produced less wax esters than the *MaFAR/ScWS* combination.

6.1.2 Substrate specificities of the *ScWS-MaFAR* fusion protein

In previous experiments, when *MaFAR* was expressed as a separate polypeptide in the cytosol, high levels of C_{16} and C_{18} alcohols were incorporated into wax esters by different WSs (Iven *et al.*, 2015). In this study, the successful localization of *MaFAR* to the ER by fusion of *MaFAR* with *ScWS* resulted in less reduction of C_{16} and C_{18} acyl-CoAs to fatty alcohols (Figure 5.1.6 A), strongly suggesting that the substrate specificity of *MaFAR* was influenced by its localization.

Unexpectedly, the *MaFAR* catalytic domain of the *ScWS-MaFAR* fusion protein reduced high levels of C_{20} acyl substrates, especially in case of $C_{20:1}$ acyl substrates, instead of taking more polyunsaturated acyl substrates, such as 18:2-FA and 18:3-FA from the ER (Figure 5.1.6 A). In previous experiments, it was shown too that co-expression of *MaFAR* with different WSs led to the incorporation of $C_{20:1}$ fatty alcohol into wax esters (Iven *et al.*, 2015). The results obtained from this study illustrated that when *MaFAR* was fused to the C-terminal end of *ScWS*, the specificity of *ScWS* to C_{20} substrates highly influenced the substrate preference of *MaFAR*, and this effect was even stronger as compared to the influence of the subcellular localization. The fusion might directly affect the catalytic specificities of both wax synthesizing enzymes by either changing the protein itself or the accessibility for the substrates. This may be explained by the fact that the elongation of $C_{18:1}$ to $C_{20:1}$ takes place in the same membrane.

Interestingly, with more available very long-chain and unsaturated fatty alcohols, the *ScWS* catalytic domain of the *ScWS-MaFAR* fusion protein showed a trend to utilize higher levels of $C_{20:1}$ acyl-CoAs instead of $C_{18:1}$ acyl-CoAs for wax ester biosynthesis (Figure 5.1.6 B), which probably illustrated that

the higher level of available C_{20:1} alcohols further promoted the substrate preference of ScWS for the fatty acyl-CoAs with similar chain-length and desaturation degree. This could also be one explanation of the low catalytic efficiency of the ScWS-*MaFAR* fusion protein, as the pool of C_{20:1} acyl-CoA for either the reaction of the *MaFAR* domain or the reaction of the ScWS domain is very limited in seeds of *A. thaliana*.

6.2 Bifunctional enzyme *AbWSD1* from *A. baylyi* ADP1

6.2.1 *AbWSD1*

The *AbWSD1* from *A. baylyi* ADP1 was the first characterized member of WS/DGAT enzymes (Kalscheuer and Steinbüchel, 2003). It catalyzes the synthesis of wax esters or TAGs from fatty acyl-CoAs with fatty alcohols or DAGs, respectively. To date, many WSs similar with *AbWSD1* have been identified to be responsible for the biosynthesis of wax esters or TAGs in several bacterial species (Röttig and Steinbüchel, 2013). The heterologous expression of *AbWSD1* in a quadruple mutant of *S. cerevisiae* without feeding fatty alcohol did not result in the formation of wax esters, while *AbWSD1* led to the accumulation of both TAG and fatty ethyl esters (Kalscheuer *et al.*, 2004). In the present study, the heterologous expression of a plant codon optimized *AbWSD1* (PCO*AbWSD1*) in *S. cerevisiae* with feeding fatty alcohol led to the accumulation of wax esters in yeast cells without the formation of TAGs (Figure 5.2.4), proving that fatty alcohols and DAGs are competitive substrates for *AbWSD1*.

Co-expression of *AbWSD1* with *MaFAR* resulted in that low amounts of wax esters were accumulated in seeds of *A. thaliana* and *C. sativa* (Figure 5.2.6; Supplementary Material 5). This might be due to the fact that the codon usage of *AbWSD1* was optimized for expression in *E. coli* in a previous study, and the enzyme probably could not be expressed at a high level in plant cells (Supplementary Material 6). Even though the optimization of *AbWSD1* for plant codon usage further promoted the formation of wax esters (12 mg g⁻¹ of seeds instead of 4 mg g⁻¹), the resulting yield was still very low (Figure 5.2.6 A). There are several possible explanations for these results. The *AbWSD1* is an enzyme from bacteria and its catalytic activity in plant cells might be strongly restricted due to the distinct intercellular environment from its original host cells. The expression level of PCO*AbWSD1* could be still very low, because only the first 20 codons instead of the full sequence of *AbWSD1* was optimized for *A. thaliana*. *AbWSD1* is a WS/DGAT enzyme, diacylglycerols and fatty alcohols are the competitive substrates for its activities (Kalscheuer and Steinbüchel, 2003). Upon expression in seeds of *A. thaliana*, the DGAT activity of *AbWSD1* might limit the WS activity. The bacterial-type WS/DGAT enzymes majorly utilized fatty acyl-ACPs not fatty acyl-CoAs as substrates for wax ester biosynthesis (Röttig and Steinbüchel, 2013). However, *AbWSD1* is a cytosolic enzyme, associated to the ER in plant cells as demonstrated by expression in onion cells (Figure 5.2.5 B) and is not able to access the fatty acyl-ACP substrate pool of the plastids. Thus, the catalytic abilities of *AbWSD1* was probably restricted in plant cells with its unfavorable acyl-CoA substrates.

In the present study, the substrate specificity of *AbWSD1* was studied in detail. It was reported that *AbWSD1* can accept C_{14} – C_{18} acyl-CoAs with the highest activity to C_{16} acyl-CoAs (Stöveken *et al.*, 2005). Upon expression in *A. thaliana* Col._0 background, *AbWSD1* showed higher preference for 18:1 and resulted in higher levels of 20:1/18:1 and 18:1/18:1 in the total wax esters in comparison to *ScWS* in the same background (Figure 5.2.2 A; Iven *et al.*, 2015). The *MaFAR/AbWSD1* combination tends to incorporate high levels of C_{18} alcohols into wax esters, but not higher than that incorporated by the *MaFAR/ScWS* combination (Figure 5.2.8 A). Moreover, *AbWSD1* tends to combine 20:1-OH with C_{18} acyl-CoAs, forming over 20 mol% of 20:1/18:1 (Figure 5.2.2 A), although C_{18} alcohols were the predominant alcohol species produced by *MaFAR* (Figure 5.2.7 A), while the *MaFAR/ScWS* combination predominantly produced 18:1/20:1 in seeds of *A. thaliana* Col._0 background (Iven *et al.*, 2015). These results illustrated that the preference of *MaFAR* to C_{18} substrates did not adapt the specificity of *AbWSD1* to these fatty alcohols. In addition, in Col._0 background, *AbWSD1* was found to have less preference for monounsaturated substrates in comparison to *ScWS*, instead, taking more saturated and dienoic substrates (Figure 5.2.8 C and D). Only in the *A. thaliana fad2 fae1* double mutant, *AbWSD1* utilized monounsaturated substrates to a high level (Figure 5.2.8 C and D), because of the great amount of 18:1-OH synthesized by *MaFAR* (Figure 5.2.2 A) and strong preference of *AbWSD1* for $C_{18:1}$ acyl-CoA (Figure 5.2.2 B). Overall, *AbWSD1* is beneficial for the formation of 18:1/18:1 in a high oleic background.

6.2.2 TMMmAWAT2-*AbWSD1*

Expression of mCherry-tagged PCO*AbWSD1* in onion epidermal cells indicated that *AbWSD1* alone is associated with the ER membrane in plant cells too (Figure 5.2.5). The ER localization of *AbWSD1* might be due to the hydrophobic region in its sequence, which might also influence activity and substrate specificity of *AbWSD1* (Stöveken *et al.*, 2005; Röttig and Steinbüchel, 2013). Even though it seems that re-localization of *AbWSD1* by adding the transmembrane domains is meaningless, actually, the TMMmAWAT2-*AbWSD1* fusion protein showed higher activity and different substrate specificities in comparison to *AbWSD1*. Although upon expression in *S. cerevisiae*, the TMMmAWAT2-*AbWSD1* fusion protein showed DGAT activity, it produced more wax esters than PCO*AbWSD1* (Figure 5.2.4). With the transmembrane domains of *MmAWAT2*, the TMMmAWAT2-*AbWSD1* fusion protein contains a huge stretch of an eukaryotic protein, which might help the enzyme to be better expressed than PCO*AbWSD1* in *S. cerevisiae*. The anchoring in the ER during translation may also help to avoid the degradation of the foreign protein, thereby increasing the level of the TMMmAWAT2-*AbWSD1* fusion protein. Interestingly, in *A. thaliana* Col._0 background, the *MaFAR/TMMmAWAT2-AbWSD1* combination showed higher specificity to 18:1-OH compared with the *MaFAR/AbWSD1* combination (Figure 5.2.7 A). As consequence, the *MaFAR/TMMmAWAT2-AbWSD1* combination incorporated higher levels of C_{18} alcohols and less saturated alcohols into wax esters in comparison to the *MaFAR/AbWSD1* combination (Figure 5.2.8 A and C). In addition, TMMmAWAT2-*AbWSD1* showed

slightly higher preference for C₁₈ acyl substrates (Figure 5.2.8 B), which might be the influence of the transmembrane domains of *MmAWAT2*.

6.3 Wax synthases from *M. aquaeolei* VT8

Even though the four WS from *M. aquaeolei* VT8 being homologous to *AbWSD1* were identified as WSs by BLAST (Holtzapfle and Schmidt-Dannert, 2007), in fact, these enzymes displayed distinct activities upon expression in *S. cerevisiae* (Figure 5.3.2). Different from the published results of an *in vitro* assay (Holtzapfle and Schmidt-Dannert, 2007), *MaWS1* showed to accept a broader range of acyl acceptors and not only being limited to fatty alcohols or DAGs. *MaWS3* was not detected to be active *in vivo*. *MaWS4* is actually not a WS but displayed unclear activity. A novel WS from *M. aquaeolei* VT8, *MaWS5*, was identified in addition to the already-studied *MaWS2*.

6.3.1 *MaWS1*

The *MaWS1* from *M. aquaeolei* VT8 was before identified as a bifunctional WS/DGAT enzyme in an *in vitro* assay, producing both wax esters and triacylglycerols (Holtzapfle and Schmidt-Dannert, 2007). In the present study, *in vivo* assays of *MaWS1* resulted in three additional products that accumulated in *S. cerevisiae* (Figure 5.3.2 A), suggesting a broader spectrum of substrates utilized by this enzyme. The chemical structures of these three unknown compounds produced by *MaWS1* were not identified in this study, but what already is known, that they are esters of fatty acyl-CoAs with unknown acyl acceptors. Analysis of these unknown compounds will be helpful for better understanding the enzymatic activity of *MaWS1*.

MaWS1 was reported to be very similar with *AbWSD1*, as it shares the highest amino acid identity (45%) with *AbWSD1* of the five WSs from *M. aquaeolei* VT8, meanwhile has similar enzymatic activity and substrate specificities as *AbWSD1* (Holtzapfle and Schmidt-Dannert; 2007). In the present study, *MaWS1* was therefore not regarded as a good candidate for the plant expression experiment, as *AbWSD1* was already expressed in seeds of *A. thaliana* but did not result in high yield of wax esters.

6.3.2 *MaWS2*

MaWS2 only harbors WS activity according to the *in vitro* assay (Holtzapfle and Schmidt-Dannert, 2007). Expression of *MaWS2* in *S. cerevisiae* led to accumulation of wax esters with feeding fatty alcohol and no production of any neutral lipids without fatty alcohols (Figure 5.3.2 A), proving that also *in vivo* *MaWS2* only displays WS activity. *MaWS2* was reported to be significantly more active than *MaWS1* as well as *AbWSD1* for the production of wax esters from hexadecanol-CoA and palmitoyl-CoA *in vitro* (Holtzapfle and Schmidt-Dannert, 2007). In contrast, another comparative test

showed opposite results saying that *MaWS1* is 3-fold more active than *MaWS2* with hexadecanol as acyl acceptor (Barney *et al.*, 2012). In the present study, expression of *MaWS2* in *S. cerevisiae* always led to higher amounts of wax esters compared with *MaWS1* in several replicated experiments. However, it is uncertain that the WS activity of *MaWS2* is higher than *MaWS1* without measuring the expression levels of these two protein in yeast cells.

Co-expression of *MaWS2* with *MaFAR* in seeds of *A. thaliana* did not cause high yield of wax esters (Figure 5.3.3), which was similar to the results with *AbWSD1*. The fact that the gene sequence of *MaWS2* was not codon usage optimized for expression in plant cells might be one of the reasons for this result. Moreover, the wax ester production ability of *MaWS2* in plant cells was low, perhaps because *MaWS2* is a bacterial-type enzyme and tend to utilize fatty acyl-ACPs instead of fatty acyl-CoAs for wax ester biosynthesis, while the level of fatty acyl-ACPs in plant cells is limited and restricted to the plastids as already has been discussed for *AbWSD1*. In addition, *MaWS2* has high specificity to C₁₈ saturated and monounsaturated acyl substrates (Holtzapple and Schmidt-Dannert, 2007; Barney *et al.*, 2012). However, there are low levels of C_{18:0} and C_{18:1} acyl substrates, but high amounts of polyunsaturated acyl substrates (such as C_{18:2} and C_{18:3}) in seeds of *A. thaliana* (Lemieux *et al.*, 1990), which are not the favorite substrates for *MaWS2*. Thus, the low yield of wax esters produced by the *MaFAR/MaWS2* combination in seeds of *A. thaliana* probably could be thus explained by the low availability of suitable substrates for *MaWS2*.

The composition of wax esters produced in *A. thaliana* showed that *MaWS2* has quite similar substrate specificities compared to *AbWSD1*, harboring high preference for C₁₈ acyl substrates, especially for C_{18:0} acyl-CoA and C_{18:1} acyl-CoA (Figure 5.2.7; Figure 5.3.4). *MaWS2* also showed high specificity to C₁₈ alcohols in the present study, predominantly incorporating 18:1-OH into wax esters. This is possibly the case because the substrate preference of *MaFAR* for C_{18:1} acyl-CoA resulted in a high level of 18:1-OH in the fatty alcohol substrate pool. Besides, it is also reasonable to speculate that as *MaWS2* and *MaFAR* originate from the same bacteria, their substrate specificities would be quite similar. In this study, the *MaFAR/MaWS2* combination was not expressed in the seeds of *A. thaliana fad2 fae1* double mutant, but it could be expected that the *MaFAR/MaWS2* combination might produce similar or even higher level of 18:1/18:1 in comparison to the *MaFAR/AbWSD1* combination, due to the high preference of *MaWS2* for both C₁₈ acyl and alcohols as substrates.

6.3.3 *MaWS3*

MaWS3 was reported not to be active in a previous *in vitro* assay (Holtzapple and Schmidt-Dannert, 2007). In this study, *MaWS3* did not show any enzymatic activity upon heterologously expression in *S. cerevisiae* too (Figure 5.3.2). One assumption for the inactive *MaWS3* is that this enzyme may use an entirely different set of substrates that are not involved in neutral lipid biosynthesis (Holtzapple and

Schmidt-Dannert, 2007), so that its reaction products were not detected by TLC in this study. Furthermore, the highly conserved acyltransferase motifs HHXXXDG that were found in *AbWSD1* and the other four WS genes from *M. aqualeolei* VT8, was different from the catalytic motif of *MaWS3* that was found to be HHXXXDA (Supplementary Material 7). Therefore, likely is that the substitution of the conserved glycine with alanine might negatively influence the activity of *MaWS3* as was already discussed previously by Holtzapfle and Schmidt-Dannert (2007).

6.3.4 *MaWS4*

Holtzapfle and Schmidt-Dannert (2007) tried to clone WS4 (Maqu_3711) from *M. hydrocarbonoclasticus* strain 8798, but found that it is a pseudogene with a stop codon that truncates its ORF. Hence, the activity of WS4 was not ever tested *in vitro* or *in vivo*. *M. hydrocarbonoclasticus* and *M. aqualeolei* had been proposed to be heterotypic synonyms (Márquez and Ventosa, 2005), and *MaWS4* (Maqu_3711) is not a product of a truncated pseudogene in *M. aqualeolei* VT8. In the present study, *in vivo* assays of *MaWS4* showed that it is neither a WS nor a DGAT, producing no wax esters or TAGs in *S. cerevisiae*; instead, *MaWS4* was active in producing an unknown compound that also accumulated in the yeast cells with *MaWS1* (Figure 5.3.2 B), indicating that *MaWS4* is an acyltransferase and has a partly similar catalytic activity as *MaWS1*. Besides, the capability of *MaWS4* to synthesize the unknown compound was observed to be inhibited by fatty alcohols, because this unknown compound was only accumulated when the yeast cells were not fed with fatty alcohol (Figure 5.2.3).

6.3.5 *MaWS5*

In this study, additional to the four WS homologous described by Holtzapfle and Schmidt-Dannert (2007), a fifth homologous gene of WS (*MaWS5*) was found to have 19% amino acid identity with *AbWSD1* (Supplementary Material 7). *MaWS5* was identified as a novel WS first by expression in *S. cerevisiae* (Figure 5.3.2), and then this discovery was confirmed by *in vitro* assays (Figure 5.3.7). *MaWS5* is a monofunctional enzyme only synthesizing wax esters like *MaWS2*. Expression of *MaWS5* resulted in higher level of wax esters accumulation in *S. cerevisiae* in comparison to *MaWS1* and *MaWS2*, but the assumption that *MaWS5* has higher WS activity than *MaWS1* and *MaWS2* need to be confirmed by measuring the quantity of these proteins in yeast cells or by enzyme kinetic analysis.

MaWS5 should be a cytosolic soluble protein since it contains neither transmembrane domains nor hydrophobic areas. During the purification of *MaWS5*-6xHis from *E. coli*, most of the *MaWS5*-6xHis proteins could be dissolved in the cell lysate supernatant; thus, *MaWS5*-6xHis was easily purified by NAC. SEC purification of *MaWS5*-6xHis resulted in four signals. The elution volumes of these four signals corresponded to aggregates, a tetramer of *MaWS5*-6xHis at about 220 kDa, a dimer of *MaWS5*-

6xHis at about 116 kDa and a monomer of *MaWS5*-6xHis at about 23 kDa. A huge signal of aggregates was observed and low concentration of the monomeric protein was obtained, when Tris-HCl buffer was used as the SEC elution buffer. This showed that *MaWS5*-6xHis tended to stay as polymer in the Tris-HCl buffer, resulting in the loss of the protein through SEC. Potassium phosphate buffer was previously used for purification of *MaWS1* and *MaWS2* (Brett *et al.*, 2012), and was also used for further purification of *MaWS5*-6xHis as the SEC buffer in this study. It was found that potassium phosphate was helpful for the stability of *MaWS5*-6xHis protein through SEC, and the detergent (CHAPS) in the buffer prevented most of the protein from being eluted as aggregates.

Even though the purified *MaWS5*-6xHis protein was already quite pure, the purification processes need to be further optimized, to use the purified *MaWS5*-6xHis protein for the studies of enzyme kinetics, substrate specificity and crystallization. Adding detergent into the NAC elution buffer might help to avoid the aggregation of the proteins from the beginning of the purification process, thereby increasing the concentration of proteins loaded onto the SEC column and decrease aggregate formation. Additionally, adding 5 - 10% glycerol to the SEC buffer might also be useful for enhancing the stability of *MaWS5*.

To date, no 3D structure of WS has been published. The structure of *MaWS2* was ever predicted by homology modeling (Juan *et al.*, 2013), but the provided information was limited and not very accurate. The researches about identifying the amino acid residues that influence the substrate specificities of WSs are also scarce. The species of tested substrates were restricted to the ones with C₈ - C₁₈ chain length, while very long-chain and unsaturated substrates have never been examined (Brett *et al.*, 2012a; Brett *et al.*, 2012b). A finding concerning *MaWS1* indicated that the alanine residue at position 360 is essential for the selectivity of this enzyme to the fatty alcohol chain length (Barney *et al.*, 2012). *MaWS5* and *MaWS1* were predicted as soluble cytosolic proteins with no transmembrane domains or hydrophobic areas (Supplementary Material 1), and are suitable for a rapid purification process (this study; Barney *et al.*, 2012). Thus, these two enzymes can be good candidates for studying their structure, catalytic mechanism and substrate specificities exemplary of bacterial-type WSs. For instance, mutant studies of *MaWS1* and *AbWSD1* showed that large amino acids may improve the binding of short-chain alcohols to the active sites of WSs (Brett *et al.*, 2012), and this speculation can probably be verified by mutating of specific amino acid residues of *MaWS5*. It is also possible to figure out why some bacterial-type enzymes only have WS activity while the others are bifunctional WS/DGAT enzymes by comparing the structures of *MaWS5* with *AbWSD1*.

6.4 Down-regulation of CsDGAT1 by amiRNAs

In a previous study done by Dr. Sofia Marmon, three amiRNAs targeting *CsDGAT1* were expressed in seeds of *C. sativa* as single constructs. The total TAG contents that accumulated in seeds of amiDGAT1

transgenic lines were not significantly different from the wild-type. But an obvious alteration was found for the fatty acid profile of the seed oil in the three amiDGAT1 transgenic lines, especially in amiDGAT1.2 and amiDGAT1.3 lines. Higher levels of 18:3 and less 18:1 and 20:1 fatty acids were observed.

Similar to the previous results, in this study, expression of amiDGAT1 with *MaFAR* and *ScWS* in seeds of *C. sativa* did not affect the TAG content of *C. sativa* seeds (Figure 5.4.2 B). However, the amiDGAT1.2/*MaFAR/ScWS* transgenic lines were found to contain obviously increased levels of 18:3-FA in TAGs compared with the *MaFAR/ScWS* combination, and the amiDGAT1.3/*MaFAR/ScWS* lines contained slightly increased levels of 18:3-FA in TAGs (Figure 5.4.3). According to the variation of TAG compositions in the amiDGAT1.2/*MaFAR/ScWS* as well as amiDGAT1.3/*MaFAR/ScWS* lines, it is very likely that amiDGAT1.2 and amiDGAT1.3 successfully down-regulated *CsDGAT1* that perhaps has substrate specificity to monounsaturated fatty acids. Once *CsDGAT1* was down-regulated, there were other enzymes in seeds of *C. sativa* taking the place of *CsDGAT1* and transferring $C_{18:3}$ acyl-CoA into the *sn*-3 position of DAGs; therefore, the levels of TAGs in seeds of *C. sativa* were constant only with changes in the fatty acid profile. Meanwhile, these enzymes might also affect the fatty acid editing cycle, thereby changing the fatty acid profile of the seed oil. According to the results of Dr. Sofia Marmon, expression of amiDGAT1.1 in seeds of *C. sativa* had the smallest effects on the fatty acid profile of seed oil, which was also shown in this study. Co-expression of amiDGAT1.1 with *MaFAR* and *ScWS* neither decreased the TAG content nor altered the fatty acyl profile of TAGs (Figure 5.4.2 B; Figure 5.4.3), indicating that amiDGAT1.1 was probably inefficient in down-regulating *CsDGAT1*.

There are extensive studies about the knock-out mutants of the DGAT1 from *A. thaliana* (*AtDGAT1*) leading to decreased seed oil content (Routaboul *et al.*, 1999; Zou *et al.*, 1999). It was expected that down-regulation of *CsGDAT1* would result in a similar phenotype of decreased TAG content as the *Atdgat1* mutants. However, the results obtained by Dr. Sofia Marmon and in this study are strikingly different from those in *A. thaliana*, which demonstrated that the model plant *A. thaliana* for certain aspects could not be a good model for crop plants of the *Brassicaceae* family. On the other hand, the *Atdgat1* mutants contain increased level of 18:3 and reduced levels of 18:1 and 20:1 (Routaboul *et al.*, 1999), and similar phenotypes were also observed in the *C. sativa* transgenic lines with amiDGAT1. These results could possibly illustrate the resemblance of *AtDGAT1* and *CsGDAT1* on substrate specificities.

Most of the amiDGAT1/*MaFAR/ScWS* lines produced less wax esters compared with *MaFAR/ScWS*, only two individual lines with amiDGAT1.2/*MaFAR/ScWS* produced similar amounts or slightly higher yields of wax esters (Figure 5.4.2 A). This might be because the numbers of resulting amiDGAT1/*MaFAR/ScWS* transgenic lines were very limited. In previous experiments, over 70 transgenic lines with *MaFAR/ScWS* were created and screened by TLC, while only 19 lines for amiDGAT1.2/*MaFAR/ScWS* and 6 lines for amiDGAT1.3/*MaFAR/ScWS* were obtained in this study

(Table 5.4.1). If more amiDGAT1/*MaFAR/ScWS* transgenic lines were available, there might be more individual lines of the amiDGAT1.2/*MaFAR/ScWS* accumulating similar or even higher amounts of wax esters with the *MaFAR/ScWS* combination.

The molecular species of wax esters produced by the amiDGAT1/ *MaFAR/ScWS* lines were obviously changed due to the action of amiDGAT1. Higher level of C_{18:3} acyl-CoA but lower levels of C_{18:1} acyl-CoA and C_{20:1} acyl-CoA were incorporated into wax esters by the three amiDGAT1/*MaFAR/ScWS* lines in comparison to *MaFAR/ScWS* (Figure 5.4.4 B), probably because more 18:3 while less 18:1 and 20:1 in the fatty acid pool are available in the amiDGAT1/*MaFAR/ScWS* transgenic line as the single amiDGAT1 lines created by Dr. Sofia Marmon. Interestingly, all three amiDGAT1/*MaFAR/ScWS* combinations incorporated more 20:1-OH into wax esters compared with the *MaFAR/ScWS* combination (Figure 5.4.4 A), indicating the presence of amiDGAT1 somehow possibly promoted the preference of *MaFAR* for 20:1 in the condition of less available of 20:1. In addition, high levels of C_{18:0} acyl-CoA were utilized by amiDGAT1.1/*MaFAR/ScWS* and amiDGAT1.3/*MaFAR/ScWS* (Figure 5.4.4 B), but the reasons for these results are unclear.

The *AtDGAT1* was reported to highly influence the seed weight and shape (Jako *et al.*, 2001; Routaboul *et al.*, 1999). The seeds of amiDGAT1.1/*MaFAR/ScWS* lines were distorted and smaller compared with those of wild-type, while the seeds of amiDGAT1.2/*MaFAR/ScWS* were bigger in size (Supplementary Material 22). These phenotypes may probably due to the down-regulation of *CsDGAT1*; on another aspect perhaps because the amiRNAs of *CsDGAT1* off-targeted other enzymes that are involved in the determination of seed size and shape. However, it is more likely that they harbor simply more starch and water, because TAG biosynthesis is affected, thus leading to larger seeds.

6.5 Optimization of wax ester composition in the seeds of *C. sativa*

Expression of *MaFAR/ScWS* or *MaFAR/AbWSD1* in *A. thaliana fad2 fae1* double mutant resulted in over 60 mol% 18:1/18:1 in all wax ester molecular species (Iven *et al.*, 2015; Figure 5.2.2), regardless of the substrate specificities of the wax ester producing enzymes. This suggests that the profile of the fatty acyl substrate pool is more important than the substrate specificities of the enzymes for determining the molecular species of wax esters. In this study, the same strategy of adjusting the fatty acyl substrate pool was transferred to *C. sativa*.

6.5.1 Modification of fatty acid profile by amiRNAs

To tailor the wax ester composition for producing higher levels of 18:1/18:1, the first step should be modifying the fatty acid profile of the seed oil for higher levels of oleic acid. In this study, amiRNAs were designed to knock-down *CsFAD2*, *CsFAD3*, *CsFAE1* and *CsFatB*. These amiRNAs were expressed in

seeds of *C. sativa* as single constructs; however, the effects of all single amiRNAs were not that obvious as expected. No significant differences in the fatty acid profile were observed between the single amiRNA lines and wild-type (Figure 5.5.1 - Figure 5.5.4). There may be several reasons that probably could explain these results. (1) There were limited numbers of transgenic lines for each single amiRNA obtained in this study. If a greater number of transgenic lines were created and studied, significant effects of single amiRNAs might be seen. (2) The designed amiRNAs did not successfully target the mRNAs of *CsFAD2*, *CsFAD3*, *CsFAE1* or *CsFatB*. However, this may be unlikely, because some individual lines with single amiRNAs were observed to have an altered fatty acid profile. For instance, several individual lines with amiFAD2 had lower levels of polyunsaturated fatty acids and a little higher level of oleic acid (Figure 5.5.1), and individual lines with amiFatB contained higher levels of stearic acid and oleic acid compared with wild-type (Figure 5.5.4). These changes might be the influences of amiFAD2 and amiFatB, and to verify whether the single amiRNAs successfully down-regulated *CsFAD2*, *CsFAD3*, *CsFAE1* or *CsFatB* or not, quantification of the mRNA levels of these enzymes in developing seeds of transgenic lines should to be conducted. However, cultivation of single amiRNA lines to the next generation to collect developing seeds for quantification of mRNAs would take four months more, so it was not done in this study due to the time limitation. (3) To clone two amiRNAs for *CsFAE1*, a quick cloning method described by Carbonell *et al.* (2014) was used, different from the cloning method for amiFAD2, amiFAD3 and amiFatB. The two 21 bp annealing oligonucleotide pairs of amiFAE1 were directly cloned into the pEntry vector, so that the transcribed amiRNA constructs of *CsFAE1* were much shorter than the 415 bp for amiFAD2, amiFAD3 and amiFatB. Although the amiRNAs cloned with the method of Carbonell *et al.* (2014) should show high efficiency in *A. thaliana*, the efficiency in *C. sativa* could not be confirmed in this study. (4) Although artificial microRNA technology is one of the most widely used and convenient approaches for down-regulating specific enzymes in crop plants, actually expression of amiRNA constructs could not be effective in 100% of the cases (Alvarez *et al.*, 2006; Ossowski *et al.*, 2008). In addition, amiRNAs have potential off-targeting effects and might result in unexpected phenotypes. (5) The fatty acid editing pathway of *C. sativa* is super active due to its hexaploid genome (Kagale *et al.*, 2014; Nguyen *et al.*, 2013). It means that there are always three homologous genes of each enzyme, for example, three homologous genes were found for *CsFAD2* (Kang *et al.*, 2011). Even though the amiRNAs used in this study were designed to be complementary to all three copies of each enzyme, the transcription levels of amiRNAs were probably insufficient for efficiently targeting all the mRNAs transcribed from three homologous genes.

6.5.2 *MaFAR/ScWS* &HO crosses

In a previous study, the combination of *MaFAR* with *ScWS* in *A. thaliana fad2 fae1* double mutant resulted in 61 mol% 18:1/18:1 in all wax ester molecular species, indicating that the optimization of acyl-CoA pool has a high influence on the formation of 18:1/18:1 (Iven *et al.*, 2015). In this study, in

parallel to modify the fatty acid profile of *C. sativa* seeds by amiRNAs using a Suneson wild type, an *Atfad3/Csfad2/Csfae1* line (RNAi) was donated by Prof. E. Cahoon, and crossed with six wax ester producing lines. The generated six independent *MaFAR/ScWS* & HO crosses showed the biosynthetic abilities to yield the highest levels of desirable wax ester molecular species, producing about 40 mol% 18:1/18:1 (over 50 mol% for the best cross lines; Figure 5.5.7), suggesting that the metabolic engineering of the fatty acid substrate pool for higher levels of 18:1 is most beneficial for the formation of 18:1/18:1 wax esters in seeds of *C. sativa*. The yields of wax esters produced by *MaFAR/ScWS* in *fad2 fae1* double mutant were slightly decreased compared with *MaFAR/ScWS* in Col.₀ background (Iven *et al.*, 2015). However, in this study, the best performing *MaFAR/ScWS* & HO cross accumulated similar amounts of wax esters in the seeds of *C. sativa* compared with the *MaFAR/ScWS* lines (Figure 5.5.5 A). Over 60% 18:1 was found in the cotyledons of six *MaFAR/ScWS* & HO crosses (Supplementary Material 23), illustrating that the six *MaFAR/ScWS* & HO cross lines successfully inherited the traits of parent lines.

Furthermore, expression of *MaFAR/ScWS* in *A. thaliana fad2 fae1* double mutant resulted in around 60 mol% 18:1/18:1 (Iven *et al.*, 2015), which was much higher than the over 40 mol% 18:1/18:1 of *MaFAR/ScWS* in *C. sativa* HO line. This difference could possibly be explained by the fact that the *A. thaliana fad2 fae1* double mutant contains over 80% 18:1 in all fatty acid species, while the *C. sativa* HO line was generated by an RNAi approach, and the achieved highest percentage of 18:1 is therefore only 65% (Nguyen *et al.*, 2013). Thus, the six *MaFAR/ScWS* & HO crosses actually accumulated the smaller amounts of 18:1/18:1 in seeds compared with the *MaFAR/ScWS* *A. thaliana* lines, due to less available of oleic substrates and lower yields of wax esters in seeds of *C. sativa*.

In addition, the molecular species of wax esters produced by *MaFAR/ScWS* & HO crosses showed that 18:1-OH was predominantly incorporated into wax esters, indicating the high specificity of *MaFAR* against C_{18:1} substrates upon exposition to high amounts of 18:1. Therefore, the usage of *MaFAR* in HO background is beneficial for the formation of 18:1/18:1. However, there were still over 10 mol% 18:1/20:1 and around 8 mol% 20:1/20:1 that accumulated in the seeds of *MaFAR/ScWS* & HO crosses (Figure 5.5.3 B), showing that *ScWS* has a very high preference for C_{20:1} substrates.

6.6 The threshold of wax ester yield and the white cotyledon phenotype

Until now, *MaFAR/ScWS* is still our best performing combination, producing over 100 mg g⁻¹ wax esters in seeds of *A. thaliana* and more than 40 mg g⁻¹ in seeds of *C. sativa*, respectively. It means the *MaFAR/ScWS* combination accumulated wax esters up to around 50% of total neutral lipids in seeds of *A. thaliana* and about 20% of total neutral lipids in seeds of *C. sativa*. The yield of wax esters in seeds of *C. sativa* with *MaFAR/ScWS* is less than half of the amount in seeds of *A. thaliana* with the same construct, showing that due to an unknown reason, *C. sativa* seeds seem to be more sensitive

for wax esters than *A. thaliana* seeds. On one aspect, this may be explained by the fact that *C. sativa* is a hexaploid plant and there are probably a greater number of homologous genes expressing functional enzymes that are involved in the TAG biosynthesis; on the other aspect, this might be due to the napin promotor is less active in *C. sativa* seeds (Iven *et al.*, 2015). This result also revealed that transferring an effective strategy exploited in a model plant sometimes would not lead to equal effects on a crop plant.

However, the transgenic *A. thaliana* and *C. sativa* lines accumulating relatively high amount of wax esters had white cotyledons, and the seedlings of transgenic lines were delayed in the early stage of development, illustrating that the big amounts of wax esters in seeds have negative influences on the seed germination. The reasons for the white cotyledon phenotype are not clear, but it is known that the phenotype is not due to the lack of TAG for germination, as there are still enough amounts of TAG accumulated in the wax ester producing lines. Providing the seeds with sugar neither complemented the phenotype nor prevented the delay in germination (communicating with Dr. Ellen Hornung), so it might be not related to the shortage of energy or biosynthetic precursors.

The cDNA of ScWS was expressed previously in seeds of *A. thaliana* in combination with cDNA of ScFAR and a β -ketoacyl-CoA synthase from *Lunaria annua*, resulting in the highest levels of wax esters which represent up to 70% of total neutral lipids in individual seeds (Kathryn *et al.*, 2000). But we never tested the levels of wax esters in individual seeds, so there might be *A. thaliana* seeds of the MaFAR/ScWS combination containing even higher amounts of wax esters. Similarly, there is a great possibility that some seeds of transgenic *C. sativa* with even higher yields of wax esters were obtained in this study, but these seeds did not germinate or the seedlings did not grow to the mature plants.

7 OUTLOOK

In order to further enhance the total yields of wax esters and optimize the compositions of wax esters in seeds of *C. sativa*, several experimental approaches are interesting to be further studied.

As there is still no structure model of WSs available, it would be interesting to use *MaWS5* as a candidate for crystallization. Being a soluble protein, *MaWS5* was not only produced in large amounts in *E. coli* but easily purified by NAC. Hence, the optimization of purification conditions of *MaWS5* could produce enough pure protein for crystallization. Furthermore, the structure model of *MaWS5* might show putative channels for both the active site and substrates, so it would be interesting to make site directed mutagenesis of interesting amino acid residuals to change the activity or the substrate specificity of this enzyme. In addition, *MaWS5* is also a good candidate to be co-expressed with *MaFAR* in seeds of *A. thaliana* and *C. sativa*. Considering that acyl-ACPs instead of acyl-CoAs might be favored substrates of the WSD/bacterial-type WSs, it would be better to locate *MaWS5* in plastids upon expression in plant seeds.

MaWS1 is predicted to be soluble and have no transmembrane domains, so it is also interesting to purify this protein for crystallization. *MaWS1* is a bifunctional enzyme, while *MaWS5* only has WS activity. A pure WS (*MaWS5*) and a bifunctional enzyme (*MaWS1*) from the same bacteria then can be compared on the structure basis, so that interesting amino acid residues that are responsible for the bifunctionality can be determined. Additionally, *MaWS1* shows activities to other substrates besides fatty alcohols and DAGs, producing three unknown products upon heterologously expression in yeast. It might be interesting to identify the chemical structure of these reaction products, for better understanding the catalytic characters of *MaWS1*.

The attempts to down-regulate *CsDGAT1* in this study, as well as the results that obtained from the *Atdgat1* mutant lines (Jako *et al.*, 2001; Routaboul *et al.*, 1999) suggested that *DGAT1* importantly influences the TAG biosynthesis, and down-regulation of only this enzyme was insufficient to completely block the biosynthesis of TAGs. Thus, in order to efficiently down regulate TAG biosynthesis and thereby promoting the production of wax esters, some other enzymes that are involved in the Kennedy Pathway, such as *CsDGAT2*, *CsPAP* and *CsLPAAT*, are also good candidates to be down-regulated. Furthermore, it is also interesting to study which acyltransferases took the place of *CsDGAT1* and preferred to transfer linolenic acyl-CoA to the *sn*-3 position of DAGs, thereby altering the fatty acid composition of TAGs that were produced by the *amiDGAT1.2/MaFAR/ScWS* and *amiDGAT1.3/MaFAR/ScWS* transgenic lines.

In this study, expression of a single amiRNA targeting *CsFAD2*, *CsFAD3*, *CsFAE1* or *CsFatB* did not show obvious effects on the fatty acid profile of Camelina seed oil. Measurement of the transcription levels of these enzymes by quantification PCR therefore should be done to make sure whether these

enzymes were really down-regulated by the expressed single amiRNA constructs. Furthermore, the hexaploid genome of *C. sativa* is possibly a big challenge for the modification of lipid metabolism. There are always three homologous genes for each enzyme in *C. sativa*, but the efficiency of artificial microRNAs sometimes could not be 100% guaranteed. In addition, amiRNAs have potential unspecificity of targeting, which might disturb functions of other enzymes and result in undesired phenotypes. Therefore, to modify the lipid metabolic fluxes of *C. sativa*, it might be better to utilize the genetic tools that have higher efficiency than the artificial microRNA technology. In recent years, a variety of genome editing technologies provide novel ways to create mutants in a target gene. The emergence of CRISPR/Cas9 technology has shown a high efficiency in inducing targeted gene mutants in plant systems, such as *A. thaliana* and rice (Belhaj *et al.*, 2013). Similar to RNA interference pathways, the CRISPR system relies on a single-strand guide RNA which confers the specificity of gene targeting and the expression of a nuclease (Cas9) to invading nucleic acids. The DNA sequence of both Cas9 enzyme and a single-strand guide RNA can be easily carried by a binary vector and transformed into *A. thaliana* by standard floral dipping method (Zhang *et al.*, 2013). More importantly, the mutations can be induced into genome effectively and inherited stably to the posterity. With the promise of CRISPR/Cas9 technology, the endogenous fatty acid editing cycle of *C. sativa* could be altered by genetic knockout of key enzymes on the genomic level. This means that the level of 18:1 in seed oil of *C. sativa* possibly will be higher than the 65% of *Atfad3/Csfad2/Csfae1* line.

8 ABSTRACT

Wax esters are the esters of primary long-chain fatty alcohols and long-chain fatty acids in various combinations, including different chain length and a variety of desaturation degrees. Wax esters cover a wide range of chemical and physical properties, therefore are interesting for many industrial applications. 18:1/18:1 is the most favorable wax ester species for the lubrication purpose. To establish a heterologous pathway for wax ester biosynthesis in plants, only two enzymes are necessary, a FAR and a WS. In previous studies, the introduction of FARs and WSs from different organisms into the seeds of *C. sativa* resulted in the accumulation of wax esters, but the yields of wax esters as well as the levels of 18:1/18:1 were still low for industrial applications. Attempts of producing higher yields of wax esters, and especially promoting the formation of 18:1/18:1 in seeds of *C. sativa* for industrial purpose were conducted, and several approaches were tried in the present study.

In opposition to the previous studies that always focus on the eukaryotic WSs, the abilities of a bifunctional WS/DGAT enzyme from *A. baylyi* ADP1 and several WSs from *M. aquaeolei* VT8 were tested in the present study. An enzyme from *M. aquaeolei* VT8 was identified as a novel WS by both *in vivo* and *in vitro* assays. Co-expression of bacterial-type WSs with *MaFAR* in seeds of *A. thaliana* did not result in big amounts of wax esters. However, the compositions of the wax esters produced by the bacterial-type WSs was more favorable for lubrication. The optimization of a bacterial-type WS led to increased levels of wax esters, but the resulting yields were still lower than in the *MaFAR/ScWS* lines that were obtained in a previous experiment. The co-localization of *MaFAR* together with *ScWS* to the ER was not able to increase the yields of wax esters in seeds of *A. thaliana*, while led to obvious alternations in the compositions of wax esters. This work provides better insights into the enzymatic characteristics and the substrate specificities of several wax ester production enzymes.

The attempt to down-regulate *CsDGAT1* neither block the last step of TAG biosynthesis nor further promote the biosynthesis of wax esters in seeds of *C. sativa*. Whereas, co-expression of *amiDGAT1* with *MaFAR* and *ScWS* unexpectedly altered the compositions of TAGs and wax esters in seeds of *C. sativa*. Expression of *MaFAR* with *ScWS* in a high oleic acid *C. sativa* background by crossing the *MaFAR/ScWS* lines with an *Atfad3/Csfad2/Csfae1* line did not affect the yields of wax esters, whilst led to the accumulation of 18:1/18:1 up to 40 mol% of all wax ester molecular species. This study suggested the importance of acy-CoA pool for tailoring the compositions of wax esters, and also showed that the biosynthesis of valuable chemical stocks at a big amount in plant seeds is still a challenge.

9 REFERENCES

- Aarts, M. G., Dirkse, W. G., Stiekema, W. J., & Pereira, A.** (1993). Transposon tagging of a male sterility gene in Arabidopsis. *Nature*, *363*, 715 – 717.
- Aaij, C., & Borst, P.** (1972). The gel electrophoresis of DNA. *Biochimica et Biophysica Acta (BBA)-Nucleic Acids and Protein Synthesis*, *269*(2), 192-200.
- Agegenehu, M., & Honermeier, B.** (1997). Effects of seeding rates and nitrogen fertilization on seed yield, seed quality and yield components of false flax. *Die Bodenkultur*, *48*(1), 15-20.
- Altman, A., & Hasegawa, P. M.** (2011). Plant biotechnology and agriculture: prospects for the 21st century. *Academic press*.
- Alvarez, J. P., Pekker, I., Goldshmidt, A., Blum, E., Amsellem, Z., & Eshed, Y.** (2006). Endogenous and synthetic microRNAs stimulate simultaneous, efficient, and localized regulation of multiple targets in diverse species. *The Plant Cell*, *18*(5), 1134-1151.
- Alvarez, H. M.** (2016). Triacylglycerol and wax ester-accumulating machinery in prokaryotes. *Biochimie*, *120*, 28-39.
- An, D., & Suh, M. C.** (2015). Overexpression of Arabidopsis WRI1 enhanced seed mass and storage oil content in Camelina sativa. *Plant Biotechnology Reports*, *9*(3), 137-148.
- Aichholz, R., & Lorbeer, E.** (1999). Investigation of combwax of honeybees with high-temperature gas chromatography and high-temperature gas chromatography–chemical ionization mass spectrometry: I. High-temperature gas chromatography. *Journal of Chromatography A*, *855*(2), 601-615.
- Ausubel, F. M., Brent, R., Kingston, R. E., Moore, D. D., Seidman, J. G., Smith, J. A.,...& Struhl, K.** (1989). Current protocols in molecular biology. *Greene Publishing Associates and Wiley-Interscience*. New York.
- Bansal, S., & Durrett, T. P.** (2016). Camelina sativa: An ideal platform for the metabolic engineering and field production of industrial lipids. *Biochimie*, *120*, 9-16.
- Barney, B. M., Wahlen, B. D., Garner, E., Wei, J., & Seefeldt, L. C.** (2012). Differences in substrate specificities of five bacterial wax ester synthases. *Applied and Environmental Microbiology*, *78*(16), 5734-5745.
- Barney, B. M., Mann, R. L., & Ohlert, J. M.** (2013). Identification of a residue affecting fatty alcohol selectivity in wax ester synthase. *Applied and Environmental Microbiology*, *79*(1), 396-399.

- Bassam, N. E.** (2013). Energy plant species: their use and impact on environment and development. *Routledge*.
- Bates, P. D., & Browse, J.** (2011). The pathway of triacylglycerol synthesis through phosphatidylcholine in Arabidopsis produces a bottleneck for the accumulation of unusual fatty acids in transgenic seeds. *The Plant Journal*, *68*(3), 387-399.
- Bates, P. D., Stymne, S., & Ohlrogge, J.** (2013). Biochemical pathways in seed oil synthesis. *Current Opinion in Plant Biology*, *16*(3), 358-364.
- Bart, J. C. J., Gucciardi, E., & Cavallaro, S.** (2013). Renewable feedstocks for lubricant production. *Biolubricants: Science and Technology*, 121-248.
- Benson, A. A., & Lee, R. F.** (1972). Wax esters: major marine metabolic energy sources. *Biochemical Journal*, *128*(1), 10P.
- Belhaj, K., Chaparro-Garcia, A., Kamoun, S., & Nekrasov, V.** (2013). Plant genome editing made easy: targeted mutagenesis in model and crop plants using the CRISPR/Cas system. *Plant Methods*, *9*(1), 1.
- Biester, E. M., Hellenbrand, J., Gruber, J., Hamberg, M., & Frentzen, M.** (2012). Identification of avian wax synthases. *BMC Biochemistry*, *13*(1), 1.
- Biermann, U., Friedt, W., Lang, S., Lühs, W., Machmüller, G., Metzger, J. O., ... & Schneider, M. P.** (2000). New syntheses with oils and fats as renewable raw materials for the chemical industry. *Angewandte Chemie International Edition*, *39*(13), 2206-2224.
- Bimboim, H. C., & Doly, J.** (1979). A rapid alkaline extraction procedure for screening recombinant plasmid DNA. *Nucleic Acids Research*, *7*(6), 1513-1523.
- Boyer, H. W.** (1971). DNA restriction and modification mechanisms in bacteria. *Annual Reviews in Microbiology*, *25*(1), 153-176.
- Bradford, M. M.** (1976). A rapid and sensitive method for the quantitation of microgram quantities of protein utilizing the principle of protein-dye binding. *Analytical Biochemistry*, *72*(1-2), 248-254.
- Brown, A. P., Affleck, V., Fawcett, T., & Slabas, A. R.** (2006). Tandem affinity purification tagging of fatty acid biosynthetic enzymes in *Synechocystis* sp. PCC6803 and *Arabidopsis thaliana*. *Journal of Experimental Botany*, *57*(7), 1563-1571.
- Bryn, K., Jantzen, E., & Bøvre, K.** (1977). Occurrence and patterns of waxes in Neisseriaceae. *Microbiology*, *102*(1), 33-43.

- Budin, J. T., Breene, W. M., & Putnam, D. H.** (1995). Some compositional properties of camelina (*Camelina sativa* L. Crantz) seeds and oils. *Journal of the American Oil Chemists' Society*, 72(3), 309-315.
- Bugnarug, C., & Borcean, I.** (2000). A study on the effect of fertilizers on the crop and oil content of *Camelina sativa* L. *Lucrări Științifice-Agricultură, Universitatea de Științe Agricole și Medicină Veterinară a Banatului Timișoara*, 32(2), 541-544.
- Butte, W.** (1983). Rapid method for the determination of fatty acid profiles from fats and oils using trimethylsulphonium hydroxide for transesterification. *Journal of Chromatography A*, 261, 142-145.
- Cagliari, A., Margis-Pinheiro, M., Loss, G., Mastroberti, A. A., de Araujo Mariath, J. E., & Margis, R.** (2010). Identification and expression analysis of castor bean (*Ricinus communis*) genes encoding enzymes from the triacylglycerol biosynthesis pathway. *Plant Science*, 179(5), 499-509.
- Carbonell, A., Takeda, A., Fahlgren, N., Johnson, S. C., Cuperus, J. T., & Carrington, J. C.** (2014). New generation of artificial microRNA and synthetic trans-acting small interfering RNA vectors for efficient gene silencing in Arabidopsis. *Plant Physiology*, pp-113.
- Carlsson, A. S., Yilmaz, J. L., Green, A. G., Stymne, S., & Hofvander, P.** (2011). Replacing fossil oil with fresh oil—with what and for what?. *European Journal of Lipid Science and Technology*, 113(7), 812-831.
- Chacón, M. G., Fournier, A. E., Tran, F., Dittrich-Domergue, F., Pulsifer, I. P., Domergue, F., & Rowland, O.** (2013). Identification of amino acids conferring chain length substrate specificities on fatty alcohol-forming reductases FAR5 and FAR8 from Arabidopsis thaliana. *Journal of Biological Chemistry*, 288(42), 30345-30355.
- Chen, H., Kim, H. U., & Weng, H.** (2011). Malonyl-CoA synthetase, encoded by ACYL ACTIVATING ENZYME13, is essential for growth and development of Arabidopsis. *The Plant Cell*, 23(6), 2247-2262.
- Chen, W., Yu, X. H., Zhang, K., Shi, J., De Oliveira, S., Schreiber, L., & Zhang, D.** (2011). Male Sterile2 encodes a plastid-localized fatty acyl carrier protein reductase required for pollen exine development in Arabidopsis. *Plant Physiology*, 157(2), 842-853.
- Cheng, J. B., & Russell, D. W.** (2004). Mammalian wax biosynthesis II. Expression cloning of wax synthase cDNAs encoding a member of the acyltransferase enzyme family. *Journal of Biological Chemistry*, 279(36), 37798-37807.
- Chung, H., & Carroll, S. B.** (2015). Wax, sex and the origin of species: dual roles of insect cuticular hydrocarbons in adaptation and mating. *Bioessays*, 37(7), 822-830.
- Ciubota-Rosie, C., Ruiz, J. R., Ramos, M. J., & Pérez, Á.** (2013). Biodiesel from *Camelina sativa*: a comprehensive characterisation. *Fuel*, 105, 572-577.

- Conn, K. L., Browne, L. M., Tewari, J. P., & Ayer, W. A.** (1994). Resistance to *Rhizoctonia solani* and presence of antimicrobial compounds in *Camelina sativa* roots. *Journal of Plant Biochemistry and Biotechnology*, 3(2), 125-130.
- Dewitt, S., Ervin, J. L., Howes-Orchison, D., Dalietos, D., Neidleman, S. L., & Geigert, J.** (1982). Saturated and unsaturated wax esters produced by *Acinetobacter* sp. HO1-N grown on C16-C20 n-alkanes. *Journal of the American Oil Chemists' Society*, 59(2), 69-74.
- Doan, T. T., Domergue, F., Fournier, A. E., Vishwanath, S. J., Rowland, O., Moreau, P., & Hofvander, P.** (2012). Biochemical characterization of a chloroplast localized fatty acid reductase from *Arabidopsis thaliana*. *Biochimica et Biophysica Acta (BBA)-Molecular and Cell Biology of Lipids*, 1821(9), 1244-1255.
- Du, W., Li, W., Sun, T., Chen, X., & Liu, D.** (2008). Perspectives for biotechnological production of biodiesel and impacts. *Applied Microbiology and Biotechnology*, 79(3), 331-337.
- Du, X., Herrfurth, C., Gottlieb, T., Kawelke, S., Feussner, K., Rühling, H., & Maniak, M.** (2014). *Dictyostelium discoideum* Dgat2 Can Substitute for the Essential Function of Dgat1 in Triglyceride Production but Not in Ether Lipid Synthesis. *Eukaryotic Cell*, 13(4), 517-526.
- Dyer, J. M., Stymne, S., Green, A. G., & Carlsson, A. S.** (2008). High-value oils from plants. *The Plant Journal*, 54(4), 640-655.
- ELONGASE, F. A.** (1999). Producing wax esters in transgenic plants by expression of genes derived from jojoba. *Perspectives on New Crops and New Uses*, 220.
- Enjalbert, J. N., Zheng, S., Johnson, J. J., Mullen, J. L., Byrne, P. F., & McKay, J. K.** (2013). Brassicaceae germplasm diversity for agronomic and seed quality traits under drought stress. *Industrial Crops and Products*, 47, 176-185.
- Eynckl, C., Shresthaz, D., Vollmann, J., Falk, K. C., Friedt, W., Singh, H. P., & Obeng, E.** (2013). Sustainable oil crops production. *Biofuel Crop Sustainability*, 165.
- Feng, Z., Zhang, B., Ding, W., Liu, X., Yang, D. L., Wei, P., & Zhu, J. K.** (2013). Efficient genome editing in plants using a CRISPR/Cas system. *Cell Research*, 23, 1229-1232
- Friedt, W., & Lühs, W.** (1998). Recent developments and perspectives of industrial rapeseed breeding. *Lipid/Fett*, 100(6), 219-226.
- Fixter, L. M., Nagi, M. N., McCormack, J. G., & Fewson, C. A.** (1986). Structure, distribution and function of wax esters in *Acinetobacter calcoaceticus*. *Microbiology*, 132(11), 3147-3157.
- Gehringer, A., Friedt, W., Lühs, W., & Snowdon, R. J.** (2006). Genetic mapping of agronomic traits in false flax (*Camelina sativa* subsp. *sativa*). *Genome*, 49(12), 1555-1563.

- Gimpel, J. A., Specht, E. A., Georgianna, D. R., & Mayfield, S. P.** (2013). Advances in microalgae engineering and synthetic biology applications for biofuel production. *Current Opinion in Chemical Biology*, 17(3), 489-495.
- Gietz, R. D., & Schiestl, R. H.** (2007). High-efficiency yeast transformation using the LiAc/SS carrier DNA/PEG method. *Nature Protocols*, 2(1), 31-34.
- Gugel, R. K., & Falk, K. C.** (2006). Agronomic and seed quality evaluation of *Camelina sativa* in western Canada. *Canadian Journal of Plant Science*, 86(4), 1047-1058.
- Guy, S. O., Wysocki, D. J., Schillinger, W. F., Chastain, T. G., Karow, R. S., Garland-Campbell, K., & Burke, I. C.** (2014). *Camelina*: Adaptation and performance of genotypes. *Field Crops Research*, 155, 224-232.
- Haslam, R. P., Sayanova, O., Kim, H. J., Cahoon, E. B., & Napier, J. A.** (2016). Synthetic redesign of plant lipid metabolism. *The Plant Journal*, 87, 76–86.
- Hagemann, J. W., & Rothfus, J. A.** (1979). Oxidative stability of wax esters by thermogravimetric analysis. *Journal of the American Oil Chemists' Society*, 56(6), 629-631.
- Hagström, Å. K., Liénard, M. A., Groot, A. T., Hedenström, E., & Löfstedt, C.** (2012). Semi-selective fatty acyl reductases from four heliothine moths influence the specific pheromone composition. *PLoS One*, 7(5), e37230.
- Heilmann, M., Iven, T., Ahmann, K., Hornung, E., Stymne, S., & Feussner, I.** (2012). Production of wax esters in plant seed oils by oleosomal cotargeting of biosynthetic enzymes. *Journal of Lipid Research*, 53(10), 2153-2161.
- Hobbs, D. H., Lu, C., & Hills, M. J.** (1999). Cloning of a cDNA encoding diacylglycerol acyltransferase from *Arabidopsis thaliana* and its functional expression. *FEBS Letters*, 452(3), 145-149.
- Hofvander, P., Doan, T. T., & Hamberg, M.** (2011). A prokaryotic acyl-CoA reductase performing reduction of fatty acyl-CoA to fatty alcohol. *FEBS Letters*, 585(22), 3538-3543.
- Holtzapple, E., & Schmidt-Dannert, C.** (2007). Biosynthesis of isoprenoid wax ester in *M. hydrocarbonoclasticus* DSM 8798: identification and characterization of isoprenoid coenzyme A synthetase and wax ester synthases. *Journal of Bacteriology*, 189(10), 3804-3812.
- Hood, E. E., Gelvin, S. B., Melchers, L. S., & Hoekema, A.** (1993). New agrobacterium helper plasmids for gene transfer to plants. *Transgenic Research*, 2(4), 208-218.
- Hrastar, R., Abramovič, H., & Košir, I. J.** (2012). In situ quality evaluation of *Camelina sativa* landrace. *European Journal of Lipid Science and Technology*, 114(3), 343-351.

- Hunsaker, D. J., French, A. N., Clarke, T. R., & El-Shikha, D. M.** (2011). Water use, crop coefficients, and irrigation management criteria for camelina production in arid regions. *Irrigation Science*, 29(1), 27-43.
- Ito, H., Fukuda, Y. A. S. U. K. I., Murata, K., & Kimura, A.** (1983). Transformation of intact yeast cells treated with alkali cations. *Journal of Bacteriology*, 153(1), 163-168.
- Iven, T., Herrfurth, C., Hornung, E., Heilmann, M., Hofvander, P., Stymne, S., & Feussner, I.** (2013). Wax ester profiling of seed oil by nano-electrospray ionization tandem mass spectrometry. *Plant Methods*, 9(1), 1.
- Iven, T., Hornung, E., Heilmann, M., & Feussner, I.** (2016). Synthesis of oleyl oleate wax esters in *Arabidopsis thaliana* and *Camelina sativa* seed oil. *Plant Biotechnology Journal*, 14(1), 252-259.
- James, D. W., Lim, E., Keller, J., Plooy, I., Ralston, E., & Dooner, H. K.** (1995). Directed tagging of the *Arabidopsis* FATTY ACID ELONGATION1 (FAE1) gene with the maize transposon activator. *The Plant Cell*, 7(3), 309-319.
- Jako, C., Kumar, A., Wei, Y., Zou, J., Barton, D. L., Giblin, E. M., ... & Taylor, D. C.** (2001). Seed-specific over-expression of an *Arabidopsis* cDNA encoding a diacylglycerol acyltransferase enhances seed oil content and seed weight. *Plant Physiology*, 126(2), 861-874.
- Jenks, M. A., Tuttle, H. A., Eigenbrode, S. D., & Feldmann, K. A.** (1995). Leaf epicuticular waxes of the eceriferum mutants in *Arabidopsis*. *Plant Physiology*, 108(1), 369-377.
- Jetter, R., & Kunst, L.** (2008). Plant surface lipid biosynthetic pathways and their utility for metabolic engineering of waxes and hydrocarbon biofuels. *The Plant Journal*, 54(4), 670-683.
- Jolivet, P., Roux, E., d'Andrea, S., Davanture, M., Negroni, L., Zivy, M., & Chardot, T.** (2004). Protein composition of oil bodies in *Arabidopsis thaliana* ecotype WS. *Plant Physiology and Biochemistry*, 42(6), 501-509.
- Kagale, S., Koh, C., Nixon, J., Bollina, V., Clarke, W. E., Tuteja, R., & Higgins, E. E.** (2014). The emerging biofuel crop *Camelina sativa* retains a highly undifferentiated hexaploid genome structure. *Nature Communications*, 5.
- Kalscheuer, R., Luftmann, H., & Steinbüchel, A.** (2004). Synthesis of novel lipids in *Saccharomyces cerevisiae* by heterologous expression of an unspecific bacterial acyltransferase. *Applied and Environmental Microbiology*, 70(12), 7119-7125.
- Kang, J., Snapp, A. R., & Lu, C.** (2011). Identification of three genes encoding microsomal oleate desaturases (FAD2) from the oilseed crop *Camelina sativa*. *Plant Physiology and Biochemistry*, 49(2), 223-229.

- Kalscheuer, R., Luftmann, H., & Steinbüchel, A.** (2004). Synthesis of novel lipids in *Saccharomyces cerevisiae* by heterologous expression of an unspecific bacterial acyltransferase. *Applied and Environmental Microbiology*, *70*(12), 7119-7125.
- Kalscheuer, R., Stöveken, T., Malkus, U., Reichelt, R., Golyshin, P. N., Sabirova, J. S., & Steinbüchel, A.** (2007). Analysis of storage lipid accumulation in *Alcanivorax borkumensis*: evidence for alternative triacylglycerol biosynthesis routes in bacteria. *Journal of Bacteriology*, *189*(3), 918-928.
- Karvonen, H. M., Aro, A., Tapola, N. S., Salminen, I., Uusitupa, M. I., & Sarkkinen, E. S.** (2002). Effect of alpha-linolenic acid rich *Camelina sativa* oil on serum fatty acid composition and serum lipids in hypercholesterolemic subjects. *Metabolism*, *51*(10), 1253-1260.
- Kawelke, S. J.** (2016). Structure-function relationships in wax producing enzymes. Doctoral dissertation, Georg-August Universität, 2014.
- Kawelke, S., & Feussner, I.** (2015). Two predicted transmembrane domains exclude very long chain fatty acyl-CoAs from the active site of mouse wax synthase. *PLoS One*, *10*(12), e0145797.
- Khan, A. A., & Kolattukudy, P. E.** (1973). Control of synthesis and distribution of acyl moieties in etiolated *Euglena gracilis*. *Biochemistry*, *12*(10), 1939-1948.
- Kaup, M. T., Froese, C. D., & Thompson, J. E.** (2002). A role for diacylglycerol acyltransferase during leaf senescence. *Plant Physiology*, *129*(4), 1616-1626.
- King, A., Nam, J. W., Han, J., Hilliard, J., & Jaworski, J. G.** (2007). Cuticular wax biosynthesis in petunia petals: cloning and characterization of an alcohol-acyltransferase that synthesizes wax-esters. *Planta*, *226*(2), 381-394.
- Kirkhus, B., Lundon, A. R., Haugen, J. E., Vogt, G., Borge, G. I. A., & Henriksen, B. I.** (2013). Effects of environmental factors on edible oil quality of organically grown *Camelina sativa*. *Journal of Agricultural and Food Chemistry*, *61*(13), 3179-3185.
- Konishi, T., Shinohara, K., Yamada, K., & Sasaki, Y.** (1996). Acetyl-CoA carboxylase in higher plants: most plants other than gramineae have both the prokaryotic and the eukaryotic forms of this enzyme. *Plant and Cell Physiology*, *37*(2), 117-122.
- Kunst, L., Jetter, R., & Samuels, A. L.** (2008). Biosynthesis and transport of plant cuticular waxes. *Annual Plant Reviews*, *23*, 182-215.
- Lange, R., Schumann, W., Petrzika, M., Busch, H., & Marquard, R.** (1995). Glucosinolate in *Leindottersamen*. *Lipid/Fett*, *97*(4), 146-152.

- Lardizabal, K. D., Metz, J. G., Sakamoto, T., Hutton, W. C., Pollard, M. R., & Lassner, M. W.** (2000). Purification of a jojoba embryo wax synthase, cloning of its cDNA, and production of high levels of wax in seeds of transgenic *Arabidopsis*. *Plant Physiology*, *122*(3), 645-656.
- Lemieux, B., Miquel, M., & Somerville, C.** (1990). Mutants of *Arabidopsis* with alterations in seed lipid fatty acid composition. *Theoretical and Applied Genetics*, *80*(2), 234-240.
- Li-Beisson, Y., Shorrosh, B., Beisson, F., Andersson, M. X., Arondel, V., Bates, P. D., ... & Franke, R. B.** (2013). Acyl-lipid metabolism. *The Arabidopsis Book*, *11*, e0161.
- Li, M., Wei, F., Tawfall, A., Tang, M., Saettele, A., & Wang, X.** (2015). Overexpression of patatin-related phospholipase AIII δ altered plant growth and increased seed oil content in camelina. *Plant Biotechnology Journal*, *13*(6), 766-778.
- Liu, A., Tan, X., Yao, L., & Lu, X.** (2013). Fatty alcohol production in engineered *E. coli* expressing *M. fatty acyl-CoA reductases*. *Applied Microbiology and Biotechnology*, *97*(15), 7061-7071.
- Liu, J., Rice, A., McGlew, K., Shaw, V., Park, H., Clemente, T., ... & Durrett, T. P.** (2015). Metabolic engineering of oilseed crops to produce high levels of novel acetyl glyceride oils with reduced viscosity, freezing point and calorific value. *Plant Biotechnology Journal*, *13*(6), 858-865.
- Liu, X., Brost, J., Hutcheon, C., Guilfoil, R., Wilson, A. K., Leung, S., ... & De Rocher, J.** (2012). Transformation of the oilseed crop *Camelina sativa* by *Agrobacterium*-mediated floral dip and simple large-scale screening of transformants. *In Vitro Cellular & Developmental Biology-Plant*, *48*(5), 462-468.
- Lu, C., & Kang, J.** (2008). Generation of transgenic plants of a potential oilseed crop *Camelina sativa* by *Agrobacterium*-mediated transformation. *Plant Cell Reports*, *27*(2), 273-278.
- Lu, C., Xin, Z., Ren, Z., & Miquel, M.** (2009). An enzyme regulating triacylglycerol composition is encoded by the ROD1 gene of *Arabidopsis*. *Proceedings of the National Academy of Sciences*, *106*(44), 18837-18842.
- Mang, T.** (1998). Umweltrelevante Kriterien zur Anwendung von Pflanzenölen und deren Derivaten im Schmierstoffbereich. *Lipid/Fett*, *100*(12), 524-527.
- Mansour, M. P., Shrestha, P., Belide, S., Petrie, J. R., Nichols, P. D., & Singh, S. P.** (2014). Characterization of oilseed lipids from "DHA-producing *Camelina sativa*": A new transformed land plant containing long-chain omega-3 oils. *Nutrients*, *6*(2), 776-789.
- Malhi, S. S., Johnson, E. N., Hall, L. M., May, W. E., Phelps, S., & Nybo, B.** (2014). Effect of nitrogen fertilizer application on seed yield, N uptake, and seed quality of *Camelina sativa*. *Canadian Journal of Soil Science*, *94*(1), 35-47.

- Malik, M. R., Yang, W., Patterson, N., Tang, J., Wellinghoff, R. L., Preuss, M. L., & Peoples, O. P.** (2015). Production of high levels of poly-3-hydroxybutyrate in plastids of *Camelina sativa* seeds. *Plant Biotechnology Journal*, *13*(5), 675-688.
- Márquez, M. C., & Ventosa, A.** (2005). *M. hydrocarbonoclasticus* and *M. aquaeolei* are heterotypic synonyms. *International Journal of Systematic and Evolutionary Microbiology*, *55*(3), 1349-1351.
- McCormick, K., & Kautto, N.** (2013). The bioeconomy in Europe: An overview. *Sustainability*, *5*(6), 2589-2608.
- Mhaske, V., Beldjilali, K., Ohlrogge, J., & Pollard, M.** (2005). Isolation and characterization of an *Arabidopsis thaliana* knockout line for phospholipid: diacylglycerol transacylase gene (At5g13640). *Plant Physiology and Biochemistry*, *43*(4), 413-417.
- Miklaszewska, M., & Banaś, A.** (2016). Biochemical characterization and substrate specificity of jojoba fatty acyl-CoA reductase and jojoba wax synthase. *Plant Science*, *249*, 84-92.
- Miklaszewska, M., Kawiński, A., & Banaś, A.** (2013). Detailed characterization of the substrate specificity of mouse wax synthase. *Acta Biochimica Polonica*, *60*(2), 209-215.
- Miwa, T. K.** (1971). Jojoba oil wax esters and derived fatty acids and alcohols: gas chromatographic analyses. *Journal of the American Oil Chemists Society*, *48*(6), 259-264.
- Mullis, K., Faloona, F., Scharf, S., Saiki, R., Horn, G., & Erlich, H.** (1986, January). Specific enzymatic amplification of DNA in vitro: the polymerase chain reaction. In *Cold Spring Harbor symposia on quantitative biology* (Vol. 51, pp. 263-273). Cold Spring Harbor Laboratory Press.
- Nagendramma, P., & Kaul, S.** (2012). Development of ecofriendly/biodegradable lubricants: An overview. *Renewable and Sustainable Energy Reviews*, *16*(1), 764-774.
- Nguyen, H. T., Park, H., Koster, K. L., Cahoon, R. E., Nguyen, H., Shanklin, J., & Cahoon, E. B.** (2015). Redirection of metabolic flux for high levels of omega-7 monounsaturated fatty acid accumulation in camelina seeds. *Plant Biotechnology Journal*, *13*(1), 38-50.
- Nguyen, H. T., Silva, J. E., Podicheti, R., Macrander, J., Yang, W., Nazareus, T. J., ... & Mockaitis, K.** (2013). Camelina seed transcriptome: a tool for meal and oil improvement and translational research. *Plant Biotechnology Journal*, *11*(6), 759-769.
- Nykiforuk, C. L., Furukawa-Stoffer, T. L., Huff, P. W., Sarna, M., Laroche, A., Moloney, M. M., & Weselake, R. J.** (2002). Characterization of cDNAs encoding diacylglycerol acyltransferase from cultures of *Brassica napus* and sucrose-mediated induction of enzyme biosynthesis. *Biochimica et Biophysica Acta (BBA)-Molecular and Cell Biology of Lipids*, *1580*(2), 95-109.

- Odham, G.** (1967). Studies on the Fatty Acids in the Feather Waxes of some Water-Birds. *Fette, Seifen, Anstrichmittel*, 69(3), 164-172.
- Ohlrogge, J. B., Pollard, M. R., & Stumpf, P. K.** (1978). Studies on biosynthesis of waxes by developing jojoba seed tissue. *Lipids*, 13(3), 203-210.
- Ossowski, S., Schwab, R., & Weigel, D.** (2008). Gene silencing in plants using artificial microRNAs and other small RNAs. *The Plant Journal*, 53(4), 674-690.
- Patel, S., Nelson, D. R., & Gibbs, A. G.** (2001). Chemical and physical analyses of wax ester properties. *Journal of Insect Science*, 1(1), 4.
- Pidkowich, M. S., Nguyen, H. T., Heilmann, I., Ischebeck, T., & Shanklin, J.** (2007). Modulating seed β -ketoacyl-acyl carrier protein synthase II level converts the composition of a temperate seed oil to that of a palm-like tropical oil. *Proceedings of the National Academy of Sciences*, 104(11), 4742-4747.
- Pollard, M. R., McKeon, T., Gupta, L. M., & Stumpf, P. K.** (1979). Studies on biosynthesis of waxes by developing jojoba seed. II. The demonstration of wax biosynthesis by cell-free homogenates. *Lipids*, 14(7), 651-662.
- Pond, D. W., & Tarling, G. A.** (2011). Phase transitions of wax esters adjust buoyancy in diapausing *Calanoides acutus*. *Limnology and Oceanography*, 56(4), 1310.
- Poxleitner, M., Rogers, S. W., Lacey Samuels, A., Browse, J., & Rogers, J. C.** (2006). A role for caleosin in degradation of oil-body storage lipid during seed germination. *The Plant Journal*, 47(6), 917-933.
- Putnam, D. H., Budin, J. T., Field, L. A., & Breene, W. M.** (1993). Camelina: a promising low-input oilseed. *New crops*. Wiley, New York, 314.
- Reiser, S., & Somerville, C.** (1997). Isolation of mutants of *Acinetobacter calcoaceticus* deficient in wax ester synthesis and complementation of one mutation with a gene encoding a fatty acyl coenzyme A reductase. *Journal of Bacteriology*, 179(9), 2969-2975.
- Rodríguez-Rodríguez, M. F., Sánchez-García, A., Salas, J. J., Garcés, R., & Martínez-Force, E.** (2013). Characterization of the morphological changes and fatty acid profile of developing *Camelina sativa* seeds. *Industrial Crops and Products*, 50, 673-679.
- Rottem, S.** (1980). Membrane lipids of mycoplasmas. *Biochimica et Biophysica Acta (BBA)-Biomembranes*, 604(1), 65-90.
- Routaboul, J. M., Benning, C., Bechtold, N., Caboche, M., & Lepiniec, L.** (1999). The TAG1 locus of *Arabidopsis* encodes for a diacylglycerol acyltransferase. *Plant Physiology and Biochemistry*, 37(11), 831-840.

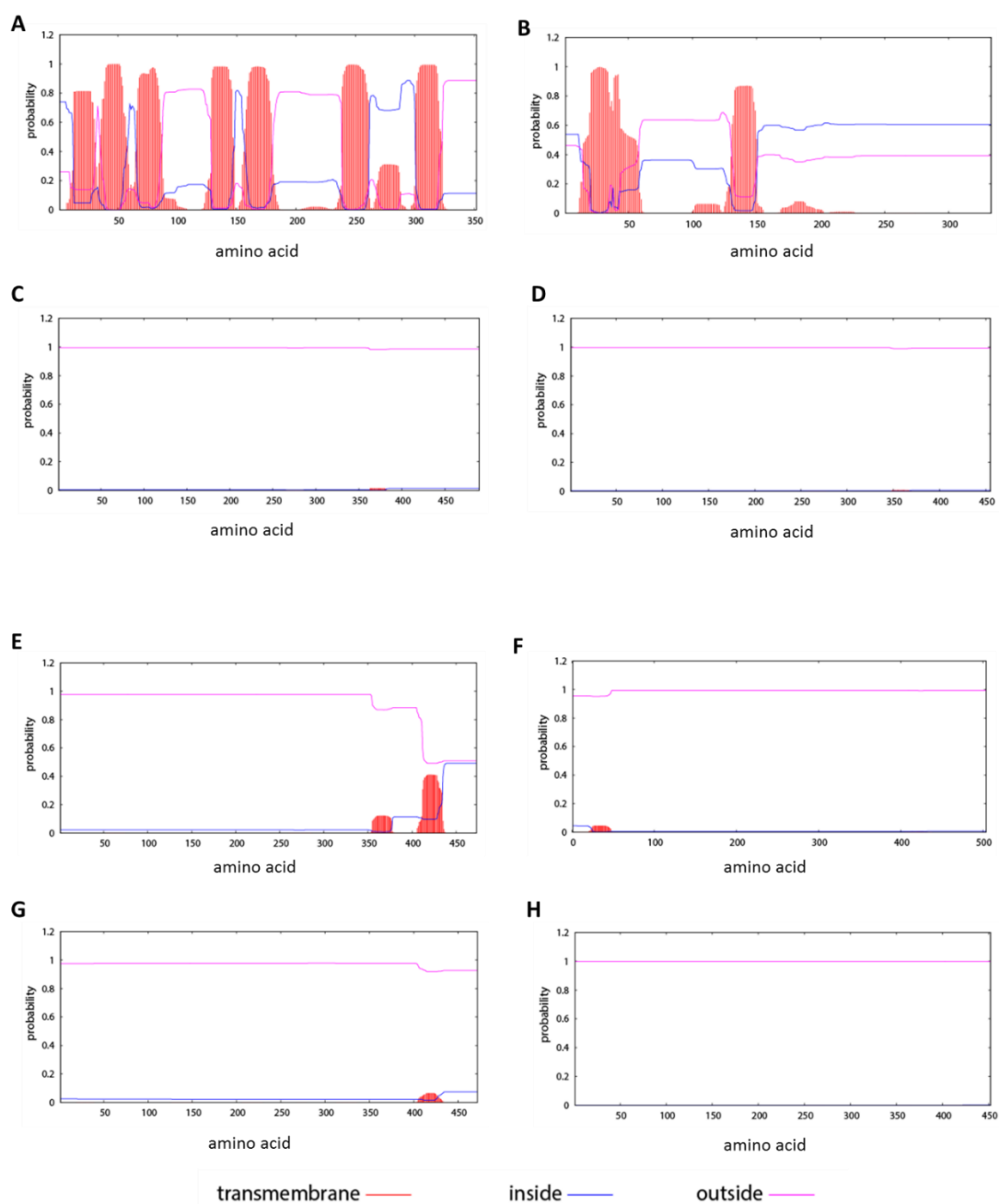
- Rouxel, T., & Balesdent, M. H.** (2005). The stem canker (blackleg) fungus, *Leptosphaeria maculans*, enters the genomic era. *Molecular Plant Pathology*, *6*(3), 225-241.
- Rowland, O., & Domergue, F.** (2012). Plant fatty acyl reductases: enzymes generating fatty alcohols for protective layers with potential for industrial applications. *Plant Science*, *193*, 28-38.
- Roy Choudhury, S., Riesselman, A. J., & Pandey, S.** (2014). Constitutive or seed-specific overexpression of Arabidopsis G-protein γ subunit 3 (AGG3) results in increased seed and oil production and improved stress tolerance in *Camelina sativa*. *Plant Biotechnology Journal*, *12*(1), 49-59.
- Rude, M. A., & Schirmer, A.** (2009). New microbial fuels: a biotech perspective. *Current Opinion in Microbiology*, *12*(3), 274-281.
- Ruiz-Lopez, N., Haslam, R. P., Napier, J. A., & Sayanova, O.** (2014). Successful high-level accumulation of fish oil omega-3 long-chain polyunsaturated fatty acids in a transgenic oilseed crop. *The Plant Journal*, *77*(2), 198-208.
- Sanford, J. C., Smith, F. D., & Russell, J. A.** (1993). Optimizing the biolistic process for different biological applications. *Methods in Enzymology*, *217*, 483-509.
- Salas, J. J., & Ohlrogge, J. B.** (2002). Characterization of substrate specificity of plant FatA and FatB acyl-ACP thioesterases. *Archives of Biochemistry and Biophysics*, *403*(1), 25-34.
- Schuster, A., & Friedt, W.** (1998). Glucosinolate content and composition as parameters of quality of *Camelina* seed. *Industrial Crops and Products*, *7*(2), 297-302.
- Saha, S., Enugutti, B., Rajakumari, S., & Rajasekharan, R.** (2006). Cytosolic triacylglycerol biosynthetic pathway in oilseeds. Molecular cloning and expression of peanut cytosolic diacylglycerol acyltransferase. *Plant Physiology*, *141*(4), 1533-1543.
- Schirmer, A., Rude, M. A., Li, X., Popova, E., & Del Cardayre, S. B.** (2010). Microbial biosynthesis of alkanes. *Science*, *329*(5991), 559-562.
- Schwab, R., Ossowski, S., Riester, M., Warthmann, N., & Weigel, D.** (2006). Highly specific gene silencing by artificial microRNAs in *Arabidopsis*. *The Plant Cell*, *18*(5), 1121-1133.
- Séguin-Swartz, G., Eynck, C., Gugel, R. K., Strelkov, S. E., Olivier, C. Y., Li, J. L., & Falk, K. C.** (2009). Diseases of *Camelina sativa* (false flax). *Canadian Journal of Plant Pathology*, *31*(4), 375-386.
- Sharma, G., Kumar, V. D., Haque, A., Bhat, S. R., Prakash, S., & Chopra, V. L.** (2002). Brassica coenospecies: a rich reservoir for genetic resistance to leaf spot caused by *Alternaria brassicae*. *Euphytica*, *125*(3), 411-417.

- Shimada, T. L., Shimada, T., Takahashi, H., Fukao, Y., & Hara-Nishimura, I.** (2008). A novel role for oleosins in freezing tolerance of oilseeds in *Arabidopsis thaliana*. *The Plant Journal*, *55*(5), 798-809.
- Shi, J., Tan, H., Yu, X. H., Liu, Y., Liang, W., Ranathunge, K., & Shanklin, J.** (2011). Defective pollen wall is required for anther and microspore development in rice and encodes a fatty acyl carrier protein reductase. *The Plant Cell*, *23*(6), 2225-2246.
- Shockey, J. M., Gidda, S. K., Chapital, D. C., Kuan, J. C., Dhanoa, P. K., Bland, J. M., ... & Dyer, J. M.** (2006). Tung tree DGAT1 and DGAT2 have nonredundant functions in triacylglycerol biosynthesis and are localized to different subdomains of the endoplasmic reticulum. *The Plant Cell*, *18*(9), 2294-2313.
- Shonnard, D. R., Williams, L., & Kalnes, T. N.** (2010). Camelina-derived jet fuel and diesel: Sustainable advanced biofuels. *Environmental Progress & Sustainable Energy*, *29*(3), 382-392.
- Slack, C. R., Campbell, L. C., Browse, J. A., & Roughan, P. G.** (1983). Some evidence for the reversibility of the cholinephosphotransferase-catalysed reaction in developing linseed cotyledons in vivo. *Biochimica et Biophysica Acta (BBA)-Lipids and Lipid Metabolism*, *754*(1), 10-20.
- Snapp, A. R., Kang, J., Qi, X., & Lu, C.** (2014). A fatty acid condensing enzyme from *Physaria fendleri* increases hydroxy fatty acid accumulation in transgenic oilseeds of *Camelina sativa*. *Planta*, *240*(3), 599-610.
- Spencer, G. F.** (1979). Alkoxy-Acyl combinations in the wax esters from winterized sperm whale oil by gas chromatography-mass spectrometry. *Journal of the American Oil Chemists' Society*, *56*(6), 642-646.
- Stoveken, T., Kalscheuer, R., & Steinbuchel, A.** (2009). Both histidine residues of the conserved HHXXDYG motif are essential for wax ester synthase/acyl-CoA: diacylglycerol acyltransferase catalysis. *European Journal of Lipid science and Technology*, *111*(2), 112.
- Siloto, R. M., Findlay, K., Lopez-Villalobos, A., Yeung, E. C., Nykiforuk, C. L., & Moloney, M. M.** (2006). The accumulation of oleosins determines the size of seed oilbodies in *Arabidopsis*. *The Plant Cell*, *18*(8), 1961-1974.
- Stymne, S., & Stobart, A. K.** (1984). Evidence for the reversibility of the acyl-CoA: lysophosphatidylcholine acyltransferase in microsomal preparations from developing safflower (*Carthamus tinctorius* L.) cotyledons and rat liver. *Biochemical Journal*, *223*(2), 305-314.
- Taube, E.** (1952). Carnuba wax—Product of a Brazilian palm. *Economic Botany*, *6*(4), 379-401.
- Teerawanichpan, P., Robertson, A. J., & Qiu, X.** (2010). A fatty acyl-CoA reductase highly expressed in the head of honey bee (*Apis mellifera*) involves biosynthesis of a wide range of aliphatic fatty alcohols. *Insect biochemistry and molecular biology*, *40*(9), 641-649.

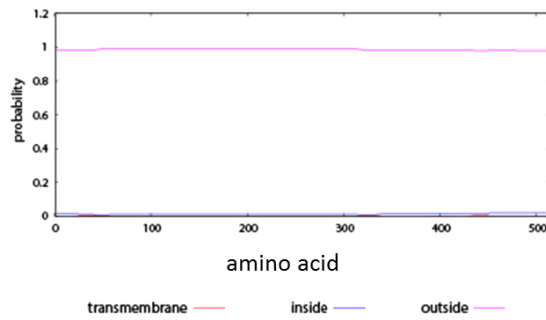
- Tower, W. S.** (1907). A history of the American whale fishery. *Publication for the University*.
- Truter, E. V.** (1956). Wool wax: chemistry and technology. *Cleaver-Hume Press*.
- Toncea, I., Necseriu, D., Prisecaru, T. U. D. O. R., Balint, L. N., Ghilvacs, M. I., & Popa, M.** (2013). The seed's and oil composition of Camelia—first romanian cultivar of camelina (*Camelina sativa*, L. Crantz). *Romanian Biotechnological Letters*, 18(5), 8594-8602.
- Tulloch, A. P.** (1970). The composition of beeswax and other waxes secreted by insects. *Lipids*, 5(2), 247-258.
- Urbaniak, S. D., Caldwell, C. D., Zheljzkov, V. D., Lada, R., & Luan, L.** (2008). The effect of cultivar and applied nitrogen on the performance of *Camelina sativa* L. in the Maritime Provinces of Canada. *Canadian Journal of Plant Science*, 88(1), 111-119.
- Vanhercke, T., Wood, C. C., Stymne, S., Singh, S. P., & Green, A. G.** (2013). Metabolic engineering of plant oils and waxes for use as industrial feedstocks. *Plant Biotechnology Journal*, 11(2), 197-210.
- Vollmann, J., & Eynck, C.** (2015). Camelina as a sustainable oilseed crop: Contributions of plant breeding and genetic engineering. *Biotechnology Journal*, 10(4), 525-535.
- Vollmann, J., Steinkellner, S., & Glauninger, J.** (2001). Variation in resistance of *Camelina sativa* [L.] Crtz.) to downy mildew. *Journal of Phytopathology*, 149, 129–133.
- Wang, Z., Xu, C., & Benning, C.** (2012). TGD4 involved in endoplasmic reticulum-to-chloroplast lipid trafficking is a phosphatidic acid binding protein. *The Plant Journal*, 70(4), 614-623.
- Wältermann, M., Hinz, A., Robenek, H., Troyer, D., Reichelt, R., Malkus, U., & Steinbüchel, A.** (2005). Mechanism of lipid-body formation in prokaryotes: how bacteria fatten up. *Molecular Microbiology*, 55(3), 750-763.
- Weber, L., Meigel, W. N., & Rauterberg, J.** (1977). SDS-polyacrylamide gel electrophoretic. *Archives of Dermatological Research*, 258(3), 251-257.
- Weiss, B., & Richardson, C. C.** (1967). Enzymatic breakage and joining of deoxyribonucleic acid, I. Repair of single-strand breaks in DNA by an enzyme system from *Escherichia coli* infected with T4 bacteriophage. *Proceedings of the National Academy of Sciences*, 57(4), 1021-1028.
- Willis, L. B., Omar, W. S. W., Sambanthamurthi, R., & Sinskey, A. J.** (2008). Non-radioactive assay for acetyl-CoA carboxylase activity. *Journal of Oil Palm Research*, 2, 30-36.
- Wisniak, J.** (1987). The chemistry and technology of jojoba oil. *The American Oil Chemists Society*.

- White, S. W., Zheng, J., Zhang, Y. M., & Rock, C. O.** (2005). The structural biology of type II fatty acid biosynthesis. *Annual Review Biochemistry*, *74*, 791-831.
- Woodman, M. E.** (2008). Direct PCR of intact bacteria (colony PCR). *Current Protocols in Microbiology*, *9:3D:A.3D.1–A.3D.6*.
- Wysocki, D. J., Chastain, T. G., Schillinger, W. F., Guy, S. O., & Karow, R. S.** (2013). Camelina: seed yield response to applied nitrogen and sulfur. *Field Crops Research*, *145*, 60-66.
- Yao, K., Bacchetto, R. G., Lockhart, K. M., Friesen, L. J., Potts, D. A., Covello, P. S., & Taylor, D. C.** (2003). Expression of the Arabidopsis ADS1 gene in Brassica juncea results in a decreased level of total saturated fatty acids. *Plant Biotechnology Journal*, *1*(3), 221-229.
- Zhang, M., Fan, J., Taylor, D. C., & Ohlrogge, J. B.** (2009). DGAT1 and PDAT1 acyltransferases have overlapping functions in Arabidopsis triacylglycerol biosynthesis and are essential for normal pollen and seed development. *The Plant Cell*, *21*(12), 3885-3901.
- Zealand, F. S. A. N.** (2003). Erucic Acid in Food: A Toxicological Review and Risk Assessment. *Canberra: Food Standards Australia New Zealand*, 17-23.
- Zou, J., Wei, Y., Jako, C., Kumar, A., Selvaraj, G., & Taylor, D. C.** (1999). The Arabidopsis thaliana TAG1 mutant has a mutation in a diacylglycerol acyltransferase gene. *The Plant Journal*, *19*(6), 645-653.
- Zubr, J.** (1997). Oil-seed crop: Camelina sativa. *Industrial crops and products*, *6* (2), 113-119.
- Zubr, J., & Matthäus, B.** (2002). Effects of growth conditions on fatty acids and tocopherols in Camelina sativa oil. *Industrial Crops and Products*, *15*(2), 155-162.

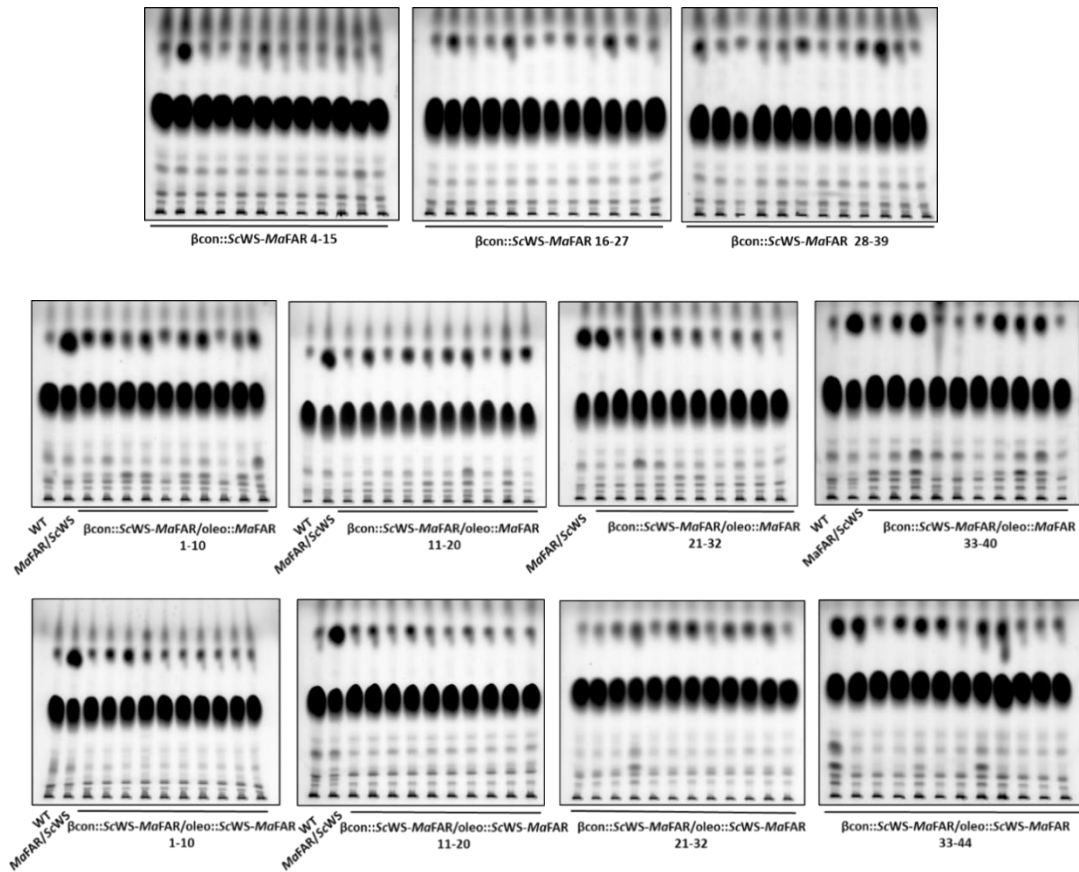
SUPPLEMENTARY MATERIALS



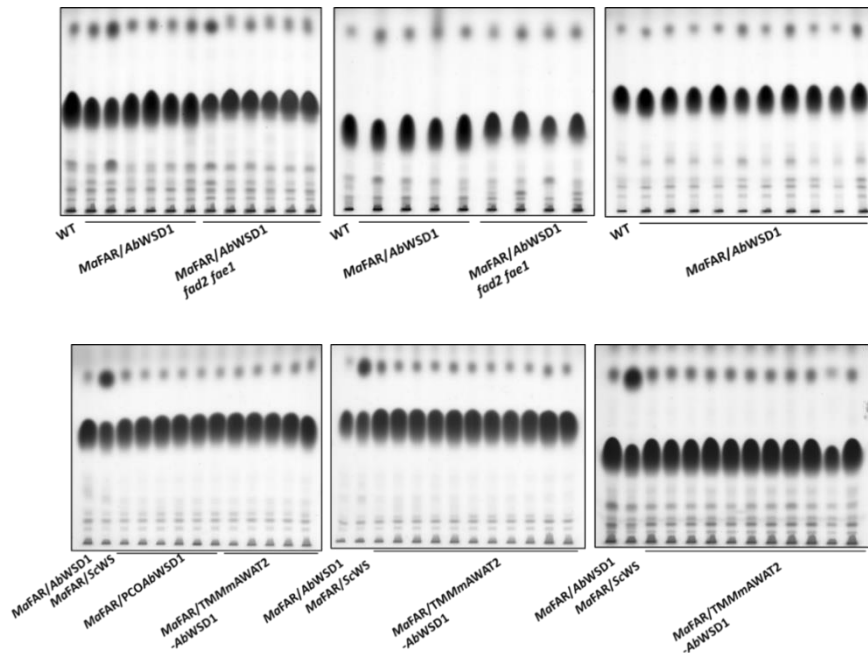
Supplementary Material 1. Predicted transmembrane structure of acyltransferases used in this study. (A) *ScWS* (B) *MmAWAT2* (C) *AbWSD1* (D) *MaWS1* (E) *MaWS2* (F) *MaWS3* (G) *MaWS4* (H) *MaWS5*. Data for respective plots were generated with the TMHMM online service (Sonnhammer *et al.*, 1998).



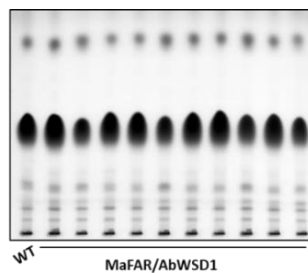
Supplementary Material 2. Predicted transmembrane structure of *MaFAR*. Data for respective plots were generated with the TMHMM online service (Sonnhammer *et al.*, 1998).



Supplementary Material 3. TLC screen of neutral lipid accumulation in seeds of wild-type, *A. thaliana* transformed with *MaFAR/ScWS*, β con::*ScWS-MaFAR*, β con::*ScWS-MaFAR* / oleo::*ScWS-MaFAR*, β con::*ScWS-MaFAR* /oleo-*MaFAR*. Thin layer chromatography (TLC) was performed with hexane: diethyl ether: acetic acid (80:20:1, v/v/v) as a running solvent, after incubating dry TLC plates in CuSO_4 solution, the plate was heated at 190 °C till to the appearance of lipid spots. TLC plate showing the spots of TAG and wax esters.



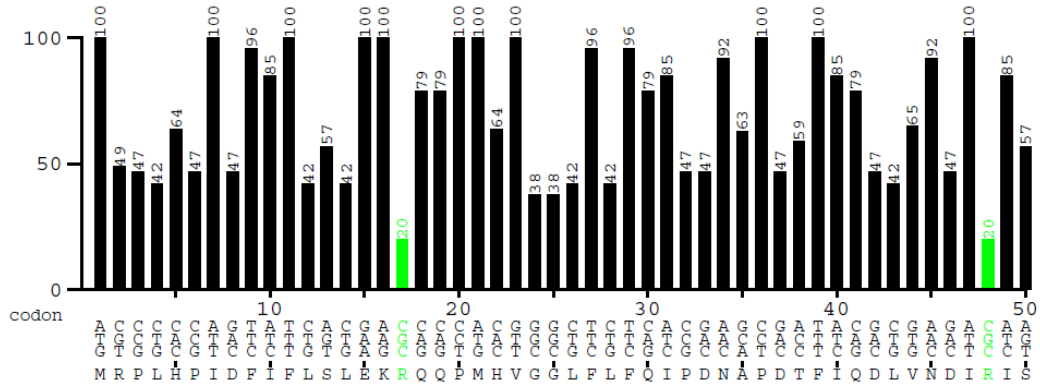
Supplementary Material 4. TLC screen of neutral lipid accumulation in seeds of wild-type, *A. thaliana fad2 fae1* double mutant transformed with *MaFAR/AbWSD1*, Col_0 background transformed with *MaFAR/AbWSD1*, *MaFAR/PCOAbWSD1* and *MaFAR/TMMmAWAT2-AbWSD1*. Thin layer chromatography (TLC) was performed with hexane: diethyl ether: acetic acid (80:20:1, v/v/v) as a running solvent, after incubating dry TLC plates in CuSO₄ solution, the plate was heated at 190 °C till to the appearance of lipid spots. TLC plate showing the spots of TAG and wax esters.



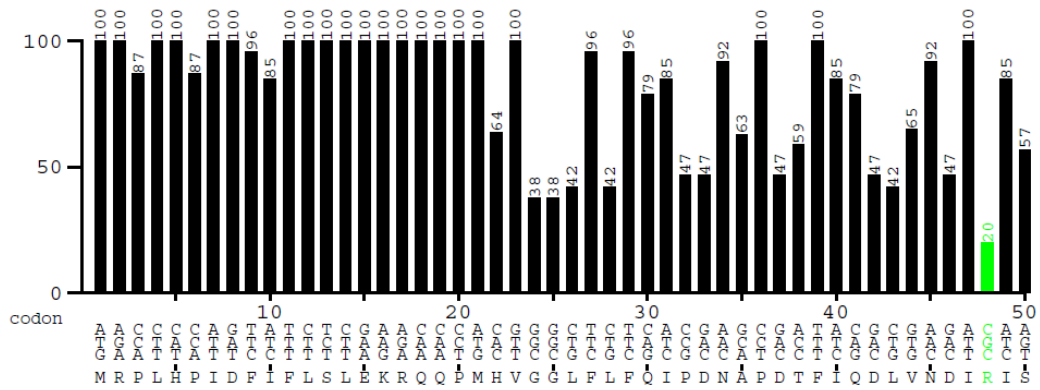
Supplementary Material 5. TLC screen of neutral lipid accumulation in seeds of wild type, *C. sativa* transformed with *MaFAR/ScWS* and *MaFAR/AbWSD1*. Thin layer chromatography (TLC) was performed with hexane: diethyl ether: acetic acid (80:20:1, v/v/v) as a running solvent, after incubating dry TLC plates in CuSO₄ solution, the plate was heated at 190 °C till to the appearance of lipid spots. TLC plate showing the spots of TAG and wax esters.

SUPPLEMENTARY MATERIALS

AbWS
 sequence derived from *Escherichia_coli*
 Codontable:
 Arabidopsis_thaliana
 Ordinate (y-axis): relative adaptiveness <20% <10%

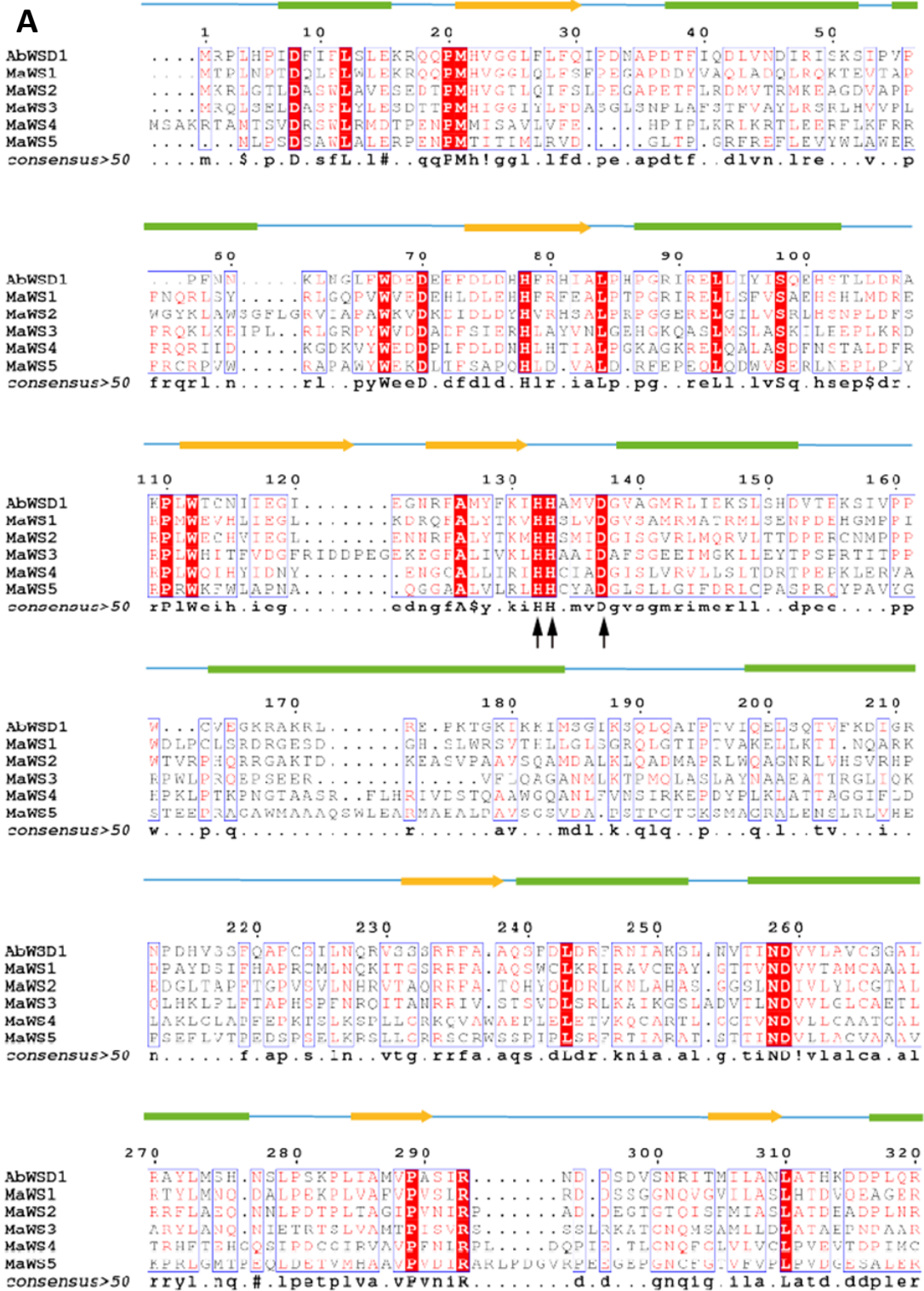


AbWS
 sequence derived from *Escherichia_coli*
 Codontable:
 Arabidopsis_thaliana
 Ordinate (y-axis): relative adaptiveness <20% <10%

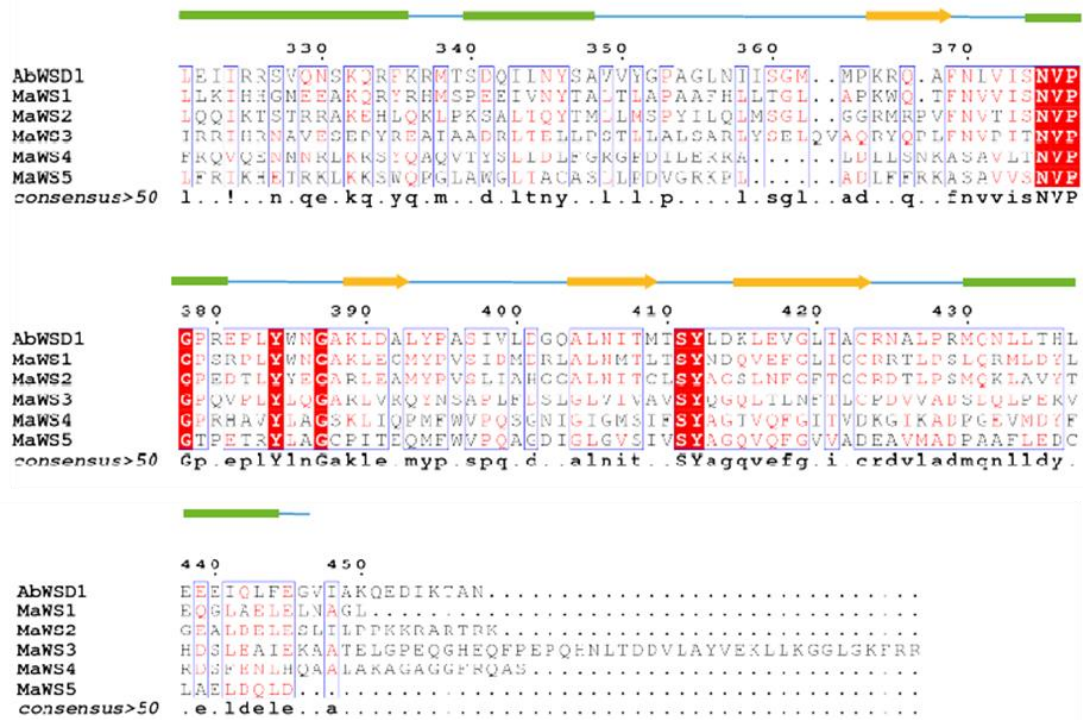


Supplementary Material 6. Codon usage frequency values of the first 50 amino acids of *AbWSD1*. Values were determined using the graphical codon usage analyzer online tool (Fuhrmann *et al.*, 2004).

A



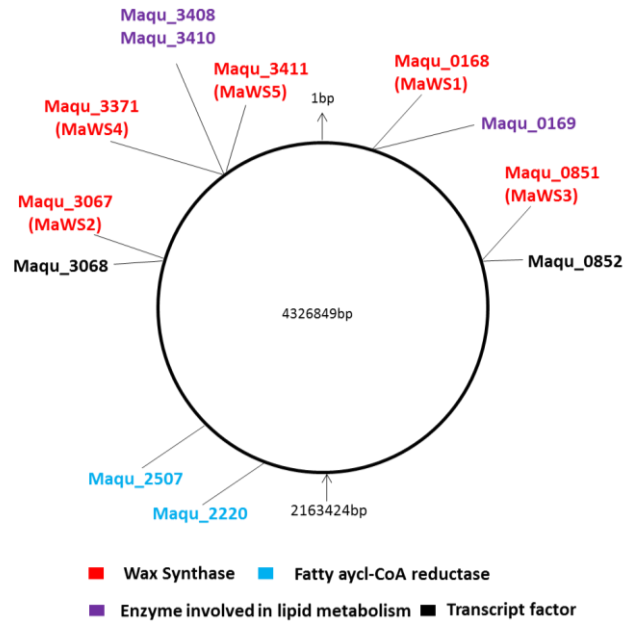
SUPPLEMENTARY MATERIALS



B

	<i>MaWS4</i>	<i>MaWS5</i>	<i>MaWS3</i>	<i>MaWS2</i>	<i>AbWSD1</i>	<i>MaWS1</i>
<i>MaWS4</i>	100	32.7	22.5	24	20.4	23.8
<i>MaWS5</i>	32.7	100	24	24.1	18.9	22.9
<i>MaWS3</i>	22.5	24.0	100	30.5	27.1	28.4
<i>MaWS2</i>	24.1	24.1	30.5	100	37.2	38
<i>AbWSD1</i>	20.4	18.9	27.1	37.2	100	45.2
<i>MaWS1</i>	23.8	22.9	28.4	38	45.2	100

Supplementary Material 7. Multiple sequence alignments of *AbWSD1* and the five putative WSs from *M. aquaeolei* VT8. (A) Identical residues are shown in white on a red background, and similar residues are shown in red. The HHXXXDG(A) active site is indicated with black arrow. The secondary structure elements of *MaWS5* are shown above the alignment. Secondary structure representation is colored green for alpha helices, yellow for beta sheets and blue for connecting loops. The multiple sequence alignments were conducted by using the online program ESPript 2.2. **(B)** The numbers show the peptide sequence identity (% ID) to related enzymes. The analysis was conducted using Multiple Sequence Alignment MUSCLE online service.

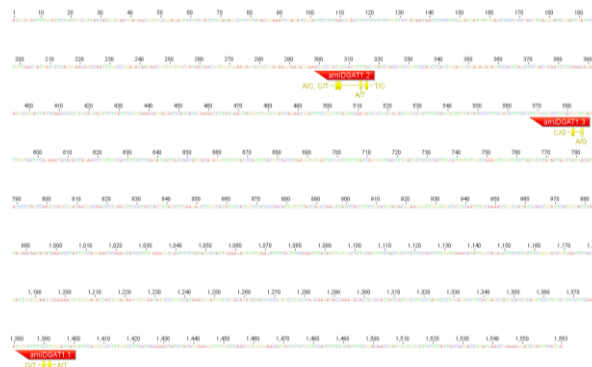


Supplementary Material 8. The positions of two FARs and five putative WSs and in the genome of *M. aquaeolei* VT8.

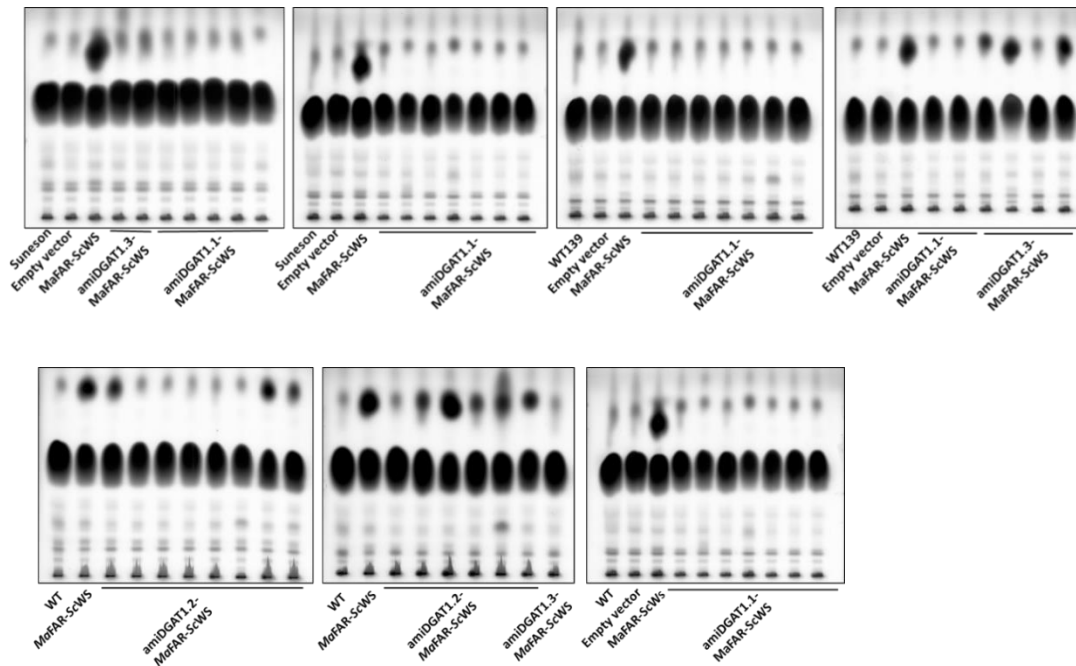
A

amiRNA	Sequence	Targeting position 5' - 3'
amiDGAT1.1	ATAATCCCTATAAAAGCCCA	299 - 319
amiDGAT1.2	CGCATACGTAGTCTCGGCGT	568 - 588
amiDGAT1.3	TCGACGGTAAAGGCAGCCAA	1381 - 1401

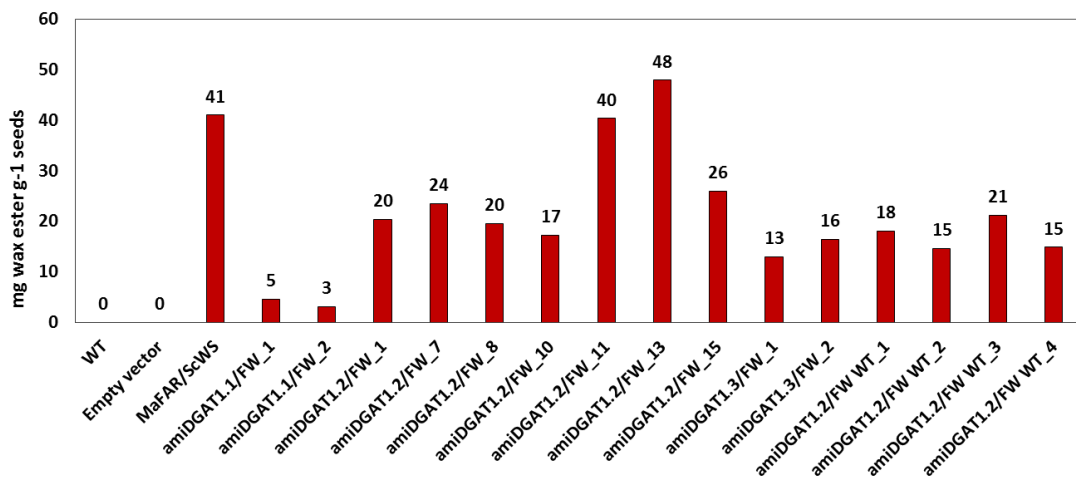
B



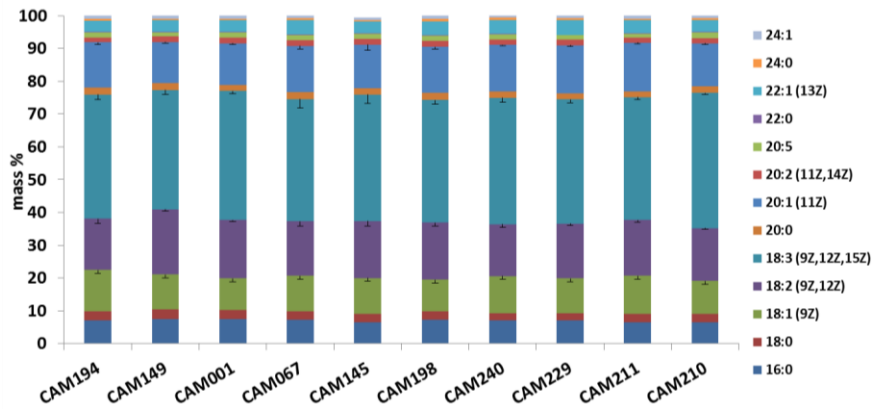
Supplementary Material 9. The sequences of three amiDGAT1 and their positions to target the DGAT1 enzyme. The artificial microRNAs were designed according to the guide offered by WMD3-Web MicroRNA Designer.



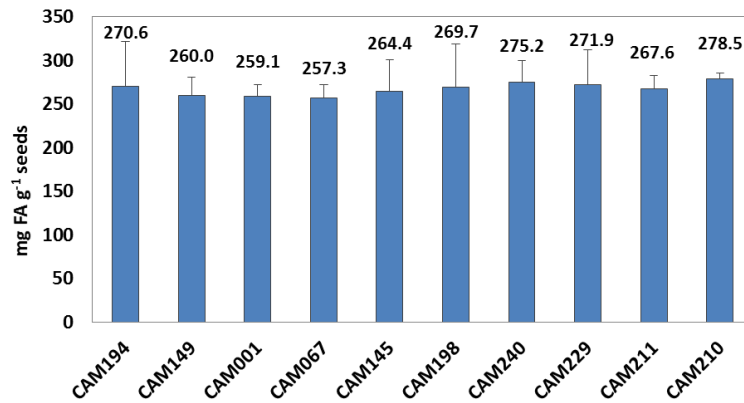
Supplementary Material 10. TLC screen of neutral lipid accumulation in seeds of wild-type, *C. sativa* transformed with empty vector, *MaFAR/ScWS*, *amiDGAT1.1/MaFAR/ScWS*, *amiDGAT1.2/MaFAR/ScWS*, *amiDGAT1.3/MaFAR/ScWS*. Thin layer chromatography (TLC) was performed with hexane: diethyl ether: acetic acid (80:20:1, v/v/v) as a running solvent, after incubating dry TLC plates in CuSO_4 solution, the plate was heated at 190 °C till to the appearance of lipid spots. TLC plate showing the spots of TAG and wax esters.



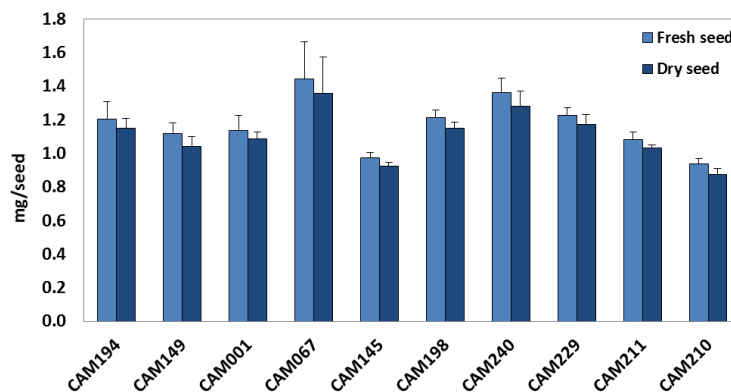
Supplementary Material 11. Wax ester contents of *C. sativa* wild-type, empty vector line, *MaFAR/ScWS* line, two *amiDGAT1.1/MaFAR/ScWS* lines, seven *amiDGAT1.2/MaFAR/ScWS* lines and two *amiDGAT1.3/MaFAR/ScWS* lines. The data represent the mean of each individual line determined with two extraction replicates of seed oil by GC-FID.



Supplementary Material 12. Fatty acid profile of the ten wild-type *C. sativa* lines. The data were determined with three extraction replicates for each line.



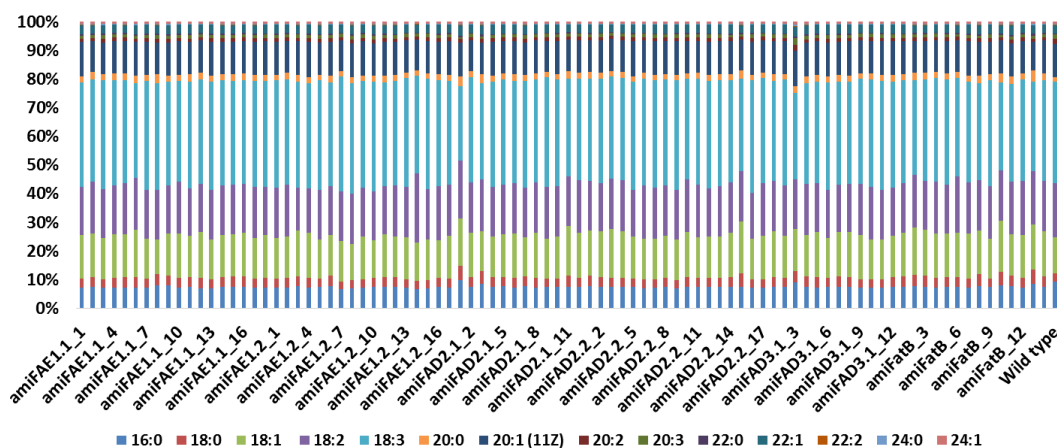
Supplementary Material 13. Total fatty acid content of the ten wild-type *C. sativa* lines. The data were determined with three extraction replicates for each line.



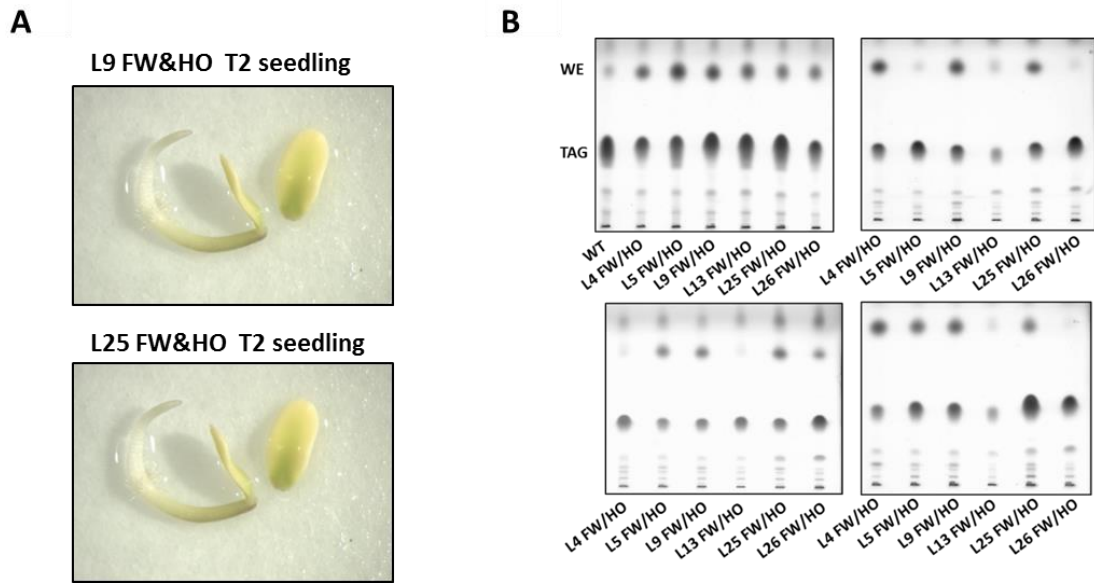
Supplementary Material 14. Fresh seed and dry seed weight of the ten wild-type *C. sativa* lines. The data were determined with three extraction replicates for each line.

amiRNA	Sequence	Targeting position 5' - 3'
amiFAD2.1	TATCGCATTATAATGTGGCAT	973 – 993
amiFAD2.2	TATCGTAGTGAGGCAACGCAT	833 – 853
amiFAD3.1	TAATAGTTGTTAGTCCTGCAC	113 – 133
amiFAD3.2	TTATTGCCGCCCTTACATCAC	845 – 865
amiFAE1.1	TATTTATGCTGGCGAAAACAC	820 – 840
amiFAE1.2	TAGGTAATCATCGGTGCGCTT	1101 – 1121
amiFatB	TTGTGAGCGACTGAACGACAC	1079 – 1098

Supplementary Material 15. The sequences of amiFAD2.1, amiFAD2.2, amiFAD3.1, amiFAE1.1, amiFAE1.2 and amiFatB. The artificial microRNAs were designed according to the guide offered by WMD3-Web MicroRNA Designer. The 21 bp artificial microRNAs were designed to target the 3' end of coding region, and no mismatch between positions 2 - 12 of amiFARs for all targets, and absolute hybridization energy is between -35 and -38 kcal/mole.

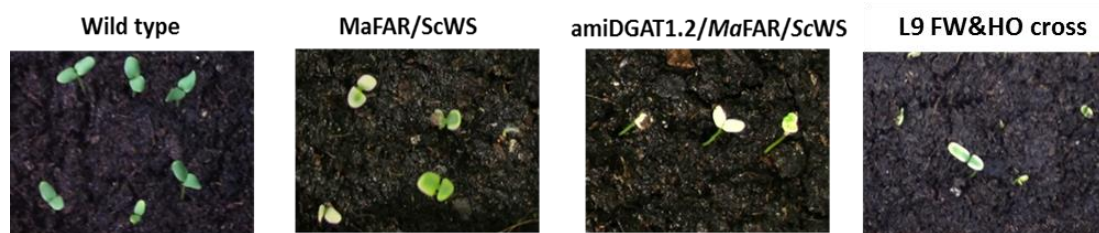


Supplementary Material 16. Fatty acid profile of seed oil of wild-type *C. sativa*, transformed with empty vector, amiFAD2.1, amiFAD2.2, amiFAD3.1, amiFAE1.1, amiFAE1.2 and amiFatB. The data represent the mean of each individual line determined with two extraction replicates of seed oil by GC-FID.

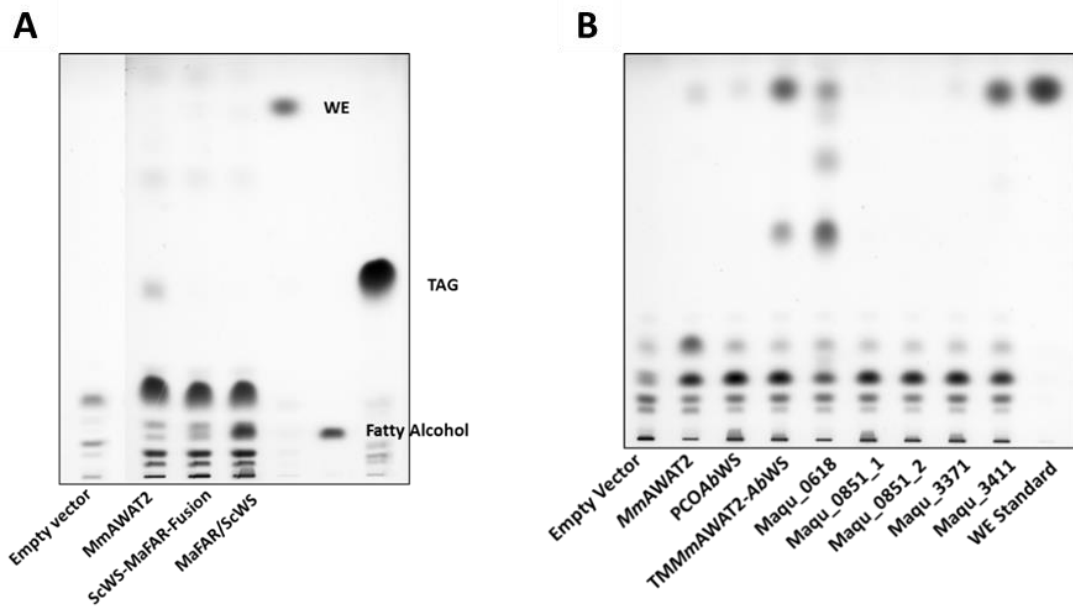


Supplementary Material 17. Selection of transgenic lines of six *MaFAR/ScWS* & HO crosses by cotyledon analysis.

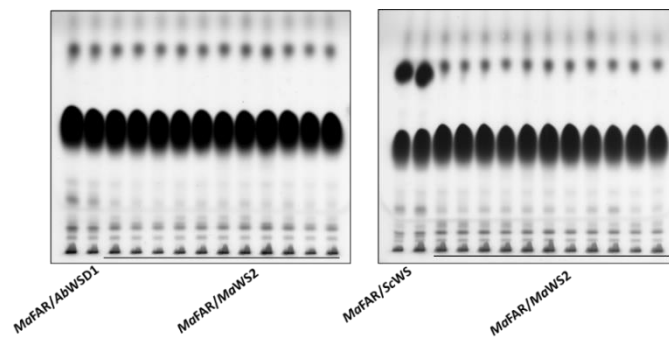
(A) Photo of seedlings where one of the two cotyledons was cut off. (B) Thin layer chromatography (TLC) was performed with hexane: diethyl ether: acetic acid (80:20:1, v/v/v) as a running solvent, after incubating dry TLC plates in CuSO_4 solution, the plate was heated at 190 °C till to the appearance of lipid spots. TLC plate showing that the wax ester accumulation in the cut-off cotyledons. The seedlings with relatively high level of wax esters in cotyledons were grown up.



Supplementary Material 18. 3-day seedlings of wild-type *C. sativa*, *MaFAR/ScWS* lines, and *amiDGAT1.2/MaFAR/ScWS* lines and L9 *MaFAR/ScWS* & HO crossing lines. The seedlings of transgenic lines producing high levels of wax esters have white cotyledons and delayed in development in the first two weeks.

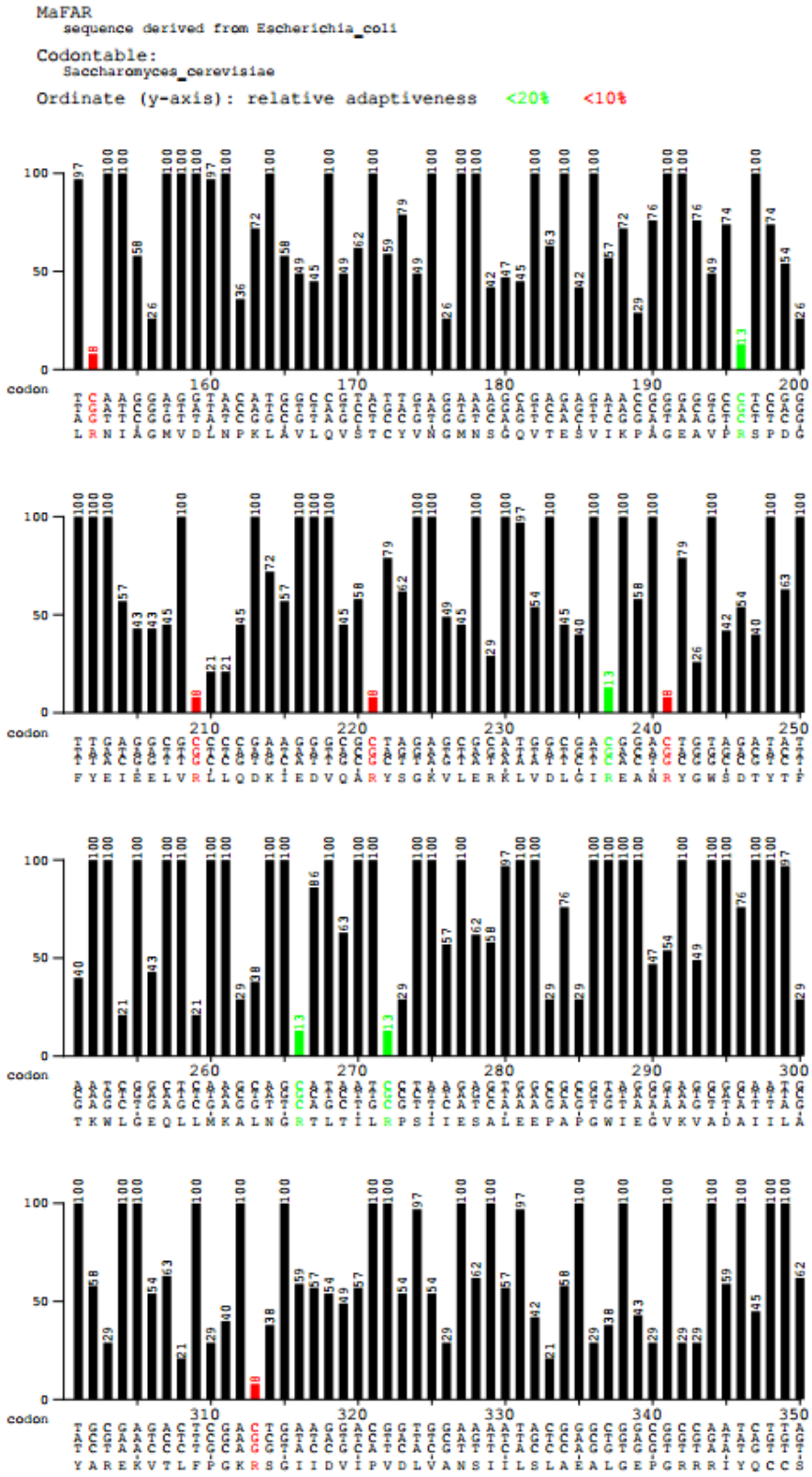


Supplementary Material 18. Accumulation of total lipids in *S. cerevisiae* H1246 strain transformed with empty vector, *MmAWAT2*, *ScWS-MaFAR*-fusion, *MaFAR/ScWS*, *PCOAbWS*, *TM MmAWAT2-AbWS*, *MaWS1* (*Maqu_0168*), *MaWS3* (*Maqu_0851*), *MaWS4* (*Maqu_3371*), *MaWS5* (*Maqu_3411*). (A) Yeast cells were not fed with fatty alcohol. (B) Yeast cells were fed with 16:0-OH. Thin layer chromatography (TLC) was performed with hexane: diethyl ether: acetic acid (80:20:1, v/v/v) as a running solvent, after incubating dry TLC plates in CuSO_4 solution, the plate was heated at 190 °C till to the appearance of lipid spots.

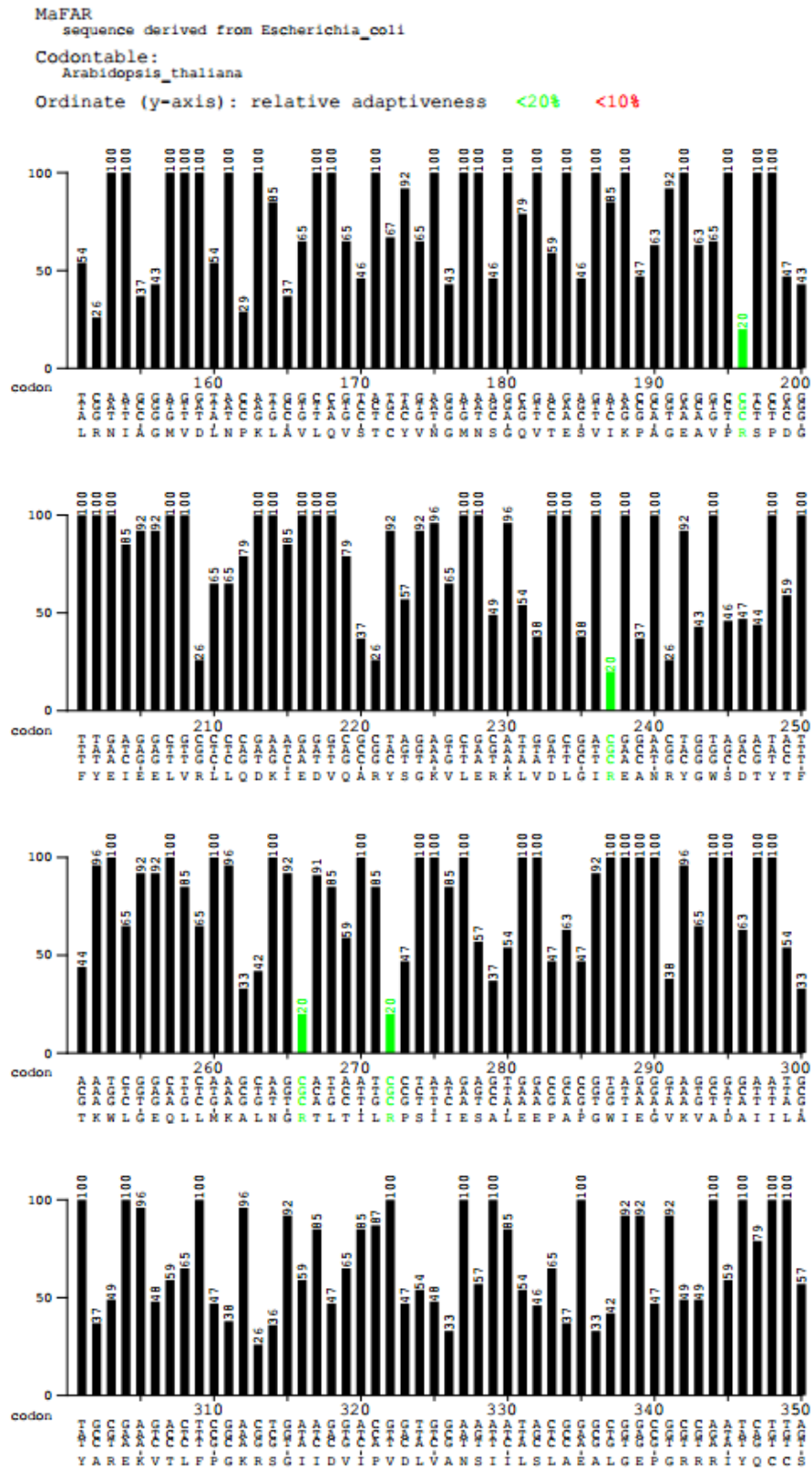


Supplementary Material 19. TLC screen of neutral lipid accumulation in seeds of *A. thaliana* transformed with *MaFAR/AbWS*1, *MaFAR/ScWS* and *MaFAR/MaWS*2. Thin layer chromatography (TLC) was performed with hexane: diethyl ether: acetic acid (80:20:1, v/v/v) as a running solvent, after incubating dry TLC plates in CuSO_4 solution, the plate was heated at 190 °C till to the appearance of lipid spots. TLC plate showing the spots of TAG and wax esters.

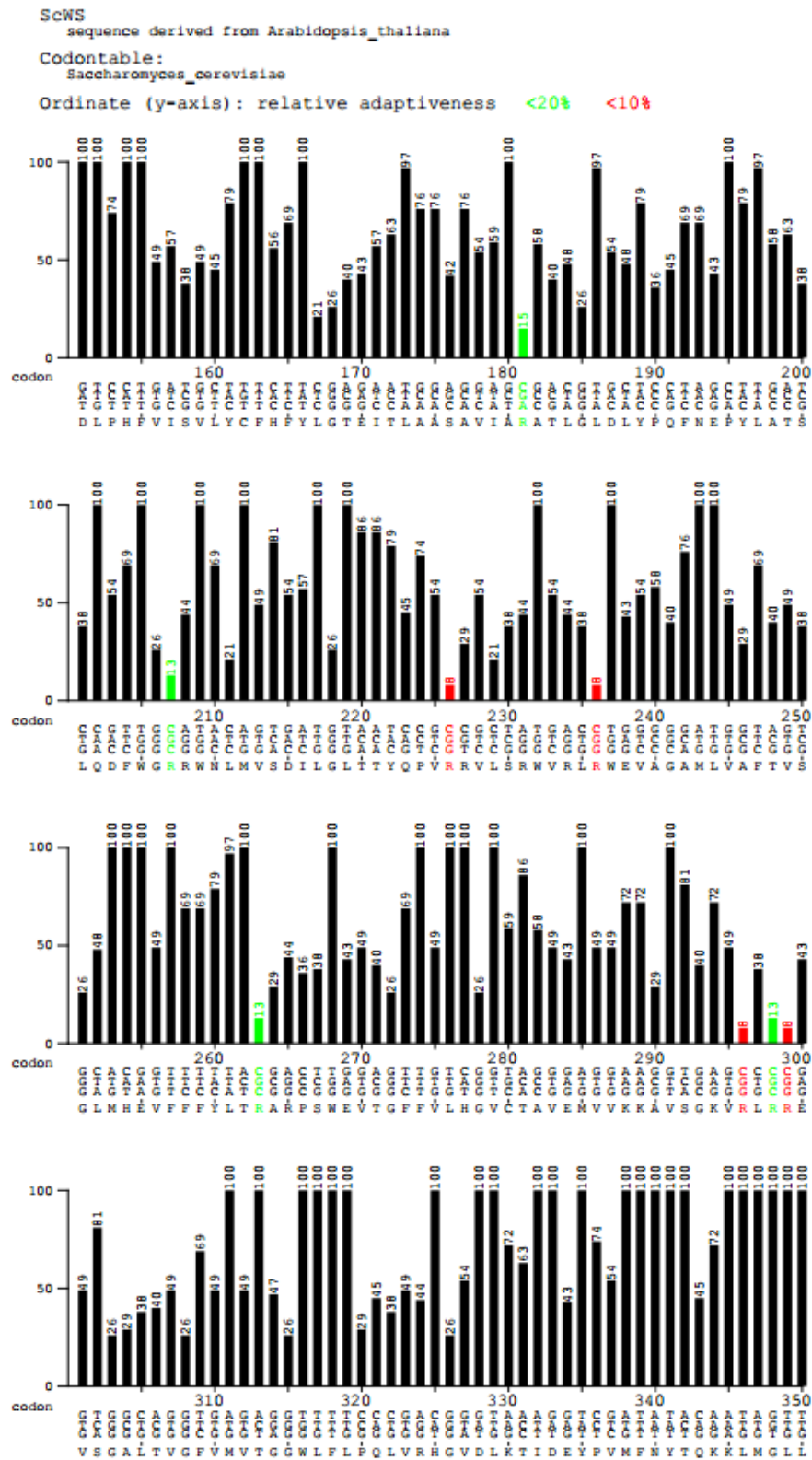
A



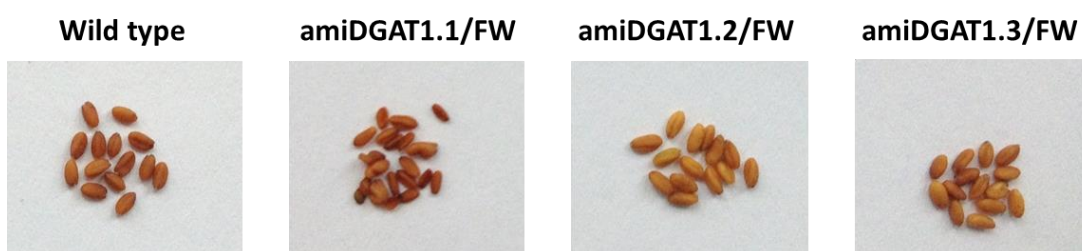
B



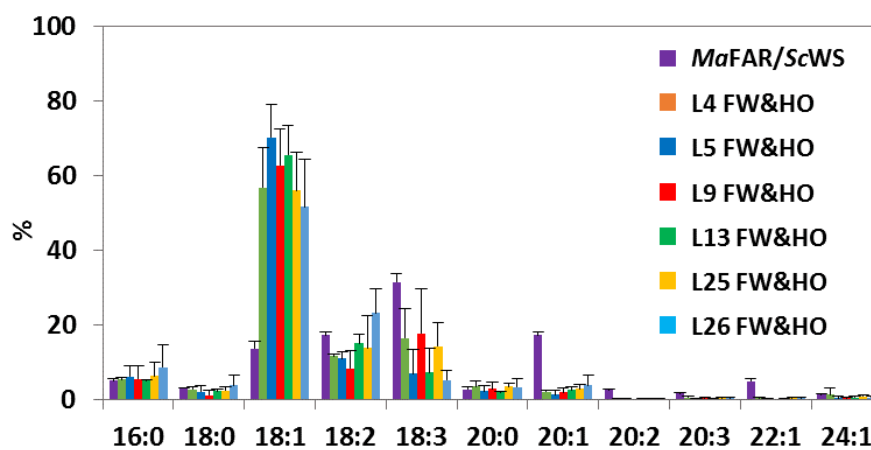
Supplementary Material 20. Codon usage frequency values of MaFAR for expressing in *S. cerevisiae* and *A. thaliana*. (A) *S. cerevisiae*. (B) *A. thaliana*. MaFAR was optimized for *E. coli* and the photo shows the 151 – 350 amino acids of MaFAR. Values were determined using the graphical codon usage analyzer online tool (Fuhrmann *et al.*, 2004).



Supplementary Material 21. Codon usage frequency values of ScWS for expressing in *S. cerevisiae*. The photo shows the 151 – 350 amino acids of ScWS. Values were determined using the graphical codon usage analyzer online tool (Fuhrmann *et al.*, 2004).



Supplementary Material 22. T2 seeds of wild-type, *C. sativa* transformed with amiDGAT1.1/*MaFAR/ScWS*, amiDGAT1.2/*MaFAR/ScWS* and amiDGAT1.3/*MaFAR/ScWS* lines.



Supplementary Material 23. Fatty acid profile of oil in cotyledons of six *C. sativa* *MaFAR/ScWS* & HO cross lines. The data were determined with five extraction of cotyledons for each cross.

LIST OF ABBREVIATIONS

Alcohol and acyl chain nomenclature

The alcohol and acyl chains of wax esters are abbreviated by a number code in this thesis. In this code, the number in front of the colon stands indicates the number of carbon atoms of the alcohol or acyl chain, while the number behind the colon indicates the number of double bounds. For instance, 18:1-OH and 18:1-FA represent the alcohol and acyl chain consists of 18 carbon atoms with one double bond. Wax esters are abbreviated by the combination of alcohol chains and acyl chains, in the case of 18:1/20:1, it is the wax ester species of 18:1 alcohol with 20:1 acyl chain.

Abbreviation	Meaning
18:1	oleic acid
TAGs	triacylglycerols
tri-15:0	tripentadecanoate
di-17:0	heptadecanoyl heptadecanoate
FA	fatty acid
DAGs	diacylglycerol
WS	wax synthase
WSD	bifunctional wax synthase/acyl-CoA:diacylglycerol O-acyltransferase
CoA	coenzyme A
ACP	acyl carrier protein
LD	lipid droplet
FAR	fatty acyl reductase
FALDR	fatty aldehyde reductase
MaFAR	fatty acyl reductase from <i>M. aquaeolei</i> VT8
ScWS	wax synthase from <i>S. chinensis</i>

LIST OF ABBREVIATIONS

DGAT	acyl-CoA : diacylglycerol-O-acyltransferase
<i>Ab</i> WSD1	wax synthase from <i>A. baylyi</i> ADP1
PCO <i>Ab</i> WSD1	plant codon optimized <i>Ab</i> WSD1
<i>Mm</i> AWAT2	wax synthase from <i>Mus musculus</i>
TMM <i>Mm</i> AWAT2- <i>Ab</i> WSD1	<i>Ab</i> WSD1 fused with transmembrane domains of <i>Mm</i> AWAT2
<i>Ma</i> WS	wax synthase from <i>M. aquaeolei</i> VT8
CsDGAT1	<i>C. sativa</i> acyl-CoA : diacylglycerol-O-acyltransferase 1
amiDGAT1	artificial microRNA of <i>C. sativa</i> DGAT1
FADs	fatty acid desaturases
CsFAD2	<i>C. sativa</i> oleate desaturase
CsFAD3	<i>C. sativa</i> linoleate desaturase
CsFAE1	<i>C. sativa</i> fatty acid elongase 1
CsFatB	<i>C. sativa</i> acyl-ACP thioesterase B
FAS	fatty acid synthase complex
KAS	keto acyl-ACP synthase
SAD	stearoyl desaturase
LACS	long-chain acyl-CoA synthase
PC	phosphatidylcholine
PA	phosphatidic acid
LPA	lysophosphatidic acid
LPC	2-lysophosphatidylcholine
LPCAT	2-lysophosphatidylcholine acyltransferase
PDAT	phospholipid: diacylglycerol acyltransferase
PAP	phosphatidic acid phosphatase

LIST OF ABBREVIATIONS

LPAAT	lyso-phosphatidic acid acyltransferase
G3P	glycerol-3-phosphate
GPAT	glycerol-3-phosphate acyltransferase
PLA2	phospholipase A2
β con	soybean β -conglycinin promotor
oleo	soybean oleosin promotor
ER	endoplasmic reticulum
BSTFA	N,O-Bis (trimethylsilyl) trifluoroacetamide
DTNB	5-(3-Carboxy-4-nitrophenyl) disulfanyl-2-nitrobenzoic acid
BASTA	phosphinothricin
SDS	sodium dodecyl sulfate
CHAPS	3-[(3-cholamidopropyl) dimethylammonio]-1-propanesulfonate
FAMES	fatty acid methyl esters
OHS	fatty alcohol methyl esters
TLC	thin layer chromatography
GC-MS	gas chromatography-coupled mass spectrometry
GC-FID	gas chromatography with flame ionization detector
ESI-MS/MS	electrospray ionization mass spectrometry
6xHis	hexahistidine-tagged
NAC	nickel affinity chromatograph
SEC	size exclusion chromatography
HO	high oleic acid
T_m	melting temperature
<i>Atfad3/Csfad2/Csfae1</i>	<i>AtFAD2-RNAi+CsfAD3-RNAi+CsfAE1-RNAi</i>

LIST OF FIGURES

Figure 1.1	Chemical structure of wax esters.	4
Figure 1.2	Two-step enzymatic reactions of wax ester synthesis.	6
Figure 1.3	Hypothetical wax biosynthesis pathway in (A) plant, (B) bacteria, (C) insect and (D) vertebrate.	8
Figure 1.4	Phylogenetic tree showing relationships among different types of fatty acyl reductases.	9
Figure 1.5	Domain structure of fatty acyl reductases.	11
Figure 1.6	Phylogenetic tree showing relationships among different types of wax synthases.	13
Figure 1.7	Domain structure of three types of wax synthases.	14
Figure 1.8	Proposed catalytic mechanism of wax synthases	16
Figure 1.9	Overview of fatty acid biosynthesis, elongation and desaturation pathways in a plant cell.	18
Figure 1.10	Hypothesis pathways of wax ester and TAG biosynthesis in plant seed.	20
Figure 1.11	Relative distribution of nutrient components in <i>C. sativa</i> seeds.	22
Figure 1.12	Fatty acid profile of the seed oil from canola, sunflower, soybean and <i>C. sativa</i> .	23
Figure 4.1	Standard curve for determination of molecular weights according to SEC.	57
Figure 4.2	Reaction scheme of the DTNB-reaction.	60
Figure 5.1.1	Structure domain of the ScWS- <i>MaFAR</i> fusion protein.	67
Figure 5.1.2	Accumulation of lipids in <i>S. cerevisiae</i> transformed with empty vector, <i>MaFAR</i> , ScWS, ScWS- <i>MaFAR</i> fusion protein, <i>MaFAR</i> /ScWS co-expression.	68

LIST OF FIGURES

Figure 5.1.3	DNA constructs used for the seed-specific expression of ScWS- <i>MaFAR</i> fusion protein.	68
Figure 5.1.4	Neutral lipids accumulation in seeds of wild-type, <i>A. thaliana</i> transformed with <i>MaFAR/ScWS</i> , β con:: <i>ScWS-MaFAR</i> , β con:: <i>ScWS-MaFAR/oleo::ScWS-MaFAR</i> and β con:: <i>ScWS-MaFAR/oleo::MaFAR</i> .	69
Figure 5.1.5	Quantification of wax esters in seeds of <i>A. thaliana</i> transformed with <i>MaFAR/ScWS</i> , β con:: <i>ScWS-MaFAR</i> , β con:: <i>ScWS-MaFAR/oleo::ScWS-MaFAR</i> and β con:: <i>ScWS-MaFAR/oleo::MaFAR</i> .	70
Figure 5.1.6	Alcohol and acyl moieties of wax esters in seeds of <i>A. thaliana</i> transformed with <i>MaFAR/ScWS</i> , β con:: <i>ScWS-MaFAR</i> , β con:: <i>ScWS-MaFAR/oleo::ScWS-MaFAR</i> and β con:: <i>ScWS-MaFAR/oleo::MaFAR</i> .	71
Figure 5.1.7	Relative abundance of alcohol and acyl moieties of wax esters in seeds of <i>A. thaliana</i> transformed with <i>MaFAR/ScWS</i> , β con:: <i>ScWS-MaFAR</i> , β con:: <i>ScWS-MaFAR/oleo::ScWS-MaFAR</i> and β con:: <i>ScWS-MaFAR/oleo::MaFAR</i> .	72
Figure 5.2.1	<i>AbWSD1</i> catalyzes the synthesis of TAG or wax ester from fatty acyl-CoA and diacylglycerol or fatty alcohol, respectively.	73
Figure 5.2.2	Molecular species of wax esters in seeds of <i>A. thaliana</i> transformed with <i>MaFAR/AbWSD1</i> .	74
Figure 5.2.3	Structure domain of the <i>TMMmAWAT2-AbWSD1</i> fusion protein.	76
Figure 5.2.4	Accumulation of total lipids in <i>S. cerevisiae</i> H1246 strain transformed with empty vector, <i>MmAWAT2</i> , <i>PCOAbWSD1</i> and <i>TMMmAWAT2-AbWSD1</i> .	77
Figure 5.2.5	Localization of mCherry-tagged <i>TMMmAWAT2-AbWSD1</i> and <i>PCOAbWSD1</i> in onion epidermal cells.	78
Figure 5.2.6	Quantification of wax esters in seeds of <i>A. thaliana</i> Col._0 transformed with <i>MaFAR/ScWS</i> , <i>MaFAR/AbWSD1</i> , <i>MaFAR/PCOAbWSD1</i> and <i>MaFAR/TMMmAWAT2-AbWSD1</i> , <i>A. thaliana fad2 fae1</i> double mutant transformed with <i>MaFAR/AbWSD1</i> .	79
Figure 5.2.7	Alcohol and acyl moieties of wax esters in seeds of <i>A. thaliana</i> Col._0 background transformed with <i>MaFAR/ScWS</i> , <i>MaFAR/AbWSD1</i> ,	80

LIST OF FIGURES

	<i>MaFAR/PCOAbWSD1</i> and <i>MaFAR/TMMmAWAT2-AbWSD1</i> , <i>A. thaliana fad2 fae1</i> double mutant background transformed with <i>MaFAR/AbWSD1</i> .	
Figure 5.2.8	Relative abundance of alcohol and acyl moieties of wax esters in seeds of <i>A. thaliana</i> Col._0 background transformed with <i>MaFAR/ScWS</i> , <i>MaFAR/AbWSD1</i> , <i>MaFAR/PCOAbWSD1</i> and <i>MaFAR/TMMmAWAT2-AbWSD1</i> , <i>A. thaliana fad2 fae1</i> double mutant background transformed with <i>MaFAR/AbWSD1</i> .	82
Figure 5.3.1	Structure domain of 5 five putative wax synthases from <i>M. aquaeolei</i> VT8.	83
Figure 5.3.2	Accumulation of total lipids in <i>S. cerevisiae</i> H1246 strain transformed with empty vector and 5 five putative wax synthases from <i>M. aquaeolei</i> VT8.	85
Figure 5.3.3	Quantification of wax esters in seeds of <i>A. thaliana</i> transformed with <i>MaFAR/ScWS</i> and <i>MaFAR/MaWS2</i> .	86
Figure 5.3.4	Alcohol and acyl moieties of wax esters in seeds of <i>A. thaliana</i> transformed with <i>MaFAR/ScWS</i> and <i>MaFAR/MaWS2</i> .	87
Figure 5.3.5	Relative abundance of alcohol and acyl moieties of wax esters in seeds of <i>A. thaliana</i> transformed with <i>MaFAR/ScWS</i> and <i>MaFAR/MaWS2</i> .	88
Figure 5.3.6	Nickel affinity chromatography (NAC) purification of heterologous <i>MaWS5</i> from <i>E. coli</i> .	89
Figure 5.3.7	<i>In vitro</i> activity test of purified <i>MaWS5-6xHis</i> eluted from Ni-NTA agarose column.	89
Figure 5.3.8	Size exclusion chromatography (SEC) of the <i>MaWS5-6xHis</i> .	90
Figure 5.3.9	<i>In vitro</i> activity test of purified <i>MaWS5-6xHis</i> eluted from SEC.	91
Figure 5.4.1	Neutral lipid accumulation in seeds of wild-type, <i>C. sativa</i> transformed with empty vector, <i>MaFAR/ScWS</i> , <i>amiDGAT1.1/MaFAR/ScWS</i> , <i>amiDGAT1.2/MaFAR/ScWS</i> , <i>amiDGAT1.3/MaFAR/ScWS</i> .	93

LIST OF FIGURES

Figure 5.4.2	Wax ester and TAG accumulation in seeds of <i>C. sativa</i> transformed with empty vector, <i>MaFAR/ScWS</i> , <i>amiDGAT1.1/MaFAR/ScWS</i> , <i>amiDGAT1.2/MaFAR/ScWS</i> , <i>amiDGAT1.3/MaFAR/ScWS</i> .	94
Figure 5.4.3	Fatty acyl profile of TAG in seeds of <i>C. sativa</i> transformed with empty vector, <i>MaFAR/ScWS</i> , <i>amiDGAT1.1/MaFAR/ScWS</i> , <i>amiDGAT1.2/MaFAR/ScWS</i> , <i>amiDGAT1.3/MaFAR/ScWS</i> .	95
Figure 5.4.4	Alcohol and acyl moieties of wax esters in seeds of <i>C. sativa</i> transformed with empty vector, <i>MaFAR/ScWS</i> , <i>amiDGAT1.1/MaFAR/ScWS</i> , <i>amiDGAT1.2/MaFAR/ScWS</i> , <i>amiDGAT1.3/MaFAR/ScWS</i> .	96
Figure 5.4.5	Relative abundance of alcohol and acyl moieties of wax esters in seeds of <i>C. sativa</i> transformed with <i>MaFAR/ScWS</i> , <i>amiDGAT1.1/MaFAR/ScWS</i> , <i>amiDGAT1.2/MaFAR/ScWS</i> , <i>amiDGAT1.3/MaFAR/ScWS</i> .	97
Figure 5.5.1	Mol% of oleic acid, linoleic acid plus linolenic acid of seed oil of <i>C. sativa</i> wild-type, transformed with empty vector, <i>amiFAD2.1</i> and <i>amiFAD2.2</i> .	100
Figure 5.5.2	Fatty acid profile of seed oil of <i>C. sativa</i> wild-type, transformed with empty vector and <i>amiFAD3.1</i> .	100
Figure 5.5.3	Mol% of oleic acid, gondoic acid of <i>C. sativa</i> wild-type, transformed with empty vector, <i>amiFAE1.1</i> and <i>amiFAE1.2</i> .	101
Figure 5.5.4	Mol% of palmitic acid, stearic acid plus oleic acid of seed oil of <i>C. sativa</i> wild-type, transformed with empty vector and <i>amiFatB</i> .	101
Figure 5.5.5	Wax ester and TAG accumulation in seeds of <i>C. sativa</i> containing high level of oleic acid (HO), transformed with <i>MaFAR/ScWS</i> (FW), six crosses of <i>MaFAR/ScWS</i> with the HO line (FW/HO).	103
Figure 5.5.6	Alcohol and acyl moieties of wax esters in seeds of six <i>C. sativa</i> <i>MaFAR/ScWS</i> & HO cross lines.	104
Figure 5.5.7	Wax ester profiles of six <i>C. sativa</i> <i>MaFAR/ScWS</i> & HO cross lines.	106

LIST OF TABLES

Table 3.1	List of chemicals	29
Table 3.2	List of machines and equipments	29
Table 3.3	List of software and web-based services	31
Table 3.4	List of kits and consumables	32
Table 3.5	List of standards and markers	33
Table 3.6.1	The composition of LB medium	33
Table 3.6.2	The composition of ZY medium	33
Table 3.6.3	Single drop-out powder without Uracil	34
Table 3.6.4	The composition of SD medium	34
Table 3.6.5	The composition of TBS buffer	34
Table 3.6.6	The composition of 50 X TAE buffer	34
Table 3.6.7	List of antibiotics	35
Table 3.7	List of columns for chromatography	35
Table 3.8	List of enzymes	35
Table 3.9	List of strains and organisms	36
Table 3.10	List of oligonucleotides	37
Table 3.11	List of the DNA constructs	41
Table 3.12	List of transgenic plant lines	43
Table 4.1	The sample composition for standard PCR	45
Table 4.2	The sample composition of colony PCR	46
Table 4.3	The composition of TAE buffer	47
Table 4.4	The composition of 6 X loading buffer	47

LIST OF TABLES

Table 4.5	The Composition of blunt-end ligation reaction	47
Table 4.6	Blunting reaction	48
Table 4.7	Ligation reaction of sticky-end cloning	48
Table 4.8	Cloning strategy of artificial microRNAs	48
Table 4.9	Site-directed PCR reaction (a) (b) (c)	49
Table 4.10	Overlapping PCR reaction (d)	49
Table 4.11	The composition of oligo annealing buffer	50
Table 4.12	The composition of TFB buffer	51
Table 4.13	The composition of YPD medium	52
Table 4.14	The composition of solution A	52
Table 4.15	The composition of solution B	52
Table 4.16	The composition of solution C	52
Table 4.17	The composition of Mix A solution	54
Table 4.18	The composition of 1000 x metal mix	55
Table 4.19	The composition of 50 x 5052	55
Table 4.20	The composition of 20 x NPS	55
Table 4.21	Auto-induction medium	55
Table 4.22	Buffer A for HisTrap	56
Table 4.23	Buffer B for HisTrap	56
Table 4.24	Tris-HCl buffer for SEC	57
Table 4.25	Phosphate buffer for SEC	57
Table 4.26	Stacking gels (4%) for SDS-PAGE	58
Table 4.27	Separation gels (12%) for SDS-PAGE	58
Table 4.28	The composition of 10 x gel running buffer	59

LIST OF TABLES

Table 4.29	The composition of 4 X sample loading buffer	59
Table 4.30	The composition of staining buffer	59
Table 4.31	The composition of destaining buffer	59
Table 4.32	The composition of bradford-reagent	60
Table 4.33	The composition of FAME Solution	62
Table 5.1.1	Numbers of harvested T2 <i>A. thaliana</i> transgenic lines transformed with β con::ScWS- <i>MaFAR</i> , β con::ScWS- <i>MaFAR/oleo</i> ::ScWS- <i>MaFAR</i> and β con::ScWS- <i>MaFAR/oleo</i> :: <i>MaFAR</i> , numbers of transgenic lines analyzed by TLC and GC-FID.	69
Table 5.2.1	Numbers of T2 transgenic lines with <i>MaFAR/AbWSD1</i> , <i>MaFAR/PCOAbWSD1</i> and <i>MaFAR/TMMmAWAT2-AbWSD1</i> in Col._0 background, lines with <i>MaFAR/AbWSD1</i> in <i>fad2 fae1</i> double mutant; numbers of transgenic lines analyzed by TLC and GC-FID.	79
Table 5.3.1	Number of harvested T2 <i>A. thaliana</i> transgenic lines transformed with <i>MaFAR/MaWS2</i> , number of transgenic lines analyzed by TLC and GC-FID.	85
Table 5.4.1	Numbers of harvested T2 <i>C. sativa</i> transgenic lines transformed with <i>amiDGAT1.1/MaFAR/ScWS</i> , <i>amiDGAT1.2/MaFAR/ScWS</i> , <i>amiDGAT1.3/MaFAR/ScWS</i> , numbers of transgenic lines analyzed by TLC and GC-FID.	92
Table 5.5.1	Numbers of harvested T2 <i>C. sativa</i> transgenic lines transformed with empty vector, <i>amiFAD2.1</i> , <i>amiFAD2.2</i> , <i>amiFAD3.1</i> , <i>amiFAE1.1</i> , <i>amiFAE1.2</i> and <i>amiFatB</i> .	99

ACKNOWLEDGEMENTS

This work was conducted in a period of three years in the Department of Plant Biochemistry of the Georg-August University of Göttingen under the supervision of Prof. Dr. Ivo Feußner. I am highly appreciate for his support during this time. He not only contributed significant ideas to this project but also positively supported my own ones. I am also grateful for the many inspiring discussions with him, he always point out the right orientation of my research works when I was not sure about what to do next.

I furthermore got a lot of important guidance and suggestions from Dr. Ellen Hornung. I got many advising from her accompanied with the molecular biology and cloning technology. She could always help me to go through the troubles I met in experiments, or told me who was the right person specialized in a research method. Beside of the various questions she answered every day in the last three years, her energetic personality enriched the everyday laboratory life, and her fantastic baking skill made me fall in love with cakes.

One important contribution of Dr. Tim Iven to this study was the analytic method of wax ester composition by nano-ESI-MS/MS. His previous works supplied a good foundation for this study. Without his work, it would not be possible to identify the molecular species of wax esters produced by the different enzyme combinations in my studies.

I gratitude for the work of Dr. Sofia Marmon. She designed and cloned three artificial microRNAs of CsDGAT1. In addition, she also gave me many helpful advices for both my research work and personal life.

I also want to thank Nina Zaremba, who contributed to my studies during her bachelor thesis. She did great job to clone the gene of *ScWS-MaFAR* into pYES2/CT vector for expressing the fusion protein in yeast.

Furthermore, I want to thank Dr. Jennifer Popko for helping me with the Gateway Reaction to clone *amiDGAT1/MaFAR/ScWs* as a multiple construct. Dr. Martin Fulda and Dr. Till Ischebeck helped me with the fluorescent microscopy, and Dr. Martin Fulda kindly provided the ER marker. Dr. Cornelia Herrfurth and Pia Meyer were patient to help me operate GC and GC-MS. I am also appreciate Susanne Mester to take good care of my plants and Andrea Nickel sometimes helped to harvest my seeds.

Apart from the members from the Department of Plant Biochemistry of the Georg-August University of Göttingen, I would like to give acknowledgment to our collaborator, Prof. Dr. Edgar Cahoon kindly provided the seeds of high oleic acid *C. sativa* line and the DNAs of soybean beta-conlycinin promoter and oleosin promotor.

ACKNOWLEDGEMENTS

I am very grateful for the supervision and guidance from all the members of my thesis committee. In the course of our meeting, Prof. Christiane Gatz and Prof. Dr. Andrea Polle also provided constructive feedback and helpful suggestions for my project.

I also want to thank all the members in the Department of Plant Biochemistry to be super nice and contribute for a relaxed and harmonious working atmosphere, so that I could collect a lot of happy memories. Especially, I spent much great time with the 'first floor hard workers', so thank Benjamin to be handsome and humorous, Steffen to be obliging and reliable, and Julia to be lovely and smart.

Prof. Dr. Ivo Feußner, Dr. Ellen Hornung, Dr. Sofia Marmon and Dr. Amelie Kelly carefully read this thesis and gave me a lot of valuable suggestions. I am high grateful for their supports during my writing process. I also thank Prof. Dr. Ivo Feußner, Prof. Christiane Gatz, Prof. Dr. Andrea Polle, Prof. Dr. Volker Lipka, Dr. Thomas Teichmann and Dr. Marcel Wiermer to be the members of the examination board.

Finally, I would not have chance to come to Göttingen or write this thesis without the support of my parents, thank you for standing by my side even though I could not accompany with you in the last three years. Thanks Shaobo for making me happy, encouraging me when I felt depressed. Last, I want to thank for myself to be a brave woman and please continue to work hard in the future.

CURRICULUM VITAE

Personal Information

Name: Dan Yu

Date of birth: 05.09.1987

Place of birth: Fuxin, China

Nationality: Chinese

Scientific Education

Doctor of Philosophy **2013-2016**

Doctoral thesis "Production of wax esters in *Camelina sativa*"

In the group of Prof. Dr. Ivo Feußner, Department of Plant Biochemistry, Albrecht-von-Haller-Institute of Plant Sciences, Georg-August-University of Göttingen, Germany within the doctoral program "Molecular Science and Biotechnology of Crops and trees-BIONUTZ"

Master of Science **2010-2013**

Master thesis "Low-molecular organic fertilizers regulate the growth and metabolism of horticultural plants"

In group of Prof. Dr. Weiling Wang, Department of Plant Science, Northwest A & F University, China

Bachelor of Engineering **2006-2010**

Bachelor thesis: "The microbial populations and the activities of soil enzymes in soil grown with different vegetation species".

In group of Prof. Dr. Wenfang Hao, Department of Plant Science, Northwest A & F University, China

Scholarships

2013-2016 Doctoral scholarship, Georg-August-University

2010-2013 First prize of graduate student fellowship, Northwest A&F University

2006-2010 First prize of undergraduate scholarship, Northwest A&F University

Studies

2003-2006 First-class Key High School, Fuxin, China

1999-2003 First-class Key Middle School, Fuxin, China

1994-1999 Zhonghua Road Primary School, Fuxin, China